Regulation of MITF and Brn2 in melanoma

Sarina Agkatsev

Brasenose College

University of Oxford

A thesis submitted for the degree of Doctor of Philosophy in Oncology

Department of Oncology, University of Oxford

Trinity Term 2014

Supervised by: Prof Leonard W. Seymour and Prof Colin R. Goding

Declaration of Authentication

The work presented in this thesis was performed entirely by me. It does not form part of any other thesis or academic work submitted to this or any other university. Contributions by others have been acknowledged. The work performed was supervised by Professor Leonard W. Seymour, Department of Oncology, Division of Medical Sciences, University of Oxford and Professor Colin R. Goding, Ludwig Institute for Cancer Research, Nuffield Department of Medicine, University of Oxford.

Sarina Agkatsev

Oxford, October 2014

Regulation of MITF and Brn2 in melanoma

Sarina Agkatsev

Brasenose College, University of Oxford

A thesis submitted for the degree of Doctor of Philosophy in Oncology to the Department of Oncology, University of Oxford

Trinity Term 2014

Abstract

Melanoma is the most aggressive skin cancer with high recurrence and low survival rate. In addition to genetic mechanisms, resistance also arises from phenotypic heterogeneity in which a proportion of cells, the so-called melanoma stem or initiating cells, survive therapy. Due to a lack of reliable markers, however, there is still debate about the existence of these cells in melanoma. Consistent with phenotypic heterogeneity, previous observations in our laboratory have demonstrated that cells in melanoma can reversibly segregate *in vivo* into different subpopulations with different properties, such as differentiation or increased invasive capacity (potentially attributed to the existence of de-differentiated stem-like cells). To characterise these cells, a dual reporter lentiviral system was engineered, expressing fluorescent proteins under cell stage/phenotype-specific promoters. The promoters for the transcription factors *POU3F2* (*Brn2*) (to mark de-differentiated cells) and the *microphthalmia*-associated transcription factor (*MITF*) (to mark proliferating and differentiated cells) were chosen. Lentivirally-transduced cells were used to screen a library of kinase inhibitors for their potential to affect promoter activity *in vitro*. The RhoA/ROCK pathway, known to contribute to invasion and metastases, was identified to play a role in *Brn2* promoter activity and exhibited differential effects on both the *MITF* and *Brn2* promoters in 501mel and SKmel28 cell lines. Through investigation of other signalling pathways involved in melanoma metastasis, we also identified the co-activator Mastermind-like 1 (MAML1), previously reported to act in the Notch pathway, as an activator of the *Brn2* promoter via the transcription factor TCF3, and the *MITF* promoter through the lymphoid-enhancer binding factor 1 (LEF1). The effects of MAML1 on *Brn2* and *MITF* promoter activity were potentiated by β-catenin. These findings provide new opportunities for the identification of therapeutic targets to prevent metastases formation in melanoma.

Dedication

Ахуыры фæндагыл мæ размæ бирæ хæстæ сæвæрдтон. Уыдон мæ къухы бафтыдысты мæ ныййарджыты, мæ бинонты руаджы. Уымæн æмæ æз цы къæпхæнмæ схызтæн, уымæ мæ уыдон разæнгард кодтой, уыдон мыл сагътой базыртæ, уыдон мæ ныфсджын кодтой. Мæ сæрæй сын ныллæг кувын. Ме ’нтыстытæ нывонд кæнын мæ мыггагæн, Æгкацатæн, мæ Ирыстонæн. Кæд абон дард дæн мæ райгуырæн бæстæйæ, уæддæр мын зынаргъ у, æмæ мæ фæнды, цæмæй алы ирон хæдзары амонд цæра æгъдау æмæ æфсармимæ. Нæ фыдæлты фарнæй Ирыстоны кæстæртæ рæствæндаг уæнт!

Acknowledgements

I would firstly like to thank my supervisors Professor Len Seymour and Professor Colin Goding for having given me the opportunity to work in their labs. I am very grateful for your constant guidance and support and your encouragements when experiments did not always go according to plan.

I am also very grateful for the help and advice I received from all members of the Seymour lab. In particular, my sadeekati Aliaa, who encouraged me throughout this whole process and helped me through some difficult situations, Clemens, who always found a sympathetic ear and Gray, who has been a great cloning teacher.

Equally, I would like to thank everybody in the Goding lab. Despite not having been an official member, everybody treated me as if I had been, which I really appreciated. In particular, I would like to thank Rasmus, who helped me set up the project, Kao Chin, who helped me with the kinase inhibitor library screen and Paola, who always made time for my questions and shared her expertise with me.

Throughout my time in Oxford I have met extraordinary people who became some of my closest friends. Ruth, Carmen, Anna, Emma, Ruxy and Aliaa – thank you so much for your support. Thanks also to my close friends from home: Leo, Nina and Lena – it has been invaluable knowing you were always there for me.

I would next like to thank my parents, Anjela and Vladimir, and my brother, Achsarbeck, who have helped me immensely through this, at times, incredibly gritty process and kept me grounded throughout. Last but not least, I cannot imagine what this journey would have been like without my husband Dan, who has been my rock and always knew the right words to cheer me up when I felt down.

Finally, I would like to thank the Medical Research Council for awarding me the studentship to undertake my DPhil studies.

Table of Contents

Declaration of Authentication ..... **i**
Abstract ..... **ii**
Dedication ..... **iii**
Acknowledgements ..... **iv**
Table of Contents ..... **v**
List of Abbreviations ..... **ix**
Introduction **1**
1.1 Metastatic melanoma **1**
1.2 Melanocyte development **2**
1.3 MAP kinase pathway **3**
1.4 PI3K/AKT pathway **6**
1.5 Canonical Wnt pathway **7**
1.5.1 Canonical Wnt pathway in development 7
1.5.2 Canonical Wnt pathway in melanoma 9
1.6 Notch pathway **10**
1.6.1 Notch pathway in development 10
1.6.2 Notch pathway in melanoma 12
1.7 Melanoma treatment **14**
1.7.1 Chemotherapy 14
1.7.2 Targeted therapy 15
1.7.3 Immunotherapy 16
1.8 Cancer stem cell theory **17**
1.8.1 CSCs in solid tumours 19
1.8.2 CSCs in melanoma 20
1.8.3 CSC markers in melanoma 20
1.8.4 Phenotype-switching theory 21
1.9 Microphthalmia-associated transcription factor (MITF) **23**
1.9.1 MITF and development 23
1.9.2 MITF in cancer 24
1.10 Brn2 (POU3F2) transcription factor **26**
1.10.1 Brn2 in development 26
1.10.2 Brn2 in melanoma 27
1.11 Aims of the project **28**
2 Materials and Methods **30**
2.1 Cell culturing **30**
2.1.1 Cell lines 30
2.1.2 Cell passaging 31
2.1.3 Freezing cell lines and storage 31
2.1.4 Cell plating 32

2.1.5 Virus generation 33
2.1.6 Puromycin selection 34
2.1.7 Cell line selection and FACS 35
2.2 *In vivo* mouse work 36
2.2.1 Housing conditions 36
2.2.2 Inoculation of CD-1® nude mice with human melanoma cell lines 36
2.2.3 Tumour cell preparation 37
2.2.4 Analysis of tumour cell suspensions using flow cytometry 38
2.3 Immunofluorescence (IF) 40
2.4 DNA transfections 41
2.5 Luciferase expression *in vitro* 43
2.5.1 Protein quantification 44
2.5.2 Data processing and statistical analysis of the luciferase results 45
2.6 Kinase inhibitor library screening 46
2.6.1 Statistical analysis of the screen results 47
2.7 Gel electrophoresis and western blotting 48
2.7.1 Protein preparation 48
2.7.2 SDS-PAGE 49
2.7.3 Protein transfer 51
2.7.4 Western blotting 52
2.8 Molecular Biology Protocols – DNA plasmid preparation 53
2.8.1 Plasmid amplification 53
2.8.2 Picking colonies 53
2.8.3 Plasmid extraction and purification 54
2.9 Molecular Biology Protocols - Cloning 55
2.9.1 Restriction digest 55
2.9.2 Agarose gel electrophoresis 55
2.9.3 Polymerase chain reaction (PCR) 56
2.9.4 Primers 58
2.9.5 Cloning 58
2.9.6 Sequencing of plasmids 59
2.9.7 Construction of primers 59
3 Generation of fluorescent lentiviral reporter constructs 61
3.1 Introduction 61
3.1.1 Rheostat model of MITF 61
3.1.2 Relationship between Brn2 and MITF 62
3.1.3 Lentiviral particles 63
3.1.4 Chapter objectives 67
3.2 Results 68
3.2.1 The MITF and Brn2 promoters are functional and responsive to Sox10 68
3.2.2 pMITF-mCherry: Engineering and testing the reporter plasmid 70
3.2.3 pBrn2-GFP: Engineering and testing the reporter plasmid 81

3.2.4 Dual lentiviral plasmid: engineering and functionality in vitro 90
3.3 Clonal cell lines express mCherry and GFP and potentially exhibiting signs of phenotype-switching *in vitro* 98
3.3.1 501mel cells express mCherry and GFP after viral transduction 98
3.3.2 mCherry$^+$ polyclonal cells express both fluorescent proteins 103
3.3.3 Kinase inhibitor screen 113
3.4 *In vivo* transplantation of the dual reporter cell lines 116
3.4.1 GFP and mCherry expression in dual reporter cell lines after in vivo transplantation 117
3.5 Discussion 121
4 The RhoA/ROCK pathway affect *Brn2* and *MITF* promoter activity in 501mel and SKmel28 cells 127
4.1 Introduction 127
4.1.1 Metastasis and invasion in melanoma 127
4.1.2 The Rho/ROCK pathway 128
4.1.3 Rho/ROCK proteins in tumourigenesis 130
4.1.4 Rho/ROCK proteins and Brn2 131
4.1.5 Chapter objectives 133
4.2 Results 134
4.2.1 RhoA activates the Brn2 promoter 134
4.2.2 RhoA-induced pBrn2 activation is not dependent on TCF/LEF1 binding site 136
4.2.3 Cytoplasmic vs nuclear β-catenin expression in 501mel and SKmel28 cells 140
4.2.4 Ectopic RhoA affects endogenous Brn2 protein expression 142
4.2.5 RhoA decreases pMITF activity in 501mel and increases activity in SKmel28 cells 144
4.2.6 ROCK1 decreases pBrn2 activity in 501mel and increases activity in SKmel28 cells 145
4.2.7 ROCK1 decreases pMITF activity in 501mel and SKmel28 cells 147
4.2.8 ROCK inhibitors increase Brn2 and decrease MITF protein expression 148
4.2.9 ROCK inhibitor treatment leads to a short-term increase in Brn2, β-catenin and MITF protein levels in 501mel cells 150
4.3 Discussion 151
4.3.1 Key findings – Brn2 promoter 151
4.3.2 Key findings – MITF promoter 153
4.3.3 Rho family proteins and cancer 155
4.3.4 Rho family proteins and ROCK in the clinic 156
4.3.5 Future work 158
5 Differential regulation of the *MITF* and *Brn2* promoters by MAML1 and β-catenin 159
5.1 Introduction 159
5.1.1 Notch pathway 159
5.1.2 Interaction of Notch and the Wnt pathway in cancer 159
5.1.3 The Notch pathway, Brn2 and MITF 161
5.1.4 Chapter objectives 162
Results 163
5.1.5 MAML1 activates the WT and Δ268 Brn2 promoter 163

5.1.6 MAML1 does not cooperate with Pax3 to activate the Brn2 promoter 165
5.1.7 Sox10 activates WT pBrn2 without cooperating with MAML1 to induce pBrn2 activation 166
5.1.8 MAML1 and β-catenin show a synergistic activation of the WT pBrn2 168
5.1.9 MAML1- and β-catenin-induced activation of the pBrn2 is dependent on the TCF/LEF1 binding site in SKmel28 cells 169
5.1.10 MAML1 and β-catenin-induced pBrn2 activation is mediated by the TCF/LEF1 site ... 173
5.1.11 MAML1- and β-catenin-induced pBrn2 activation is mediated through TCF3 175
5.1.12 MAML1- and β-catenin-induced pMITF activation is mediated through LEF1 178
5.1.13 MAML1 effects on endogenous MITF protein expression in 501mel and SKmel28 cells 180
5.1.14 MAML1 affects endogenous β-catenin protein expression in 501mel and SKmel28 cells 182
5.1.15 Silencing of MAML1 decreases MITF and β-catenin protein 183
5.1.16 Silencing of β-catenin decreases MAML1 levels in 501mel cells 186
5.2 Discussion 187
5.2.1 Key findings 187
5.2.2 MAML1 and cancer 189
5.2.3 Differential regulation of the Brn2 and MITF promoters 191
5.2.4 Future work 192
6 Discussion 194
6.1 Summary 194
6.2 Key findings 194
6.2.1 Chapter 3: Generation and testing of fluorescent lentiviral reporter constructs 194
6.2.2 Chapter 4: RhoA/ROCK pathway affects pBrn2 and pMITF activities 195
6.2.3 Chapter 5: Differential regulation of pBrn2 and pMITF by MAML1 195
6.3 Implications for melanoma biology 196
6.3.1 Implications of phenotype-switching for treatment of melanoma 196
6.3.2 Implications of the roles of MITF and Brn2 in invasion and metastasis 198
6.4 Limitations of this project 200
6.5 Future work 202
6.6 Conclusion 204
7 References 205
8 Appendix 224
8.1 Funding secured as a result of this thesis 224
8.2 Presentations relating to this thesis 224

List of Abbreviations

3' and 5'	3' and 5' end of RNA and DNA
α-H	Anti-human
α-M	Anti-mouse
µg	Microgram/s
µL	Microlitre/s
µM	Micromolar
AB	Antibody
Acrylamide	Acrylamide/Bis-acrylamide
ALL	Acute myeloid leukaemia
ANOVA	Analysis of variance
APAR	Advanced Protein Assay
APC	Allophycocyanin
APC	Adenomatous polyposis coli
APS	Ammonium persulfate
bp	Basepair
BCA	Bicinchoninic acid
BSA	Bovine serum albumin
C	Cytosine
CA	Constitutively-active
CBP	CREB-binding protein
CD	Cluster of differentiation
CDK	Cyclin-dependent kinase
CDK2	Cyclin-dependent kinase 2
CDK4	Cyclin-dependent kinase 4
CIAP	Calf Intestinal Alkaline Phosphatase
CMV	Cytomegalovirus
CO_2	Carbon dioxide
CRISPRs	Clustered regularly interspaced short palindromic repeats
CSC	Cancer stem cell
CSL	CBF-1, Su (H), Lag-1
CTL	Control
CTLA-4	Cytotoxic T Lymphocyte-associated antigen 4
CXCR4	C-X-C chemokine receptor type 4
d	Days
DAPT	N-S-phenyl-glycine-t-butyl ester
DCT	Dopachrome tautomerase
Dia1	Diaphanous-related formin-1

DLL1	Delta-like 1
DMSO	Dimethyl sulfoxide
DMEM	Dulbecco's Modified Eagle Medium
DNA	Deoxyribonucleic acid
dNTPs	Deoxyribonucelotide triphosphates
DPBS	Dulbecco's Phosphate Buffered Saline
DSH	Dishevelled
E	Embryonic day
ECL	Enhanced Chemiluminescence
E.coli	Escherichia coli
EDTA	Ethylenedinitrilotetraacetic acid
EMT	Epithelial-to-mesenchymal
ERK	Extracellular Signal-regulated Kinase
EtBr	Ethidium bromide
FACS	Fluorescent activated cell sorting
FBS	Foetal bovine serum
FDA	Food and Drug Administration
g	gram/s
G	Guanine
Gag	Group antigens
GDP	Guanosine diphosphate
GFP	Green fluorescent protein
GSI	Gamma-secretase inhibitor
GSK3-β	Glycogen synthase kinase 3-β
GTP	Guanosine triphosphate
h	Hour/s
H_2O	Water
HBSS	Hank's Balanced Salt Solution
HCl	Hydrogen chloride
HEK293-T	Human embryonic kidney
Hes1	Hairy/Enhancer of Split
Hey-1	Hairy/E (spl)-related with YRPW
HIV-1	Human immunodeficiency virus-1
HLA	Human leukocyte antigen
HRP	Horseradish peroxidase
IF	Immunofluorescence
IgG	Immunoglobulin G
iPS cells	Induced pluripotent stem cells

JAG2	Jagged2
L	Litre
LB-agar	Lysogeny broth agar
LB-medium	Lysogeny broth medium
LEF1	Lymphoid-enhancer binding factor 1
LTR	Long Terminal Repeat
kb	Kilobases
kDa	Kilodaltons
M	Molar
mA	Milliampere
mM	Millimolar
MAP	Mitogen-activated protein
MAML1	Mastermind-like 1
Maxiprep kit	QIAGEN Plasmid *Plus* Maxi Kit
MEF2C	Myocyte-specific enhancer factor 2C
MEK	Mitogen-activated protein kinase kinase
mg	Milligram/s
Mg^{2+}	Magnesium ions
MIA	Melanoma inhibitory activity
min	Minute/s
Miniprep kit	QIAprep Spin Miniprep kit
miR	microRNA
MITF	Microphthalmia-associated transcription factor
mL	Millilitre/s
MLC	Myosin regulatory light chain
mRNA	Messenger RNA
mTOR	Mammalian target of rapamycin
NaCl	Sodium chloride
NaOH	Sodium hydroxide
NEB	New England Biolabs
NICD	Notch intracellular domain
nm	Nanometres
NOD/SCID	Non-obese diabetic mice with severe combined immunodeficiency disease
OCT	Optimal cutting temperature
O_2	Oxygen
PAC	Puromycin *N*-acetyl-transferase
Pax3	Paired box 3

p*Brn2*	*Brn2* promoter
p*Brn2*-Luc	p*Brn2*-luciferase
PBS-T	PBS containing 0.1% Tween
PCR	Polymerase chain reaction
PD-1	Programmed cell death-1
PDK1	3-phosphoinositide-dependent protein kinase 1
PE	Phycoerythrin
PI3K	Phosphatidylinositol-4,5-bisphosphate 3-kinase
PIP_2	Phosphatidylinositol-4,5-bisphosphate
PIP_3	Phosphatidylinositol-3 phosphate
p*MITF*	*MITF* promoter
p*MITF*-Luc	p*MITF*-luciferase
pmol	Picomol
Pol	Polymerase
Poly(A)	Polyadenylation and transcription pause sites
Polybrene	Hexadimethrine bromide
POU3F2	POU domain, class 3, factor 2 / Brn2
P/S	Penicillin/Streptomycin
PVDF	Polyvinylidene fluoride
PTEN	Phosphate and tensin homologue
Rb1	Retinoblastoma
RCF	Relative centrifugal force
RCL	Replication competent lentiviruses
RGP	Radial growth phase
Rho-GAP	Rho-GTPase-activating proteins
Rho-GEF	Rho guanine nucleotide exchange factor
RLU	Relative light units
RNA	Ribonucleic acid
ROCK	Rho-associated coiled-coil forming kinase
ROCKi	ROCK inhibitor
RPMI	Roswell Park Memorial Institute 1640
s	Second/s
SDS	Sodium dodecyl sulphate
SDS-PAGE	SDS-polyacrylamide gel electrophoresis
shRNA	Short hairpin RNA
siβ	siRNAs against β-catenin
siRNA	small interfering RNA
Sox10	SRY (sex determining region Y)-box 10
SUMO	Small ubiquitin-like modifiers
TACE	TNF-a-converting enzyme

TAE	Tris-acetate-EDTA
T-ALL	T-cell acute lymphoblastic leukaemia/lymphoma
TB	Transcription blocker
TCF	T-cell factor
T/E	Trypsin
TEMED	N,N,N',N'-Tetramethlethylenediamine
TGF-β	Transforming growth factor-β
T_m	Melting temperature
TREtight	"Tight" promoter
Tyrp1	Tyrosinase-related protein 1
U	Units
UTR	Untranslated region
UV	Ultraviolet
VGP	Vertical growth phase
VSV-G	Vesicular stomatitis virus envelope glycoprotein
WT	Wild-type

1 Introduction

1.1 Metastatic melanoma

Cutaneous metastatic melanoma is one of the most aggressive types of cancer. It arises from melanocytes, which are pigment cells that provide protection from ultraviolet (UV) light-induced damage (Cheli et al., 2010). In 2012 the estimated incidence and mortality of melanoma in Europe was 2.9% and 1.3% per 100,000 people, respectively (World Health Organization - International Agency for Research on Cancer, 2014). The reason for the high mortality in patients diagnosed with melanoma is most likely due to the aggressive nature of the cancer and its progression. Initially, a melanoma lesion typically expands radially by increasing its size on the surface of the skin (Al Dhaybi et al., 2010). If the tumour growth is stopped at this stage, the patient still has good chances for survival as the tumour would have not metastasised yet (Al Dhaybi et al., 2010; Clark, 1991). After the radial growth phase (RGP), however, the tumour enters the second phase, which is referred to as the vertical growth phase (VGP). At this stage it becomes more difficult to intervene medically as the tumour might have formed metastases very quickly (Clark et al., 1989). Unfortunately, not all melanoma lesions follow this model of expansion. Some might have a short and potentially undetectable RGP and enter the VGP quicker and therefore lead to metastasis formation before it is even possible to intervene in the RGP and minimise spread to other organs. However, when the tumour is treated while it is still in the RGP, the five-year survival rate is over 95% (Balch et al., 2009) while by the time the tumour has started metastasising the prognosis for patients is poor with a median survival of 8-18 months (Balch et al., 2009). One of the reasons for this drastic drop in survival with cancer progression is associated with melanoma's high potential to invade other organs and generate metastases (Clark, 1991).

The progression of the cancer is measured by different methods, one of them being the Clark scale, which assesses the size and the thickness of the primary tumour (Clark et al., 1984). Generally, the lower the scale the less progressed the tumour and the better the survival chances for the patient. Patients in stage I have a survival rate of 90%, while in stage II it is 70% (Francken et al., 2008; Liew et al., 2011). However, there is a striking drop in survival rates as soon as the tumour reaches stages III and IV. In stage III the five year survival rate is 25-50%, while in stage IV it is 10% (Francken et al., 2008; Liew et al., 2011).

1.2 Melanocyte development

Melanocytes are specialised pigmented cells that originate from progenitor cells in the neural crest (Thomas and Erickson, 2008). From the neural crest, the cells migrate to the basal layer of the epidermis or the hair follicle and develop into melanin-secreting cells (Thomas and Erickson, 2008). One of the main functions of melanocytes is to protect cells from DNA damage induced by UV radiation (Slominski et al., 2004). This process is mainly controlled by keratinocytes, residing in the epidermis, that tightly regulate the function of melanocytes (Haass et al., 2004; Miller and Mihm, 2006; Valyi-Nagy et al., 1993). In response to UV light exposure, keratinocytes stimulate melanin production in melanocytes in organelles called melanosomes (Raposo and Marks, 2007). These then travel through dendrites to neighbouring keratinocytes and protect their nucleus from UV light-induced DNA damage (Scott et al., 2002). The deregulation of the proliferation of melanocytes can lead to the generation of moles or naevi (Clark, 1991; Clark et al., 1989; Clark et al., 1984), which can subsequently lead to melanoma formation.

There are some genetic risk factors for melanoma, such as mutations in the cell cycle regulator genes cyclin dependent kinase (CDK) Inhibitor 2A (*CDKN2A*) (Nelson and Tsao, 2009), cyclin dependent kinase 4 (*CDK4*) (Zuo et al., 1996) and mutations in the gene for *microphthalmia-associated transcription factor* (*MITF)* at position 318 which leads to a substitution of the amino acid glutamic acid to lysine (Bertolotto, 2013). However, the main risk factor is UV light, especially associated with intermittent UV light exposure and a history of childhood burns (Bennett, 2008). Exposure to UV light might lead to the generation of mutations in different genes which will lead to melanomagenesis. In melanoma the most common mutations are found in the oncogenes *BRAF* (Davies et al., 2002) and *NRAS* (Omholt et al., 2002; Tsao et al., 2004), and in the tumour suppressor gene phosphate and tensin homologue (*PTEN*) (Guldberg et al., 1997; Tsao et al., 1998), as well as in the cell cycle control gene *CDKN2A* (Hussussian et al., 1994).

1.3 MAP kinase pathway

To gain a better understanding about melanomagenesis it is important to study some of the main signalling pathways implicated in melanocyte development since mutations in these may ultimately lead to melanomagenesis.

Under physiological circumstances the mitogen-activated protein (MAP) kinase pathway is activated by growth factors, such as stem-cell factor, fibroblast growth factor or hepatocyte growth factor (Bohm et al., 1995) and leads to the proliferation of melanocytes (Figure 1.1) (Wellbrock et al., 2004). Upon binding of the ligands to receptor tyrosine kinases at the cell membrane, a GTP-ase from the Ras family, such as KRAS, NRAS or HRAS, becomes activated and in turn activates a kinase from the Raf family (ARAF, BRAF or CRAF). The latter will subsequently phosphorylate the

mitogen-activated protein kinase kinase (MEK), upon which the MAP kinase (also referred to as Extracellular Signal-regulated Kinase (ERK)) is phosphorylated and activated, leading to the transcription of genes involved in cell cycle progression, cell migration, invasion or senescence (Yoon and Seger, 2006).

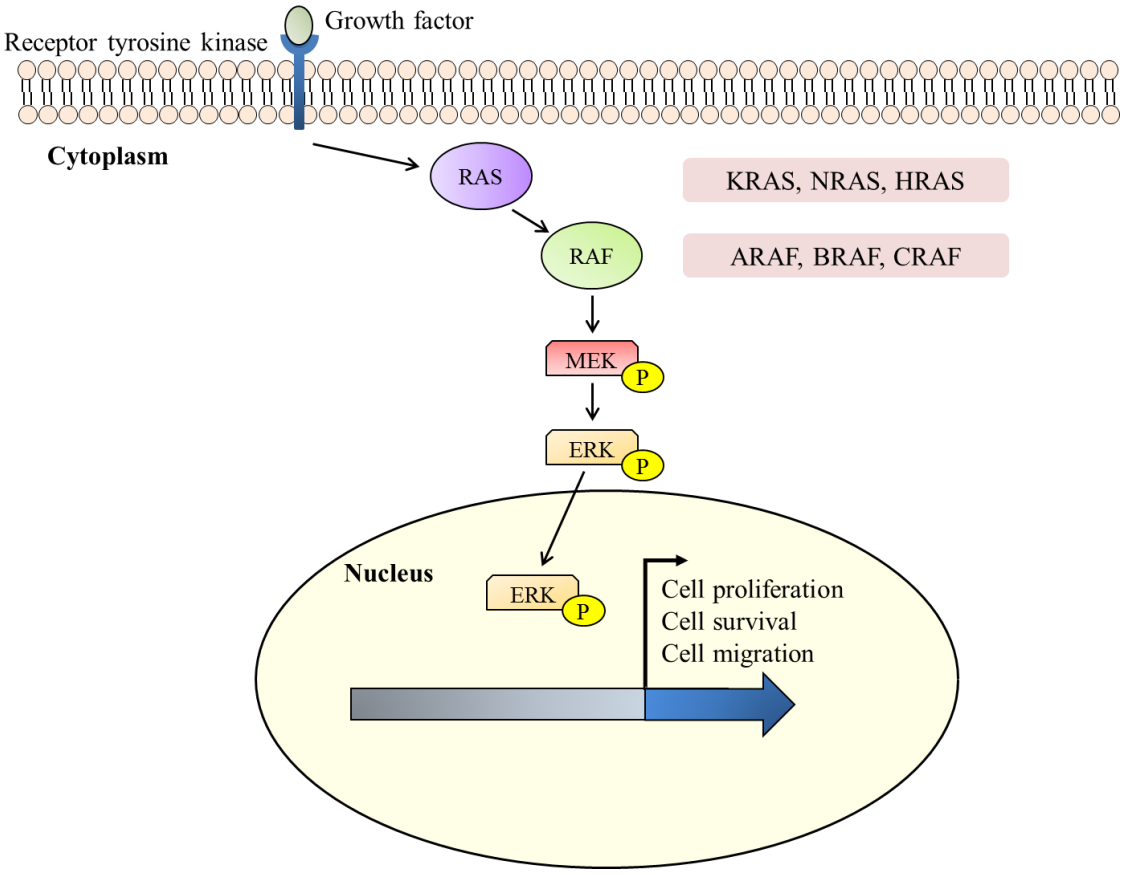


Figure 1.1: MAP kinase/ERK signalling in cancer. Upon binding of growth factors to receptor tyrosine kinases, the RAS family GTP-ases become active and induce kinase activity of the RAF family kinases. These in turn phosphorylate and activate mitogen activated protein kinase kinase (MEK), which then phosphorylates and activates ERK (also referred to as MAP kinase). This protein kinase translocates into the nucleus and induces transcription of genes implicated in cell proliferation, survival and migration. Adapted from (Wellbrock et al., 2004) and (Downward, 2008).

In 15-30% of melanomas, the *NRAS* gene is mutated, whereby the amino acid leucine is substituted for glutamine at position 61 (Q61L) (Ellerhorst et al., 2011; Omholt et al., 2002; Thomas and Erickson, 2008), leading to constitutive activation of the MAP kinase pathway (Davies et al., 2002). However, the most common mutation in melanoma is found in the *BRAF* gene ($BRAF^{V600E}$), in approximately 66% of the cases (Davies et al., 2002), suggesting that this might be an early event in melanomagenesis

(Yeh et al., 2013). Interestingly, mutations in *BRAF* and *NRAS* are mutually exclusive, as the transcription of both genes would lead to the activation of the same pathway (Gorden et al., 2003; Omholt et al., 2003). The $BRAF^{V600E}$ mutation is generated by the substitution of the amino acid glutamic acid (E) for valine (V) at the position 600, rendering the gene constitutively active (Davies et al., 2002). The effect of this mutation leads to a similar outcome as the *NRAS* mutation – the MAP kinase signalling pathway is constitutively active, resulting in cell proliferation and subsequently senescence (Michaloglou et al., 2005). The latter is mediated by the tumour suppressor protein $p16^{INK4a}$ which stops cell cycle progression from G1 phase to S phase by blocking the complex formation of CDK4 and cyclin D1. This explains how senescent melanocytic naevi often harbour $BRAF^{V600E}$ mutations. Additionally, BRAF can also activate the genes encoding MITF (Wellbrock et al., 2008) and POU domain, class 3, transcription factor 2 (POU3F2, here referred to as Brn2) (Goodall et al., 2004b), that play key roles in melanoma biology.

It is also important to note that most melanomas arise de-novo, as only 25% of melanomas arise from pre-existing naevi (Bertolotto, 2013). This also implies that mutations of the *BRAF* gene might not always arise first. In fact, sporadic melanomas might arise from cells that have homozygous deletions or mutations in the *CDKN2A* gene encoding the tumour suppressor $p16^{INK4a}$. These cells would not show a change in phenotype, but they would have lost their ability to become senescent. Subsequently all that is needed for melanoma initiation is a second mutation, such as in the *BRAF* gene, leading to unimpeded cell proliferation.

1.4 PI3K/AKT pathway

The phosphatidylinositol-4,5-bisphosphate 3-kinase (PI3K) pathway is often found to be dysregulated in melanoma, which leads to activation of the oncogene AKT (also known as protein kinase B) and promotes cell survival and growth (Gray-Schopfer et al., 2007). The pathway is activated upon binding of growth factors to cell membrane receptors, which leads to the generation of the second messenger phosphatidylinositol-3, 4, 5-phosphate (PIP_3) through conversion of the cell membrane-bound phosphatidylinositol-4,5-bisphosphate (PIP_2) (Figure 1.2) (Bertolotto, 2013).

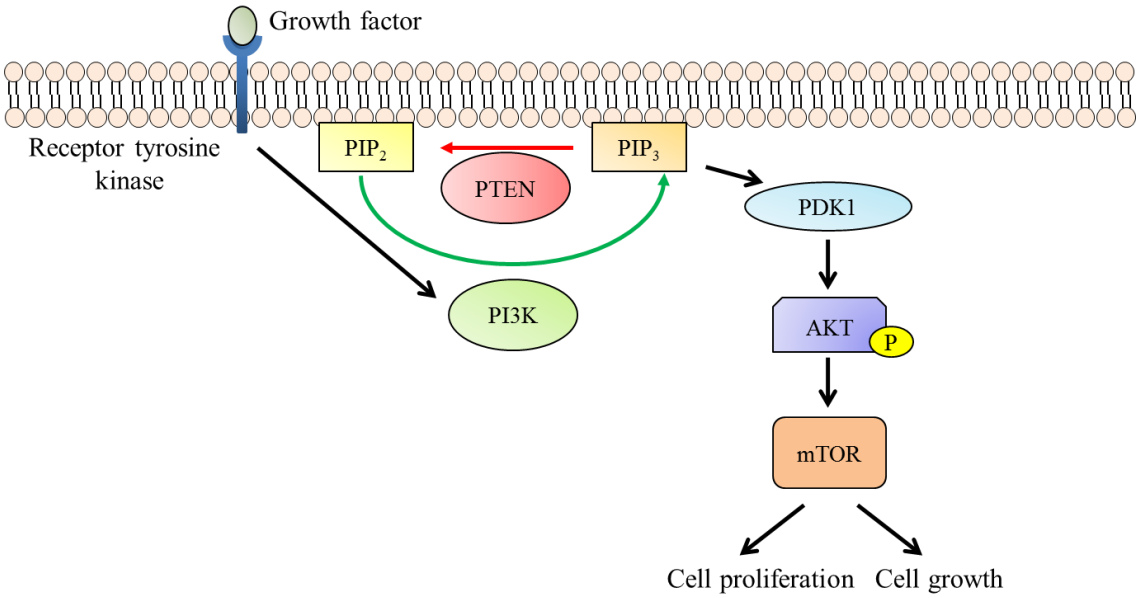


Figure 1.2: PI3K signalling cascade. Upon binding of growth factors to receptor tyrosine kinases, PI3K is activated and converts phosphatidylinositol-4, 5-bisphosphate (PIP_2) to phosphatidylinositol-3, 4, 5-triphosphate (PIP_3). The reverse process is mediated by the tumour-suppressor PTEN. PIP_3 activates phosphatidylinositol-dependent kinase 1 (PDK1), which in turn phosphorylates and activates AKT, also known as protein kinase B. AKT then activates the mammalian target of rapamycin (mTOR) which induces cell proliferation and growth. Adapted from (Cully et al., 2006).

The second messenger PIP_3 can then activate 3-phosphoinositide-dependent protein kinase 1 (PDK1), which in turn phosphorylates and activates the serine/threonine kinase AKT (Bertolotto, 2013). Subsequently, AKT will activate the mammalian target of rapamycin (mTOR), which will induce transcription of target genes implicated in cell growth (Wullschleger et al., 2006) and cell proliferation (Skeen et al., 2006). AKT is activated by mutation in approximately 60% of melanomas (Stahl et al., 2004). In these

cases, AKT will act as an oncogene, leading to unrestricted cell growth and proliferation (Stahl et al., 2004). To terminate the PI3K-induced signalling, the tumour suppressor PTEN converts the second messenger PIP_3 back to PIP_2 (Bertolotto, 2013) (Figure 1.2). While mutations in PI3K are rare in melanoma (Omholt et al., 2006), mutations in the gene encoding *PTEN* are present in 5% to 20% of late-stage melanomas (Wu et al., 2003). Mutations in PTEN allow cells to overcome $BRAF^{V600E}$- or NRAS-induced cell senescence and thereby continue to proliferate and promote melanomagenesis (Bertolotto, 2013). While the mutation in BRAF producing the constitutively active form $BRAF^{V600E}$ is an early event in melanomagenesis, mutations in the PI3K/AKT pathway generally take place later during disease progression (Bertolotto, 2013).

1.5 Canonical Wnt pathway

1.5.1 Canonical Wnt pathway in development

The Wnt pathway is crucial for melanocyte development and plays an important role in neural crest cell differentiation into melanoblasts (Dunn et al., 2000). The main effector of this pathway is β-catenin. Under physiological conditions when the Wnt pathway is not engaged, β-catenin is bound to the multiprotein 'destruction' complex consisting of the scaffold protein Axin, the tumour suppressor adenomatous polyposis coli (APC) protein, glycogen synthase kinase 3-β (GSK3-β) and the casein kinase 1 complex (Bertolotto, 2013). Within this complex β-catenin is phosphorylated, which triggers its ubiquitylation and subsequent proteasomal degradation (Bertolotto, 2013) (Figure 1.3). However, upon activation of the Wnt pathway, by the binding of Wnt proteins to their receptor Frizzled, the phosphoprotein Dishevelled (DSH) is activated and recruits Axin to the membrane, which leads to its degradation and the disruption of the 'destruction

complex'. Subsequently, β-catenin levels rise in the cytoplasm, leading to the translocation of β-catenin to the nucleus (Bertolotto, 2013). Once in the nucleus, β-catenin interacts with the transcription factor family T-cell factor (TCF) and the lymphoid-enhancer binding factor 1 (LEF1) to induce transcription of target genes (Bertolotto, 2013)

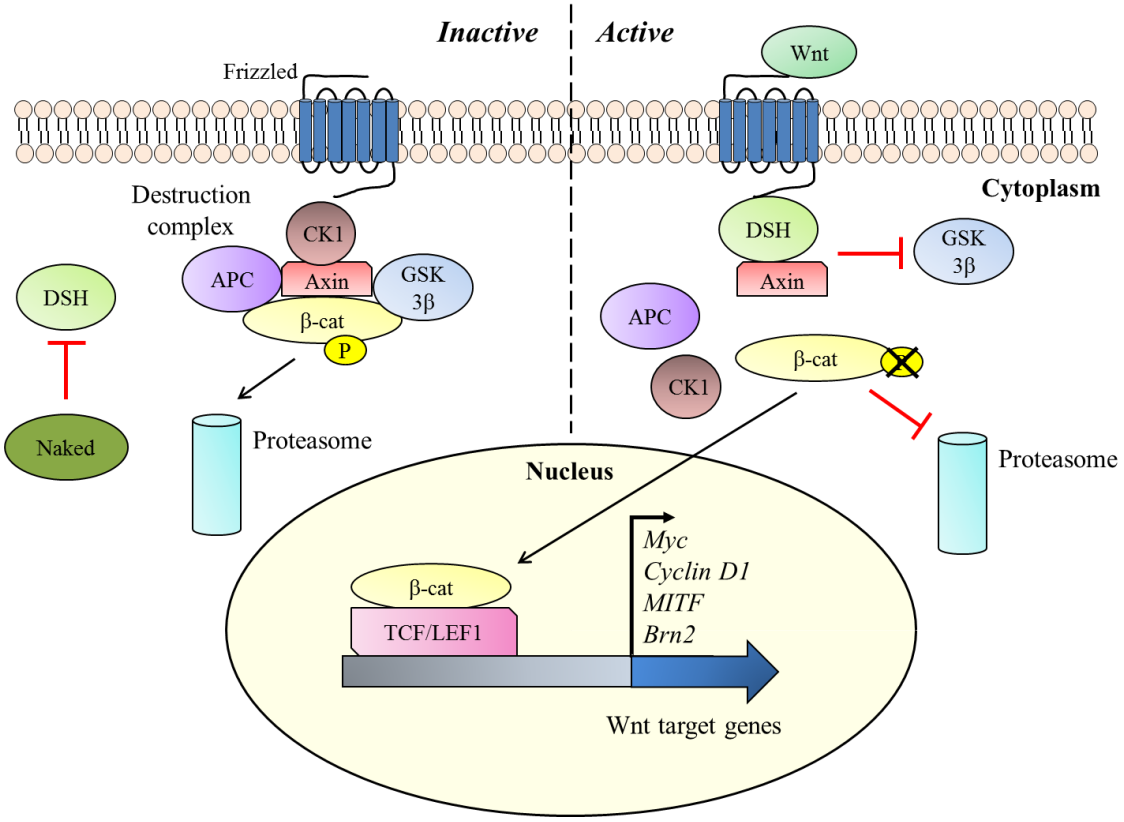


Figure 1.3: Wnt signalling pathway. In cells where the Wnt pathway is not activated, β-catenin is sequestered in the destruction complex consisting of the adenomatous polyposis coli protein (APC), the scaffold protein Axin, casein kinase 1 (CK1) and glycogen synthase kinase 3-β (GSK3-β). While in this complex, β-catenin is phosphorylated, which induces its ubiquitylation followed by its proteasomal degradation. Upon binding of the Wnt ligand to its receptor Frizzled, the phosphoprotein Dishevelled (DSH) is recruited to the activated receptor. DSH in turn recruits Axin and inhibits the function of GSK3-β, allowing β-catenin to translocate to the nucleus and bind to the transcription factors TCF and LEF1 (transcription factor family T-cell factor and lymphoid-enhancer binding protein 1). This induces transcription of genes such as *myc*, *cyclin D1*, *MITF* and *Brn2*. Adapted from (Takebe et al., 2011).

Because of the diverse effects of this pathway, Wnt signalling has been studied extensively in the context of melanocyte development and melanoma. In zebrafish, overexpression of β-catenin messenger ribonucleic acid (mRNA) promoted pigment-cell formation rather than neuronal and glial cell development (Dorsky et al., 1998). Equally, in transgenic mice, overexpression of Wnt1 in neural-crest derived

melanocytes led to their proliferation and differentiation (Dunn et al., 2000). The role of Wnt signalling in melanocyte differentiation was demonstrated when overexpression of Wnt-3a induced the expression of the lineage-determination factor MITF (Takeda et al., 2000) (see below). Additionally, when the activity of the Wnt pathway was disrupted, clonogenic cell growth was halted and cells were only rescued after constitutive expression of MITF (Widlund et al., 2002).

1.5.2 Canonical Wnt pathway in melanoma

The involvement of β-catenin in melanomagenesis was implicated when β-catenin was found to be expressed in the nucleus of primary melanomas in approximately a third of the cases (Rimm et al., 1999) rather than on the cell membrane (Sanders et al., 1999). Additionally, mutations preventing β-catenin from being degraded also exist in many melanoma cell lines (Rubinfeld et al., 1997). However, it is not yet known whether this is due to a mutation in the β-catenin gene *CTNNB1*, protecting it from degradation (Omholt et al., 2001), or whether there are other mutations in the Wnt pathway, such as in the *APC* gene in colorectal cancer (Morin et al., 1997) that might lead to the accumulation of β-catenin.

Whilst the studies above have demonstrated a role for β-catenin in differentiation and proliferation of melanoma cells, there are other studies that show how stabilised β-catenin reduces the number of melanoblasts *in vivo* and induces immortalization of primary skin melanocytes in culture through repressing $p16^{INK4a}$ transcription and expression (Delmas et al., 2007). Using a mouse model, it was also shown that β-catenin can induce proliferation together with activated NRAS, demonstrating the interplay between the Wnt and the MAP kinase pathway (Delmas et al., 2007). Therefore, whether the role of β-catenin is pro- or anti-proliferative might depend on

the cell stage and the cell context (Delmas et al., 2007), such as in the case of β-catenin-induced MITF activation (Takeda et al., 2000), the outcome of which would depend on the amount of MITF present in the cell (Delmas et al., 2007).

Additionally, the role of β-catenin in metastasis formation is not well understood. Some studies demonstrate that β-catenin might suppress invasion (Arozarena et al., 2011; Chien et al., 2009; Kageshita et al., 2001; Maelandsmo et al., 2003), while others show how an increase in β-catenin might induce more melanoma metastases *in vitro* and *in vivo* (Damsky et al., 2011; Murakami et al., 2001; Zuidervaart et al., 2007). Again, this could be explained by the effect of different cell contexts on β-catenin function (Delmas et al., 2007).

1.6 Notch pathway

1.6.1 Notch pathway in development

Notch signalling was originally investigated in drosophila where a mutation in the *Notch* gene led to an irregular shape of the drosophila wings (termed 'notched') (Morgan, 1917). Notch is a transmembrane receptor of which there are four types (Notch 1 to Notch 4) (Takebe et al., 2011). Upon binding of its ligand (Delta 1, 3 or 4 or Jagged 1 or 2), the Notch receptor undergoes two proteolytic cleavages. The first is mediated by the metalloprotease TNF-α-converting enzyme (TACE) (Brou et al., 2000), while the second cleavage is performed by a γ-secretase complex (De Strooper et al., 1999). This cleavage releases the Notch intracellular domain (NICD) of the receptor into the cytoplasm where it translocates to the nucleus (Schroeter et al., 1998). Here it binds to the transcription factor CSL (CBF-1, Su (H), Lag-1), also known as RBP-Jκ, and the co-factor mastermind-like 1 (MAML1) (Wu et al., 2000) (Figure 1.4).

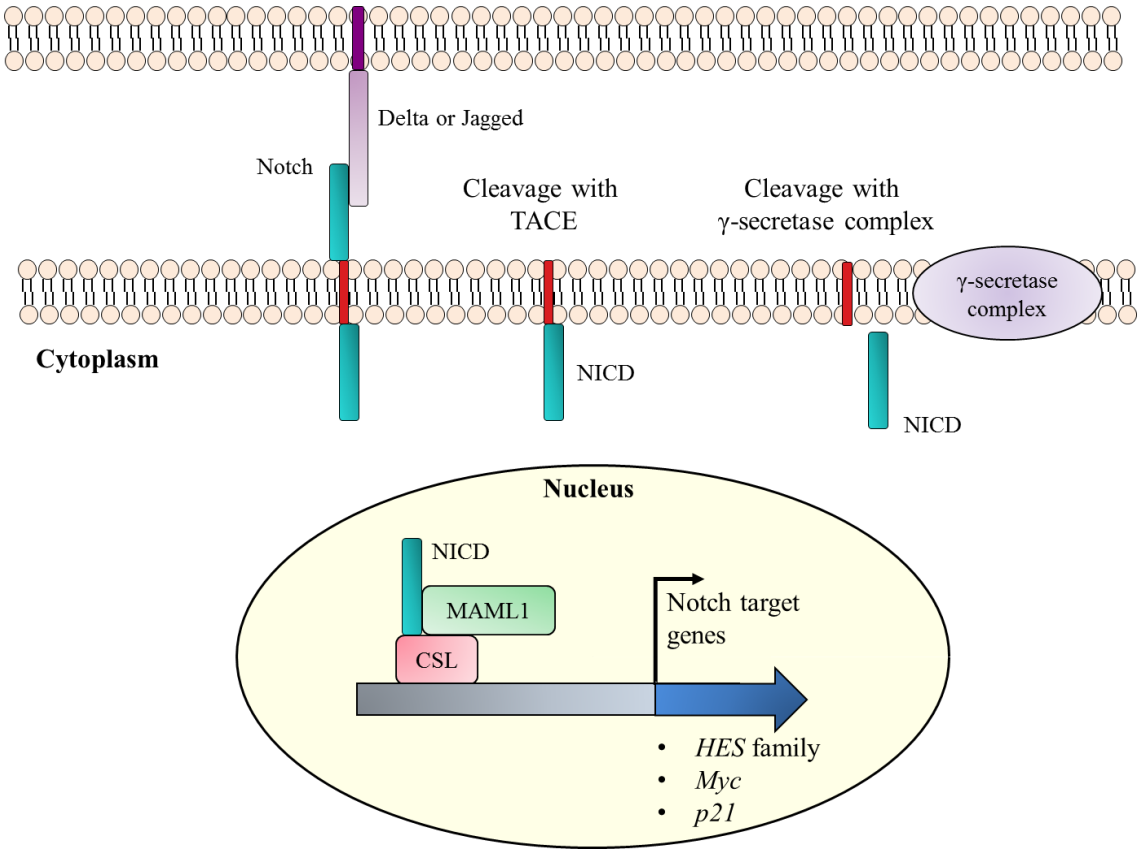


Figure 1.4: Notch signalling pathway. Upon binding of the ligand Delta or Jagged to its Notch receptor, located on the cell membrane, the latter undergoes two proteolytic cleavages. The first one is mediated by the TNF-α-converting enzyme (TACE) and the second by γ-secretase complex. This releases the Notch intracellular domain (NICD) into the cytoplasm from where it translocates to the nucleus and binds to the transcriptional co-activator mastermind-like 1 (MAML1) and the transcription factor CSL (CBF-1, Su (H), Lag-1). This complex initiates transcription of Notch target genes such as *Hes-1* and *Hey-1*, belonging to the *HES* family, *myc* and *p21*. Adapted from (Takebe et al., 2011).

This induces the transcription of target genes such as Hairy/Enhancer of Split (Hes-1) and Hairy/E (spl)-related with YRPW (Hey-1) (Iso et al., 2003; Maier and Gessler, 2000). In the absence of Notch signalling, CSL is bound to deoxyribonucleic acid (DNA) and recruits histone deacetylases and other repressors to inhibit gene transcription (Kao et al., 1998).

The role of Notch signalling has been studied in the context of melanocyte stem cell and melanoblast survival and maintenance in murine models (Moriyama et al., 2006), by demonstrating that ablation of RBP-Jκ in the melanocyte lineage leads to unpigmented hair and absence of melanocyte-derived cells in the lower permanent portion of the hair follicle (Moriyama et al., 2006). These findings are supported by

experiments performed in skin from embryonic day 13.5 (E13.5) mouse embryos (Moriyama et al., 2006). Treating the skin with a pharmacological inhibitor of the Notch pathway, the γ-secretase inhibitor N-S-phenyl-glycine-t-butyl ester (DAPT), followed by transplantation into immunodeficient mice, apoptosis of melanoblasts as well as unpigmented hair was observed (Moriyama et al., 2006). Similarly, treatment of melanocytic lineage cells expressing Hes-1 in transgenic mice with DAPT, the hair was still pigmented and the melanoblast population was present (Moriyama et al., 2006).

Despite advances of our understanding of the Notch pathway and its involvement in murine melanocyte development, less is known about the Notch pathway in human melanocytes. Nonetheless, in processes such as myogenesis, neurogenesis and B-cell lymphogenesis Notch signalling inhibits differentiation (Iso et al., 2003).

1.6.2 Notch pathway in melanoma

The Notch pathway has long been known to have a role in development (see above) but in 1987 Reynolds and colleagues demonstrated the involvement of this pathway in the generation of T-cell acute lymphoblastic leukaemia/lymphoma (T-ALL) (Reynolds et al., 1987). A chromosomal translocation was demonstrated to drive the constitutive expression of an active Notch1 protein, later defined as NICD, by the T-cell receptor β (Ellisen et al., 1991). As this receptor was expressed in T-cells, the truncated Notch1 protein was constitutively expressed in these cells and led to the development of T-ALL (Ellisen et al., 1991). After demonstrating the involvement of Notch signalling in the generation of haematological cancers, solid tumours (including melanoma), were subsequently investigated for increased Notch signalling. However, the role of Notch in melanoma is not well defined. While some studies advocate a tumour suppressor role of Notch1 (Nicolas et al., 2003), others demonstrated Notch1 to behave like an oncogene

(Balint et al., 2005). The former was supported by Nicolas and colleagues (Nicolas et al., 2003) who used a cre-loxP technology to generate a knockout mouse model, lacking Notch1, and suggested that the loss of this protein led to hyperplasia of the epithelium and the cornea. Additionally, knockdown of Notch1 led to the expression of Gli2, a transcription factor involved in the Hedgehog signalling pathway (Matise and Joyner, 1999), as well as an increase in β-catenin signalling, which could be reversed by adding a dominant-active form of the Notch1 receptor (Nicolas et al., 2003). These results indicated that under normal circumstances Notch1 inhibits β-catenin signalling and assumes a tumour suppressive function (Nicolas et al., 2003).

On the other hand, Balint and colleagues firstly blocked, then constitutively activated the Notch1 pathway which led to increased cell proliferation and more metastatic primary melanoma cells *in vitro* and *in vivo* (Balint et al., 2005). Additionally, Notch1 activation induced β-catenin expression and inhibition of β-catenin reversed the tumour growth and metastases induced by Notch1 (Balint et al., 2005). This notion was further supported by Bedogni and colleagues who demonstrated that mRNA levels of the Notch target gene *HEY1* were elevated in human melanoma samples compared to normal skin or benign naevi (Bedogni et al., 2008). Also, in 53% of the human melanoma samples Notch1 protein levels were substantially elevated, again suggesting that Notch signalling might play a role in melanomagenesis (Bedogni et al., 2008). These results were supported by *in vivo* studies, whereby cells previously treated with a γ-secretase inhibitor (GSI) or short hairpin RNAs (shRNAs) against Notch1, showed delayed tumour formation when transplanted into mice (Bedogni et al., 2008).

As the use of GSIs seemed to affect tumour formation *in vivo* (Bedogni et al., 2008; Qin et al., 2004), new pharmacological GSIs, such as RO4929097 and MK-0752, have been developed and tested in Phase I trials (Krop et al., 2012; Tolcher et al., 2012). Despite

great advances in this field, there is still more to learn about the mechanism of action of the Notch pathway and its precise contribution to melanomagenesis.

1.7 Melanoma treatment

1.7.1 Chemotherapy

Currently the treatment options for melanoma are very limited. When the tumour is still local and has not metastasised (stage 1) the first line of treatment is surgical excision (Bertolotto, 2013). However, once metastases in other parts of the body have developed (stage 4), surgical excision of the primary tumour is followed by chemotherapy (Bertolotto, 2013). Traditional chemotherapy consists of dacarbazine and temozolomide, which mainly targets fast dividing cells by inducing apoptosis (Bertolotto, 2013). The problem with chemotherapy in general is that chemotherapeutic drugs target proliferating cells, leading to significant side effects. In melanoma in particular, cells that are quiescent or dormant might be resistant against these drugs (phenotypic resistance) (Hoek and Goding, 2010; Roesch et al., 2013) and after a seemingly successful therapy, previously dormant or quiescent cells might be able to re-grow the whole tumour (Ossowski and Aguirre-Ghiso, 2010). Depending on the underlying reason for the resistance (phenotypic (Roesch et al., 2013) vs genetic (Nazarian et al., 2010)), it is conceivable that these secondary tumours might be more resistant to the initial treatment. While phenotypic resistance is mediated by the developmental cell stage, such as quiescent vs proliferating cells, genetic resistance can manifest itself through the activation of pathways bypassing the effects of targeted inhibitors, such as BRAF inhibition (see below) or evasion of apoptosis.

1.7.2 Targeted therapy

1.7.2.1 BRAF^{V600E} inhibitor

To overcome the problem of the significant side effects induced by traditional chemotherapy, vemurafenib has a more specific mechanism of action and was approved by the U.S. Food and Drug Administration (FDA) in 2011 (Kim et al., 2014). Vemurafenib, is a kinase inhibitor that targets the V600E mutated form of BRAF (**V**600**E** **mu**tated B**RAF** inhibition), which is present in approximately 60% of melanoma cases (Davies et al., 2002). While this drug works well in the initial stages of cancer treatment (Sosman et al., 2012), patients often develop resistance and relapse. Different types of drugs that also target the MAPK pathway are MEK inhibitors, such as PD184352 (Collisson et al., 2003). These have been shown to inhibit BRAF^{V600E}-induced proliferation and invasion *in vitro* and decrease metastases formation as well as promote regression of already existing metastases (Collisson et al., 2003).

1.7.2.2 Resistance to treatment

It is widely known that melanoma patients undergoing treatment with vemurafenib can develop resistance against the drug (Montagut et al., 2008; Nazarian et al., 2010). There are multiple mechanisms underlying the development of resistance. Inhibition of BRAF^{V600E} can enable resistant cells that already contain a mutation in the genes for *NRAS* (Nazarian et al., 2010) or *CRAF* (Montagut et al., 2008; Villanueva et al., 2010) to proliferate, leading again to stimulation of the MEK/Erk pathway. Other mechanisms of resistance include activating mutations in MEK itself (Wagle et al., 2011) or BRAF amplifications (Shi et al., 2012). Another well-studied mechanism is the upregulation of receptor tyrosine kinases, such as platelet derived growth factor receptor-β (Nazarian et al., 2010) or insulin growth factor receptor, followed by the activation of PI3K

signalling (Villanueva et al., 2010), which would allow cells to bypass the MAPK pathway and therefore induce resistance to vemurafenib. Furthermore, loss of *PTEN* has also been demonstrated to contribute to vemurafenib-induced resistance (Paraiso et al., 2011).

1.7.3 Immunotherapy

In order to address the problem faced with chemotherapy (drug specificity) and targeted therapy, such as with vemurafenib (development of resistance), additional therapeutic options have been investigated. A new way of treating melanoma is by activating the immune system using immunotherapeutic drugs such as interleukin-2 (Schatton et al., 2010) or ipilimumab (Lacy et al., 2012). Both drugs activate T-cells and induce their proliferation, but while interleukin-2 acts on T-cells directly (Lacy et al., 2012), ipilimumab stops inhibitory signals acting through the T-cell receptor and thereby enhances their activity (Lacy et al., 2012). Ipilimumab was approved by the U.S. FDA in 2010 (Yervoy™, Bristol-Myers Squibb). It is a monoclonal antibody against the inhibitory immune-checkpoint receptor Cytotoxic T Lymphocyte-associated antigen 4 (CTLA-4) found on T-cells (Korman and Fisher, 2013). Upon activation of a T-cell through the binding of an antigen to the T-cell receptor, multiple inhibitory receptors are expressed subsequently on the cell surface (Murphy et al., 2014), such as CTLA-4. Activation of this receptor leads to down-modulation of T-cell activity.

Interestingly, as melanoma is considered to be an immunogenic tumour, an immune response is mounted but suppressed. Possible explanations for this are that the cells can evade the immune system or that the immune cell activity is decreased (Schatton et al., 2010). One mechanism is the activation of the CTLA-4 receptor, which leads to the inhibition of the immune system and prevents it from becoming active (Walunas et al.,

1994). To overcome this negative regulation, ipilimumab can bind to the receptor and block the inhibitory signal produced by CTLA-4 activation and thereby allow T-cells expressing cluster of differentiation 4 ($CD4^+$) to become activated and target the melanoma cells (Kitano et al., 2013).

Another immunotherapeutic drug, which has gone through Phase I trials (Weber et al., 2013) and is currently going through Phase III trials in the US is nivolumab. The mechanism of action of this drug is similar to ipilimumab but instead of targeting CTLA-4, this monoclonal antibody blocks the activation of the inhibitory programmed cell death-1 (PD-1) receptor, allowing T-cells to become fully activated and target cancer cells (Mamalis et al., 2014).

1.8 Cancer stem cell theory

Despite the major advances in our understanding of the nature and causes of melanoma, a high percentage of patients who have undergone seemingly successful treatment still experience relapse.

As traditional drugs and treatments mainly target proliferating cells, they leave behind a potentially small population of quiescent, non-motile cells. These cells might be more adapted to survive drug treatment through alternative pathways of resistance (such as increased expression of drug efflux transporters (Frank et al., 2005)) and potentially become even more aggressive and metastasise upon leaving their quiescent state to generate new tumours at different sites in the body. Therefore, these cells exhibit properties of self-renewal and give rise to more differentiated progeny which is in physiological settings reserved for tissue stem cells. However, the cell population that survives treatment with chemotherapeutic or other drugs seems to behave similarly to

stem cells, which is why these cells are often referred to as cancer stem cells (CSCs) (Sharma et al., 2010).

The first time the existence of such cells was demonstrated was in acute myeloid leukaemia (AML) (Lapidot et al., 1994). This discovery was soon followed by another report by Bonnet and Dick in 1997 (Bonnet and Dick, 1997). The group showed that only the $CD34^{+}/CD38^{-}$ cells in AML were able to produce tumours in limiting dilution assays in non-obese diabetic mice with severe combined immunodeficiency disease (NOD/SCID mice). They also concluded that due to the similarity of CSCs and physiological stem cells, which were able to repopulate within the mouse model, the CSCs might have originated through a transformation of primitive cells rather than committed progenitor cells.

Based on these observations, the CSC theory was formulated, postulating that a tumour might contain a small population of cells that have the ability to a) self-renew through symmetric or asymmetric division and b) give rise to differentiated progeny (Murphy et al., 2014), and therefore contain the ability to regrow a whole tumour comprising phenotypically heterogeneous subpopulations of cells. Additional characteristics of the CSCs might be drug-resistance (Elliott and Al-Hajj, 2009; Frank et al., 2005). This finding can explain why patients experience relapse: once the bulk of the tumour, made up of proliferating cells, is eradicated it might seem that the treatment was successful. But in fact, a small population of CSCs, not detectable at the stage of primary treatment, might have remained viable and are now able to re-grow the tumour. Thus a small drug-resistant CSC population left behind after drug treatment, would not only be able survive and proliferate in response to a changing microenvironment, but it could also migrate to other parts of the body and establish new tumours. One resulting

problem is that the new tumour might contain a higher percentage of CSCs compared to the parental tumour, which in turn, might make it more difficult to treat.

1.8.1 CSCs in solid tumours

After the first discovery of CSCs in AML (Bonnet and Dick, 1997), many researchers have attempted to prove the existence of CSCs in other tumour types and therefore reconcile the observations of drug-resistance in tumours, relapse and metastases.

The "gold-standard" method to identify CSCs is to isolate them using a (surface) marker and perform serial xenograft transplantations and *in vivo* limiting dilution assays in xenograft models (Murphy et al., 2014; Quintana et al., 2010; Quintana et al., 2008). Serial xenograft transplantations are performed by implanting cells into mice, followed by the excision of the established tumour and dissociation of the tumour cells (Murphy et al., 2014). These differ from limiting dilution assays as instead of using the same number of cells in each round of re-transplantation, increasing dilutions of cells are injected back into the xenografts. If the cell suspension contains CSCs, it will generate tumours in the new animal after having gone through a round of dissociation and re-transplantation. Additionally, limiting dilution assays will allow an estimation of the cell number required to establish a tumour and therefore indicate the percentage of CSCs present in the tumour.

Using this method, CSCs have been demonstrated to exist in glioblastoma (Singh et al., 2004), breast carcinoma (Al-Hajj et al., 2003) and colon carcinoma (Ricci-Vitiani et al., 2007). The markers, however, used to isolate these cells differ from one cancer to another. In glioblastoma and colon cancer, $CD133^{+}$ cells were demonstrated to enrich for cells with stem-like properties (Singh et al., 2004), while in breast carcinoma $CD44^{+}/CD24^{-}$ cells showed CSC characteristics (Al-Hajj et al., 2003).

Despite the fact that CSCs have been accepted to exist in many haematological and solid tumours, it is still a matter of dispute if CSCs are also present in melanoma (Fang et al., 2005; Quintana et al., 2010). In addition, there is no consensus concerning markers used to isolate and identify potential melanoma CSCs.

1.8.2 CSCs in melanoma

Despite evidence supporting the existence of CSCs in the cancers mentioned above, opinions are still divided over the existence of CSCs in melanoma (Boiko et al., 2010; Fang et al., 2005; Quintana et al., 2010; Quintana et al., 2008; Schatton et al., 2008). While Quintana and colleagues demonstrated that 25% of unselected single cells from human melanoma samples (primary and metastatic) successfully generated tumours in immunocompromised mice, the percentage of single cell-transplants, generated from xenotransplants from four patients, was as high as 27% (Quintana et al., 2008). This directly opposed the notion that the CSC population was supposed to be small. Subsequently, the same laboratory tested many markers that were previously published to enrich for CSCs in melanoma, but no enrichment of the CSC population was observed (Quintana et al., 2010). Similarly, Kelly and colleagues demonstrated that, contrary to the assumption that haematological malignancies consist of a small CSC population, at least 10% of cells from lymphomas and leukaemias were able to form tumours in histocompatible mice (Kelly et al., 2007).

1.8.3 CSC markers in melanoma

Opposing the views from the Morrison laboratory (Quintana et al., 2010; Quintana et al., 2008), there were many reports that demonstrated an enrichment of the CSC population in melanoma (Boiko et al., 2010; Fang et al., 2005; Frank et al., 2005;

Schatton et al., 2008). Many laboratories reported markers that had been used to isolate this population and demonstrated its tumour-forming capabilities *in vivo*, as well as the lack thereof when cells negative for the marker were used in transplantation experiments. The most well-researched markers are the drug efflux pump ABCB5 (Schatton et al., 2008), CD20 (Fang et al., 2005; Pinc et al., 2012; Schlaak et al., 2012), CD271 (Boiko et al., 2010; Civenni et al., 2011), aldehyde dehydrogenase (Luo et al., 2012) and JARID1B (Roesch et al., 2010).

It is important to note that the discrepancies between the reports describing varying numbers of CSCs within melanoma, might arise from the preparation of the cells prior to transplantation experiments, the *in vivo* models used, and the treatment of the cells *ex vivo*. These points need to be considered also in the case of the findings coming from the Morrison laboratory who reported the existence of the CSC population to be as high as 25-27% (Quintana et al., 2010). A straightforward reason that biased this estimation might have been due to the more immunocompromised mouse model used. As other researchers have performed xenotransplants in NOD/SCID mice (Civenni et al., 2011; Monzani et al., 2007; Schatton and Frank, 2008), Quintana and colleagues have utilised a NOD/SCID mouse containing an additional mutation in the interleukin-2 receptor gamma chain (Quintana et al., 2010), which might make the microenvironment more permissive for any cell to establish a tumour and could explain the increased tumour-forming ability of melanoma cells observed by this group (Fukunaga-Kalabis et al., 2011; Murphy et al., 2014).

1.8.4 Phenotype-switching theory

To reconcile the seemingly controversial findings of Quintana et al (Quintana et al., 2010; Quintana et al., 2008) and Kelly et al (Kelly et al., 2007) with the laboratories

that have been able to demonstrate the existence of CSC on the basis of specific cell markers (Boiko et al., 2010; Civenni et al., 2011; Frank et al., 2005; Luo et al., 2012; Schatton et al., 2008), the phenotype-switching theory (Hoek and Goding, 2010; Pinner et al., 2009; Roesch et al., 2010) emerged (Figure 1.5). This theory states that any cancer cell, including differentiated cells, might have the capacity to adapt their phenotype in response to changes in the microenvironment (Hoek and Goding, 2010). This might trigger non-invasive cancer cells to leave their differentiated state to become proliferating or ultimately invasive and generate a CSC (Hoek and Goding, 2010).

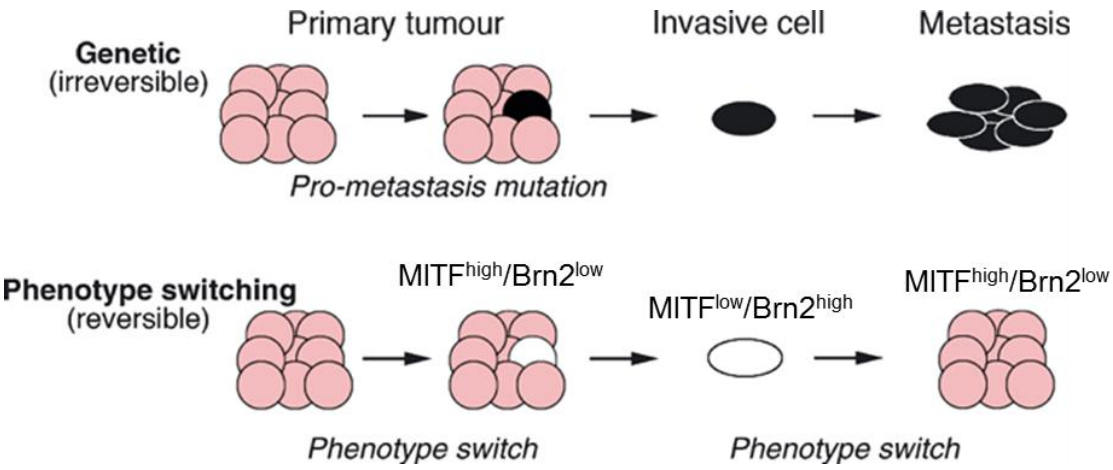


Figure 1.5: Metastasis generation according to the genetic and the phenotype-switching model. In the genetic model cells from a primary tumour can only generate metastases if they acquire irreversible pro-metastatic mutations (top). In the phenotype-switching model, however, changes in the microenvironment could affect any cell in the tumour to reversibly change their phenotypes from a proliferative to a more stem-like and invasive phenotype, allowing cells to generate metastases at secondary sites. Depending on the new microenvironment, cells will either stay in the same phenotype or revert back to their previous proliferative phenotype. Adapted from (Hoek and Goding, 2010).

Another implication of the phenotype-switching model is that cells can cycle between different phenotypes and may therefore be more difficult to eradicate, as they will constantly adapt to their environments (Hoek and Goding, 2010). In the same way, it is conceivable that the measurements that were conducted by the groups mentioned above were done under conditions where the microenvironments might have been different, e.g. through treatment with trypsin or collagenase, thereby influencing the proportion of cells that become stem-like. In both cases, what these types of assessments actually

measure is the ability of cells to survive in a new environment and proliferate, rather than their ability to form new tumours.

1.9 Microphthalmia-associated transcription factor (MITF)

1.9.1 MITF and development

A transcription factor that has been shown to play a role in melanomagenesis and potentially phenotype-switching is MITF. Due to its many effects MITF is often referred to as the melanocyte 'master regulator' (Bell and Levy, 2011). The first time the importance of MITF was demonstrated was in 1993 by Hodgkinson and colleagues and subsequently in 1994 by Hughes and colleagues (Hodgkinson et al., 1993; Hughes et al., 1994). When this transcription factor was inactivated it led to mice with microphthalmic eyes and white fur colour (Steingrimsson et al., 2004). Since then it has been demonstrated that MITF influences melanocyte differentiation, as it induces the expression of genes involved in melanin production and storage, such as *Tyrosinase* (Bentley et al., 1994; Du et al., 2003), *dopachrome tautomerase* (*DCT*) (Bertolotto et al., 1998) and *Pmel17* (Du et al., 2003). MITF also plays a role in cell proliferation and survival through its control of the transcription factor of the T-box family, *TBX2* (Bejar et al., 2003; Carreira et al., 2000). TBX2 represses the cyclin-dependent kinase (CDK) inhibitor 1A ($p21^{Cip1}$) and CDK inhibitor 2A ($p19^{ARF}$) that leads to a block in senescence (Jacobs et al., 2000; Prince et al., 2004; Vance et al., 2005). Later, the regulation of other cell cycle control proteins such as cyclin-dependent kinase 2 (CDK2) by MITF was demonstrated (Du et al., 2004). Additionally, short-term depletion of MITF decreases the expression of diaphanous-related formin Dia1 (Carreira et al., 2006), leading to a cell cycle arrest mediated by the CDK inhibitor 1B, $p27^{Kip1}$ (Carreira et al., 2006). Interestingly, long-term inhibition of MITF induces cell

senescence through a DNA damage response and upregulation of p53 (Giuliano et al., 2010). The effect of MITF on proliferation was also demonstrated *in vivo* when MITF-heterozygous mice had fewer melanoblasts which were shown to proliferate faster (Hornyak et al., 2001). In addition to controlling differentiation and cell cycle control genes, MITF also affects cell survival by regulating the pro-apoptotic gene *BCL2 in vitro* and *in vivo* (McGill et al., 2002).

1.9.2 MITF in cancer

MITF in the context of melanoma has also been referred to as a 'lineage addiction' or 'lineage survival' oncogene (Garraway and Sellers, 2006; Garraway et al., 2005a; Goodall et al., 2004b). This is due to DNA microarray analyses of melanoma cell lines and metastatic disease, which demonstrated an amplification of the *MITF* gene (Garraway and Sellers, 2006; Garraway et al., 2005a; Garraway et al., 2005b). Furthermore, ectopic MITF expression in primary human melanocytes, also containing a $BRAF^{V600E}$ mutation, leads to the transformation of the cells (Garraway et al., 2005b). In summary, increased levels of MITF in melanoma, together with mutations in the above-mentioned cell cycle control proteins can promote melanoma formation and MITF can act as an oncogene.

Contrastingly, MITF can also act as a tumour suppressor in melanoma (Carreira et al., 2005; Carreira et al., 2006; Loercher et al., 2005; Wellbrock and Marais, 2005). Studies have demonstrated that MITF upregulates the transcription of the CDK inhibitor gene *CDKN1A*, leading to an increase in $p21^{Cip1}$ expression, which together with the consequent hypophosphorylation of the tumour suppressor retinoblastoma (Rb1) induces cell cycle arrest and cell differentiation (Carreira et al., 2005). Additionally, MITF activates the expression of the tumour suppressor $p16^{INK4a}$. This again leads to

hypophosphorylation of Rb1, cell cycle arrest and induction of differentiation (Loercher et al., 2005). Supporting the hypothesis that MITF can work as a tumour suppressor rather than an oncogene is a study performed by Wellbrock and Marais in 2005, that demonstrated how in proliferating BRAF-transformed melanoma cells, MITF expression is low and that re-introduction of MITF inhibited cell proliferation (Wellbrock and Marais, 2005). In addition, cells expressing low levels of MITF are invasive (Carreira et al., 2006), an observation supported by Cheli and colleagues who showed that melanoma cell lines that were depleted of MITF, by using small interfering RNAs (siRNAs), followed by transplantation into mice, proliferated faster and formed the bulk of the tumour mass (Cheli et al., 2011). Interestingly, following MITF depletion, the levels of the CDK inhibitor $p27^{Kip1}$, as well as of the stem cell markers Oct4 and Nanog were increased, but once $p27^{Kip1}$ was depleted alongside MITF, the size of the tumours was reduced. Similarly, in human melanoma cell lines that were grown in melanospheres to induce stemness, MITF expression was decreased while $p27^{Kip1}$ and Oct4 expression were increased (Cheli et al., 2011). Again, MITF-depleted cells developed bigger tumours in mice. These results were confirmed in freshly isolated human melanoma cells (Cheli et al., 2011).

To summarise, MITF can both promote and inhibit proliferation of melanoma cells, and low levels of MITF promote tumour formation after injection into mice, most likely because slow cycling cells can adapt more readily to the sub-cutaneous microenvironment before turning on MITF to proliferate.

1.10 Brn2 (POU3F2) transcription factor

1.10.1 Brn2 in development

Another crucial transcription factor involved in melanocyte development is Brn2 (also known as POU3F2). Brn2 belongs to the POU transcription factor family of which Oct4 possibly is the most well-known as it has been implicated in the formation of induced pluripotent stem (iPS) cells (Takahashi et al., 2007; Takahashi and Yamanaka, 2006; Wernig et al., 2007). POU transcription factors bind to DNA through the highly conserved POU domain (Sturm and Herr, 1988), consisting of an N-terminal POU-specific domain, which comprises 75 amino acids and the C-terminal POU-homeo domain consisting of 60 amino acids (Cook and Sturm, 2008). These N- and C-terminal domains form helix-turn-helix motifs that allow the POU transcription factors to bind to the DNA (Cook and Sturm, 2008). While some POU factors are widely expressed, such as Oct1 (Ohno et al., 1994), Brn2 is expressed during neuron migration (McEvilly et al., 2002), in the central nervous system in adults (Wegner et al., 1993) and in the melanocytic lineage (Cook et al., 2003). In explant cultures, Brn2 is expressed in the neural crest from embryonic day 9 (E9) (Cook et al., 2003). However, Goodall and colleagues demonstrated that in murine E11.5 neural crest or in melanoblasts *in vivo* *Brn2* mRNA is not present (Goodall et al., 2004a). Interestingly, when melanocytes were exposed to a culture medium which is used to culture melanoblasts, decreased pigmentation and an increase in Brn2 protein expression were observed (Cook et al., 2003), indicating that Brn2 is most likely involved in the maintenance of a de-differentiated state. Furthermore, forced overexpression of Brn2 in mouse melanocytes led to a less differentiated phenotype (Goodall et al., 2004b). In line with this, when melanoma cells were treated with differentiating agents, such as butyric acid or dimethyl sulfoxide (DMSO), Brn2 expression was reduced (Sturm et al., 1991).

Consequently, treatment of these cells with the depigmenting agent dithiothreitol increased Brn2 expression (Sturm et al., 1991).

To summarise, the expression of Brn2 is correlated with an undifferentiated cell state and it is inversely correlated with pigmentation, i.e. differentiation.

1.10.2 Brn2 in melanoma

Because Brn2 is expressed in unpigmented, less differentiated cells, it is unsurprising that Brn2 protein levels are higher in melanoma cell lines compared to melanocytes (Cox et al., 1988; Eisen et al., 1995; Sturm et al., 1994; Thomson et al., 1993). In line with these observations, some melanoma cell lines exhibit *Brn2* gene amplification (Thomson et al., 1995). Furthermore, comparison of non-pigmented and more differentiated, pigmented melanoma cell lines demonstrates that Brn2 protein and its DNA binding abilities are increased in non-pigmented cell lines (Cook et al., 2003). To investigate the function of Brn2 in more detail, antisense RNA was stably introduced into melanoma cells to mediate Brn2 inhibition (Thomson et al., 1995). This led to changes in morphology and the loss of differentiation markers such as MITF or tyrosinase-related protein 1 (TYRP1) (Thomson et al., 1995). Transplantation of these cells into SCID and nude mice, revealed that tumour formation was ablated (Thomson et al., 1995). These results not only suggest a contribution of Brn2 in the formation of melanocytes but also a role in tumourigenesis. Equally, downregulation of Brn2 by siRNA-mediated targeting in melanoma cell lines decreases proliferation (Goodall et al., 2004a; Goodall et al., 2004b).

1.11 Aims of the project

MITF and Brn2 are involved in processes such as differentiation, cell survival and proliferation. These transcription factors are also likely to play a role in metastasis and invasion as well as phenotype-switching in melanoma. One of the main reasons why melanoma is such a difficult cancer to treat compared to other cancers is due to the existence of multiple cell populations. The reason for this is that the process of generating heterogeneity might increase the chances of generating cells that contain the capacity to form metastases. One possibility to achieve heterogeneity is by phenotype-switching. This process can be investigated by assessing the expression of the MITF and Brn2 proteins, as these can mark potentially different cell populations in melanoma. Another important process to address in melanoma is metastasis formation. As Brn2 is expressed in invasive, less differentiated cells, which could also potentially mark melanoma stem cells, Brn2 expression may help inform on pathways that contribute to invasion and metastasis formation.

Therefore, the overall aims of this thesis are to investigate the process of phenotype-switching in melanoma and pathways that can contribute to the development of metastases. In particular, the following aims have been identified:

1. Determine if the *Brn2* and *MITF* promoters could serve as reporters to identify different phenotypic states of melanoma cells *in vitro* and *in vivo*. This was addressed by constructing dual lentiviral reporter systems and generating clonal cell lines. According to our hypothesis, *MITF* promoter activity would mark differentiated and proliferating cells, while the *Brn2* promoter would be active in cells that are less differentiated and therefore potentially more invasive and stem-like.

2. Investigate if the reporter cell lines could be used to test small molecules that can affect the activity of the *Brn2* promoter. By screening a library of kinase inhibitors for their potential to affect *Brn2* promoter activity, it might be possible to identify pathways involved in the maintenance or generation of more de-differentiated cells in melanoma.
3. Investigate signalling pathways involved in invasion and metastasis generation and their effects on the *Brn2* and *MITF* promoters. The first part of this aim will be based on further testing of the hits obtained from the kinase inhibitor screen. Due to their roles in invasion, the second part of this aim will investigate the effects of the Notch and Wnt pathways on *Brn2* and *MITF* promoter activity.

2 Materials and Methods

2.1 Cell culturing

Unless otherwise stated, laboratory plastic ware was purchased from Corning Inc or Fisher Scientific. Cells were washed with Dulbecco's Phosphate Buffered Saline (DPBS, Life Technologies) and grown in the Roswell Park Memorial Institute 1640 (RPMI, Sigma-Aldrich) medium, containing L-glutamine and sodium bicarbonate, or in Dulbecco's Modified Eagle Medium (DMEM, Sigma-Aldrich), containing 4500 mg/L glucose, L-glutamine and sodium bicarbonate. RPMI and DMEM were both supplemented with 10% foetal bovine serum (FBS, Life Technologies) and 1% penicillin (25 U/mL) / streptomycin (10 mg/mL) (P/S, Life Technologies) (Life Technologies), (further referred to as complete RPMI/DMEM), unless stated otherwise. For cell passaging, trypsin-ethylenedinitrilotetraacetic acid (EDTA) consisting of 0.5 g/L porcine trypsin and 0.2 g/L EDTA•4NA in Hank's Balanced Salt Solution with phenol red (T/E; Sigma-Aldrich) were used.

2.1.1 Cell lines

All cell lines were cultured in a 37°C incubator at 5% CO_2 and handled in a class II laminar-flow cabinet using sterile techniques.

The mouse melanoma cell line, B16F10, originating from the skin of C57BL/6J mice, and the human melanoma cell lines SKmel28 and 501mel (both derived from human malignant melanoma, all kindly donated by the Goding laboratory) were cultured in RPMI medium containing 10% FBS and 1% P/S. Human embryonic kidney cells (HEK293-T), as well as Phoenix cells (section 2.1.5), were cultured in DMEM containing 10% FBS and 1% P/S. HEK293-T cells contain the gene for the SV40 T-antigen to allow the production of high titers of infectious retrovirus. Phoenix cells

were previously created from HEK293-T cells (section 2.1.5). Cells that were virally transduced (section 2.1.5) were cultured in complete RPMI medium containing the antibiotic puromycin (2 µg/mL, Takara Bio Company and Sigma-Aldrich) (section 2.1.6). For details of cell lines and their specific growth media, see Table 2.1.

Table 2.1: Summary of the origin of cell lines used and their growth media

Cell line	Origin	Growth medium	Authenticated
SKmel28	Human malignant melanoma	RPMI, 10% FBS, 1% P/S	yes
501mel	Human malignant melanoma	RPMI, 10% FBS, 1% P/S	yes
B16F10	Mouse melanoma cell line	RPMI, 10% FBS, 1% P/S	
HEK293-T	Human embryonic kidney cells	DMEM, 10% FBS, 1% P/S	
Phoenix	Human embryonic kidney cells	DMEM, 10% FBS, 1% P/S	

2.1.2 Cell passaging

Cells were passaged when they reached 90-100% confluency by removing the media from the culture flask, washing the cells with DPBS and incubating with T/E for 5-10 minutes (min) at 37°C, 5% CO_2. To stop the activity of T/E, complete medium was added to the cells once they started to detach. Cells were then transferred to a new flask in a dilution ranging from 1:20 to 1:3.

2.1.3 Freezing cell lines and storage

To freeze cell lines, cells were grown to confluency in 175 cm^2 flasks. Medium was removed and cells were washed and treated with T/E as described above. Subsequently, complete RPMI medium was added and cells were pelleted at 250 relative centrifugal force (rcf) for 5 min at RT. The freezing medium was prepared beforehand, consisting of 90% FBS and 10% dimethyl sulfoxide (DMSO, Sigma-Aldrich). The cell pellet was resuspended in 3 mL of freezing medium and aliquoted into three cryovials. These were

wrapped in blue paper roll and positioned in a polystyrene box or placed in a Mr. Frosty and stored in a -80°C freezer until fully frozen. Subsequently, the cryovials were transferred into storage boxes and stored at -80°C.

To resuscitate frozen cells, cryovials were placed in a 37°C water bath until they were thawed. The cells were then resuspended in complete medium and seeded into a 75 cm^2 flask. Alternatively, to remove the DMSO from the freezing medium, the thawed cells were resuspended in 4 mL complete medium and spun at 250 rcf for 5 min at RT. While the supernatant was discarded, the cell pellet was resuspended in complete medium and cells were placed in a 75 cm^2 flask in a 37°C incubator.

2.1.4 Cell plating

When cells had to be further assessed or treated, they were plated into 96, 48, 24 or 6 well plates. For this, medium from the cells was removed and cells were washed with DPBS and treated with T/E as described above. Subsequently, complete medium was added and a cell suspension was generated. Cells were counted using a haemocytometer, the correct volume needed for the plating of the cells was calculated and pipetted into 50 mL Falcon tubes. Medium was added to adjust the correct total volume.

When cells were analysed by immunohistochemistry (section 2.3) they were plated onto coverslips (Ø13 mm, VWR) in 24 well plates. The coverslips were placed in the wells beforehand. Cells were plated directly onto the coverslips. Alternatively, if it was known that the cell lines detached easily from the coverslips, the latter were covered beforehand in poly-L-lysine (Sigma-Aldrich) and placed in the 37°C incubator for 5-15 min. The remaining poly-L-lysine solution was removed and stored at 4°C to be re-used at a later time. Subsequently, cells were plated onto the coverslips as described above.

2.1.5 Virus generation

In order to recover lentiviruses, Phoenix cells were used as a producer cell line. These are a helper-free retrovirus producer cell line which was created by transfecting HEK293-T cells with constructs expressing group antigens-polymerase (gag-pol) and the envelope protein for ecotropic and amphotropic viruses at the Stanford University (Nolan, 2014). Ecotropic viruses have a narrow host range and can therefore only infect host cells (ecotropism), while amphotropic viruses have a broad host range and can infect more than one species (amphotropism). To introduce the two different constructs into the cells, two different non-moloney promoters were used and the cells were treated with hygromycin and diphtheria toxin to select for cells containing both constructs.

To recover the lentiviruses, cells were seeded in a 15 mm^2 tissue culture plate in complete DMEM medium and left in the tissue culture incubator at 37°C until they reached 90-100% confluency. Despite the fact that the gag-pol and the envelope proteins were introduced into Phoenix cells previously (as described above), additional plasmids containing gag-pol and the lentiviral envelope protein were transfected into the cells alongside a lentiviral plasmid containing the genes of interest. Cells were placed back in the 37°C incubator. After 24 hours (h) the old medium was replaced with new complete medium and cells were left again in the 37°C incubator. 48 h and 72 h post-transfection, the supernatant was collected and filtered through a 0.44 µm syringe (VWR International). Subsequently, the supernatant was centrifuged at 50,000 rcf using an ultracentrifuge (Avanti J-26XP Centrifuge, Beckman Coulter) and supernatant was discarded. The pellet was resuspended in 1 mL Hank's Balanced Salt Solution (HBSS) and hexadimethrine bromide (polybrene, Sigma-Aldrich) was added. Polybrene is a cationic polymer and it enhances virus infection by neutralising the

charge repulsion between the virus particles and sialic acid (Davis et al., 2004). Sialic acid is present on the cell surface and allows virus particles to bind to it and therefore gain access to the cytoplasm.

After resuspending the particles in HBSS they were applied directly onto the cells that were plated previously into a 6 well plate and had reached a confluency of 90-100% at the time of infection. Cells were placed back in the 37°C incubator. Treatment with the antibiotic to select for infected cells was started 96 h after infection (puromycin treatment – section 2.1.6).

2.1.6 Puromycin selection

To select the cells that were successfully transduced from those cells that did not take up any virus, puromycin was applied. Puromycin is an aminonucleoside antibiotic that inhibits peptidyl transfer on prokaryotic and eukaryotic ribosomes. Unless cells took up viruses expressing the Pac resistance cassette that encodes the enzyme puromycin *N*-acetyl-transferase (Pac), the cells underwent apoptosis.

To determine the lowest concentration of puromycin needed to kill off cells lacking the PAC cassette, a puromycin viability curve was established on non-transduced wild-type (WT) cells. To accomplish this, cells were seeded in complete RPMI in a 96 well plate. A puromycin dilution series, ranging from 0-10 µg/mL was made up in complete RPMI. When cells reached a confluency of 90-100%, medium was removed and increasing concentrations of puromycin in complete RPMI were added to the cells. Cells were assessed for cell viability by microscopy every day for seven days. To quantify cell death cells were treated with the compound resazurin (Sigma-Aldrich). As only living cells retain the capacity to convert the non-fluorescent dye resazurin to the highly fluorescent dye resorufin, it was possible to quantitatively assess the number of

viable cells by fluorescence (the excitation and emission maxima of resorufin are at 579 nm and 584 nm, respectively). Prior to this, the media in the wells was removed and 100 µL of a 0.05% resazurin solution (made up in complete medium) was added to each well. The plates were left at 37°C for 1 – 3 h. Fluorescence was read at 560/590 nm for 0.5 s (seconds).

The concentration chosen for the experiments was firstly 4 µg/mL (using puromycin obtained from Takara Bio Company). However, when the viability assay was repeated with a new batch of puromycin (Sigma-Aldrich) the sensitivity increased and the working concentration of puromycin was reduced to 2 µg/mL.

2.1.7 Cell line selection and FACS

Cells resistant to puromycin were grown up from a 6 well plate, where they had been infected previously, to a 175 mm^2 flask and frozen at -80°C (section 2.1.3).

In order to analyse the behaviour and properties of the virally infected cells expressing either mCherry or GFP, or both fluorescent proteins, cells underwent fluorescent activated cell sorting (FACS). This was carried out by Andrew Worth (Jenner Institute, University of Oxford) using FACS MoFlow. Single cells were sorted into 96 or 48 well plates for exclusively expressing mCherry, GFP or both fluorescent proteins at the same time. Additionally, a larger cell number was also sorted into 48 well plates to analyse a mixed population of only mCherry or GFP expressing cells.

Cells sorted into 96 or 48 well plates were left in the incubator for a minimum of 6 days to check for colony formation as the colonies were too fragile to be analysed before this time. Fluorescence was analysed using a fluorescent microscope connected to a Nikon 80i microscope and NIS Elements Imaging Software.

2.2 *In vivo* mouse work

In vivo animal studies involving laboratory mice were conducted in accordance with the UK Home Office Animals (Scientific Procedure) Act 1986 under the project licence PPL 30/2819 and personal licence PIL 30/8452.

2.2.1 Housing conditions

The animal facility was located at Biomedical Services, John Radcliffe Hospital, Oxford. The cages were temperature and humidity-controlled (20-22°C), individually ventilated and environmentally-enriched. The mice were able to freely access sterile tap water and formulated diets.

2.2.2 Inoculation of CD-1® nude mice with human melanoma cell lines

On the basis of their genetic background, CD-1® nude mice were chosen as the host animal for the following inoculation studies. Due to the transfer of the nude gene from Crl:NU-*Foxn1*^{nu} to a CD-1 mouse, the mice lack thymi and are therefore unable to raise a T cell-dependent immune response. These mice are therefore particularly well suited for xenograft research as their genetic background allows for the inoculation of cells that originated from other species.

Prior to the inoculation of CD-1® nude mice, the mice were divided into four groups, each corresponding to the different cell type the mice were injected with: group one, received cells expressing mCherry or GFP. Group two, received GFP^{+} cells and the third group was inoculated with mCherry^{+} cells. All these groups consisted of four mice. The fourth group was a control, where two mice were injected with non-transformed 501mel cells and an additional two mice received a transplantation of the

mouse melanoma cell line B16F10 to test for the tumour generation. Groups one, two and three were divided up in three cages. The two control groups shared one cage.

Before inoculation, 501mel cells were washed with DPBS, treated with T/E and resuspended in complete RPMI. Cells were subsequently washed twice, involving centrifugation at 250 rcf for 5 min at RT and resuspension in DPBS. After the last washing step, cells were counted and a cell suspension consisting of $4x10^6$ cells was produced in DPBS. Cells were transported to the BMS on ice.

CD-1® nude mice were anaesthetised by inhalation of oxygen and isofluorane, 3-5% (University Veterinary Services) and subcutaneously inoculated with $4x10^6$ 5001mel cells in 100 µL of DPBS above the flank using a 25G needle and 1 mL syringe. This was repeated on the other side of the animal. Mice were left to recover in their corresponding cages. Tumours were left to develop and once they had reached a volume of approximately 1000 mm^3, the mice were put down through a schedule 1 method of killing. Subsequently, the tumours were excised and transported in complete RPMI at 4°C.

2.2.3 Tumour cell preparation

After the excision, tumours were dissected into five pieces, three of which were placed in 1.5 mL eppendorf tubes and immediately frozen in liquid nitrogen. This would enable us to use the cells to assess DNA, RNA and protein levels. Another part of the tumour was placed in optimal cutting temperature (OCT) compound in cryomolds and frozen in liquid nitrogen by slowly lowering the mould. The fifth part of the tumour was placed in 1.5 mL eppendorf, containing 1 mL of complete RPMI medium supplemented with collagenase type 4 (Sigma-Aldrich) and Dispase II (Roche Life Science) (both at 3 mg/mL concentration). The eppendorf tubes containing the tumour

cells were dissociated for 1.5 h at 37°C in a rotating stand. After every 30 min the cells were manually resuspended and placed back at 37°C.

Afterwards, the cells were pipetted through a 100 µm cell strainer and the resulting single cell suspension was washed by centrifugation at 250 rcf for 5 min at RT. After each centrifugation step, the supernatant was removed and the cells were resuspended in complete RPMI medium. After the last wash step, cells were resuspended in 1 mL of complete RPMI medium and counted. To analyse the fluorescence of the cell suspension by flow cytometry cytometry (section 2.2.4), 4 x 10^5 cells were placed in a flow cytometry tube. The residual cells were pipetted into two wells of a 24 well plate. If the tumour cell suspension did not contain 4x10^5 cells, $^1/_3$ of the cell suspension, 300 µL, were analysed for fluorescence using flow cytometry.

2.2.4 Analysis of tumour cell suspensions using flow cytometry

The expression of fluorescent proteins in the stable cell lines, previously transduced with virus, and in the cells taken from *in vivo* experiments, was quantitatively assessed by flow cytometry.

Briefly, for the analysis of stable cell lines, complete RPMI medium was removed, cells were washed with DPBS, treated with T/E or enzyme-free cell dissociation buffer (Life Technologies) for 5-10 min at 37 °C and neutralised with complete RPMI medium (section 2.1.2). Cells were spun at 170 rcf for 5 min, resuspended in flow cytometer solution (consisting of DPBS supplemented with 3 mM EDTA and 5% FBS) and pipetted into flow cytometer tubes in order to assess the expression of GFP and mCherry using the cell analyser BD FACSCanto (BD Biosciences).

For the analysis of GFP^+/$mCherry^+$ cells obtained from *in vivo* tumour samples (section 2.2.3), 300 µL of each tumour sample were pipetted into flow cytometer tubes. To

control for mCherry/GFP expression, $mCherry^+$ and GFP^+ cell lines were used as controls. The cells were washed with DPBS, treated with cell dissociation buffer, neutralised with complete RPMI and counted. $3x10^5$ cells were pipetted into each flow cytometer tube. Tubes containing the control cells or cells from the tumour samples, were spun at 170 rcf for 1 min at 4°C after which the medium was discarded by inverting the tubes. 300 µL or 500 µL of flow cytometer solution was added to the each tube to wash the cells. These were briefly vortexed and spun again.

In order to exclude the host mouse cells from the analysis, the cells were incubated with primary antibodies (prepared in flow cytometer solution, 50 µL/test) against mouse CD45 at 0.08 µg/test (BioLegend), mouse CD71 at 0.04 µg/test (eBioscience), mouse CD31 at 0.5 µg/test (clone 390, eBioscience) and mouse TER-119 (BioLegend, 0.3 µg/test) for 40 min at 4°C in the dark (Quintana et al., 2008).

CD45 is expressed on all hematopoietic cells except mature erythrocytes and platelets. CD71 is also known as transferrin receptor and as such it is expressed on immature proliferating cells and at low levels on resting mature lymphocytes. CD31, also known as PECAM-1, is expressed by endothelial cells and at low levels on all leukocytes and platelets. TER-119 is expressed on early proerythroblasts to mature erythrocytes but is not present on erythroid colony-forming cells.

All mouse antibodies were conjugated to allophycocyanin (APC) and therefore did not require secondary antibody incubation. APC is excited at 650 nm and emits light at 660 nm. Additionally, in order to analyse only the human 501mel cells that were implanted into the mouse, the tumour samples were also incubated with a biotinylated antibody against human leukocyte antigen (HLA)-A,B,C (Quintana et al., 2008) at 0.125 µg/test (eBioscience) for 40 min at 4°C in the dark. This protein belongs to the human major histocompatibility complex class I and is expressed on all human nucleated cells.

After the incubation, cells were washed three times by adding 300 µL or 500 µL of flow cytometer solution to each tube and centrifuging at 170 rcf for 1 min at 4°C.

Cells that were stained with the anti HLA-A,B,C antibody were subsequently incubated with a secondary streptavidin antibody against biotin, conjugated to Phycoerythrin (PE)-Cy7 for 40 min at 4°C. This antibody is excited at 480, 565, 743 nm and emits light at 767 nm. Cells were washed again three times using the flow cytometer solution and in the final step the cells were resuspended in 300 µL of flow cytometer solution and analysed using the cell analyser BD FACSCanto.

2.3 Immunofluorescence (IF)

To analyse protein expression in untreated and transfected cell lines, cells were plated in 24 well plates containing cover glasses (Ø13mm; VWR). 24 h post-plating cells, were washed, fixed in 10% formalin solution for 15 min at room temperature (Sigma-Aldrich), and washed three times with DPBS. Subsequently, cells were permeabilised with DPBS containing 0.1% Triton-X100 (Sigma-Aldrich, DPBS-T) for 10 min at RT and washed three more times with DPBS. Afterwards, cells were blocked in 2% skimmed milk (made up in DPBS-Triton, Marvel) for 30 min at room temperature. Subsequently, cells were incubated with primary antibodies at 4°C overnight and afterwards incubated with secondary antibodies for 1 h at room temperature (Table 2.2). Cells were washed three more times with DPBS and either mounted on a cover slip with a mounting medium containing the fluorescent nuclear stain DAPI (Vectashield; Vector-labs), or alternatively incubated with DAPI containing DPBS during the second wash step. Fluorescence was measured using a LSM710 confocal microscope (Zeiss) and the ZEN software.

Table 2.2: Summary of antibodies used. AB = antibody, IgG = immunoglobulin G, IF = immunofluorescence

Primary AB	***Raised in***	***Dilution in application***		***Source***
		Western	***IF***	
Anti-MITF	Rabbit polyclonal IgG	1:1000	1:200	In house
Anti-Brn2	Mouse monoclonal IgG	1:1000	1:100	In house
Anti-Brn2	Mouse IgG1 Clone 8C4.2	1:1000	1:200	Merck Millipore
Anti-FLAG	Rabbit polyclonal IgG	1:10.000	1:500	Sigma-Aldrich
Anti-Myc	Mouse monoclonal IgG, clone 4A6	1:5000	1:100	Merck Millipore
Anti-β-catenin	Mouse monoclonal IgG1	1:5000	1:500	Santa Cruz Biotechnologies
Anti-MAML1	Rabbit polyclonal	1:500	1:300	Bethyl Laboratories
Anti-β-actin	Mouse monoclonal Clone AC-74	1:1000	-	Sigma-Aldrich
Secondary AB	***Raised in***	***Dilution in application***		***Source***
		Western	***IF***	
Alexa Fluor 488 anti-rabbit IgG	Donkey	-	1:1000	Life Technologies
Alexa Fluor 546 anti-rabbit IgG	Donkey	-	1:1000	Life Technologies
Alexa Fluor 488 anti-rabbit IgG	Donkey	-	1:1000	Life Technologies
Alexa Fluor 546 anti-mouse IgG	Donkey	-	1:1000	Life Technologies
Alexa Fluor 488 anti-mouse IgG	Donkey	-	1:1000	Life Technologies
Polyclonal Anti-Mouse Immunoglobulins HRP-conjugated	Rabbit	1:1000	-	Dako
Polyclonal Anti-Rabbit Immunoglobulins HRP-conjugated	Goat	1:1000	-	Dako

2.4 DNA transfections

Depending on the experimental conditions, transfections were performed with Lipofectamine 2000, Lipofectamine LTX and Plus reagent (both Life Technologies) or GeneJuice (Novagen, Merck Millipore). 24 h prior to the transfections, cells were

plated in complete RPMI medium. For transfections with Lipofectamine 2000, DNA was pipetted into suitable containers and diluted in serum-free Opti-MEM (Life Technologies) (for amounts of DNA see separate results chapters). Volumes of Opti-MEM were pipetted according to well sizes and manufacturer's instructions. In a second container Lipofectamine 2000 was diluted in Opti-MEM and left at RT for 5 min. Subsequently, the two solutions were combined and incubated for 5 min at RT. Prior to the addition of the DNA-transfection reagent solution to the cell monolayer, the medium in the wells was replaced with RPMI medium supplemented with 10% FBS only. The solution containing the DNA and Lipofectamine 2000 was then added drop-wise to the cell monolayer. Alternatively, the fresh RPMI medium was added to the DNA-Lipofectamine 2000-Opti-MEM solution directly and added to the cells. This way it was ensured that the DNA and transfection reagent were mixed well and that each well on the cell plate received the same volume DNA and transfection reagent. After transfection, cells were placed in the 37°C incubator until analysed.

For transfections with Lipofectamine LTX and Plus reagent, the DNA was firstly diluted in Opti-MEM followed by the addition of the Plus reagent and Lipofectamine LTX (the volumes were adjusted to the wells cells were plated in and manufacturer's instructions were followed). This was followed by a 30 min incubation at RT. Prior to the drop-wise addition of the DNA-transfection reagent mix to the cells, medium in the wells was removed and replaced with fresh RPMI, only supplemented with 10% FBS. Medium was changed 4-6 h post-transfection to RPMI medium, supplemented with 10% FBS and 1% P/S, and cells were placed in 37°C incubator until analysed.

Briefly, for transfections with GeneJuice the medium in the wells was replaced with fresh medium. Subsequently, the correct amount of Opti-MEM, depending on the well size that was to be transfected, was pipetted into sterile tubes. GeneJuice transfection

reagent was then added directly to the medium and vortexed. After a 5 min incubation at RT, the correct amount of DNA was pipetted into the transfection reagent-Opti-MEM solution and mixed gently. After another incubation at RT for 5-15 min, the mixture was added drop-wise to the cells. The medium was not changed after the addition of the transfection reagents.

2.5 Luciferase expression *in vitro*

To assess the luciferase expression of cells that were transfected with plasmids encoding the transgene for firefly luciferase a luciferase assay system (Promega) was used. 20-26 h post-transfection (section 2.4), medium was removed from the wells and cells were lysed with the lysis buffer, provided in the kit (150 µL/well). The lysis buffer was previously diluted to a 1x solution using de-ionised H_2O or DPBS from a 5x concentrated solution. The plate was subsequently frozen at -80°C and thawed at RT. The wells were scraped and 25 µL of cell lysate was pipetted into a tube and placed in a luminometer (Lumat LB 9507, Berthold Technologies). In order to determine the luciferase expression in the cells, the luciferase assay substrate (25 µL of beetle luciferin) was added to each 25 µL sample. When the firefly luciferase enzyme was expressed in the cells, the luciferase assay substrate was converted to the luminescent product oxyluciferin using the co-substrates ATP and O_2, as well as Mg^{2+}. Besides oxyluciferin, AMP, PP_1, CO_2 and light were also formed. The luminescence produced by the reaction was measured for 10 s and recorded as relative light units (RLU). To control for the total amount of DNA transfected into each well, an empty plasmid control was used. To correct for the amount of protein present in each well, the protein content per well was measured (section 2.5.1) and RLU was divided by the amount of

protein. The results were subsequently expressed as a percentage of the control or as RLU per protein (RLU / (mg/mL)).

Alternatively, after transfection, the plate containing the cell lysate was shaken for 30 min at 4°C and luminescence was measured by pipetting 50 µL into a white, flat bottom 96 well plate and injecting 50 µL of luciferin (beetle luciferin). The luminescence was read by the GloMax® 96 Microplate Luminometer (Promega).

As the Lumat LB 9507 luminometer gave more reliable and precise measurements, the first method was used for further luciferase analyses.

2.5.1 Protein quantification

The protein concentration of lysed cells was determined using the QuantiPro BCA assay kit (Sigma-Aldrich), whereby a Cu^{2+}-protein complex is formed and subsequently reduced to Cu^{1+}. To detect this conversion, the bicinchoninic acid (BCA) forms a purple-blue complex with Cu^{1+} in alkaline environments. As the amount of reduction is proportional to the amount of protein present, it is possible to correlate the colour change to the amount of protein present in the sample.

Firstly, the QuantiPro working reagent, made up of the QuantiPro buffer QA ($^{25}/_{51}$ parts of the total volume), QuantiPro BCA QB ($^{25}/_{51}$ parts) and the Copper(II) sulphate solution ($^{1}/_{51}$ parts) is prepared (Table 2.3). Then, 50 µL of the working solution is added to 50 µL of cell lysate, which was previously transferred to a 96 flat-well plate. Additionally, a bovine serum albumin (BSA) dilution series (2-0 mg/mL) is made up to generate a standard curve. Incubation took place at 60°C for 1 h, 37°C for 2 hrs or overnight at RT. The absorbance was read on the spectrophotometer (Wallac 1420 Victor^2 multi label plate reader (PerkinElmer)) at 595 nm at 1 s exposure. The protein

concentration was determined by extrapolating the values from the standard curve set up with BSA.

Table 2.3: Components of the BCA assay kit

Buffers	Components
Buffer QA	Sodium carbonate
	Sodium tartate
	Sodium bicarbonate
	All in 0.2M NaOH, pH 11.25
Buffer BCA QB	4% bicinchoninic acid solution, pH 8.5
Copper(II) sulphate	4% (w/v) copper(II) sulphate, pentahydrate solution

A quicker and more accurate method to determine the protein concentration is provided by the Advanced Protein Assay (APAR, Cytoskeleton, Inc.). Again, a BSA standard curve was made up (2 - 0 mg/mL). 5 µL of cell lysate was pipetted into each well of a 96 flat-well plate and 200 µL of the APAR, diluted 1:5 with de-ionised H_2O, was added to each well. Absorbance was read immediately on the spectrophotometer (Wallac 1420 Victor^2 (PerkinElmer)) at 595 nm at 1 s exposure.

2.5.2 Data processing and statistical analysis of the luciferase results

Data was processed in Windows Excel 2010 and statistical analyses were performed in GraphPad Prism 5. Data are represented as mean with error bars showing standard deviation. Results were analysed using Student's T-test or a one-way analysis of variance (ANOVA) followed by a post-hoc Tukey's test, which compares all possible pairs of means to determine if they are significantly different from each other.

2.6 Kinase inhibitor library screening

To perform the screen, approximately 300 kinase inhibitors were obtained from Stefan Knapp (Structural Genomics Consortium, University of Oxford). All inhibitors were provided in a 96 well plate format (0.5 mM concentration, made up in DMSO). 24 h prior to the addition of the kinase inhibitors, 100 µL of a cells solution were plated in clear bottom, black 96 well plates. To prevent wells from drying out and cell death, wells on the outer edges of the plate were left empty. When cells reached 90-100% confluency, 2 µL of the kinase inhibitors were added to a 200 µL final volume in the wells (0.25 mM final concentration of the inhibitors). To control for the DMSO effect, the same volume of pure DMSO was added to the control wells. Cells were placed back in the 37°C incubator for 24 h. Subsequently, the media in the wells was removed and 100 µL of complete RPMI, containing the nuclear dye Hoechst 33258 (final concentration 0.1 µg/mL), was added to the cells. The Hoechst 33258 dye is used to stain DNA and image the cell nuclei. The excitation and emission spectra are 355 nm and 465 nm, respectively.

After a 30 min incubation at 37°C the medium containing the stain was removed and complete RPMI, without phenol red (Life Technologies), was added to the wells. Subsequently, the cells were imaged on a PerkinElmer Operetta® High Content Imaging System machine (PerkinElmer) for expression of GFP, mCherry and Hoechst 33258. Prior to imaging, the correct emission spectra for the respective fluorescent proteins were selected on the machine. In order to measure the intensity as accurately as possible, five different fields of view were selected per well. Pictures were captured in the GFP, mCherry and Hoechst 33258 channels. All compounds were tested in duplicate.

2.6.1 Statistical analysis of the screen results

The results from the screen were analysed on the Harmony® High Content Imaging and Analysis Software (Perkin Elmer). In order to calculate the intensity of the fluorescent proteins, the outline of the nuclei in every well was selected automatically by the software. Then, the outline of the cells was also determined automatically by the software. Automatic detection was done through selecting the best fitting parameters, provided on the software. Subsequently, the software calculated the intensity of green fluorescent protein (GFP) / mCherry / Hoechst 33258 per cell by taking into account all five fields of view per well.

Once the values for the fluorescence intensities were obtained, a non-parametric method was chosen and the results were analysed by Dr Sheng Yu and Dr Francesca Meteora Buffa (Computational Genomics, University of Oxford).

First, it was assessed how well the means of the negative control correlated with the means of the compounds on the plate. This was necessary to determine if the negative control DMSO, present on each plate, would be a good metric to normalise the outcome of each well to. Second, a modified z-score was calculated for each compound. This was done according to the following formula:

$$z' = \frac{x - \mu_{nt}}{\sigma_{nt}}$$

Where z' is the modified z-score, x is the mean signal of each well, μ_{nt} is the mean of the negative control and σ_{nt} is the standard deviation of the negative control. As the screen was conducted in duplicate, the z-score was calculated for each replicate. Subsequently, a rank product was determined to identify the top hits and estimate the rank of the replicates.

2.7 Gel electrophoresis and western blotting

2.7.1 Protein preparation

To assess the presence of a protein in a cell, gel electrophoresis followed by western blotting was performed. Firstly, cells were lysed in TNN lysis buffer and the amount of protein was determined by the APAR method (section 2.5.1). The correct amount of protein was pipetted into an eppendorf tube and if necessary, diluted with TNN lysis buffer (Table 2.4). Subsequently, sample buffer was added to the protein solution and the sample was denatured at 95°C for 10 min. The presence of the reducing reagent β-mercaptoethanol in the sample buffer ensured that the disulfide linkages in the proteins were broken, which lead to the loss of the tertiary and the quaternary structure of the protein. This allowed the proteins to migrate through the acrylamide gel once the electric field was applied (see section 2.7.2). In addition, the glycerol in the sample buffer decreased the density of the protein and allowed it to sink to the bottom of the well once the sample was loaded onto the gel.

Table 2.4: Composition of the TNN lysis buffer and sample buffer used for western blotting

TNN lysis buffer	
1M Tris HCl pH 7.8 (mL)	10
1M sodium chloride (NaCl) (mL)	12.5
Halt Protease inhibitor cocktail, EDTA-free (µL, Thermo Scientific)	500
IGEPAL (µL)	250
De-ionised H_2O (mL)	Up to 50

Sample buffer (3x)	
1M Tris HCl (pH 6.8) (mL)	1.5
Glycerol	2.4
10% Sodium dodecyl sulphate (SDS) (mL)	4.8
β-mercaptoethanol (mL)	1.2
Bromophenol blue (mg)	80

2.7.2 SDS-PAGE

To visualise the proteins of interest the samples were loaded onto a 10% acrylamide gel and an electric field was applied to separate the proteins by their sizes (SDS-polyacrylamide gel electrophoresis (PAGE)).

The acrylamide gels consisted of a 10% resolving gel and a 5% stacking gel, which were cast between two glass plates. Firstly, the resolving gel was prepared (for ingredients and amounts see (Table 2.5). Among other ingredients, the resolving gel contained SDS, ammonium persulfate (APS) and tetramethylethylenediamine (TEMED). While SDS served to apply a negative charge to the denatured proteins thereby allowing them to run through the gel, APS and TEMED, once added, started the polymerisation of the acrylamide and therefore had to be added last. Once APS and TEMED were added the resolving gel was cast between the two glass plates and allowed to set. To assure that the top edge of the gel was even, which was important for the running of the proteins, and to avoid evaporation, 100% ethanol was added on top of the resolving gel before it set.

Table 2.5: Composition of the resolving and stacking gel

10% Resolving gel	
Deionised H_2O (mL)	5.9
1.5M Tris HCl pH 8.8 (mL)	3.8
10% SDS (μL, Sigma-Aldrich)	0.15
30% Acrylamide/Bis-acrylamide (mL) (Acrylamide, Bio-Rad)	5
10% APS (μL) (Sigma-Aldrich)	150
TEMED (μL) (Sigma-Aldrich)	20
5% Stacking gel	
Deionised H_2O (mL)	4.1
1.5M Tris HCl pH 6.8 (mL)	0.75
10% SDS (μL, Sigma-Aldrich)	60
30% Acrylamide/Bis-acrylamide (mL) (Acrylamide, Bio-Rad)	1
10% APS (μL) (Sigma-Aldrich)	60
TEMED (μL) (Sigma-Aldrich)	15

While the resolving gel was setting, the stacking gel was prepared (Table 2.5) and pipetted onto the set resolving gel after removing the ethanol. A plastic comb (1.5 mm thick) was inserted between the two glass plates to create the wells for the loading of the protein samples. Once everything was set, the glass plates were placed in running buffer (Table 2.6) and the gel was left to equilibrate for 20-30 min at RT.

Alternatively, samples and protein standards were loaded onto pre-cast gels (Bio-Rad). Subsequently, the samples were loaded alongside protein standards (Precision Plus

Protein All Blue Standards, Bio-Rad or Spectra Multicolor Broad Range Protein Ladder Thermo Scientific), and run at 200 V for 30-40 min using a Mini-Protean electrophoresis cell (Bio-Rad).

Table 2.6: Composition of running and transfer buffer for SDS-PAGE

Running buffer pH 8.3 (5x)	
Tris base (g)	9.9
Glycine (g)	43.2
SDS (g)	3.0
Deionised H_2O (mL)	600
To be diluted five times in H_2O before use.	
Transfer buffer pH 8.3	
25 mM tris base (g)	3.029
Deionised H_2O (mL)	800
192 mM glycine (g)	14.4
Methanol (mL)	200

2.7.3 Protein transfer

The proteins that migrated through the gel and aligned according to their sizes were next transferred onto a polyvinylidene fluoride (PVDF) or nitrocellulose membrane using a Mini Trans-blot electrophoretic transfer cell. As the PVDF membranes are hydrophobic they had to be activated beforehand with methanol. For this, the membrane was incubated for a few seconds in methanol and subsequently in H_2O to wash off the excess methanol and left to equilibrate in transfer buffer until it was used.

To assemble the transfer cassette, two sheets of Watman filter paper were placed on top of a sponge. This was followed by the acrylamide gel containing the proteins. The activated PVDF membrane was then placed on top of the gel to allow the transfer of the proteins from the gel on the negative electrode side, to the PVDF membrane on the positive electrode side. To make the cassette complete, another two sheets of Watman filter paper were placed on top of the membrane, followed by another sponge. The cassette was subsequently placed in the transfer cell and transfer buffer was added to it (Table 2.6). The transfer was performed at 150 milliampere (mA) overnight at 4°C or at 300 mA for 90 min at 4°C. When proteins >140 kilodaltons (kDa) were transferred the electrophoretic transfer cell was placed in a polystyrene box with ice and the transfer was performed at 400 mA for 90 min at 4°C.

2.7.4 Western blotting

To visualise the proteins now bound to the PVDF or nitrocellulose membrane, the membrane was blocked for 30 min at RT in 5% skimmed milk, made up in PBS containing 0.1% Tween (PBS-T), to decrease the background noise by blocking non-specific binding. The primary antibodies were diluted in 5% skimmed milk (Table 2.2) and the membranes were incubated for 1-3 h at RT or overnight at 4°C, depending on the antibody. Afterwards, the membranes were washed three times in PBS-T for 10 min at RT and incubated with the secondary antibody, conjugated to horseradish peroxidase (HRP) for 1 h at RT followed by three 10 min wash steps with PBS-T at RT. To develop the membrane, Enhanced Chemiluminescence (ECL) Western Blotting Detection Reagents (Amersham, GE Healthcare) were added to the membrane and the blot was visualised by exposure to X-ray films (Fujifilm).

2.8 Molecular Biology Protocols – DNA plasmid preparation

2.8.1 Plasmid amplification

Escherichia coli (*E.coli*) bacteria were taken from the -80°C freezer and thawed on ice for 10 min before adding 1-3 µL of plasmid DNA stock and incubating for 20 min on ice. In order to heat-shock the bacteria and allow the uptake of the target DNA, the bacteria were placed in a water bath at 37°C for 3 min. 900 µL of lysogeny broth medium (LB-medium, Sigma-Aldrich) was added and the bacteria were placed back at 37°C for another 15 min. Afterwards, 100 µL of the bacterial solution was streaked out onto a bacterial plate containing lysogeny broth agar (LB-agar, Sigma-Aldrich) supplemented with 50 µg/mL of the antibiotic kanamycin or ampicillin or 170 µg/mL chloramphenicol, depending on the resistance cassette present in the plasmid. The antibiotic guarantees that only the bacteria that have taken up the plasmid that contains the gene for the enzyme that can neutralise the antibiotic will survive. The bacterial plates were placed in an incubator at 37°C overnight with the LB-agar side facing upwards.

2.8.2 Picking colonies

After the overnight incubation, the desired colonies were picked from the bacterial plate by using a 20 µL pipette and placing the colony into 5 mL of LB-medium, containing the desired antibody, in a 15 mL Falcon tube. The Falcon tube was placed in a shaker at 37°C overnight. Subsequently, if a high yield was required, a 250 µL aliquot of the bacteria was taken and added to 250 mL of LB-medium containing the desired antibiotic and shaken overnight at 37°C. This protocol was later adjusted to require less LB-medium in the last step (130 mL instead of 250 mL) and the amount of bacteria transferred from the start culture to the 130 mL was adjusted. Glycerol stocks were

generated by adding 150 µL of glycerol to 850 µL of the bacterial culture and vortexing. Glycerol stocks were stored at -80°C.

2.8.3 Plasmid extraction and purification

In order to extract the DNA from the 5 mL bacterial cultures, the QIAprep Spin Miniprep kit (miniprep kit, Qiagen) was used. Consequently, the DNA extraction of 130/250 mL was performed with the QIAGEN Plasmid *Plus* Maxi Kit (maxiprep kit, Qiagen).

Briefly, the bacteria was spun at 4500 rcf for 15-20 min at 4°C and resuspended with buffer P1. Buffer P2 was used to lyse the bacteria after which the addition of buffer N3/S1 (for 15 mL bacterial cultures and 130/250 mL, respectively) neutralised the reaction. In the case of the miniprep kit, the cell lysate was spun for 10 min at 16,000 rcf and supernatant was applied to the binding column, which was subsequently washed multiple times with the buffer PB. The maxiprep kit, however, first required the cell lysate to be incubated for 10 min at RT and then filtered through a syringe. After the addition of the buffer B1, the filtrate was drawn through a binding column using a vacuum pump. In both kits, DNA was washed using buffer PB or ETR, for the miniprep kit or maxiprep kit, respectively, and subsequently with the buffer PE. Finally, the DNA was eluted into another eppendorf tube using either buffer EB or TE (miniprep and maxiprep kit, respectively). The concentration of the DNA was measured on a spectrophotometer (NanoDrop Products).

2.9 Molecular Biology Protocols - Cloning

2.9.1 Restriction digest

To test for the presence of a specific sequence within a plasmid, a test digest with restriction endonucleases was performed on the DNA obtained from the plasmid extractions. For this a 10 µL digest was performed containing 0.5-1 µg of plasmid DNA, 1 µL of 10 x BSA (to aid the function of the enzyme), 0.2 µL of the restriction endonuclease (20,000 unit/mL), 1 µL of the appropriate reaction buffer (all New England Biolabs (NEB)), made up to 10 µL with nuclease-free H_2O. If the enzyme exhibited a low activity or if two enzymes were used together, the volumes were adjusted according to the activity of the enzymes in the different reaction buffers. This information was provided by the Double Digest Finder on the NEB website (New England BioLabs Inc., 2014). The digest took place at 37°C for 1 h after which 1 µL of the reaction mix was diluted with 9 µL of H_2O and 2 µL of 5 x sample buffer (NEB) and loaded onto an agarose gel. If DNA was digested for cloning purposes (section 2.9.5), the reaction volume was 75 µL or 100 µL and the amounts of the components were scaled up accordingly.

2.9.2 Agarose gel electrophoresis

To test for the presence of DNA and to visualise the different sized fragments resulting from the restriction digest, agarose gel electrophoresis was performed. In this assay, DNA was loaded onto an agarose gel and current was applied. As the DNA is positively charged it migrated to the negative electrode – the smaller sized fragments migrating faster than the bigger ones.

To set up the electrophoresis a 1% agarose gel was prepared. The gel was made up with tris-acetate-EDTA (TAE) buffer containing ethidium bromide (EtBr, 0.5 µg/mL,

Sigma-Aldrich). This was to allow the visualisation of nucleic acids as EtBr intercalates with DNA and fluoresces when exposed to UV light. The DNA samples were loaded onto the gel, alongside a DNA ladder (Bioline) and the gel was run for 40-60 min at 40/120 V, depending on the size of the agarose gel, or until the different-sized fragments were clearly separated. The gels were placed in the UV transilluminator Alpha Imager (Alpha Innotech, USA) and the fragments were visualised. The analyses were performed using the programme FluorChem HD2.

2.9.3 Polymerase chain reaction (PCR)

A PCR allows testing for the presence or analysis of a specific sequence within the DNA. It is comprised of five different steps: the initialisation step performed at 98°C to activate the polymerase enzyme; the annealing step, whereby the primers are allowed to bind to the DNA template – this is normally set up a few degrees lower than the melting temperature (T_m) of the primers; the elongation step, which allows the polymerase to construct a new strand complementary to the parental DNA template using new nucleotides; and the final elongation step, to ascertain that the DNA is fully extended.

In order to perform the PCR the Phusion High-Fidelity DNA Polymerase Kit (Thermo Scientific) was used. This kit provided a polymerase enzyme and a reaction buffer, already containing magnesium ions (to increase the enzyme function) and deoxyribonucelotide triphosphates (dNTPs) needed for the synthesis of the complementary DNA strand. Manufacturer's instructions were followed. Briefly, to set up the PCRs all components were pipetted into PCR tubes or into different wells on PCR plates (Table 2.7).

Table 2.7: Components for PCRs

Component	*50 µL reaction*	*10 µL reaction*
H_2O	Up to 50 µL	Up to 10 µL
2x Phusion Master Mix	25 µL	5 µL
Forward primer	0.5 µM	
Reverse primer	0.5 µM	
Template DNA	10 ng	

The PCRs were performed on a ThermoCycler (Thermo Scientific) using the cycles described above and in Table 2.8. The annealing temperature was adjusted for each primer pair. If the primers were longer than 20 nucleotides, the temperature of the cycle was set at 3°C higher than the T_m of the lower T_m primer. If the primers were smaller than, or equal to 20 nucleotides long, the annealing temperature was set up to be the same as the lower T_m primer. The extension time was adjusted according to the length and origin of the fragment that was to be amplified (Table 2.8). If the fragment was to be amplified from a plasmid or genomic DNA the extension time equalled 15 s or 30 s per 1 kb, respectively.

Table 2.8: Cycling instructions for PCRs.

Cycle step	*Temperature*	*Time*	*Cycles*
Initial denaturation	98	60 s	1
Denaturation	98	10 s	30-35
Annealing	Adjust	20 s	
Extension	72	Adjust	
Final extension – 1	72	7 min	1
Final extension – 2	4	18 h	

PCR products were subsequently tested on agarose gel electrophoresis (section 2.9.2).

2.9.4 Primers

Oligonucleotide primers were designed in the laboratory and synthesised by Sigma-Aldrich (Table 2.9).

2.9.5 Cloning

In order to construct a new plasmid, specific sequences had to be added to or removed from already existing plasmids. To accomplish this, the first step was a restriction digest in the recipient and donor plasmids (section 2.9.1) with restriction endonucleases producing compatible DNA overhangs within the recipient plasmid and the fragment from the donor plasmid. In some instances, the fragment to be ligated into the recipient vector would be generated by PCR. However, digests would take place in the same way as described for fragments originating from the donor plasmid.

To prevent re-ligation of the recipient plasmid treatment with Calf Intestinal Alkaline Phosphatase (CIAP) was performed for 1 h at 37°C. Subsequently, the recipient plasmid was purified using the miniprep kit.

The success of the restriction digests was assessed by agarose gel electrophoresis. If necessary, the desired fragment, produced from the donor plasmid or PCR, was excised from the gel and purified using the QIAquick Gel Extraction Kit (Qiagen).

For the ligation, the fragment and the recipient plasmid were incubated together with a T4 DNA ligase (NEB), ligation buffer and H_2O (made up to 20 µL reaction volume) for 1 h at RT. To control for the specificity and efficiency of the ligation, control ligations without a fragment or without T4 DNA ligase were also set up. Afterwards, the DNA

was inserted into bacteria and amplified (section 2.8.1). Colonies were picked (section 2.8.2) and grown up over the following night. Plasmid extraction (section 2.8.3) and test digests (section 2.9.1) were performed over the following days. To confirm that the ligation was performed correctly, DNA samples were sequenced (section 2.9.6).

2.9.6 Sequencing of plasmids

Sequencing of plasmids was performed at Source BioScience LifeSciences at the Wellcome Trust Centre for Human Genetics in Oxford by the Sanger method. For this, a minimum of 100 ng/μL of the sample DNA were placed in an eppendorf tube. The primers were specifically designed to bind just upstream of the start of the desired sequence to be read (5' end) and just downstream of the end of the sequence (3' end). The primers were used at a concentration of 3.2 pmol/μL. Results were subsequently visualised by the programme ABI Viewer and the plasmid editor software ApE.

2.9.7 Construction of primers

To sequence plasmids or to perform PCRs primers had to be constructed beforehand (Table 2.9). If done manually, a region of 16-24 bp upstream (5') of the sequence to be tested was selected for the forward primer. The same was done for a 16-24 bp region downstream (3') for the reverse primer. Ideal primers contained a guanine (G) or a cytosine (C) base at the 5' end, a GC-content not higher than 50% and T_m of approximately 57°C. However, this was not always possible and the conditions were chosen as closely to the ideal parameter as possible. The main requirement was that the T_ms of the primers were not further apart than 3°C. If avoidable the primers were chosen to not produce any secondary structures within themselves. The properties of the primers were analysed by the web-based programme Multi Primer Analyzer (Thermo

SCIENTIFIC, 2013). Alternatively, the web-based software Primer3 (Untergasser et al., 2012) was used to pick the forward and reverse primers once the desired sequence to be amplified was selected. The conditions for the primers were chosen as described above. Primer were subsequently synthesised by Sigma-Aldrich.

All primers synthesised are summarised in Table 2.9.

Table 2.9: Primer designed and used during the studies.

Application	***Primer sequence***
PCR	
mCherry amplification	5'-TTTAAGCTTATATGGTGAGCAAGGGCG-3'
	3'-AAATCTAGAATCTTGTACAGCTCGTCC-5'
p*MITF*-mCherry amplification	5'-CGAGCTCTTACGCGTGCTA-3'
	3'-TTTGAATTCATCTTGTACAGCTCGTCCATGC-5'
Inverse PCR of pLVX-Tight-Puro	5'-TTTTCTAGACAGATCGCCTGGAGAAGGAT-3'
	3'-TTTTCTAGATGAAGACGAAAGGGCCTCAT-5'
Sequencing	
p*MITF*-mCherry	5'-CCGGTGGTGTATCGGGATAC-3'
	3'-CACTGCATTCTAGTTGTGGTTTG-5'
pMITF-mCherry-pLVX-puro	5'-TACAGGGACAGCAGAGATCCA-3'
	3'-AAAGCAGCGTATCCACATAGCG-5'
	5'-CCGGTGGTGTATCGGGATAC-3'
pLVX-puro	5'-GGTACAGTGCAGGGGAAAGA-3'
p*Brn2*-GFP	3'-GAGCCTATGGAAAAACGC-5'
	3'-GTGGTGCAGATGAACTTCAG-5'
p*Brn2*-GFP-p*MITF*-mCherry-pLVX-puro with and without TB	5'-TACAGGGACAGCAGAGATCCA-3'
	3'-AAAGCAGCGTATCCACATAGCG-5'
	5'-CCGGTGGTGTATCGGGATAC-3'
	5'-GCAGCAGTAATAGCAAGAGCAG-3'
	5'-CTGAGCAAAGACCCCAAC-3'
WT, Δ368 and Δ261 p*Brn2*-Luc	5'-GGAGCGGCCGCAATAAAATATC-3'
	3'-GAACCAGGGCGTATCTCTTCATAG-5'

3 Generation of fluorescent lentiviral reporter constructs

3.1 Introduction

3.1.1 Rheostat model of MITF

MITF has been implicated in melanomagenesis ('lineage oncogene') (Garraway and Sellers, 2006; Garraway et al., 2005b) although on the other hand it has been shown to act as a tumour suppressor in melanoma (Carreira et al., 2006; Loercher et al., 2005; Wellbrock and Marais, 2005). This was previously discussed in Chapter 1 (section 1.9). To reconcile these apparently contradictory effects of MITF, the rheostat model was introduced to explain different effects of MITF under different conditions (Carreira et al., 2006). Based on this model, cells can be allocated into one of three differentiation states: differentiated, proliferative and invasive, potentially stem-like (Figure 3.1).

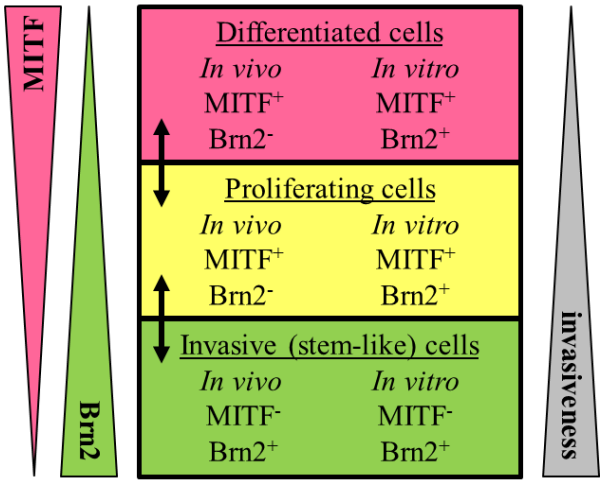


Figure 3.1: MITF and Brn2 transcription factor expression in differentiated, proliferating and invasive (potentially stem-like) cells in melanoma. *In vitro*, both markers are co-expressed, while *in vivo* there are clearly two different subpopulations, expressing either MITF or Brn2. With increasing expression of Brn2 and decreasing expression of MITF, cells become more invasive, leading to interconversion of different phenotypes in melanoma (black arrows). This phenomenon is described as phenotype-switching. Adapted from (Hoek and Goding, 2010)

While non-proliferating, differentiated cells express high levels of MITF, which activates the transcription of pigment genes, such as *Tyrosinase* (Bertolotto et al., 1996; Cheli et al., 2010; Steingrimsson et al., 2004), MITF-expressing proliferating cells would activate the transcription of genes implicated in cell proliferation and survival such as *CDK2* and *BCL2*, respectively (Du et al., 2004; Goding, 2011; McGill et al.,

2002). Invasive cells, on the other hand, would be unpigmented as MITF protein levels would be low or non-existent. Additionally, low MITF levels would also lead to cell cycle arrest and promote cells to become more invasive and prone to metastasise, and potentially acquire melanocyte stem cell-like properties (Carreira et al., 2006; Cheli et al., 2011; Goding, 2011). While the diagram summarises the expression of Brn2 and MITF in melanoma, in development Brn2 is not expressed. However, MITF is still regulated in a similar fashion but the precise mechanisms remain to be established.

3.1.2 Relationship between Brn2 and MITF

As established before, Brn2 is a potential marker for stem-like or invasive cells (Pinner et al., 2009) (section 1.10.2), which makes it an interesting candidate as a possible reporter to inform on cellular status. Furthermore, the interaction between Brn2 and MITF has been heavily investigated (Goodall et al., 2008; Wellbrock et al., 2008). In melanocytic cells one of the best-defined Brn2 targets is MITF (Goodall et al., 2008), with overexpressed Brn2 repressing MITF expression *in vitro* (Goodall et al., 2008). Similarly, *in vivo,* where expression of Brn2 and MITF were mutually exclusive in melanoma tissue, the presence of these transcription factors seems to mark different subpopulations in melanoma (Thurber et al., 2011). This is consistent with Brn2 acting as a repressor of MITF expression. Other reports affirming the same conclusions demonstrated how cells that were originally poorly pigmented, $Brn2^{low}$ melanoma cells, metastasised *in vivo* from the primary tumour through the blood system, with increased Brn2 expression (Pinner et al., 2009). Once cells had reached secondary sites, Brn2 expression was decreased again and pigmentation was re-induced (Pinner et al., 2009). While these reports confirm that *in vivo* Brn2 is indeed involved in the regulation of pigmentation genes, such as MITF (even though this was not directly demonstrated in

this study (Pinner et al., 2009)), it also shows that Brn2 might be involved in the metastasis/invasion process of melanoma cells.

Contrary to the findings above, in melanoma cell lines containing a $BRAF^{V600E}$ mutation, endogenous Brn2 increased the expression of MITF and therefore acts as an activator of MITF (Wellbrock et al., 2008). This was supported by Thurber and colleagues who demonstrated that Brn2 and MITF were co-expressed *in vitro* (Thurber et al., 2011). However, it is unclear whether the transcription factors were active at the same time *in vitro*. To reconcile the findings of Brn2 being a repressor and an activator of MITF it is possible that different microenvironments lead to different post-translational modifications, such as phosphorylation of Brn2 (Cook and Sturm, 2008; Nieto et al., 2007), that determine its capacity to regulate gene expression. Alternatively, the effect of Brn2 could also be mediated by protein levels.

Based on the interplay between Brn2 and MITF we aimed to generate a dual reporter system comprising the promoters of these two transcription factors, driving expression of two different fluorescent proteins.

3.1.3 Lentiviral particles

3.1.3.1 Introduction

To generate dual reporter cell lines, we chose to use a lentiviral system. Lentiviruses have been widely applied as vehicles for the delivery of genomic material into mammalian cells (Brambrink et al., 2008; Naldini et al., 1996). These viruses carry the genetic material in the form of RNA and contain components that will convert RNA into DNA and subsequently insert the DNA into the host genome to allow stable expression (Baltimore, 1974; Esposito and Craigie, 1999). For this, viruses make use of their own reverse transcriptase (for the conversion of RNA into DNA) and integrase

(for the integration of the DNA into the host genome) (Dropulic, 2011). The advantage of using integrating viruses over plasmid transfections reflects their ability to generate stable clonal cell lines. Daughter cells derived from virally transduced cells will contain the same genetic material and therefore should allow continuous expression of the transgene. Another advantage of using lentiviruses over other integrating viral vectors, such as Moloney murine leukaemia virus, is that lentiviruses infect a wide range of mammalian cell lines and are not dependent on cell proliferation (Naldini et al., 1996; Salmon and Trono, 2007). This has been exploited particularly in the field of stem cell research (Brambrink et al., 2008).

However, there are also disadvantages to using integrating lentiviruses. The integration event can occur in random places in the cell genome and even in often-transcribed loci (Hacein-Bey-Abina et al., 2003). This might lead to deregulation of cellular genes (including tumour suppressors and proto oncogenes) and perhaps also to constitutive expression of the transgene when in fact it is required to be transcribed only upon the activation of its own promoter (Hacein-Bey-Abina et al., 2003). The transforming consequences of this process are referred to as insertional mutagenesis and were described in a clinical trial involving patients who developed leukaemia after having received virally-transduced cells (Hacein-Bey-Abina et al., 2008; Hacein-Bey-Abina et al., 2003). In this case, the integration event of the vector led to uncontrolled cell proliferation through the interaction of the retroviral vector long terminal repeat (LTR) and the promoter of an erythropoietic gene (Hacein-Bey-Abina et al., 2008; Hacein-Bey-Abina et al., 2003). Another disadvantage of lentiviruses is the potential silencing of transgene transcription (Frame et al., 2010; Jahner and Jaenisch, 1985). Therefore, it is important to monitor the expression of the transgene continuously throughout the experiments.

3.1.3.2 Lentiviruses

Lentiviruses are a subset of the Retroviridae virus family, of which the human immunodeficiency virus-1 (HIV-1) is often used as a paradigm for a lentivirus. It comprises of a 9 kb single-stranded positive-sense RNA genome (Sakuma et al., 2012). The genome encodes three major structural proteins Gag, Pol and Env, two regulatory proteins Tat and Rev, as well as four accessory proteins Vif, Vpr, Vpu and Nef. *Gag* encodes viral core proteins and the *Pol* gene encodes enzymes required for viral replication, while *Env* encodes the viral surface glycoprotein gp160, which is exchanged for the *vesicular stomatitis virus envelope glycoprotein (VSV-G)* in lentiviral plasmids used for research. VSV-G confers broad tropisms to a variety of mammalian cell types (Emi et al., 1991; Naldini, 1998; Naldini et al., 1996). The accessory proteins are responsible for viral transcription, splicing and nuclear exports of viral transcripts. Additionally, the genome also contains LTRs that allow viral transcription, reverse transcription and integration.

Viral HIV particles enter the target cell through attaching to the CD4 receptor and its co-receptor C-X-C chemokine receptor type 4 (CXCR4) (Duquenne et al., 2014) and subsequently fusing with the cell membrane. The viral components are then released into the cytoplasm and the RNA is converted into DNA, which is transported to the nucleus and integrated into the host's genome. Subsequently, new viral particles are generated and shed from cells to infect new host cells.

To avoid the generation of replication competent lentiviruses (RCL) the genetic material was separated into three components: two helper plasmids, containing the genes for the structural and enzymatic proteins *Gag* and *Pol* on one plasmid and the gene for *VSV-G* on another. The third plasmid encodes the transgene-of-interest. To further decrease the risk for recombination and RCL generation, the accessory proteins

were deleted. To avoid activating the transcription of host genomic genes by the viral LTRs, which can serve as enhancers for host transcription factor binding (Sakuma et al., 2012), the 3'LTR was deleted to render self-inactivating lentiviral vectors (Yu et al., 1986).

3.1.3.3 Application of lentiviral particles in the current project

To generate dual reporter lentiviral plasmids, lentiviruses from the Lenti-Tet-on-inducible system were modified to render the backbone for lentiviral plasmid engineering. The Tet-inducible system allows the regulation of gene transcription upon the addition of the antibiotic doxycycline. However, for the current project, this level of regulation was not required and as the clonal cell lines were engineered to react to physiological changes, the Tet-related components were removed to render the lentiviral plasmid pLVX-puro. Together with two helper plasmids expressing gag, pol, rev and VSV-G the lentiviral plasmid containing the genes of interest were transfected into Phoenix cells. These produced viral particles that were harvested and subsequently used to transduce 501mel cells (Figure 3.2). Fluorescent protein expression was analysed by flow cytometry and fluorescence microscopy.

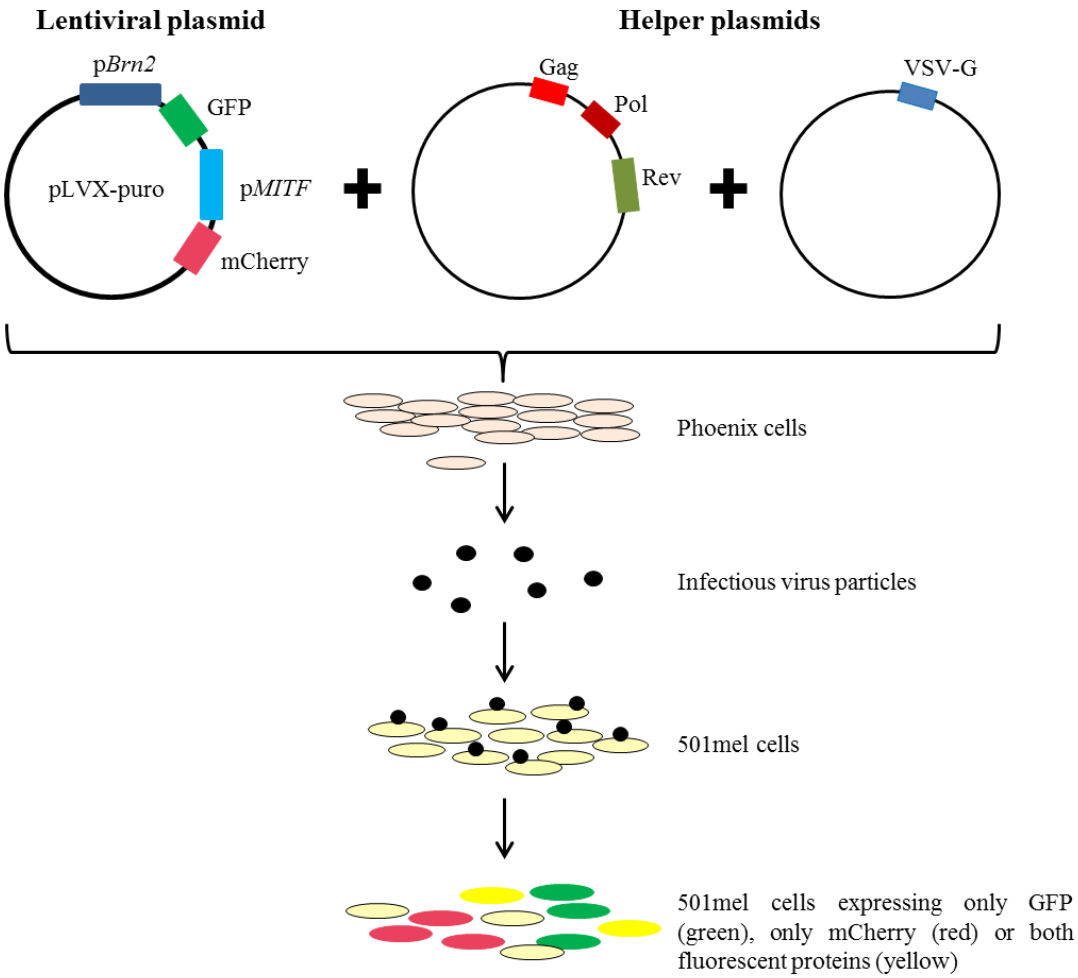


Figure 3.2: Schematic diagram of the generation of lentiviral particles. To generate lentiviral particles encoding the genes of interest, the lentiviral plasmid pLVX-puro together with two helper plasmids were co-transfected into Phoenix cells. Viral particles were harvested and 501mel cells were transduced. Expression of the fluorescent proteins GFP and mCherry was assessed by fluorescence microscopy and flow cytometry.

3.1.4 Chapter objectives

- Construction of dual lentiviral plasmids using the promoters for *MITF* and *Brn2* to express fluorescent proteins mCherry and GFP, respectively.
- Recovery of lentiviral particles and production of stable clonal human melanoma cell lines.
- Kinase inhibitor library screening using the stable clonal cell lines.
- *In vivo* transplantation of monoclonal cell lines to investigate phenotype-switching.

3.2 Results

3.2.1 The MITF and Brn2 promoters are functional and responsive to Sox10

To generate the lentiviral reporter plasmids containing the promoters for *MITF* and *Brn2*, we needed to ensure that the exogenous promoters were functional and responding to external factors.

As starting material, plasmids were used that expressed luciferase upon activation of the human *MITF* or the mouse *Brn2* promoters (p*MITF*-Luc and p*Brn2*-Luc, respectively) (Figure 3.3). While the *MITF* promoter is well defined, less is known about the *Brn2* promoter. The human *MITF* promoter contains binding sites for the transcription factors SRY (sex determining region Y)-box 10 (Sox10), a known activator of the *MITF* promoter (Lee et al., 2000), paired box 3 (Pax3), LEF1, the cAMP response element-binding protein (CREB) (Vance and Goding, 2004) and for Brn2 (Figure 3.3A). The p*MITF*-Luc construct consists of a 2435 bp promoter fragment upstream of the 5' UTR, followed by the luciferase gene. The *Brn2* promoter contains binding sites for the transcription factors TCF and LEF1 flanked by the binding sites for Pax3 (Bonvin et al., 2012). Similar to the p*MITF*-Luc plasmid, the p*Brn2*-Luc construct comprises a 1743 bp mouse *Brn2* promoter fragment upstream of the 5' UTR, followed by the luciferase gene (Figure 3.3B).

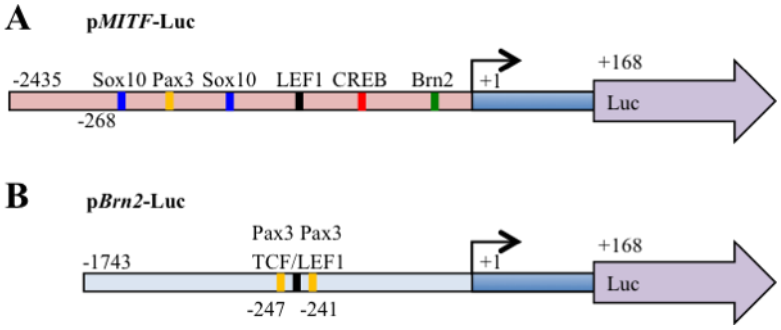


Figure 3.3: Schematic diagram of the human *MITF* (A) and mouse *Brn2* (B) promoters in luciferase expression plasmids. The *MITF* promoter (A) contains a 2.4 kb fragment upstream of the 5' UTR, while the *Brn2* promoter (B) consists of a 1.7 kb fragment. Both promoter constructs comprise a 168 bp 5' UTR followed by the luciferase gene. (A) Adapted from (Vance and Goding, 2004).

To test the activity of the *MITF* promoter, the p*MITF*-Luc plasmid was transfected into the human melanoma cell lines 501mel and SKmel28, together with a plasmid expressing Sox10 (Figure 3.4).

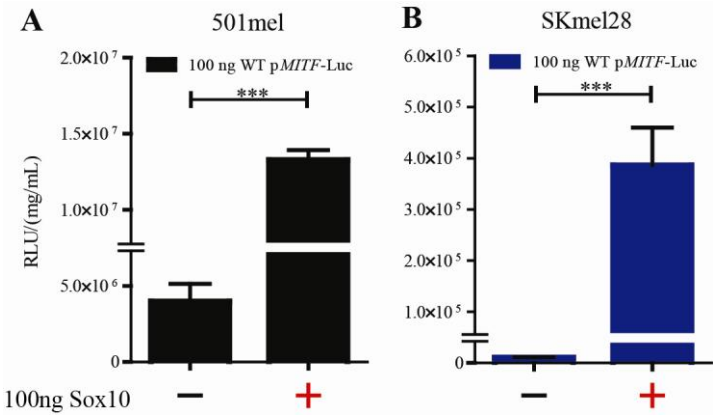


Figure 3.4: Sox10 activates the *MITF* promoter in 501mel and SKmel28 cells. 501mel (**A**) and SKmel28 (**B**) cells were co-transfected with 100 ng p*MITF*-Luc plasmid together with 100 ng of an empty plasmid control or 100 ng of a Sox10 expression plasmid. Luciferase expression was measured 24 h post-transfection and normalised to the protein content per well. The results are expressed as mean ± standard deviation (S.D.), n=3. Statistical analysis was performed using a Student's T-test. *** = $p<0.001$

Transfection of the p*MITF*-Luc plasmid on its own induced luciferase expression in 501mel and SKmel28 cells (Figure 3.4A and B, respectively). Upon co-transfections with the Sox10 expression plasmid luciferase expression increased over 2-fold in 501mel cells and 35-fold in SKmel28 cells compared to the control ($p<0.001$ for both conditions) (Figure 3.4A and B, respectively), demonstrating that the *MITF* promoter is still responsive in these cell lines.

To assess the functionality and responsiveness of the p*Brn2*-Luc reporter construct, transfections were performed with plasmids expressing Pax3 and Sox10 (Figure 3.5). Pax3 is a transcription factor that activates the *Brn2* promoter (Bonvin et al., 2012).

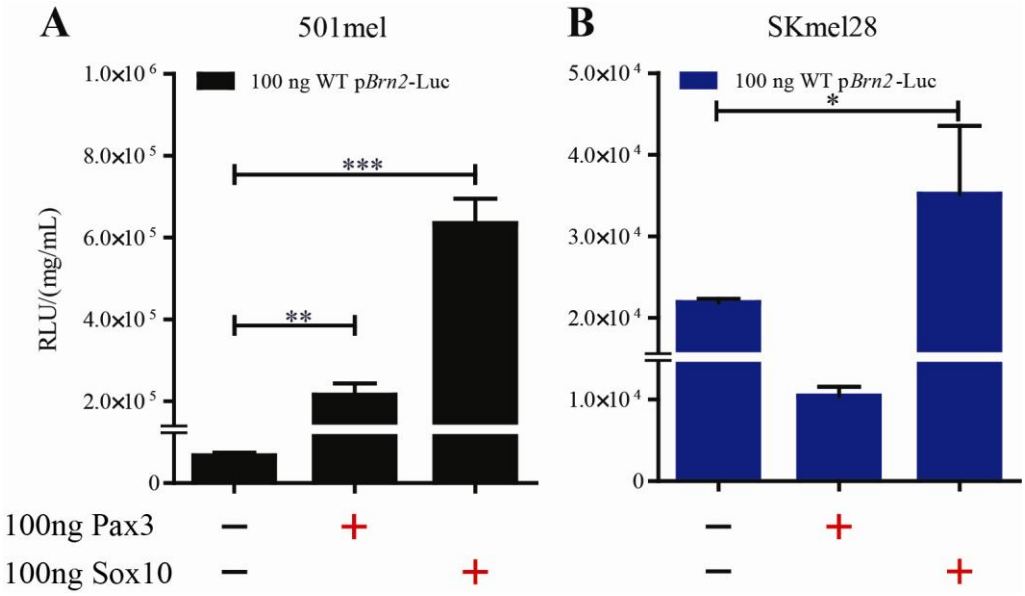


Figure 3.5 Sox10 activates the *Brn2* promoter in 501mel and SKmel28 cells. 501mel (**A**) and SKmel28 (**B**) cells were co-transfected with 100 ng p*Brn2*-Luc plasmid together with 100 ng of an empty plasmid control or with 100 ng of a Pax3 or Sox10 expression plasmid. Luciferase expression was measured 24 h post-transfection and normalised to the protein content per well. The results are expressed as mean ± S.D., n=3. Statistical analysis was performed using a one-way ANOVA followed by a post-hoc Tukey's test. * = p<0.05, ** = p<0.01, *** = p<0.001

In 501mel cells, transfections with the Pax3 and Sox10 expression plasmids induced more than a 3-fold (p<0.01) and a 9.5-fold (p<0.001) activation of the *Brn2* promoter, respectively, compared to the control (Figure 3.5A). While the regulation of the *Brn2* promoter by Pax3 was demonstrated before (Bonvin et al., 2012), the Sox10-induced activation of the *Brn2* promoter is a novel finding.

However, in SKmel28 cells, Pax3 induced a non-significant decrease in *Brn2* promoter activity (50%) while Sox10 activated the promoter by 60% (p<0.05).

3.2.2 pMITF-mCherry: Engineering and testing the reporter plasmid

Once it was demonstrated that the plasmids are functional and responding to promoter activators in the melanoma cell lines, lentiviral plasmids were engineered.

3.2.2.1 The pMITF-mCherry reporter plasmid is functional in vitro

To generate a fluorescent p*MITF* reporter plasmid, the luciferase gene in the p*MITF*-Luc plasmid (p*MITF*-pGL3) was replaced with the mCherry gene (mCherry plasmid was kindly donated by Rasmus Freter, Goding lab).

To clone the mCherry gene from its plasmid into p*MITF*-pGL3, mCherry was PCR-amplified using forward and reverse primers, flanked with unique restriction enzyme sites for HindIII and XbaI, also present in the target plasmid (Figure 3.6).

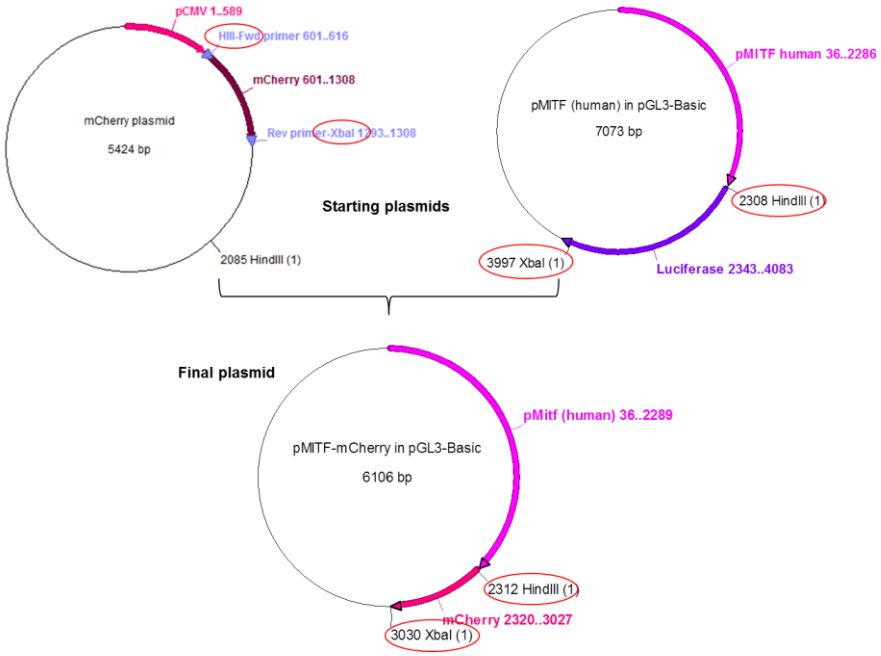


Figure 3.6: Schematic diagram of the generation of the pGL3 plasmid containing the p*MITF*-mCherry fragment. After PCR amplification, the mCherry fragment containing the restriction enzyme ends for HindIII and XbaI, as well as the target plasmid p*MITF*-pGL3 were treated with restriction enzymes for 1 h at 37°C. Subsequently, the mCherry fragment was ligated into the p*MITF*-pGL3 plasmid, resulting in the final plasmid p*MITF*-mCherry-pGL3.

To clone the PCR fragment into the target plasmid, both were subjected to restriction digests with the enzymes HindIII and XbaI, followed by ligation of the fragment into the target plasmid. After the ligation, five colonies (C1-C5) were picked. To test the presence and the correct orientation of the p*MITF*-mCherry fragment in the backbone,

restriction digests with the enzymes MscI and PsiI were performed on C1-C5 (Figure 3.7).

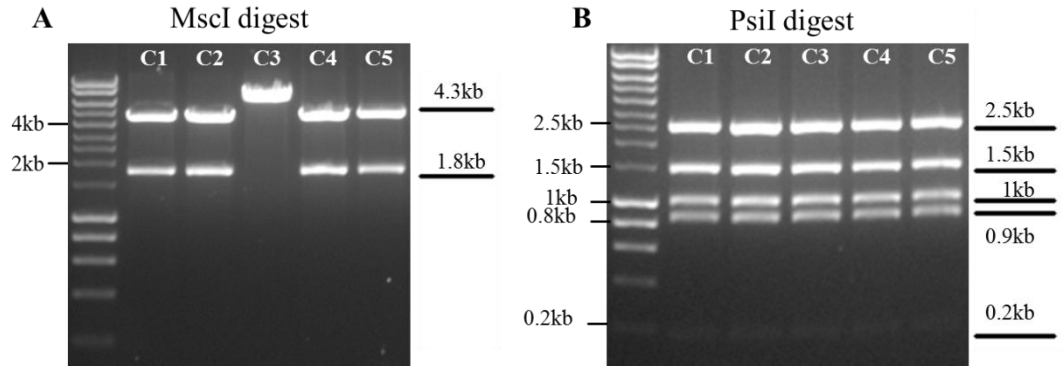
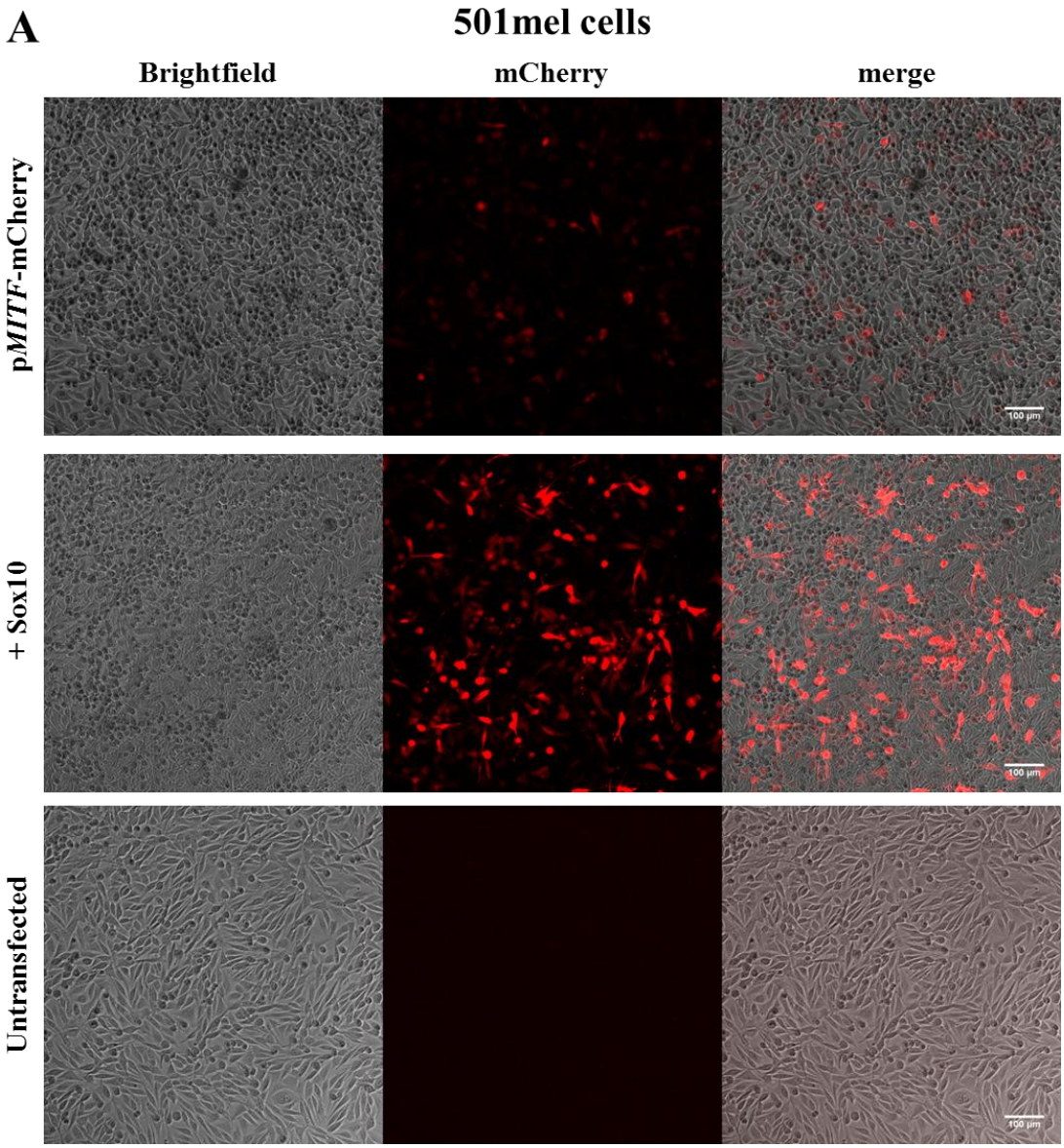


Figure 3.7: Colonies C1, 2, 4 and 5 exhibit the correct digest pattern. Colonies C1-C5 were digested with the restriction enzymes MscI (**A**) and PsiI (**B**) for 1 h at 37°C and subsequently analysed on a 1% agarose gel by electrophoresis. The predicted digest outcomes are to the right of the actual digests, demonstrating that colonies C1, 2, 4 and 5 were correct.

After the digests with MscI (Figure 3.7A) colonies C1, 2, 4 and 5 produced the correct digest pattern, while all colonies showed the correct pattern after treatment with PsiI (Figure 3.7B).

For the next step, one of the clones was chosen and sequenced to confirm that it was correct. To assess its functionality, transfections were performed on 501mel and SKmel28 cells and fluorescence was assessed by microscopy (Figure 3.8).


A
501mel cells
Brightfield
mCherry
merge
pMITF-mCherry
+ Sox10
Untransfected
100 µm
100 µm
100 µm

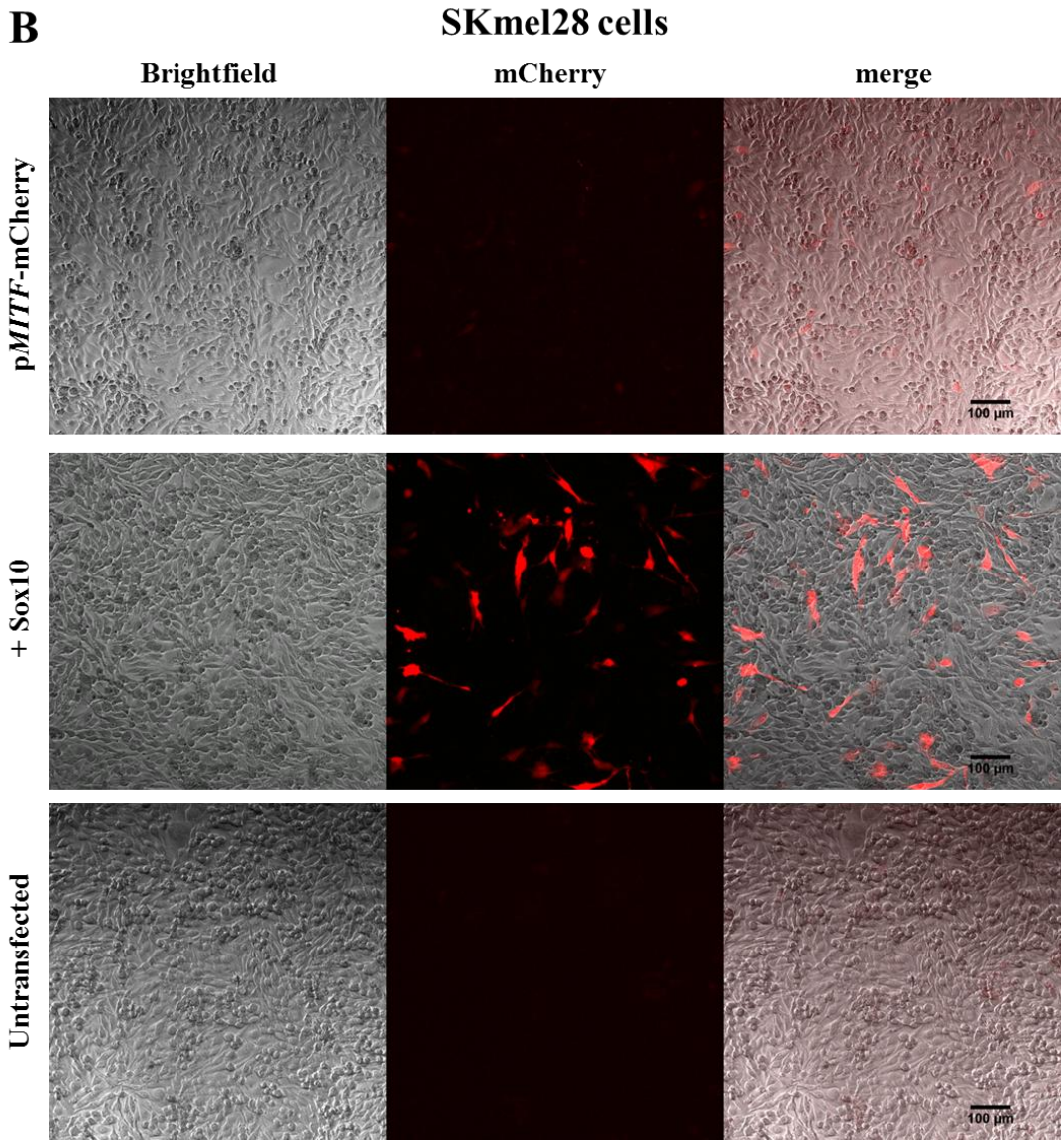


Figure 3.8: mCherry is expressed in 501mel and SKmel28 cells. 400 ng of the reporter plasmid p*MITF*-mCherry and 200 ng of an empty or a Sox10 expression plasmid were transfected into 501mel (**A**) and SKmel28 (**B**) cells (first row and second row, respectively) and mCherry expression was measured 48 h post-transfection. Fluorescence was also measured from untransfected cells to control for background signal. Scale bar represents 100 µm.

Upon transfection of 501mel and SKmel28 cells with the reporter plasmid alone, mCherry expressing cells were detected, although their fluorescence was weak (Figure 3.8 A and B, first row). Co-transfections with a Sox10 expression plasmid increased mCherry expression, suggesting that Sox10 activated the *MITF* promoter in 501mel and SKmel28 cells (Figure 3.8 A and B, second row). To ensure that the increase in mCherry was due to a specific effect of Sox10 on the *MITF* promoter rather than an

increase in general transcription due to an increased amount of DNA, an empty plasmid was co-transfected with the reporter p*MITF*-mCherry plasmid (Figure 3.8 A, first row).

To quantify the increase in mCherry expression, flow cytometry was performed on 501mel and SKmel28 cells after co-transfections (Figure 3.9). In 501mel cells, mCherry expression increased from 0.14% of the live, untransfected cell population to 6.64% in the cells transfected with the reporter plasmid p*MITF*-mCherry (Figure 3.9A, second column). Upon co-transfections with a Sox10 expression plasmid, mCherry expression increased to 15.3% (Figure 3.9A, third column).

In SKmel28 cells, after transfection with p*MITF*-mCherry alone mCherry expression was not detectable by flow cytometry (Figure 3.9B, second column). However, upon co-transfection with a Sox10 expression plasmid, mCherry expression increased to 4.98% (Figure 3.9B, third column).

In both cell lines, these results confirm that Sox10 activates the *MITF* promoter and increases mCherry expression. Nonetheless, this increase is more striking in microscopy than in flow cytometry. This might stem from the fact that flow cytometry measures the number of cells that detectably express fluorescent proteins, while cells expressing low levels of MITF might be not detected. This was also reflected in transfections with the reporter plasmid alone, particularly in SKmel28 cells (Figure 3.8B, first row vs Figure 3.9B).

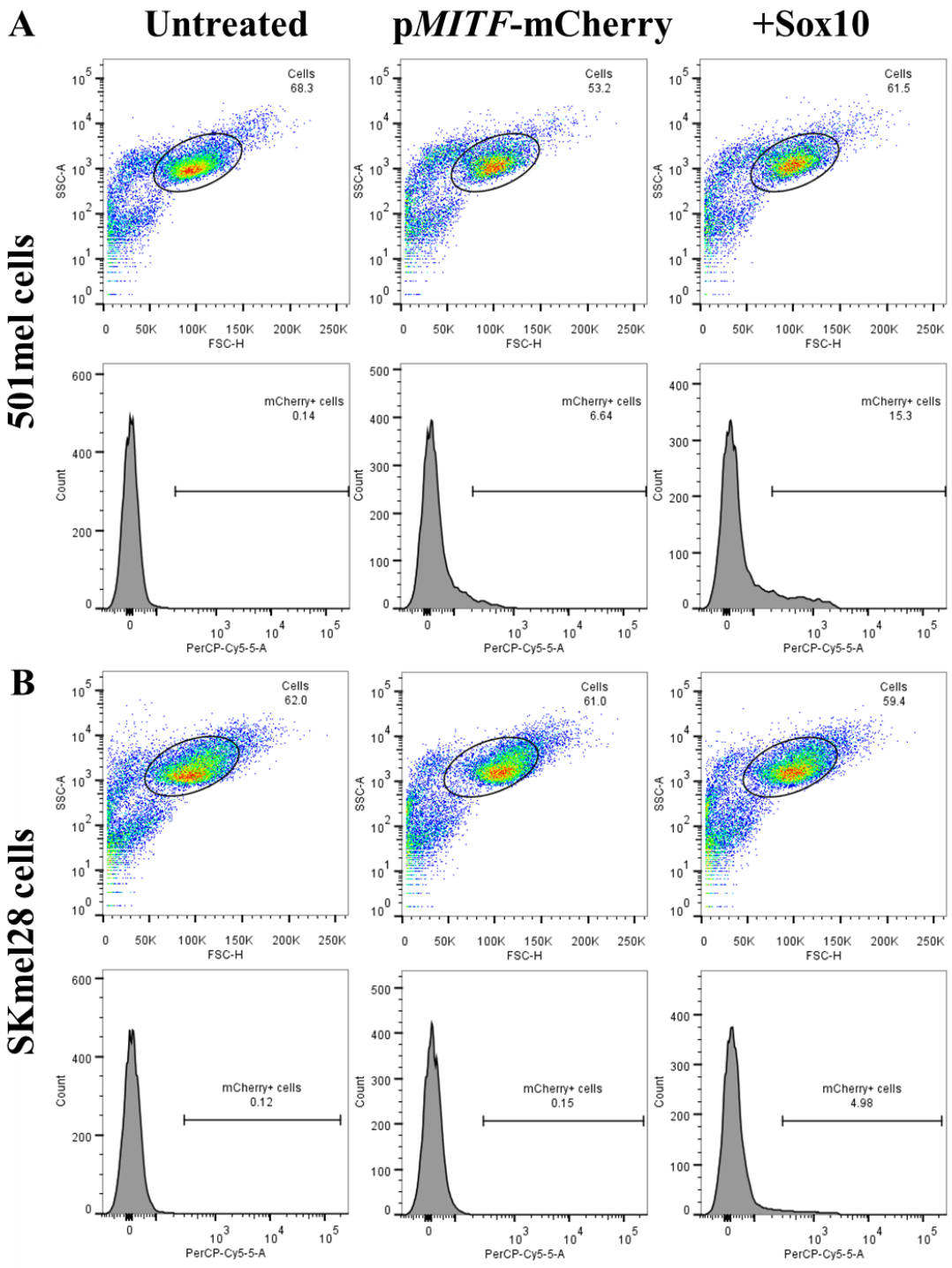


Figure 3.9: Sox10 increases mCherry expression in 501mel and SKmel28 cells. 400 ng of the reporter plasmid p*MITF*-mCherry were co-transfected with 200 ng of an empty plasmid or a Sox10 expression plasmid into 501mel (**A**) and SKmel28 (**B**) cells. Fluorescence was measured 24 h post-transfection using flow cytometry.

3.2.2.2 The lentiviral pMITF-mCherry reporter plasmid is functional in vitro

Having established that the p*MITF*-mCherry reporter plasmid was functional, the next step was to engineer lentiviral plasmids. To this end, the lentiviral plasmid pLVX-

Tight-Puro was used (section 3.1.3.3). To generate this lentiviral plasmid, the p*MITF*-mCherry fragment from the pGL3-Basic plasmid was PCR-amplified with forward and reverse primers containing restriction sites for the enzymes MluI and EcoRI, respectively (Figure 3.10). Restriction sites for both enzymes were also present in the target plasmid pLVX-Tight-Puro. Once the fragment was amplified, a restriction digest with the above-mentioned enzymes was performed, together with the pLVX-Tight-Puro plasmid, and ligated into the latter (Figure 3.10).

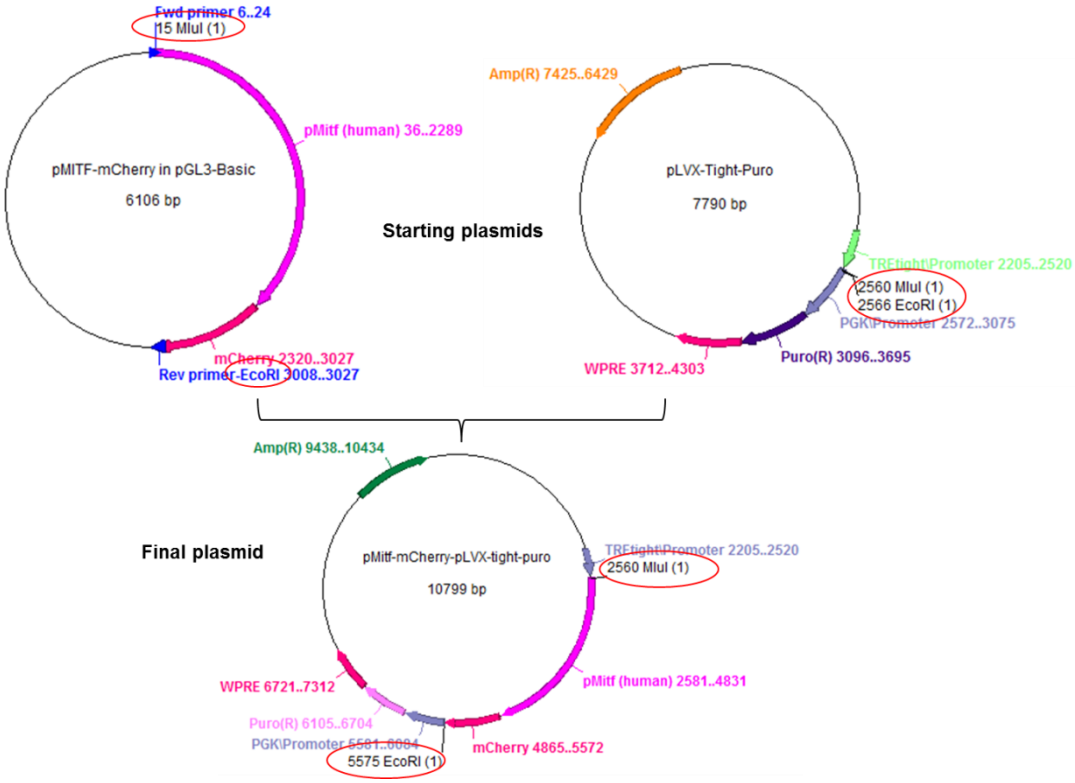


Figure 3.10: Schematic diagram of the generation of the lentiviral plasmid pLVX-Tight-Puro containing the p*MITF*-mCherry fragment. After PCR amplification of the p*MITF*-mCherry fragment, the target plasmid and the fragment were digested with the restriction endonucleases MluI and EcoRI for 1 h at 37°C. The fragment was ligated into the target plasmid, resulting in the final plasmid p*MITF*-mCherry-pLVX-Tight-Puro.

After the ligation, *E.coli* bacteria were transformed and five colonies were picked (C1-C5). Restriction digests were performed using the enzymes PvuII and PsiI on C1-C5 to assess the ligation success and the orientation of the fragment (Figure 3.11). Sequence analyses were performed to confirm that the resulting plasmids p*MITF*-mCherry-pLVX-Tight-Puro were correct.

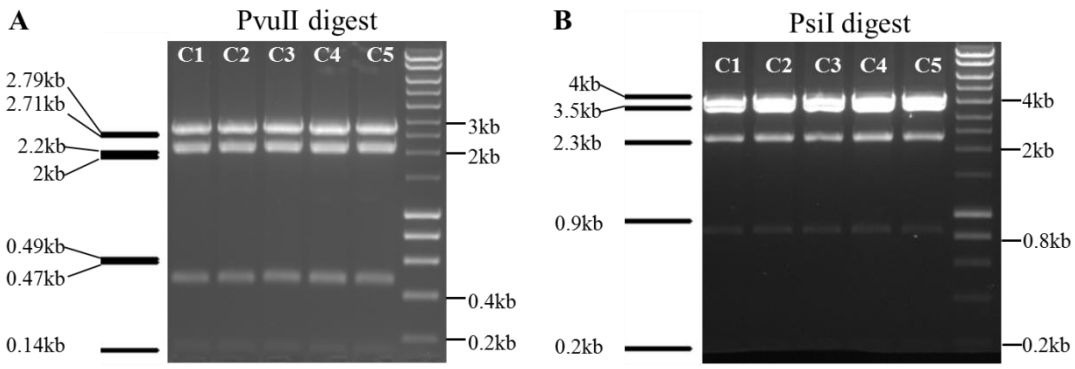


Figure 3.11: Colonies C1 to C5 exhibit the correct restriction digest pattern. Colonies C1 to C5 were digested with the restriction enzymes PvuII (**A**) and PsiI (**B**) for 1 h at 37°C and subsequently analysed on a 1% agarose gel by electrophoresis. The predicted digest outcomes, to the left of the actual digests, demonstrated that the ligation was successful in all colonies.

As demonstrated on the agarose gel, all colonies digested with PvuII and PsiI (Figure 3.11A and B, respectively) showed the correct digest pattern.

Next, the p*MITF*-mCherry-pLVX-Tight-Puro plasmid was transfected into 501mel cells to assess the functionality of the *MITF* promoter by measuring mCherry expression using fluorescence microscopy (Figure 3.12).

Transfections of 501mel cells with the p*MITF*-mCherry-pLVX-Tight-Puro plasmid induced mCherry expression (Figure 3.12, second row). To increase the *MITF* promoter activity and therefore mCherry expression, a Sox10 expressing plasmid was co-transfected with the lentiviral plasmid (Figure 3.12, third row). To quantify and confirm mCherry expression, flow cytometry was performed on transfected 501mel cells (data not shown).

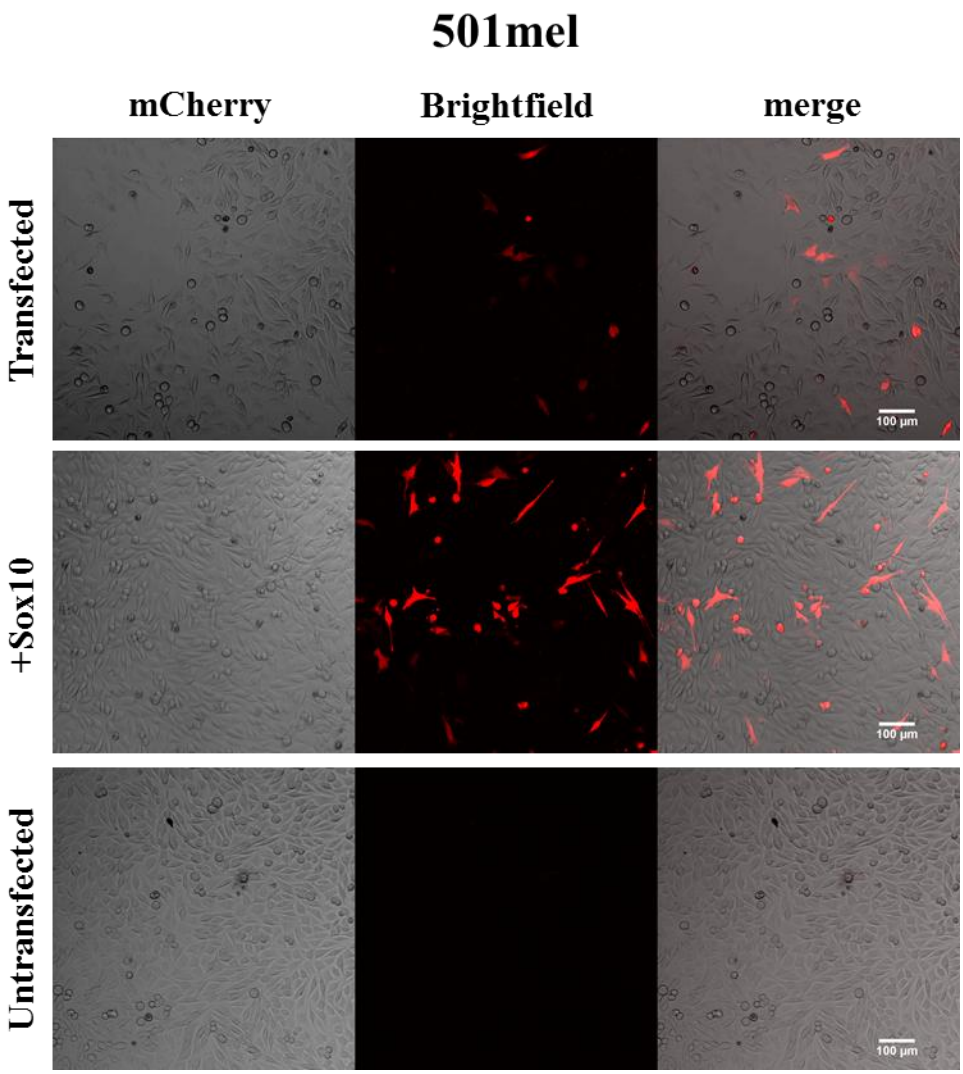


Figure 3.12: mCherry is expressed in 501mel cells. 501mel cells were transfected with 750 ng of the p*MITF*-mCherry-pLVX-tight-puro plasmid alone (second row) or together with 250 ng of a Sox10 expression plasmid (third row). Fluorescence was measured 24 h post-transfection.

The pLVX-Tight-Puro construct allows the strict regulation of transcription through the "Tight" promoter (TREtight). As this level of regulation was not required for our system the "Tight" promoter was removed through restriction digests utilising the two restriction enzyme sites flanking the promoter (Figure 3.13).

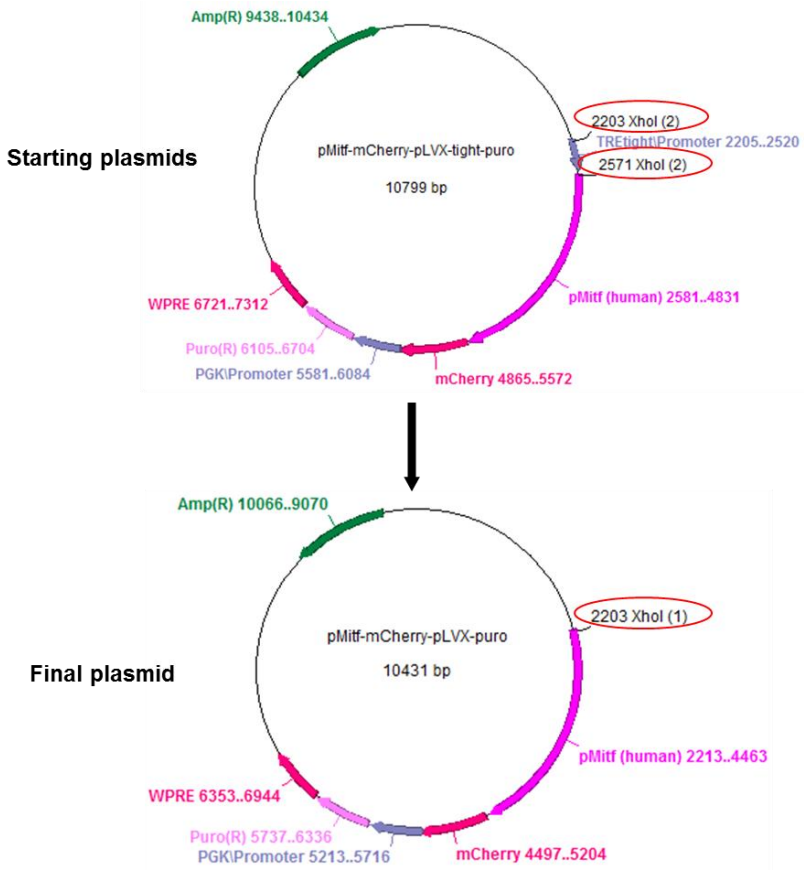


Figure 3.13: Schematic diagram of the generation of the p*MITF*-mCherry-pLVX-puro plasmid. p*MITF*-mCherry-pLVX-Tight-Puro was digested with the restriction enzyme XhoI for 1 h at 37°C and re-ligated to result in the final plasmid p*MITF*-mCherry-pLVX-puro.

After the re-ligation of the plasmid and transformation of *E.coli* bacteria, colonies were picked and digested with restriction enzymes to ensure that the "Tight" promoter was removed (Figure 3.14).

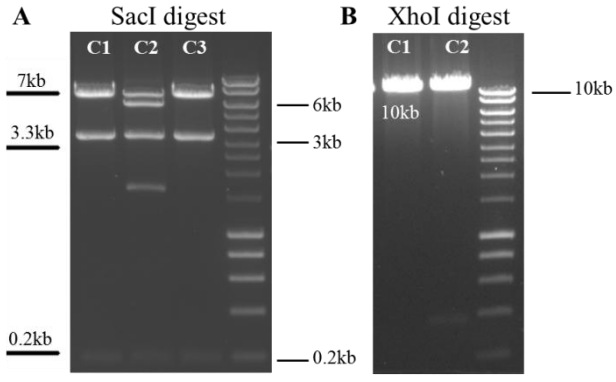


Figure 3.14: Colonies C1 and 3 exhibit the correct restriction digest pattern. Colonies C1-3 were digested with SacI (**A**) and XhoI (**B**) for 1 h at 37°C and subsequently analysed on a 1% agarose gel by electrophoresis. The predicted digest outcomes, to the left (for SacI) and right (for XhoI) of the actual digests, demonstrated that the ligation had been successful in C1 and C3.

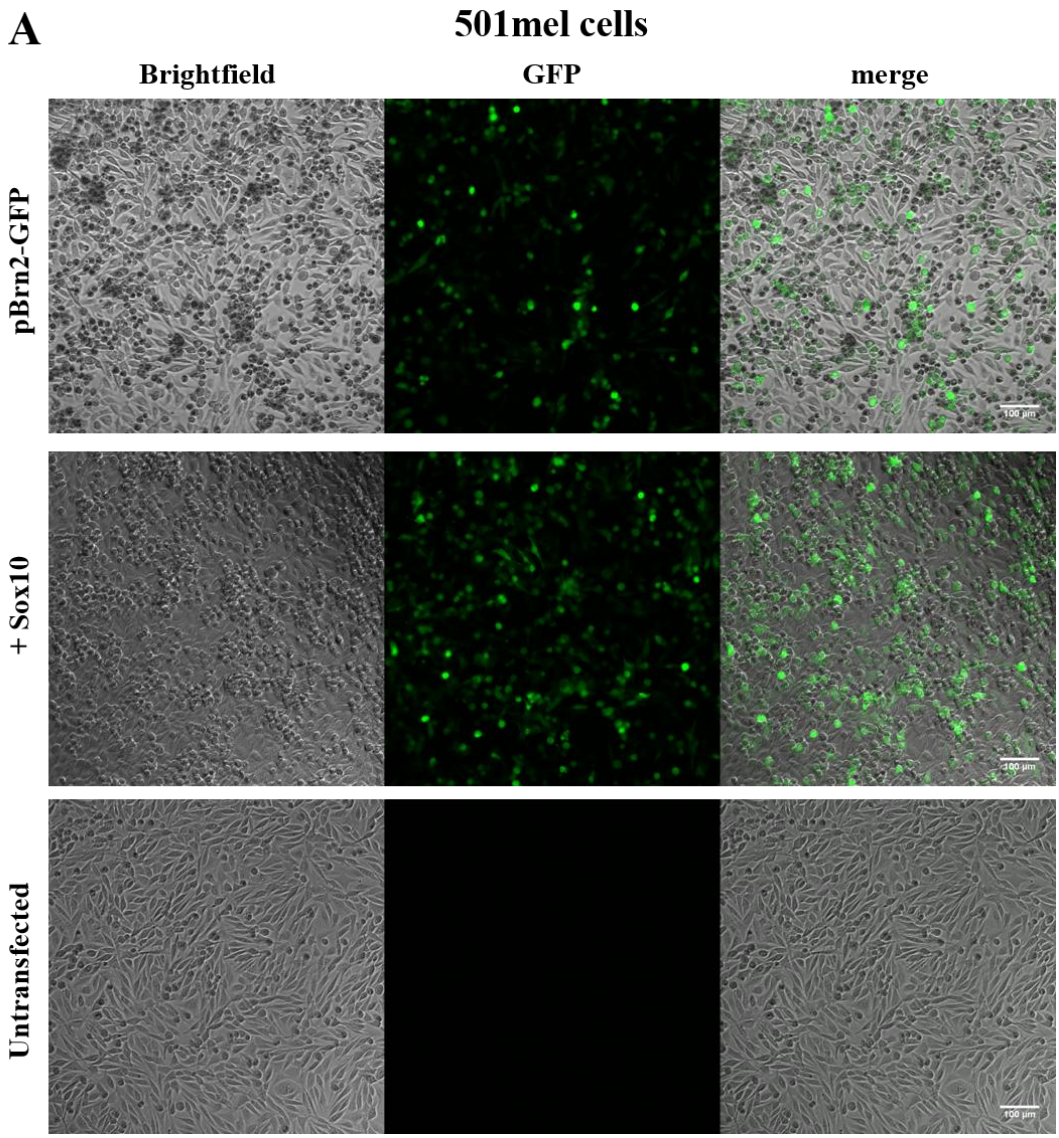
The digest pattern obtained with SacI and XhoI (Figure 3.14A and B, respectively) demonstrated that two out of the three colonies had been correctly re-ligated, which was confirmed by sequencing analysis.

3.2.3 pBrn2-GFP: Engineering and testing the reporter plasmid

3.2.3.1 The pBrn2-GFP reporter plasmid is functional in vitro

The starting material for the generation of the reporter lentiviral plasmid containing the reporter for stem-like cells, Brn2, already existed in the form of a reporter plasmid expressing GFP which was regulated by the activity of the *Brn2* promoter (p*Brn2*-GFP plasmid). To ensure that the reporter was functioning correctly, the reporter plasmid was transfected into 501mel and SKmel28 cells both alone and in combination with the transcription factor Sox10, and the fluorescence was measured by fluorescence microscopy (Figure 3.15).

Upon transfection with the reporter plasmid, GFP expression was measured suggesting that the transfection was successful and the *Brn2* promoter was functional in 501mel cells (Figure 3.15A, first row). Co-transfections with a Sox10 expression plasmid increased the number of GFP^+ cells compared to the control condition (reporter plasmid only) (Figure 3.15A, second and first row, respectively).


A
501mel cells
Brightfield
GFP
merge
pBrn2-GFP
+ Sox10
Untransfected
100 µm

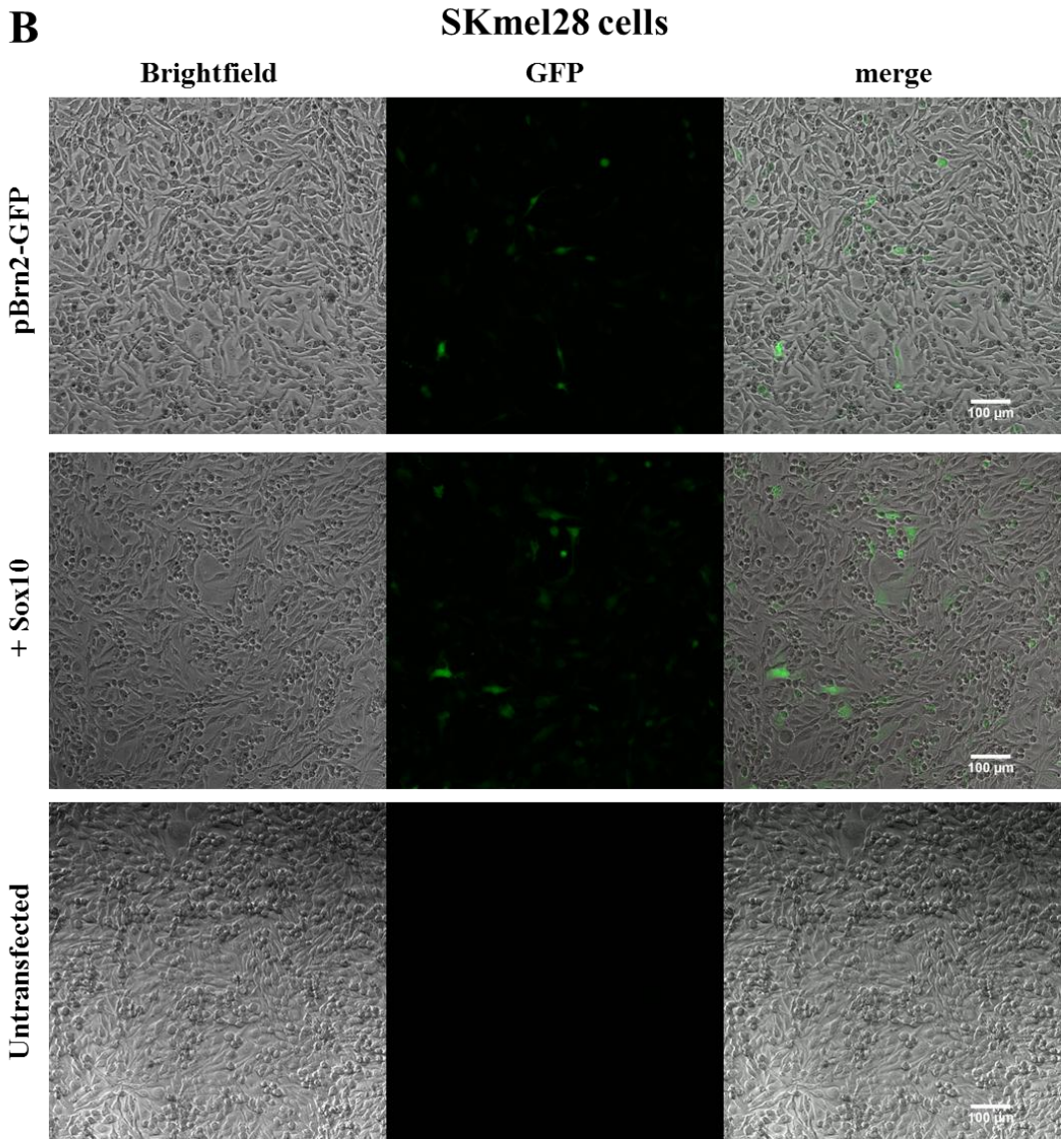


Figure 3.15: GFP is expressed in 501mel and SKmel28 cells. 400 ng of p*Brn2*-GFP were co-transfected with 200 ng of an empty plasmid (first row) or a Sox10 expression plasmid (second row) in 501mel (**A**) and SKmel28 (**B**) cells. GFP expression was measured in transfected and untreated cells (third row) 24 h post-transfection. Scale bar represents 100 µm.

In SKmel28 cells, GFP was expressed upon transfections with the reporter plasmid only (Figure 3.15B, first row) compared to the untreated control cells. Co-transfection with a Sox10 expression plasmid again increased the number of GFP^+ cells (Figure 3.15B, second row), even though this was less striking than in 501mel cells.

These results demonstrate the responsiveness of the *Brn2* promoter in 501mel and SKmel28 cells and confirmed the luciferase results (Figure 3.5). To quantify the number of fluorescent cells, flow cytometry analyses were performed (Figure 3.16).

In 501mel cells, transfections with the p*Brn2*-GFP reporter plasmid induced an increase in GFP expression to 47% from 0.15% in the untransfected control (Figure 3.16A, second column). Co-transfections with a Sox10 expression plasmid increase the number of GFP^+ cells even further to 54.5% (Figure 3.16A, third column).

In SKmel28 cells transfected with the reporter plasmid only, the number of GFP^+ cells was 20% (Figure 3.16B, second column) compared to 0.13% in untreated cell. Upon transfections with a Sox10 expression plasmid, the number of GFP^+ cells increased to 27.9% (Figure 3.16B, third column).

Results in 501mel and SKmel28 cells suggest that the *Brn2* promoter is responsive to Sox10, confirming the results obtained by luciferase assay (Figure 3.5) and fluorescence microscopy (Figure 3.15).

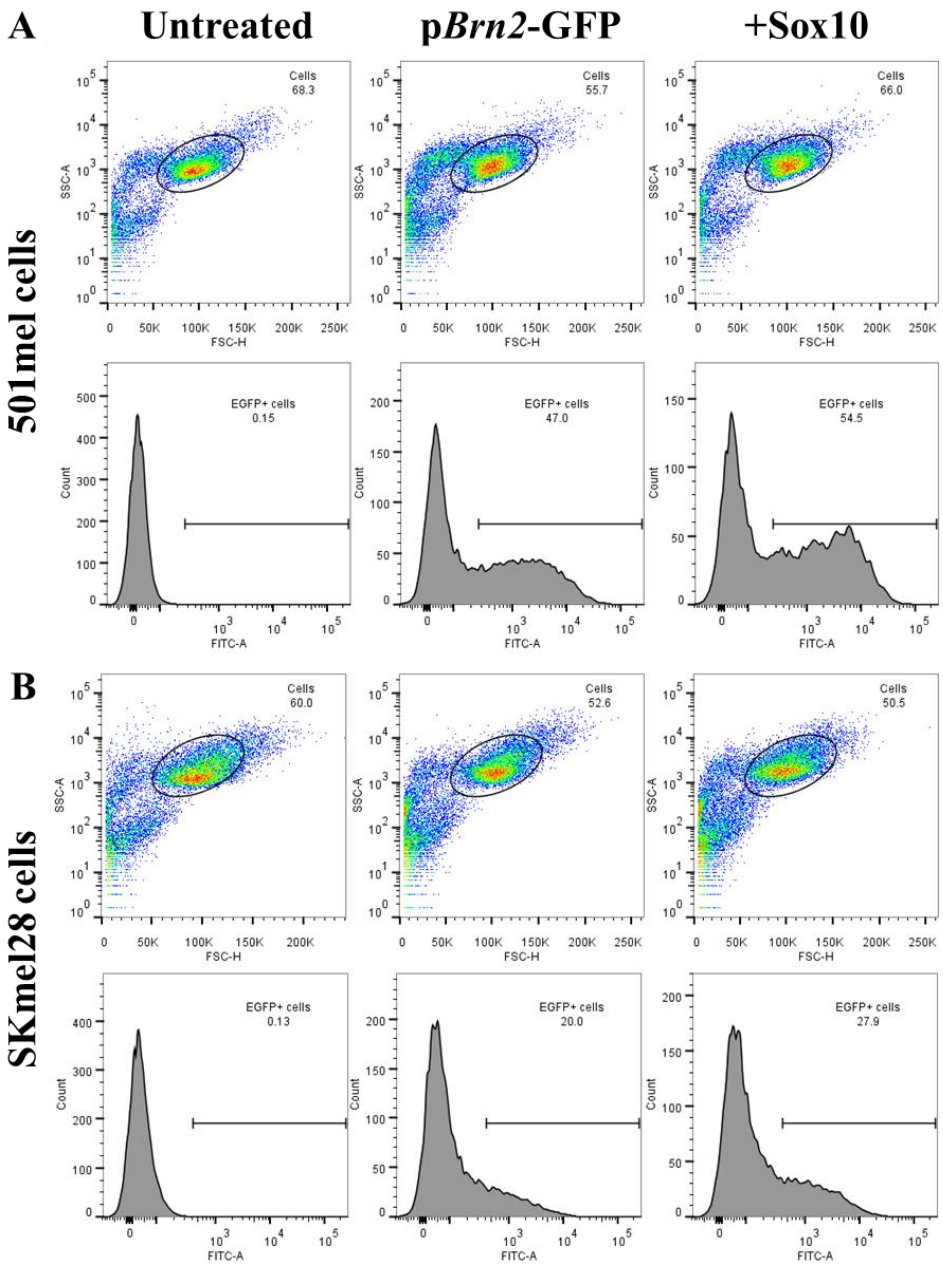


Figure 3.16: Sox10 increases GFP expression in 501mel and SKmel28 cells. 400 ng of p*Brn2*-GFP were co-transfected with 200 ng of an empty plasmid (second column) or a Sox10 expression plasmid (third column) in 501mel (**A**) and SKmel28 (**B**) cells. 24 h post-transfection, GFP expression was measured in transfected and untreated cells (third column).

3.2.3.2 The lentiviral pBrn2-GFP reporter plasmid is functional in vitro

To engineer a lentiviral plasmid containing the p*Brn2*-GFP fragment, the "tight" promoter had to be removed from the parental plasmid, pLVX-tight-puro. Due to the

fact that the *Brn2* promoter already contained an XhoI restriction site, the strategy for the removal of the tight promoter had to be changed.

Instead, an "inverse" PCR was performed with primers that were constructed to contain restriction enzyme ends for XbaI (Figure 3.17). Instead of binding to the 5' end, as designed above, the forward primer was designed to be complimentary to the 3' end of the "tight" promoter. Consequently, the reverse primer was complimentary to the 5' end, rather than the 3' end. This would allow for the amplification of the plasmid to take place but exclude the "tight" promoter. Subsequently, the PCR-amplified fragment was digested with XbaI and re-ligated to give the parental plasmid pLVX-puro (Figure 3.17).

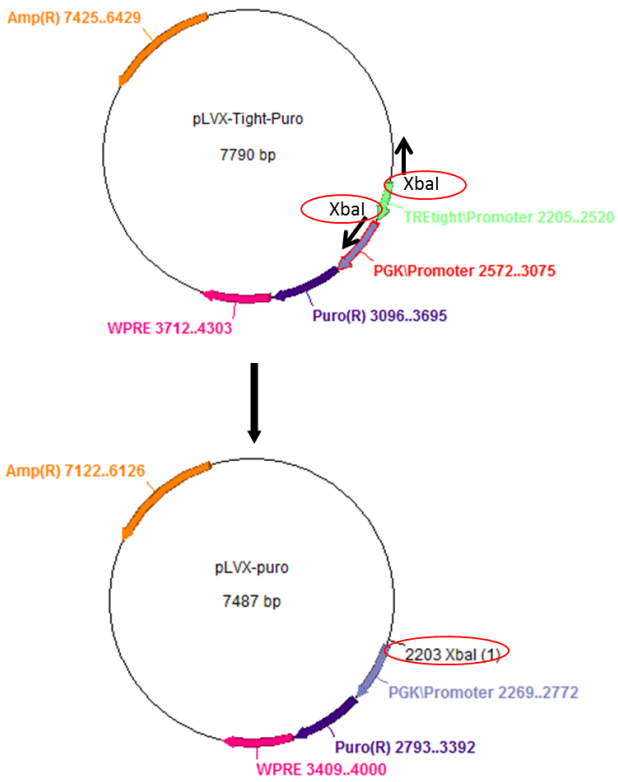


Figure 3.17: Schematic diagram of the inverse PCR of the plasmid pLVX-tight-puro. Forward and reverse primers for the PCR were designed to contain XbaI restriction sites. After the PCR was performed, the fragment was digested with XbaI for 1 h at 37°C and re-ligated to result in the final plasmid pLVX-puro.

After the re-ligation and transformation of *E.coli* bacteria, colonies were picked and restriction digests were performed to confirm that the plasmids were correct (Figure 3.18), followed by sequencing analysis.

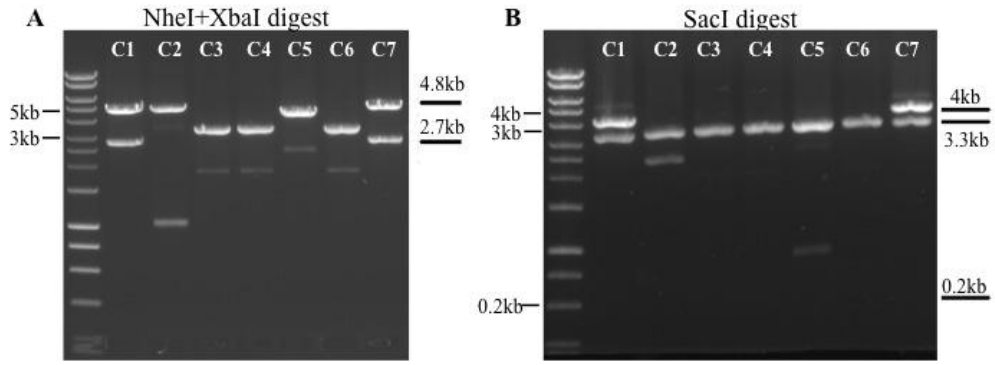


Figure 3.18: Colonies C1 and C7 exhibit the correct restriction digest pattern. Colonies C1 to C7 were digested with NheI and XbaI simultaneously (**A**) and with SacI (**B**) for 1 h at 37°C. Subsequently the digests were analysed on a 1% agarose gel by electrophoresis. The predicted outcomes, to the right of the gel, confirmed that colonies C1 and C7 were correct.

After digesting the colonies C1 to C7 with either NheI and XbaI (Figure 3.18A) or SacI alone (Figure 3.18B), only the colonies C1 and C7 exhibited the correct digest pattern. The next step was to ligate the p*Brn2*-GFP fragment into the pLVX-puro plasmid. However, the restriction enzyme sites flanking this fragment did not match the ones in the parental plasmid pLVX-puro. To circumvent this problem, the p*Brn2*-GFP fragment was next ligated into a shuttle vector (data not shown). Subsequently, the fragment was excised using the enzymes NotI and ClaI (Figure 3.19). Simultaneously, pLVX-puro was also digested with these two enzymes (Figure 3.19) and the p*Brn2*-GFP fragment was ligated into the target plasmid.

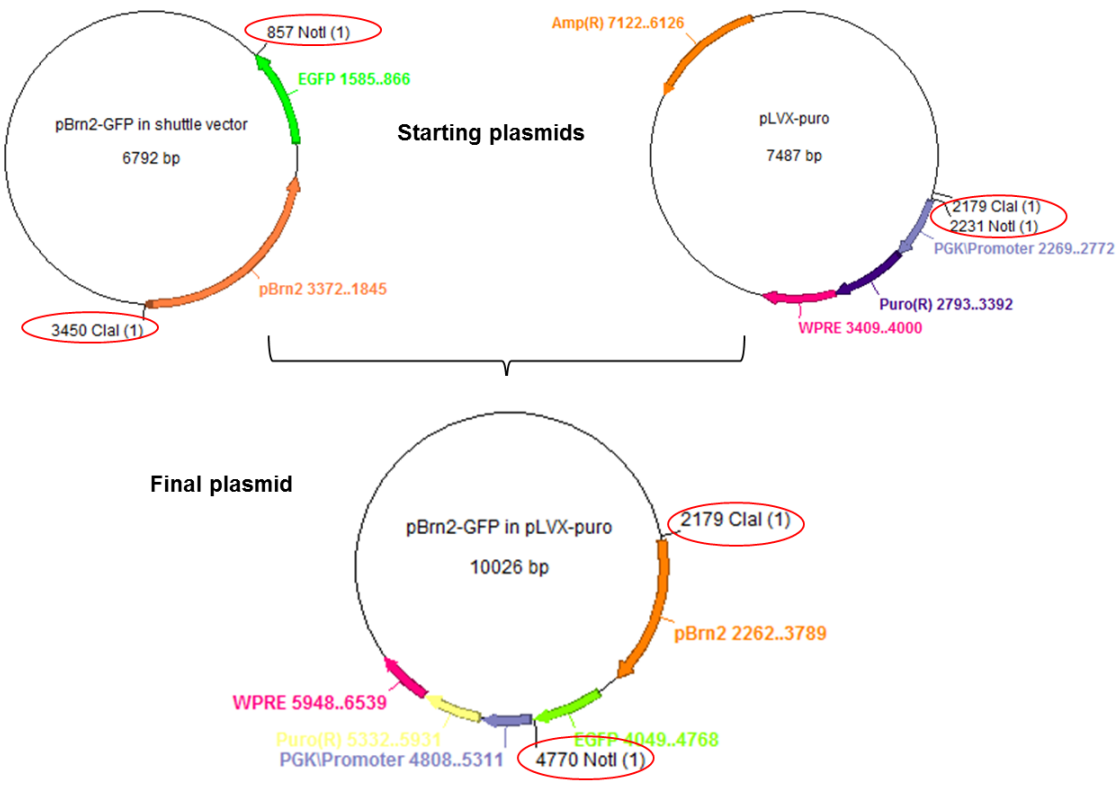


Figure 3.19: Schematic diagram of the p*Brn2*-GFP-pLVX-puro plasmid. The shuttle vector and the pLVX-puro plasmid were digested with ClaI and NotI for 1 h at 37°C, followed by a ligation to result in the final plasmid p*Brn2*-GFP-pLVX-puro.

After the ligation *E.coli* bacteria were transformed, clones were picked and digested by restriction enzymes (Figure 3.20). This was followed by sequence analysis to confirm that the resulting p*Brn2*-GFP-pLVX-puro plasmid was correct.

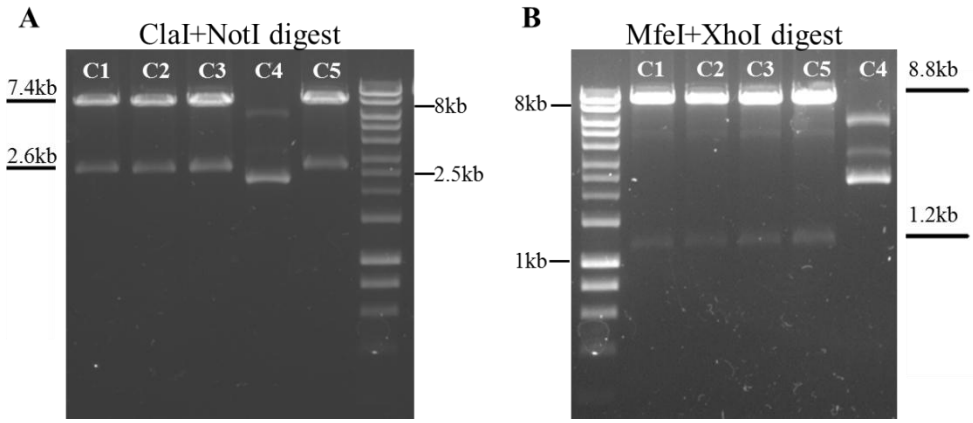


Figure 3.20: Colonies C1, 2, 3 and 5 exhibit the correct digest pattern. Colonies C1 to C5 were digested with the restriction endonuclease pairs ClaI and Not1 (**A**) and MfeI and XhoI (**B**) for 1 h at 37°C. Subsequently the digests were analysed on a 1% agarose gel by electrophoresis. The predicted outcomes, to the left (for ClaI + NotI) and to the right (for MfeI + XhoI) of the actual digests confirmed that colonies C1, 2, 3 and 5 were correct.

The restriction digest demonstrated that out of the five colonies screened, four were exhibiting the correct digest pattern after digests with the enzyme pairs ClaI + NotI and MfeI + XhoI.

To assess the functionality of this plasmid *in vitro*, SKmel28 cells were transfected with the p*Brn2*-GFP-pLVX-puro plasmid. Fluorescence was measured by microscopy (Figure 3.21).

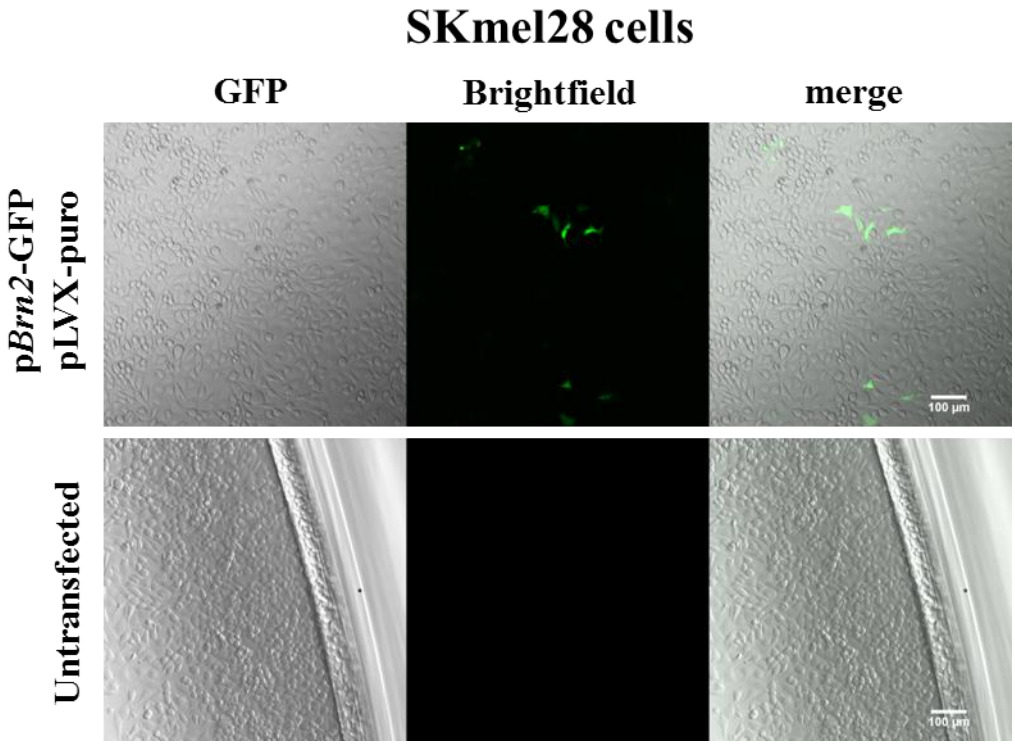


Figure 3.21: GFP is expressed in SKmel28 cells. SKmel28 cells were transfected with 500 ng of the plasmid p*Brn2*-GFP-pLVX-puro (second row) and fluorescence was measure 48 h post-transfection.

Upon transfections of SKmel28 cells with the p*Brn2*-GFP-pLVX-puro plasmid GFP expression was induced compared to the untransfected control (Figure 3.21). The small number of GFP-positive cells might be due to low transfection efficiency.

3.2.4 Dual lentiviral plasmid: engineering and functionality in vitro

Having demonstrated that the *Brn2* and *MITF* promoters are still functional in the lentiviral plasmid backbone, the next step was to engineer the dual lentiviral reporter plasmid.

To avoid that activation of one promoter led to the expression of both fluorescent proteins, the *Brn2* promoter was cloned upstream of the *MITF* promoter (Figure 3.22). The reason for this was that observations in the laboratory have shown that p*Brn2* is a weaker promoter than p*MITF*. This is determined by the ability of the transcription machinery to bind to the promoter and initiate transcription. Since transcription from the *MITF* promoter is initiated more frequently than from the *Brn2* promoter, in relative terms, the likelihood of the *MITF* promoter becoming activated following p*Brn2* activation, was lower than vice versa, when p*Brn2* was cloned upstream of p*MITF*.

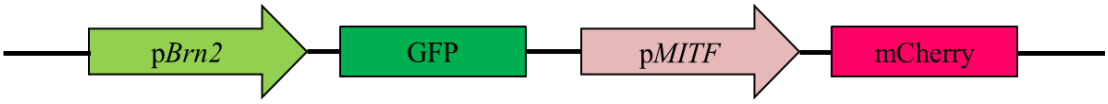


Figure 3.22: Simplified diagram of the dual lentiviral reporter plasmid containing the p*Brn2*-GFP fragment upstream (5' end) of the p*MITF*-mCherry fragment (3' end).

Due to the cloning strategy and the restriction enzymes used to generate the single lentiviral plasmids, a new strategy was applied to construct the dual plasmid. To this end, the p*MITF*-mCherry fragment was ligated into the previously engineered pLVX-puro backbone, resulting in the reporter plasmid p*MITF*-mCherry-pLVX-puro. *E.coli* were transformed and colonies were picked. Restriction digests were performed with the restriction enzymes EcoRI and MluI and StuI separately (Figure 3.23) to screen for the presence and the correct orientation of the p*MITF*-mCherry fragment.

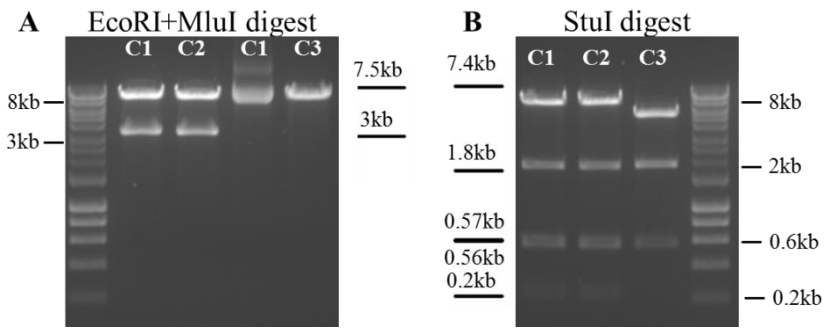


Figure 3.23: Colonies C1 and C2 exhibit the correct digest pattern. Colonies C1, 2 and 3 were digested with the restriction endonuclease pair EcoRI and MluI (left) as well as StuI (right) for 1 h at 37°C. Subsequently the digests were analysed on a 1% agarose gel by electrophoresis. The predicted outcomes, to the right (for EcoRI + MluI) and to the left (for StuI) of the actual digests confirmed that colonies C1 and C2 were correct.

Subsequently, the p*Brn2*-GFP fragment was ligated into the p*MITF*-mCherry-pLVX-puro plasmid, followed by *E.coli* transformation and picking colonies. Restriction digests with three restriction enzyme pairs (ClaI + NotI, MfeI + NdeI and MfeI + XbaI) confirmed the presence and the correct orientation of the p*Brn2*-GFP fragment (Figure 3.24).

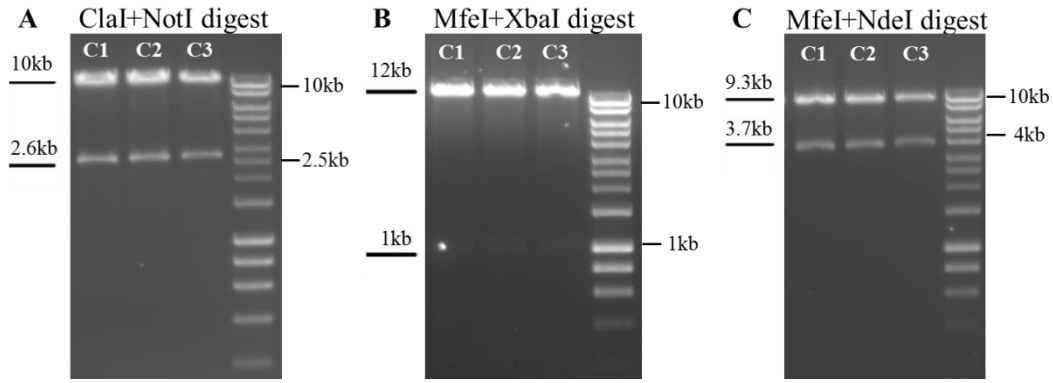


Figure 3.24: All p*Brn2*-GFP-p*MITF*-mCherry-pLVX-puro colonies exhibit the correct digest pattern. Colonies C1-3 were digested for 1 h at 37°C to check for the presence of pBrn2-GFP with the enzymes ClaI + NotI (**A**), for the correct orientation of p*MITF*-mCherry and p*Brn2*-GFP using the enzymes MfeI + XbaI (**B**) and MfeI + NdeI (**C**), respectively. The digests were analysed on a 1% agarose gel by electrophoresis. The predicted outcomes are to the left of the gels. The outcome of the digests confirmed that all three colonies were correct.

To test the functionality of the dual lentiviral plasmid p*Brn2*-GFP-p*MITF*-mCherry-pLVX-puro, the plasmid was transfected into SKmel28 and 501mel cells and fluorescence was assessed by microscopy (Figure 3.25) and flow cytometry analyses (Figure 3.26).

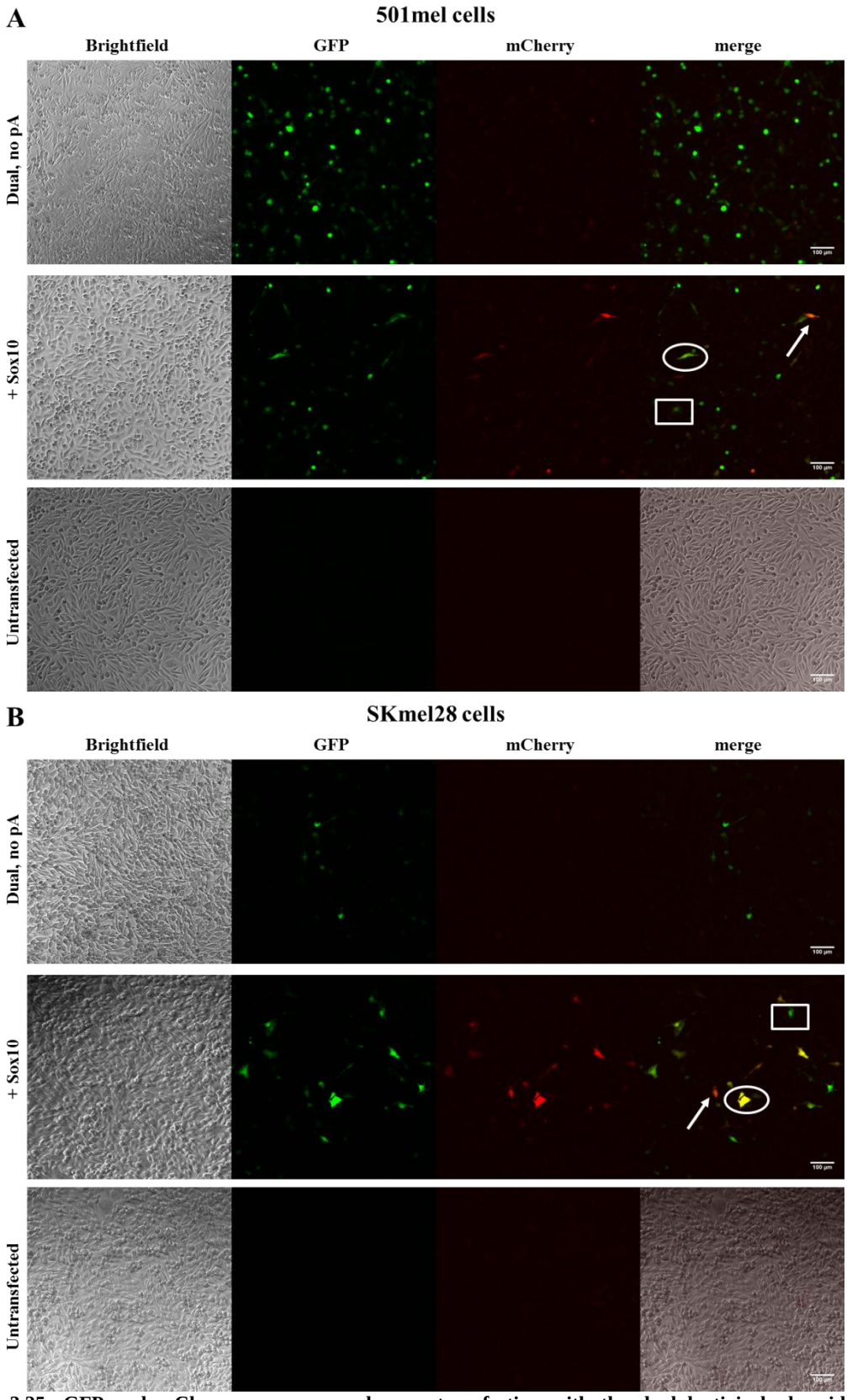


Figure 3.25: GFP and mCherry are expressed upon transfection with the dual lentiviral plasmid. Co-transfections of 200 ng of the dual lentiviral plasmid p*Brn2*-GFP-p*MITF*-mCherry-pLVX-puro with 400 ng of an empty plasmid (first row) or a Sox10 expression plasmid (second row) were transfected into 501mel (**A**) and SKmel28 (**B**) cells. 48 h post-transfection GFP and mCherry expression were measured. A merged picture of GFP and mCherry expressing cells was generated (fourth column). Cells expressing GFP and mCherry were circled while cells mainly expressing mCherry or GFP were indicated with an arrow or framed in a rectangular box, respectively. Scale bar represents 100 µm.

After transfection with the lentiviral plasmid, mCherry and GFP expression was detected in 501mel and SKmel28 cells, despite the low fluorescence intensity (Figure 3.25A and B, first row). Co-transfection of the dual plasmid and a Sox10 expression plasmid increased GFP and mCherry expression (Figure 3.25A and B, second row). Even though this was more striking in SKmel28 than in 501mel cells, this outcome confirmed the results obtained previously. Interestingly, co-transfections with the dual reporter and the Sox10 expression plasmid showed heterogeneity in p*Brn2* and p*MITF* activity: most cells were mainly positive for GFP (Figure 3.25A and B, second row, rectangle), while only some cells expressed mCherry more strongly than GFP (Figure 3.25A, second row, arrow). The majority of the transfected cells, however, co-expressed GFP and mCherry (Figure 3.25A and B, second row, circle). These results demonstrated that the activity of the two promoters varied from one cell to another, therefore demonstrating a degree of heterogeneity in both cell lines. This result validates the use of fluorescent promoters to investigate different cell populations in melanoma.

To confirm the results obtained by fluorescence microscopy, flow cytometry analyses were performed on transfected 501mel and SKmel28 cells to quantify the number of cells expressing mCherry and GFP (Figure 3.26).

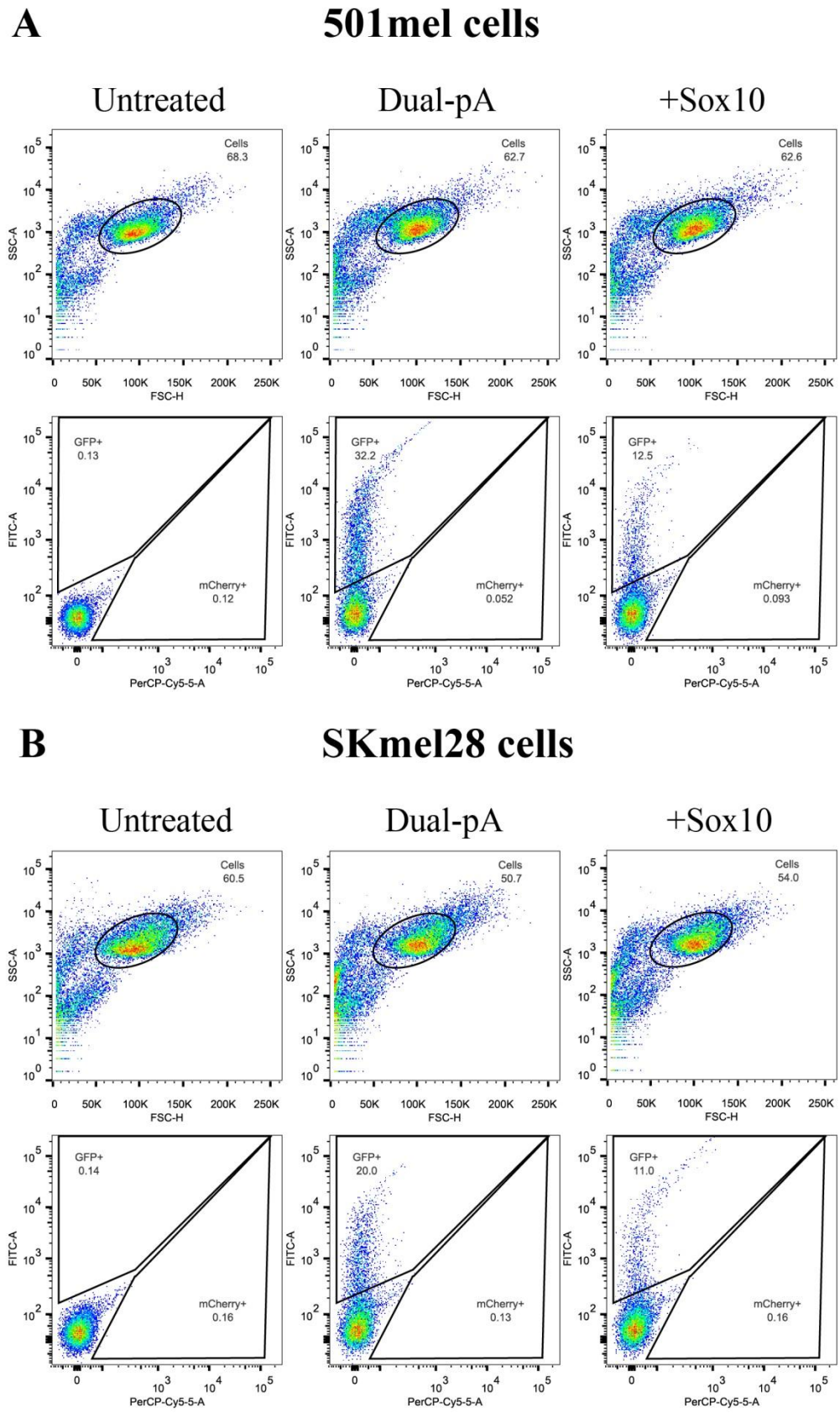


Figure 3.26: Sox10 increases *Brn2* promoter activity of the dual lentiviral plasmid. 400 ng of the dual reporter lentiviral plasmid were co-transfected with 200 ng of an empty plasmid (second column) or a Sox10 expression plasmid (third column) into 501mel (**A**) or SKmel28 cells (**B**). Fluorescence was measured 48 h post-transfection.

To assess the fluorescence of viable cells only, cells were incubated with ToPro3, a dye that is only taken up by cells that do not contain intact cell membranes. In 501mel cells, transfection with the dual plasmid demonstrated an increase in GFP^+ cells from 0.13% in the control to 32.2%, while the number of $mCherry^+$ cells was not strikingly different (Figure 3.26A second column). Co-transfections with the Sox10 expression plasmid decreased the number of GFP^+ cells (12.5%) compared to dual plasmid transfections only and did not affect the number of $mCherry^+$ cells (Figure 3.26A, third column).

In SKmel28 cells, transfections of the dual plasmid increased the GFP^+ cell number to 20% compared to 0.14% in the untreated control, while the mCherry-expressing cell number did not change (Figure 3.26B, second column). Similar to 501mel cells, co-transfections with the Sox10 expression plasmid only induced an 11% increase in GFP^+ cells and did not affect mCherry-expressing cell numbers (Figure 3.26B, third column).

These results confirmed that the dual plasmid was functional. However, despite the clear activation of the *MITF* and *Brn2* promoters with Sox10 detected by fluorescence microscopy, this activation was not as obvious when fluorescence was analysed by flow cytometry. Similarly, while in fluorescence microscopy most cells expressed both GFP and mCherry, this was not detected by flow cytometry. These discrepancies could have been due to the small number of fluorescent cells from the start and changes in fluorescence might have only affected a small population of cells which would have not been picked up by flow cytometry. Additionally, flow cytometry allows the quantification of fluorescent levels in cells that express detectable levels of fluorescent protein. However, the flow cytometry machine excited at the wavelength 488 nm, inducing a mCherry excitation of only approximately 5%. As the excitation maximum of mCherry is reached at 580 nm, optimal excitation of mCherry was not provided. Therefore, even though low levels of fluorescent protein expression might still be

detectable via fluorescent microscopy, it is likely that these levels might not be detected by flow cytometry, explaning the discrepant results obtained using these two techniques. Another reason for not detecting striking changes in mCherry^{+} cell numbers might be due to the low expression levels of mCherry. While GFP is known to be a bright fluorophore (Shaner et al., 2005), mCherry is a good general-purpose fluorescent protein (Shaner et al., 2005) but it is not as bright as GFP, explaining why it is difficult to detect its signal by microscopy and flow cytometry if the intrinsic signal is low.

However, due to the observation by fluorescence microscopy that the majority of cells expressed both mCherry and GFP, a second lentiviral reporter plasmid was constructed that contained a transcription blocker (TB), consisting of polyadenylation and transcription pause sites (poly(A)) between the p*Brn2*-GFP and p*MITF*-mCherry fragments (Figure 3.27). The poly(A) sequence would prevent expression of mCherry without activation of the *MITF* promoter.

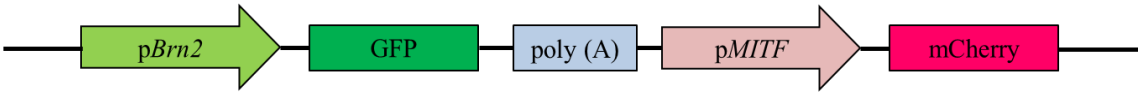


Figure 3.27: Simplified diagram of the dual reporter plasmid. A synthetic transcription blocker was inserted downstream of the p*Brn2*-GFP fragment in the dual lentiviral plasmid to prevent the transcription of the mCherry gene when only the *Brn2* promoter was active.

After PCR-amplifying TB from a separate plasmid and ligating it into the dual lentiviral plasmid, *E.coli* bacteria were transformed and clones were picked. Restriction digests and sequencing analyses confirmed that the clones were correct. To assess the functionality of the dual lentiviral plasmid containing the TB, transfection experiments were performed to confirm mCherry and GFP expression (Figure 3.28).

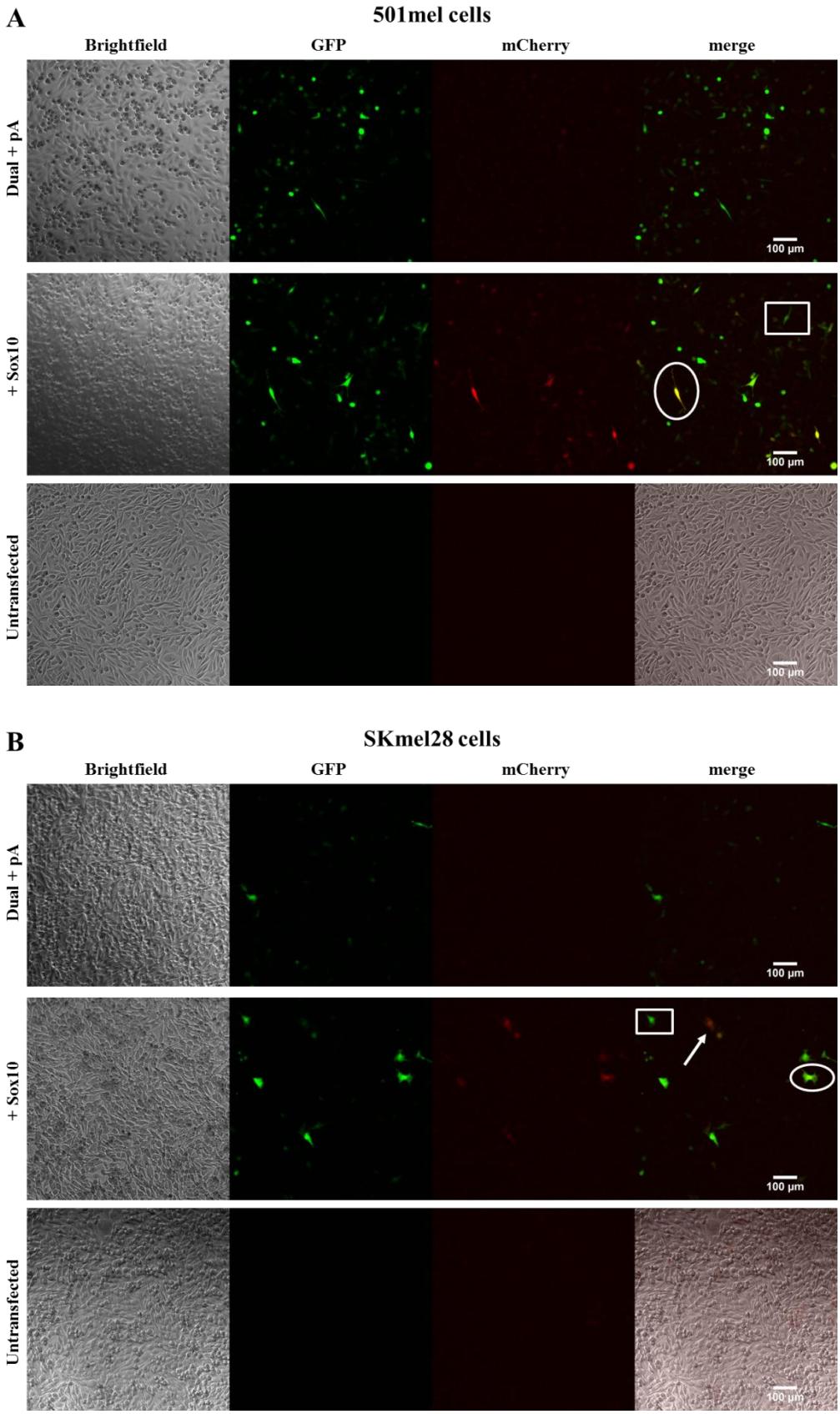


Figure 3.28: mCherry and GFP is increased after transfections with the dual reporter plasmid containing TB. 400 ng of the dual reporter plasmid with TB were co-transfected into 501mel (**A**) and SKmel28 (**B**) cells together with 200 ng of an empty plasmid (first row) or a Sox10 expression plasmid (second row). Fluorescence was measured 48 h post transfection. Scale bar represents 100 µm.

In 501mel cells, transfection of the dual reporter lentiviral plasmid containing the TB induced GFP expression, while mCherry expression was very faint (Figure 3.28A, first row). Upon co-transfection with a Sox10 expression plasmid, the number of mCherry-positive cells increased but the effect on the GFP-expressing cells was less obvious (Figure 3.28A, second row). As seen before, most cells expressed mCherry and GFP (Figure 3.28A, third row, circle), while some cells expressed GFP only (rectangle).

In SKmel28 cells, transfections with the dual plasmid alone showed a few GFP^+ cells but mCherry expression was very faint and hardly detectable (Figure 3.28B, first row). Sox10 increased mCherry expression, while also increasing GFP expression. Again, most cells expressed mCherry and GFP (Figure 3.28B, second row, circle), however, some cells expressed mainly mCherry (arrow) or mainly GFP (rectangle).

Flow cytometry analyses of 501mel and SKmel28 cells were performed similarly to cells transfected with the dual virus without TB, and confirmed fluorescent protein expression (data not shown). Despite the low fluorescent protein expression observed, we hypothesised that generation of viruses and stable integration of the promoter-fluorescent protein constructs into the cell genome will allow a stronger and more consistent activation of the promoters. Therefore, the outcome of this data justified the generation of stable clonal cell lines using lentiviral constructs.

3.3 Clonal cell lines express mCherry and GFP and potentially exhibiting signs of phenotype-switching *in vitro*

3.3.1 501mel cells express mCherry and GFP after viral transduction

Lentiviral particles were generated using dual lentiviral reporter plasmid without TB and 501mel cells were transduced. To select for the cells that were successfully infected with the lentivirus, cells were treated with the antibiotic puromycin. Once a stable

population of cells was generated, mCherry and GFP expression was assessed by fluorescence microscopy (Figure 3.29A, top row). To test activation of the promoters, a Sox10 expression plasmid was transfected into the stable cells (Figure 3.29).

After transduction and selection with puromycin, 501mel cells showed GFP expression, while mCherry expression was very weak (Figure 3.29A, first row). Even though transfections with a Sox10 expression plasmid increased mCherry and GFP expression after 24 h post-transfection, the overall number of fluorescent cells was still low (Figure 3.29A, second row, circle). Also note that the density of these cells was low. Interestingly, 6 days (d) post-transfection, the number of fluorescent cells increased strikingly in transduced and transfected stable cells (Figure 3.29B, first and second row). Three different cell populations were observed: $mCherry^+$ cells (Figure 3.29B, arrow), GFP^+ cells (Figure 3.29B, asterisk) and cells expressing both fluorescent proteins (Figure 3.29B, circle). Upon transfections with the Sox10 expression plasmid, mCherry fluorescence and GFP expression seemed to increase (Figure 3.29B, third and fourth row), but this was not as striking as with the previous plasmid transfections (Figure 3.25 and 3.26).

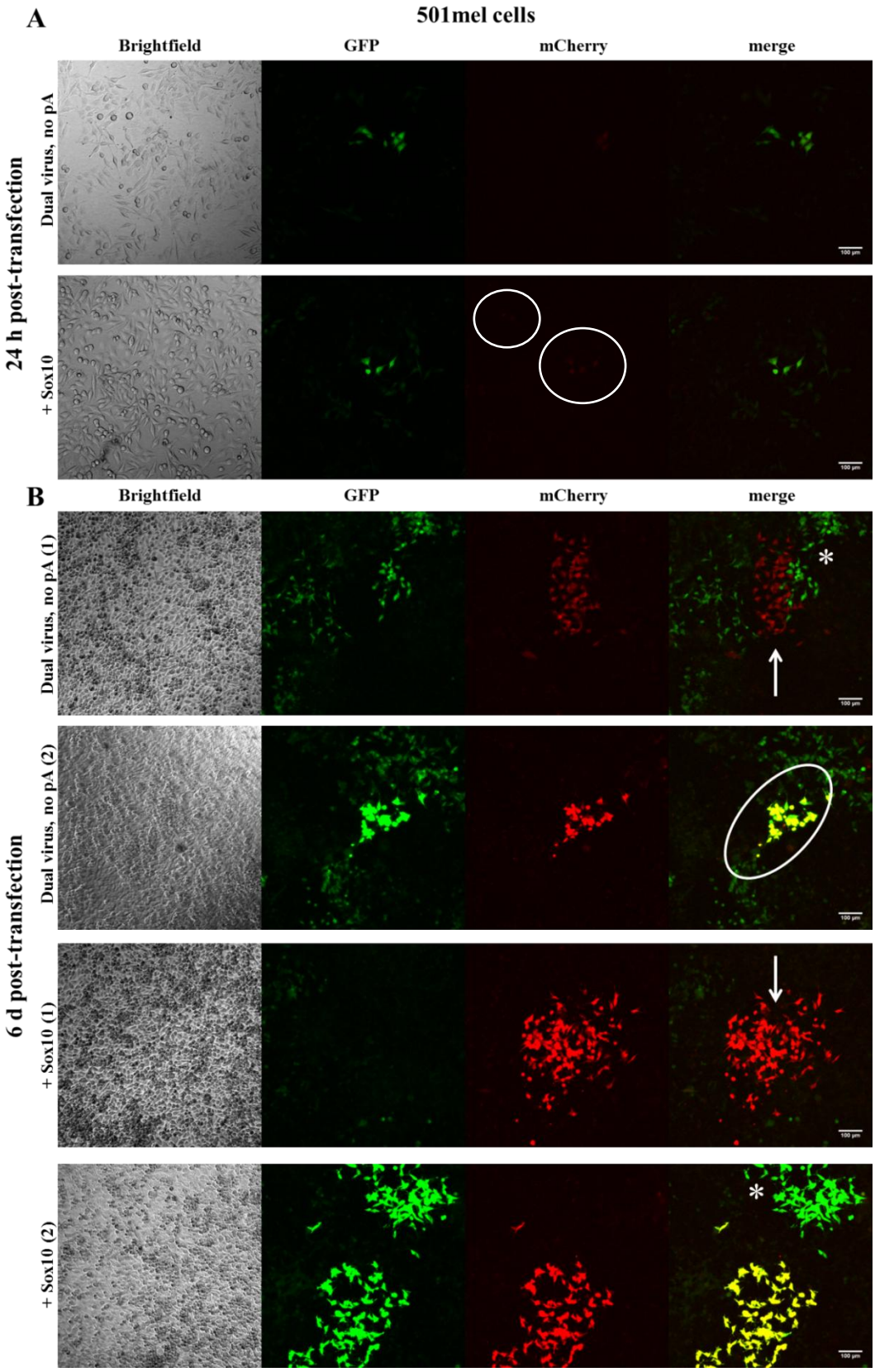


Figure 3.29: Virally transduced 501mel cells express mCherry and GFP. 501mel cells were transduced with the dual reporter lentivirus without TB and treated with puromycin to select for the cells that were infected. Subsequently, cells were transfected with a Sox10 expression plasmid (1 µg) and GFP and mCherry expression (second and third column, respectively) were measured 24 h and 6 days (d) post-transfection (A and B, respectively). These channels were also combined in a merged picture (fourth column). Cells expressing both GFP and mCherry were circled. Cells expressing solely GFP were marked with an asterisk, while populations of solely $mCherry^+$ cells were indicated with an arrow. Scale bar represents 100 µm.

What was striking about the results obtained by microscopy was the fact that more cells were fluorescent at 6 d post-seeding than 24 h post-seeding (Fig 3.29 A and B, top row). The most prominent difference between these conditions was the increased cell density at 6 d post-seeding. This suggests that changes in the microenvironment, such as cell density, might influence promoter activity. This fact in itself demonstrated that the promoters were functional and responsive to changes in cell environment.

501mel cells were subsequently transduced with the dual reporter lentivirus containing TB. Again, to confirm the functionality of the promoters, cells were transfected with a Sox10 expression plasmid (Figure 3.30).

Similar to 501mel cells transduced with the dual reporter lentivirus without TB (Figure 3.29), cells transduced with the reporter virus containing TB also expressed GFP 24 h post-seeding (Figure 3.30A, first row). mCherry expression was very faint and even after 24 h post-transfection with a Sox10 expression plasmid no striking changes in GFP and mCherry expression were detected (Figure 3.30A, second row).

However, mCherry and GFP-positive cell populations were detected in transduced cells 6 d post-seeding (Figure 3.30B, first row, arrow and asterisk, respectively), although no striking difference in GFP and mCherry expression was detected after 6 d post-transfection with the Sox10 expression plasmid (Figure 3.30B, second row).

Similar to observations of confluency-induced fluorescence in cells transduced with the reporter lentivirus without TB (Figure 3.29A vs B), increased confluency in cells transduced with the same reporter virus containing TB also increased fluorescent protein expression (Figure 3.30A vs B).

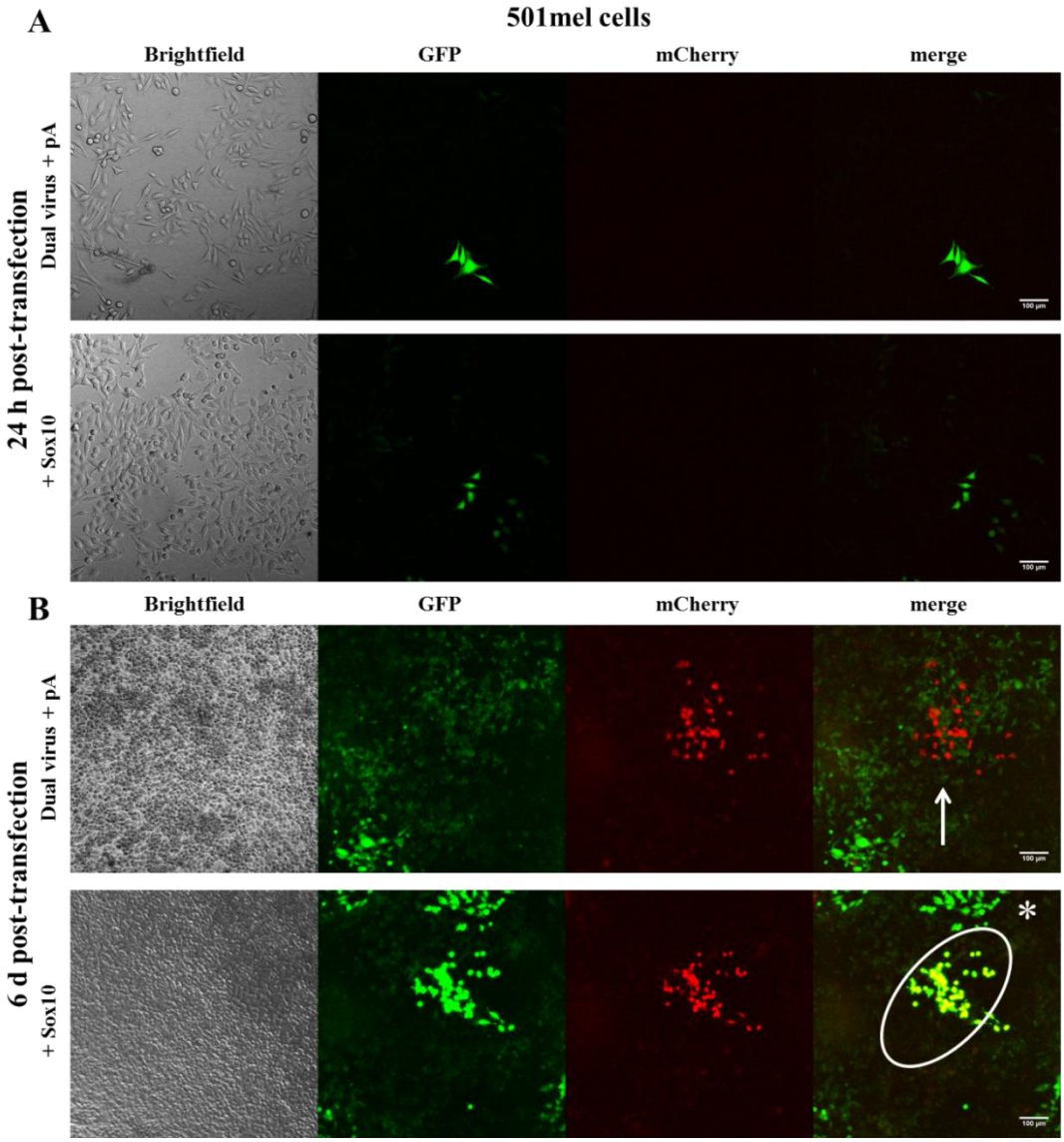


Figure 3.30: Virally transduced 501mel cells express mCherry and GFP. 501mel cells were transduced with the dual reporter lentivirus containing TB and treated with puromycin to select for the cells that were infected. Subsequently, cells were transfected with a Sox10 expression plasmid (1 µg) and GFP and mCherry expression (second and third column, respectively) were measured 24 h and 6 d post-transfection (A and B, respectively). These channels were also combined in a merged picture (fourth column). Cells expressing both GFP and mCherry were circled. Cells expressing solely GFP were marked with an asterisk, while populations of solely mCherry$^+$ cells were indicated with an arrow. Scale bar represents 100 µm.

As for the results obtained with the dual reporter virus without TB, these data also demonstrate that the *Brn2* and *MITF* promoters were functional and responsive to changes in the microenvironment.

3.3.2 mCherry$^+$ polyclonal cells express both fluorescent proteins

Having produced stably expressing cells, the next step was to generate stable clonal cell lines. These were the basis for the investigation into phenotype-switching. To this end, a cell suspension of lentivirally-tranduced cells was generated and cells were sorted by fluorescence using FACS. This was performed with the help of Andrew Worth (Jenner Institute, Oxford University).

To obtain polyclonal populations of cells transduced with the reporter lentiviruses without TB (originating from multiple mCherry$^+$ or GFP$^+$ cells), mCherry or GFP-expressing cells were seeded into 48 well plates after sorting. Fluorescence was assessed by microscopy (Figure 3.31) and flow cytometry (Figure 3.32).

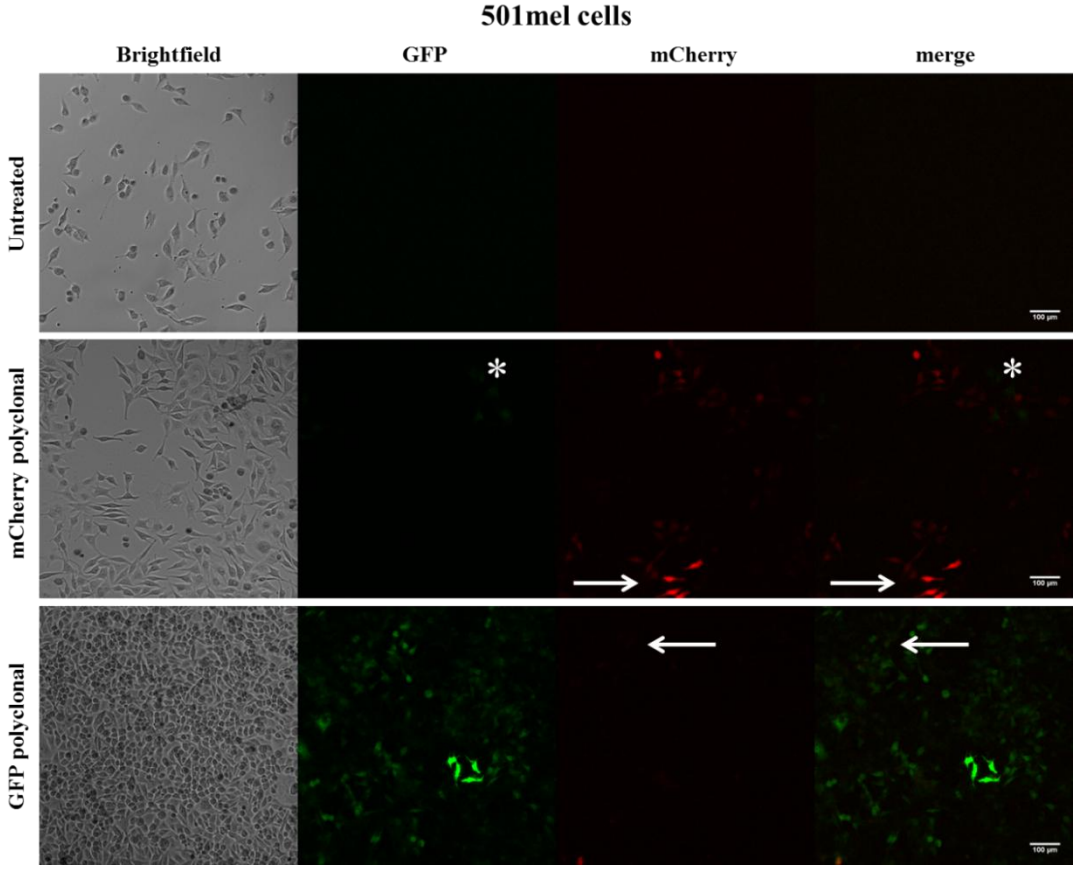


Figure 3.31: Polyclonal populations of lentivirally-transduced cells express mCherry and GFP. Fluorescence was assessed in FACS-sorted 501mel cells, transduced with the dual reporter lentivirus without TB. mCherry was detected in cells that were sorted for mCherry expression (mCherry polyclonal, second row, arrow), while GFP was detected in GFP polyclonal cell populations (GFP polyclonal, third row, asterisk). The scale bar represents 100 µm.

mCherry and GFP polyclonal cell populations both expressed the respective fluorescent proteins (Figure 3.31, second and third row, arrow and asterisk, respectively). The observation that not all cells seemed to express detectable levels of mCherry in the mCherry polyclonal population, might have been due to cell confluency, as demonstrated above. Therefore, as all cells should be expressing mCherry after FACS sorting, the only possible explanation for the low mCherry^{+} cell number was that due to heterogeneity in this cell population, it was not possible to detect mCherry expression in all cells at this low cell density. Interestingly, GFP^{+} cells were also detected in the mCherry polyclonal population (Figure 3.31, second row, asterisk). The GFP polyclonal population also seemed to contain mCherry^{+} cells, although it was unclear if this was an artefact of the confluency (Figure 3.31, third row, arrows).

Heterogeneous expression of GFP was also demonstrated in GFP polyclonal cells (Figure 3.31, third row). The high degree of heterogeneity in both cell lines indicated that *MITF* and *Brn2* promoter activity varied between cells. Another explanation for this observation might have been the difference in viral copy numbers that were present in each cell.

To confirm these results, the cell populations were analysed by flow cytometry (Figure 3.32). Using flow cytometry it was demonstrated that 5.43% within the mCherry polyclonal cell population express detectable mCherry levels, compared to 0.15% in untreated 501mel cells (Figure 3.32, second row). Even though most cells should have been expressing mCherry after FACS sorting, by flow cytometry it seemed that only a proportion of these cells expressed mCherry, again suggesting that the expression was too low to detect by these two techniques. Furthermore, as demonstrated above (Figure 3.30), mCherry expression was affected by cell density, therefore the low confluency of

the mCherry polyclonal cell population might have hampered the detection of all mCherry^{+} cells.

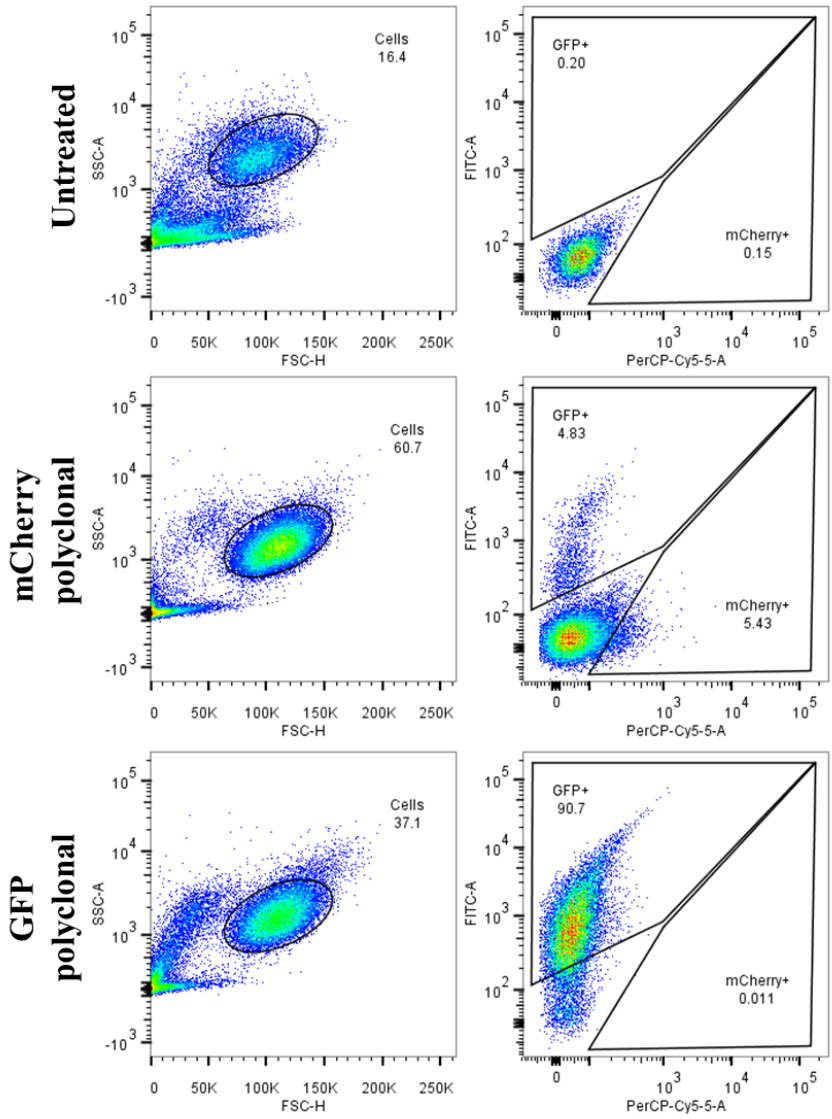


Figure 3.32: Polyclonal populations of lentivirally-transduced cells express mCherry and GFP. Fluorescence was assessed in untreated 501mel cells (first row) and FACS-sorted mCherry polyclonal (second row) and GFP polyclonal cells (third row) previously transduced with the dual reporter lentivirus without TB.

As previously demonstrated by microscopy (Figure 3.32), GFP-expressing cells were also present in the mCherry polyclonal population (4.83% compared to 0.2% in the untreated cells) (Figure 3.32, second row).

In the GFP polyclonal population 90.7% of cells expressed detectable GFP (compared to 0.2% in the untreated cells) (Figure 3.32, third row). No striking changes in mCherry cell numbers were detected, suggesting that the mCherry^{+} cells detected by microscopy

in the GFP polyclonal population, might have been an artefact of the increased cell density.

To summarise, firstly, these results demonstrate the expression of the correct fluorescent proteins in the sorted polyclonal cell populations. Secondly, GFP^+ cells were observed in mCherry-sorted cells. This suggests that there is potential for phenotype-switching. However, the other possibility is that GFP^+ cells were accidentally sorted together with $mCherry^+$ cells and might therefore be an artefact.

As these results have shown, it was not conclusive whether the heterogeneous expression of the fluorescent proteins was an indication of the activity of the promoters or only due to the transduction efficiency of the virus. To this end, stable clonal cell lines were generated to ensure that the genetic background within each population was the same (referred to as monoclonal cell population). Working with monoclonal cells would allow us to conclusively correlate changes in mCherry and GFP expression to changes in promoter activity.

To generate stable cell lines, $mCherry^+$ and GFP^+ cells, as well as cells expressing both fluorescent proteins at the time of sorting, were sorted into 96 well plates (one cell per well) to grow up colonies of monoclonal populations of cells.

To ensure that the cells had been correctly sorted and that the expression of the fluorescent proteins was maintained throughout future experiments, fluorescence was measured at different time points. The single cells sorted into 96 well plates were fragile and prone to apoptosis. Therefore fluorescence was assessed at different time points post-sorting (Figure 3.33).

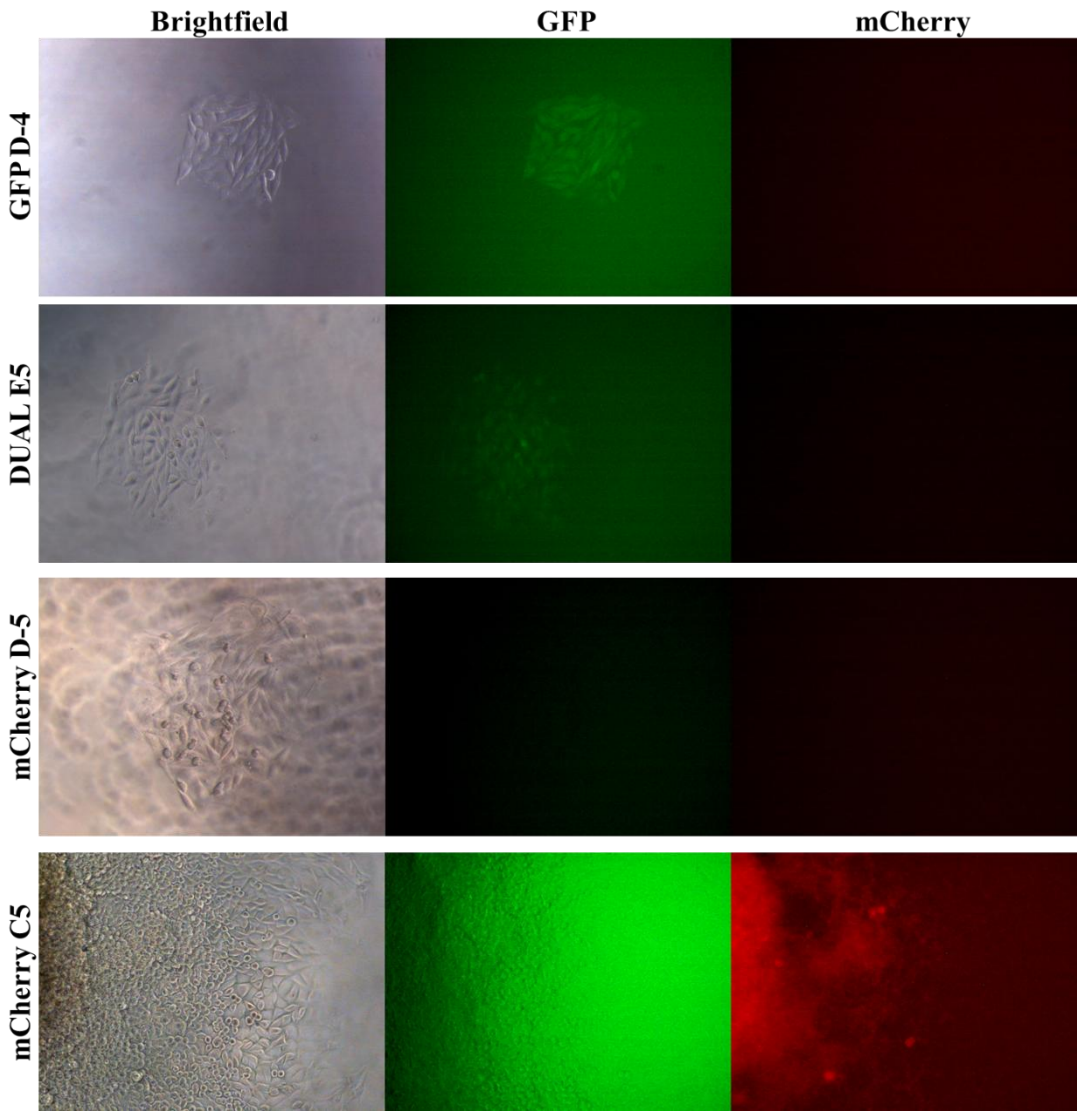


Figure 3.33: Monoclonal colonies express either mCherry or GFP after sorting. 501mel cells transduced with the dual reporter lentivirus with or without TB were FACS-sorted into single wells on a 96 well plate. Fluorescence of GFP-expressing clones GFP D-4 and DUAL E5 as well as mCherry-expressing clones mCherry D-5 and mCherry C5 was measured 6-8 d post-sorting.

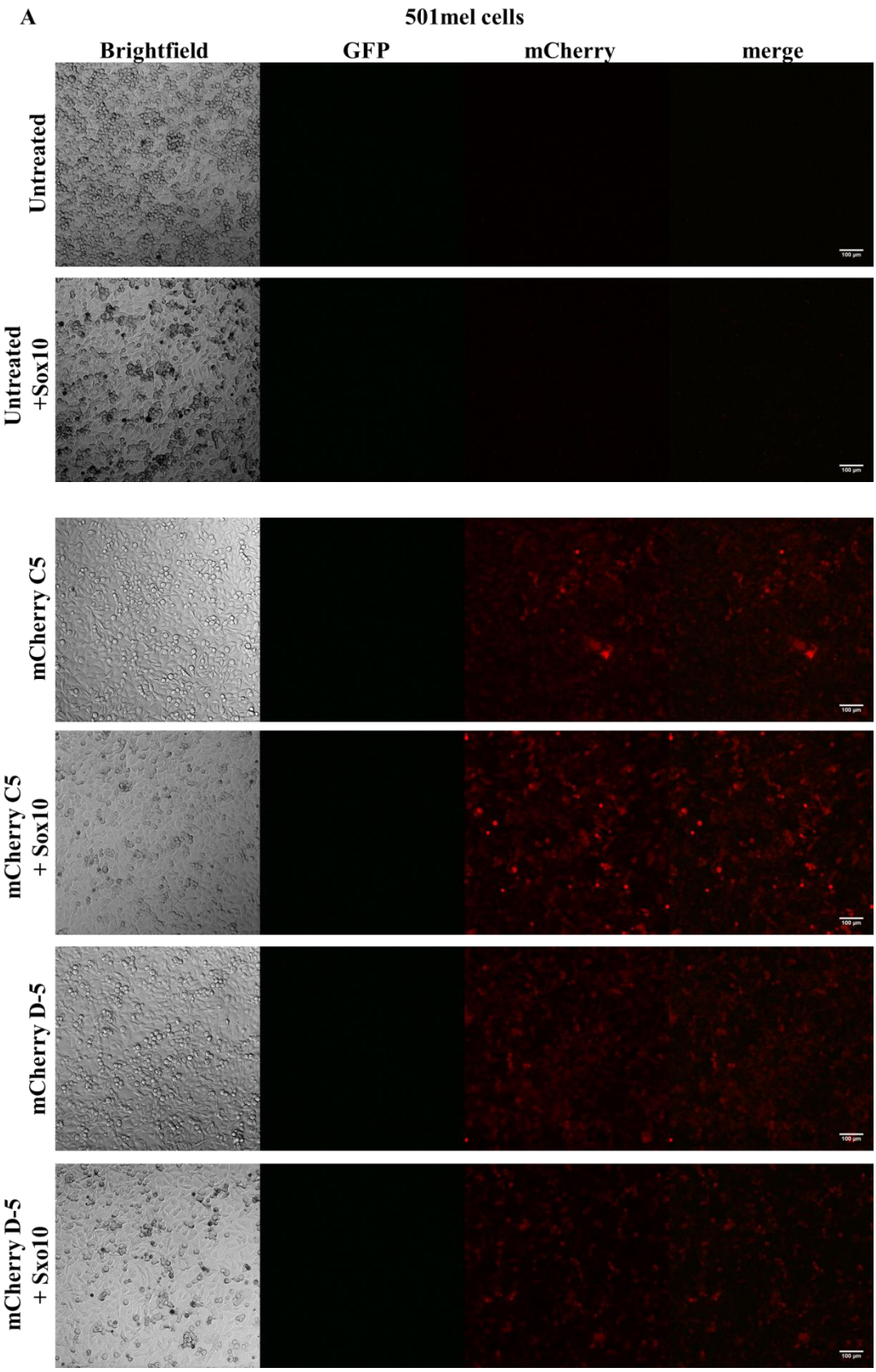
Cell colonies were picked and expanded based on the fluorescent protein expression. The GFP-expressing clone, GFP D-4, the mCherry-expressing clone mCherry D-5 and the clone expressing both fluorescent proteins DUAL E5 were imaged 6 d, 7 d and 8 d post-sorting (Figure 3.33). While GFP D-4 and mCherry D-5 were generated from the virus that did not contain the TB, in DUAL E5 the p*Brn2*-Luc and p*MITF*-Luc constructs were separated by the TB.

The colony GFP D-4 expressed GFP, while no mCherry was detected. The same was true for the colony DUAL E5. None of the clones sorted for expression of both

fluorescent proteins expressed mCherry. However, DUAL E5 showed the most reliable GFP expression and since the initial sorting was performed on the basis of mCherry expression as well as GFP expression, it was assumed that this cell clone would contain the capacity to respond to signals increasing mCherry expression. Due to the fact that mCherry expression in the clone mCherry D-5 was low, another round of FACS sorting was performed on the mCherry polyclonal population. From the second FACS sort an additional mCherry-expressing clone was chosen and expanded, mCherry C5. Similar to DUAL E5, this clone also contained a TB between the p*Brn2*-Luc and p*MITF*-mCherry constructs. The image above was taken 3 weeks after the second FACS sort, explaining the high cell density at the time when the picture was taken.

Interestingly, despite having the same genetic background, the monoclonal population also demonstrated a heterogeneous expression of GFP (GFP D-4 and DUAL E5) and mCherry expression (mCherry C5). However, as all cells originated from the same cell, the changes in mCherry and GFP expression must have been due to changes in promoter activity.

To test if the cell lines were responsive to Sox10 activation of the *MITF* and *Brn2* promoters, the stable cell lines were transfected with the Sox10 expression plasmid (Figure 3.34).


A
501mel cells
Brightfield
GFP
mCherry
merge
Untreated
Untreated +Sox10
mCherry C5
mCherry C5 + Sox10
mCherry D-5
mCherry D-5 + Sxo10

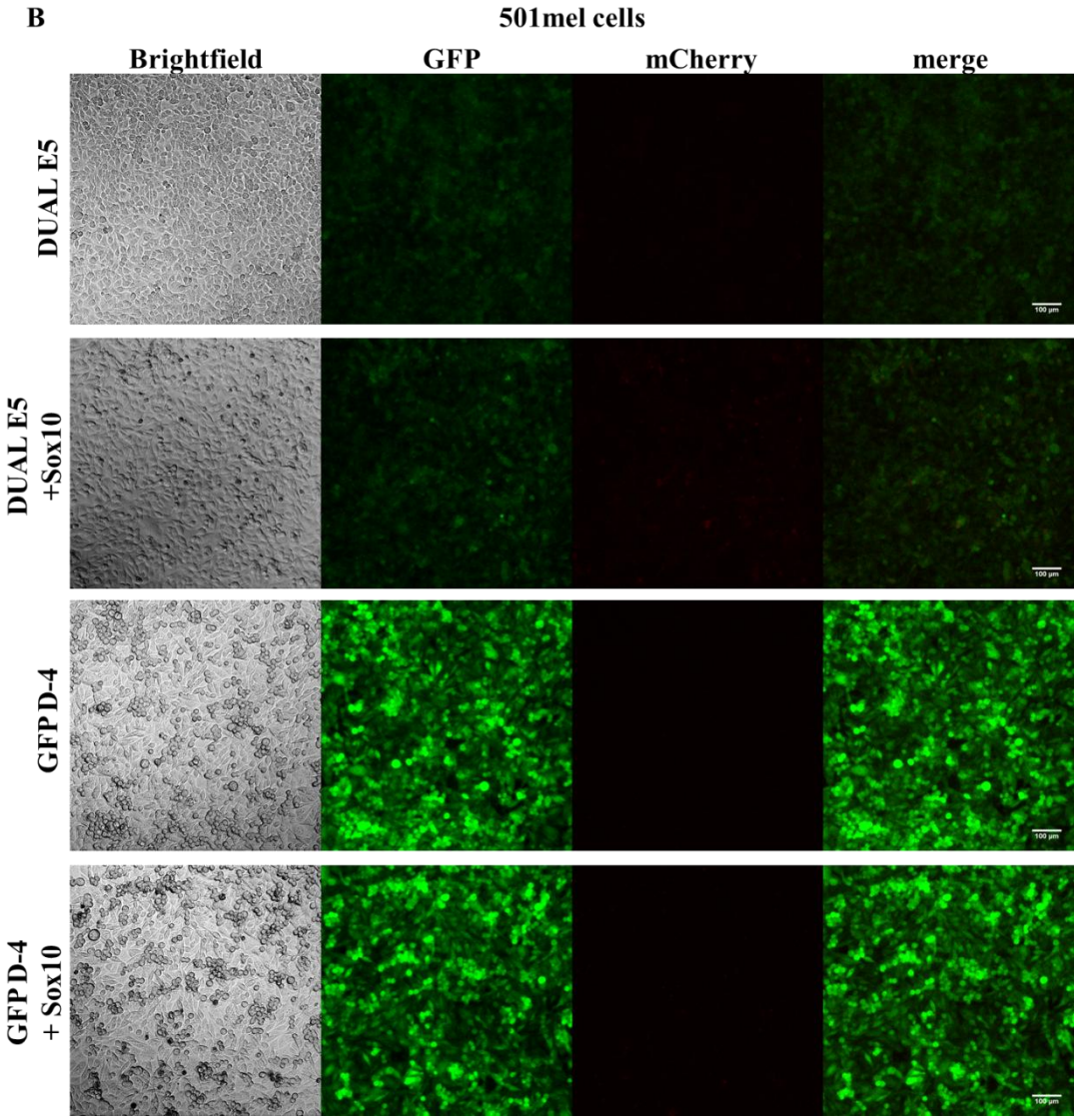


Figure 3.34: Monoclonal cell populations express GFP and mCherry. Monoclonal cell clones mCherry D-5 and C5 (both in **A**) and DUAL E5 and GFP D-4 (both in **B**) were transfected with 750 ng of the Sox10 expression plasmid and mCherry and GFP expression was measured 48 h post-transfection. Scale bar represents 100 µm.

Despite the results obtained before demonstrating Sox10-induced activation of the *MITF* and *Brn2* promoters, which led to an increase in mCherry and GFP expression, respectively, results with the stable clones were not as striking. The number of $mCherry^+$ cells in the clones C5 and D-5 was higher than in untreated 501mel cells, confirming that the clones were fluorescent (Figure 3.34A). However, following transfections with the Sox10 expression plasmid, changes in mCherry expression were difficult to observe (Figure 3.34A). Equally, GFP expression was also not induced by Sox10 in these clones. The untransfected clones DUAL E5 and GFP D-4 still

demonstrated GFP expression (Figure 3.34B). Transfections with the Sox10 expression plasmid did not seem to affect GFP expression. However, mCherry expression seemed to be slightly increased upon Sox10 transfections in the DUAL E5 cell line. To quantify these results, cells were analysed by flow cytometry (Figure 3.35). Interestingly, the results obtained by flow cytometry confirm the data obtained by fluorescence microscopy. Transfections of the untreated 501mel cells with the Sox10 expression plasmid did not change GFP expression strikingly but did increase mCherry signal from 0.13% in the control to 0.82% (Figure 3.35A, second row). As these cells did not express mCherry it must be concluded that transfections increased background fluorescence levels in the mCherry channel and this should be taken into account when considering the effects of Sox10 on clonal cell lines. mCherry C5 and D-5 on their own both expressed mCherry (9.78% and 1.4%, respectively, compared to 0.13% in the untreated control) (Figure 3.35B and C, respectively, top row). Sox10 induced an increase in mCherry expression in C5 from 9.78% to 12.5% and in D-5 from 1.4% to 2% (Figure 3.35B and C, respectively, second row). GFP expression was not affected.

In the untransfected DUAL E5 cell line 4.77% of cells expressed GFP compared to 0.12% in untreated 501mel cells (Figure 3.35D). Transfections with the Sox10 expression plasmid increased GFP expression to 6.05% (Figure 3.35D). The percentage of $mCherry^{+}$ cells within the untransfected DUAL E5 clone was 1.81%, which increased to 3.25% upon transfection with the Sox10 expression plasmid.

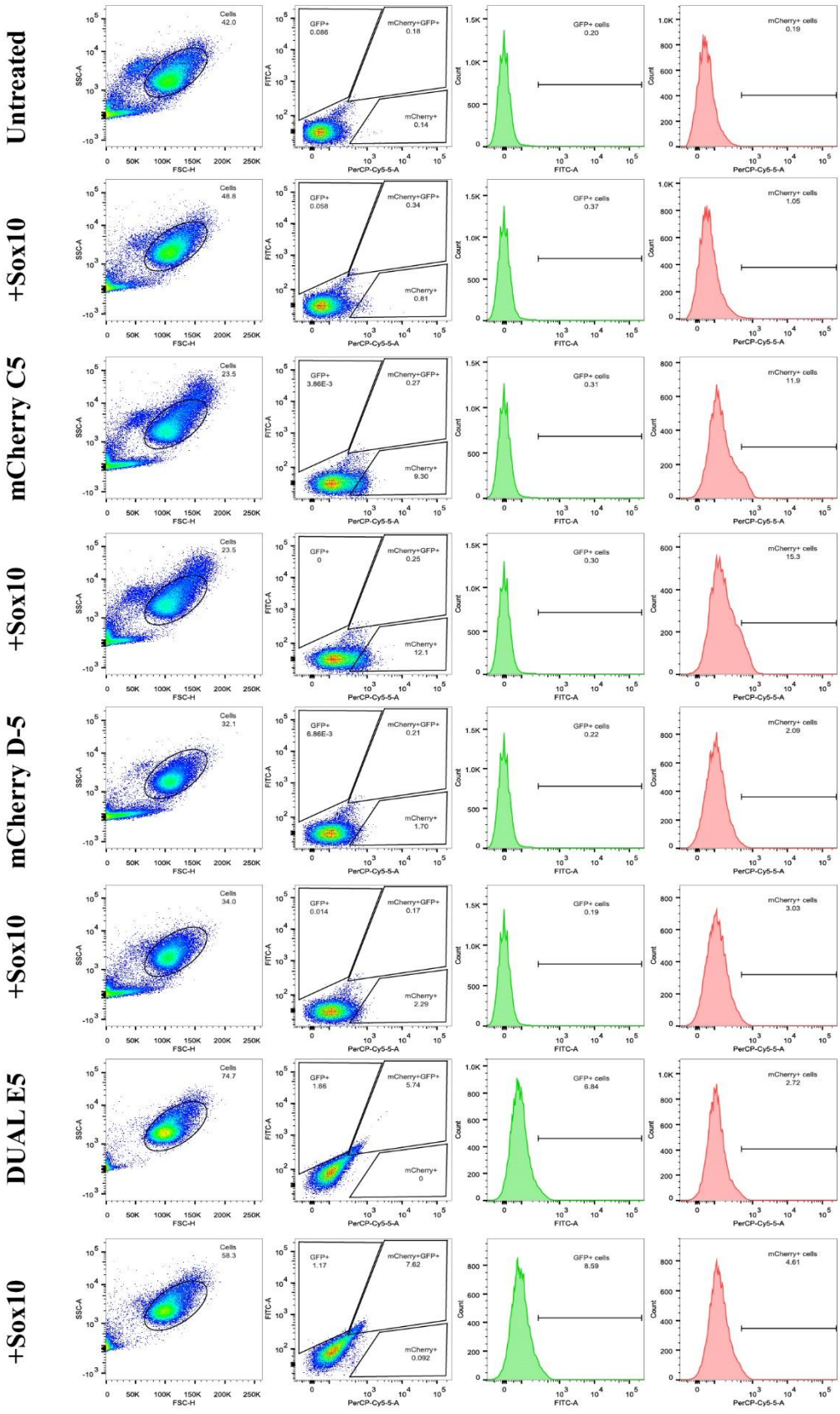

Untreated
+Sox10
mCherry C5
+Sox10
mCherry D-5
+Sox10
DUAL E5
+Sox10
Cells
GFP+
mCherry+GFP+
mCherry+
GFP+ cells
mCherry+ cells
SSC-A
FSC-H
FITC-A
PerCP-Cy5-5-A
Count

Figure 3.35: Sox10 increases mCherry expression in monoclonal cell populations. Upon transfections of untreated 501mel cells (A) and monoclonal cell populations mCherry C5 (**A**), mCherry D-5 (**B**) and DUAL E5 (**C**) with 750 ng of Sox10 expression plasmid, mCherry and GFP expression was measured 48 h post-transfection.

To summarise, transfections with Sox10 expression plasmid increased the number of GFP- or mCherry-expressing cells in all stable clones. However, as this was also observed following transfections of untreated 501mel cells with the Sox10 expression plasmid, the true effect of Sox10 on the activity of the *Brn2* and *MITF* promoters was difficult to interpret. Nonetheless, the use of the clones for further experiments was still justified as it was shown that the cells do possess the capacity to respond to changes in the microenvironment and potentially also to ectopic expression of Sox10.

3.3.3 Kinase inhibitor screen

The goal of the kinase inhibitor screen was to discover a compound that is able to affect *Brn2* and/or *MITF* promoter activity, thereby potentially inducing changes in the cell phenotype. The kinase inhibitor screen was conducted on the reporter cell line DUAL E5, as this cell line showed consistently detectable GFP expression.

Compounds were analysed for their ability to increase GFP levels, as we were interested in *Brn2* promoter regulation (Table 3.1). Kinase inhibitors were sorted in a descending order according to their rank product, which is a variable that takes into account the potential of a compound to increase GFP expression compared to the negative DMSO control, as well as how well the two replicates correlated. The top 100 hits are summarised in Table 3.1.

Some of the hits that increased GFP include p38 kinase inhibitors, GSK3 inhibitors, CDK inhibitors, transforming growth factor-β (TGF-β) inhibitor and a Rho kinase inhibitor (rank 45 and 48). As we were mainly interested in the processes of migration and invasiveness, some kinases were not assessed further as they were already known to be involved in MITF protein regulation and were being investigated by other

members of the group. We decided therefore to focus on pathways that are implicated in melanomagenesis, which led to the decision to assess Rho kinases and their inhibitors in more detail (Chapter 4). Rho kinases affect cell migration and are hypothesised to play a role in tumourigenesis (Sahai and Marshall, 2002). To date, the link between Rho kinases and Brn2 function in melanoma has not been investigated, making the Rho/Rho-associated coiled-coil forming kinase (ROCK) pathway attractive to explore and potentially target in melanoma.

Table 3.1: Top 100 hits of the kinase inhibitor library increasing GFP expression in the cell line DUAL E5

Rank	Compound	Rank product	pfp	p-value	z-score rep 1	z-score rep 2
1	TGF-β inhibitor	4.8	0.0625	0.000211	14.19	21.46
2	CRAF inhibitor	11.92	0.246	0.002078	4.79	18.17
3	CDK inhibitor	17.66	0.432143	0.00511	13.66	11.53
4	TIE-2 and VEGFR-2 inhibitor	22.78	0.628333	0.009552	2.71	17.52
5	TIE-2 and VEGFR-2 inhibitor	23.45	0.604	0.010203	31.7	3.48
6	MSK-1 inhibitor	30.41	0.690714	0.016334	2.56	16.3
7	p38 kinase inhibitor	32.56	0.695	0.018784	5.7	9.17
8	IKK-α and β kinase inhibitor	32.73	0.659412	0.018936	23.2	3.27
9	CDK2 inhibitor	32.86	0.630556	0.019172	3.4	13.29
10	JNK2 and JNK3 inhibitor	33.05	0.606579	0.019468	4.47	11.4
11	IKK-α and β kinase inhibitor	35.69	0.65575	0.022154	29.17	2.58
12	p38 kinase inhibitor	36.11	0.641667	0.022762	26.69	2.75
13	p38 kinase inhibitor	36.74	0.604565	0.023488	31.56	2.09
14	p38 kinase inhibitor	37.55	0.600208	0.024333	23.05	2.98
15	GSK3 inhibitor	40.84	0.6748	0.028497	3.35	11.6
16	p38 kinase inhibitor	44.72	0.721667	0.032914	15.87	3.62
17	Polo-like kinase 1 inhibitor	45.43	0.715	0.033818	21.41	2.66
18	p38 kinase inhibitor	50.89	0.846724	0.041478	20.75	2.55
19	ErbB-1/ErbB-2 tyrosine kinase inhibitor	53.38	0.889667	0.045084	4.54	6.43
20	GSK3 inhibitor	55.96	0.907656	0.049063	7.98	3.97
21	GSK3 inhibitor	57.23	0.859143	0.050794	12.03	3.13
22	p38 kinase inhibitor	60.01	0.912917	0.055515	20.81	1.61
23	JNK2 and JNK3 inhibitor	60.43	0.895946	0.055997	21.79	1.21
24	GSK3 inhibitor	60.66	0.878947	0.056419	4.44	5.76
25	ErbB-2 tyrosine kinase inhibitor	60.82	0.860128	0.056664	11.25	3.07
26	GSK3 inhibitor	61.64	0.854875	0.057762	16.31	2.41
27	TGF-β inhibitor	62.06	0.842805	0.05837	3.81	6.44
28	ErbB-1/ErbB-2 tyrosine kinase inhibitor	62.35	0.830714	0.058936	16.88	2.18

29	GSK3 inhibitor	62.93	0.823953	0.059848	2.91	8.57
30	RET kinase inhibitor	67.4	0.828542	0.067179	5.32	4.35
31	p38 kinase inhibitor	68.85	0.843469	0.069814	3.02	7.06
32	GSK3 inhibitor	70.46	0.8586	0.072517	1.14	11.02
33	IKK-β kinase inhibitor	70.88	0.835385	0.073378	17.52	1.32
34	TIE-2 and VEGFR-2 inhibitor	71.55	0.830377	0.074341	1.22	10.96
35	IKK-α and β kinase inhibitor	75.7	0.859375	0.081292	18.3	0.82
36	p38 kinase inhibitor	76.68	0.864474	0.083235	8.33	2.68
37	p38 kinase inhibitor	78.1	0.874224	0.08565	1.84	8.32
38	GSK3 inhibitor	79.74	0.888559	0.088556	14.27	1.52
39	GSK3 inhibitor	82.49	0.867344	0.093767	11.02	1.9
40	Polo-like kinase 1 inhibitor	83.07	0.85053	0.094823	5.84	3.06
41	p38 kinase inhibitor	83.25	0.840896	0.095169	10.9	1.97
42	IGF-1R inhibitor	87.33	0.87	0.102872	9.45	1.86
43	ErbB-2 tyrosine kinase inhibitor	87.64	0.862676	0.103463	9.71	1.79
44	ErbB-1/ErbB-2 tyrosine kinase inhibitor	90.99	0.883243	0.110405	7.37	2.29
45	Rho kinase inhibitor	91.27	0.863684	0.110878	1.83	6.63
46	p38 kinase inhibitor	91.59	0.857727	0.111563	-0.6	9.81
47	p38 kinase inhibitor	93.2	0.869551	0.114569	-1.95	9.83
48	Rho kinase inhibitor	94.44	0.876899	0.117019	1.01	8.3
49	TIE-2 and VEGFR-2 inhibitor	95.94	0.888938	0.120127	3.05	5.02
50	p38 kinase inhibitor	96.63	0.874878	0.121182	6.42	2.37
51	VEGFR-2 inhibitor	97.15	0.870542	0.122052	7.73	1.92
52	GSK3 inhibitor	99.28	0.887321	0.125904	2.11	6.09
53	GSK3 inhibitor	101.51	0.908294	0.130414	1.2	6.82
54	GSK3 inhibitor	102.03	0.894713	0.131486	0.86	7.55
55	p38 kinase inhibitor	103.42	0.902955	0.134223	0.98	6.94
56	GSK3 inhibitor	103.96	0.899551	0.135236	3.87	3.51
57	ROCK1 inhibitor	105.08	0.904556	0.137517	2.63	4.97
58	CDK2 inhibitor	107.83	0.892842	0.143277	3.06	4.43
59	TIE-2 and VEGFR-2 inhibitor	108.25	0.889896	0.144307	5.18	2.54
60	BRAF kinase inhibitor	108.73	0.886289	0.14522	-2.12	8.62
61	ErbB-1/ErbB-2 tyrosine kinase inhibitor	109.11	0.882041	0.146014	6.06	1.85
62	p38 kinase inhibitor	109.12	0.873283	0.146039	2.48	4.89
63	MSK-1 inhibitor	109.62	0.8701	0.146976	5.25	2.42
64	GSK3 inhibitor	110.91	0.876782	0.149586	4.39	2.85
65	JNK2 and JNK3 inhibitor	111.12	0.871078	0.150084	3.5	3.64
66	CRAF inhibitor	111.27	0.86432	0.15038	3.06	4.26
67	CDK2 inhibitor	111.47	0.858654	0.150845	3.69	3.48
68	BRAF kinase inhibitor	112.29	0.860429	0.15261	2.41	4.81
69	CRAF inhibitor	113.18	0.847593	0.154628	0.82	6.56
70	GSK3 inhibitor	114.47	0.840495	0.157593	1.57	5.65
71	ErbB-1/ErbB-2 tyrosine kinase inhibitor	114.49	0.833259	0.157644	2.11	5.06
72	ErbB-1/ErbB-2 tyrosine kinase inhibitor	116.1	0.838596	0.161486	1.08	6.23
73	CRAF inhibitor	116.48	0.836087	0.162416	3.84	3.16
74	EGFr and c-erbB-2 inhibitor	116.67	0.830991	0.162829	4.34	2.73
75	IKK-α and β kinase inhibitor	120.9	0.855966	0.172061	6.77	1.11

76	MSK-1 inhibitor	121.79	0.859708	0.174265	3.26	3.57
77	p38 kinase inhibitor	122.08	0.855661	0.17489	3.36	3.51
78	GSK3 inhibitor	122.33	0.851598	0.175498	3.67	3.16
79	p38 kinase inhibitor	123.64	0.839722	0.178725	2.37	4.33
80	CDK2 inhibitor	124.41	0.840945	0.180405	3.76	2.96
81	GSK3 inhibitor	125.87	0.837615	0.183936	2.01	4.76
82	GSK3 inhibitor	126.33	0.835	0.184772	1.51	5.17
83	p38 kinase inhibitor	127.02	0.835758	0.186351	2.13	4.45
84	CRAF inhibitor	128.69	0.840187	0.190177	2.57	3.89
85	CRAF inhibitor	130	0.83989	0.192948	1.18	5.53
86	p38 kinase inhibitor	131.15	0.839638	0.195726	3.86	2.68
87	Rho kinase inhibitor	133	0.850612	0.199721	1.61	4.77
88	CDK2 inhibitor	134.39	0.852092	0.202948	2.19	4.21
89	Tie-2 inhibitor	134.52	0.848239	0.203463	-0.58	6.23
90	CDK2 inhibitor	137.35	0.854069	0.209189	5.84	0.81
91	CDK2 inhibitor	140.05	0.873527	0.215431	-0.61	6.15
92	p38 kinase inhibitor	140.25	0.869966	0.216022	1.5	4.67
93	CDK inhibitor	143.63	0.882533	0.223615	1.33	4.7
94	Lck inhibitor	145.87	0.898907	0.229282	-2.43	6.18
95	GSK3 inhibitor	148.37	0.892564	0.235203	1.68	4.1
96	MSK-1 inhibitor	151	0.890062	0.242061	3.64	2.52
97	p38 kinase inhibitor	151.2	0.88571	0.242373	0.6	5
98	VEGFR inhibitor	151.79	0.879848	0.243742	3.97	1.94
99	GSK3 inhibitor	152.2	0.877424	0.244552	-0.06	5.37
100	GSK3 inhibitor	156.33	0.879064	0.253919	4	1.76

Pfp = probability of false positive, rep = replicates, TIE2 = tyrosine kinase with immunoglobulin-like and EGF-like domains, VEGFR = vascular endothelial growth factor receptor, MSK = mitogen- and stress-activated protein kinase, IKK = Inhibitor κ B kinase, JNK = c-Jun N-terminal kinase, ErbB = epidermal growth factor receptor, RET = REarranged during Transfection receptor tyrosine kinase, IGF-1R = insulin-like growth factor 1 receptor, Lck = lymphocyte-specific protein tyrosine kinase.

3.4 *In vivo* transplantation of the dual reporter cell lines

Recent publications have addressed phenotype-switching and have demonstrated that cells grown *in vitro* co-express MITF and Brn2, while the majority of cell populations *in vivo* express either MITF or Brn2 (Thurber et al., 2011).

While transfections of the clones with the Sox10 expression plasmid demonstrated a potential regulation of the *Brn2* and *MITF* promoters, changes in the microenvironment did affect GFP and mCherry expression. Consequently, it was hypothesised that the microenvironment *in vivo* might also influence promoter activity. This would contribute to our understanding of cell behaviour *in vivo*. To test this hypothesis, cells have been

inoculated in CD1 nude mice and tumours were grown until the pre-defined tumour burden was reached. Subsequently, tumours were dissociated and fluorescent protein expression was measured using flow cytometry.

3.4.1 GFP and mCherry expression in dual reporter cell lines after in vivo transplantation

Prior to the inoculation into animal models, three cell lines were selected on the basis of their consistent fluorescent protein expression (demonstrated by microscopy (Figure 3.34) and flow cytometry (Figure 3.35)): the mCherry-expressing cell line mCherry C5, the GFP-expressing cell line GFP D-4 and the GFP^+($/mCherry^+$) cell line DUAL E5 were inoculated into CD1 nude mice.

After the mouse tumours were excised and dissociated, the expression of mCherry and GFP in the cell lines was assessed by flow cytometry (Figure 3.36, 3.37, 3.38). Firstly, the tumours generated from the mCherry C5 clone were assessed (Figure 3.36). To ensure that only human cells were analysed and mouse cells were excluded from the analysis, the samples were incubated with an antibody against HLA-A,B,C present on each cell, as well as a mix of anti-mouse antibodies against TER119, CD45, CD31 and CD71 (Quintana et al., 2008). To confirm that the antibodies recognised the correct cells, they were tested on 501mel (Figure 3.36, first row) and on mouse B16F10 cells (data not shown).

mCherry expression was measured in the original mCherry C5 clone to establish that expression was still present. The percentage of $mCherry^+$ cells was 13.5% compared to 0.12% in the untreated control, while GFP was not expressed (Figure 3.36, second row). Since the clone was transplanted into both sides of the flank of the mouse, two tumours developed. The number of mCherry-expressing cells in tumour 1 was 63.2%,

while GFP was expressed in 25.8% (Figure 3.36, third row) compared to 0.14% in untreated cells. In tumour 2, the GFP^+ cell number was 17.6%, while the mCherry-expressing cell number was 50.8% (Figure 3.36, fourth row).

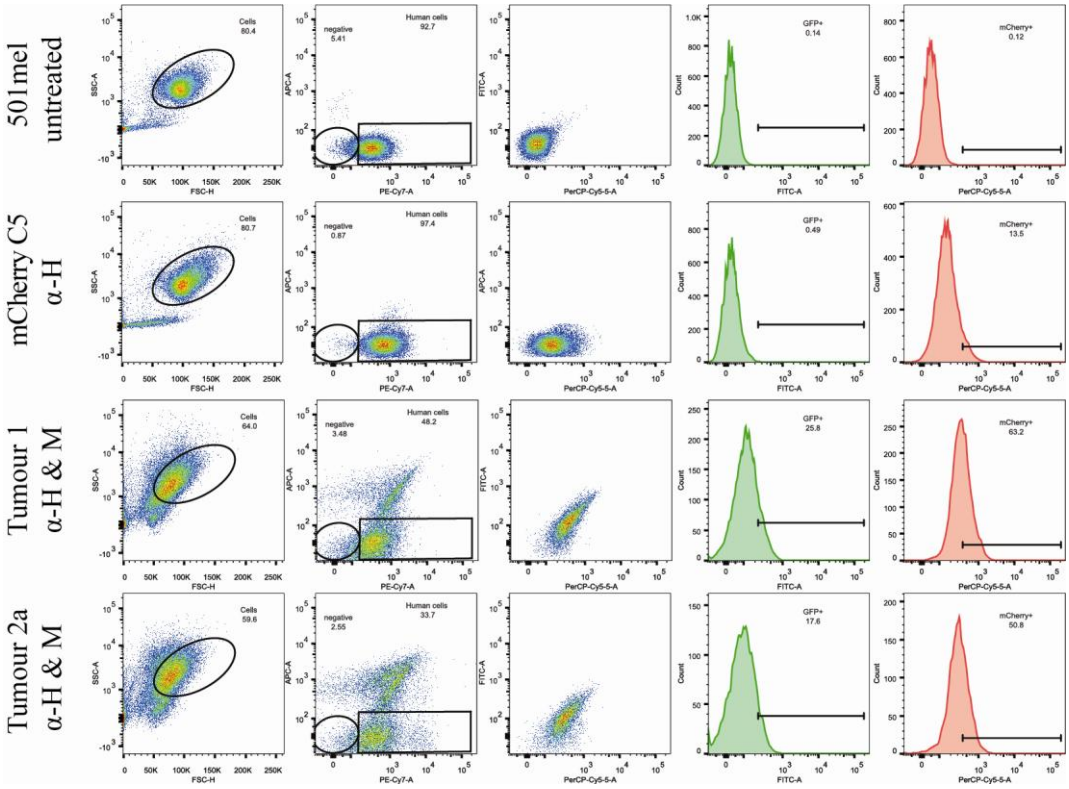


Figure 3.36: mCherry C5 clone expressed GFP and mCherry after xenotransplantation into CD1 nude mice. mCherry C5 cells generated two tumours (Tumour 1 and 2) *in vivo*. After excision of the tumour, mCherry C5 cells were dissociated and fluorescence was assessed by flow cytometry after culturing *in vivo*. Untreated 501mel and mCherry C5 cells grown *in vitro* were used as control. Cells were incubated with antibodies recognising human HLA-A, B, C (α-H) and/or mouse antibodies recognising TER-119, CD31, CD71 and CD45 (α-M).

While it was expected that the tumours would still be expressing mCherry, GFP expression was unexpected. One explanation for this finding might have been due to autofluorescence of apoptotic cells. As the tumour samples have not been treated with a live/dead stain prior to measurement, it is possible that cells undergoing apoptosis were fluorescent. However, another explanation is that the microenvironment *in vivo* might have activated the *Brn2* promoter and induced expression of GFP, a result that would be in agreement with the phenotype-switching hypothesis.

To assess the fluorescence in the GFP-expressing cell clone GFP D-4 after *in vivo* transplantation, cells were dissociated and incubated with the anti-human and-mouse antibodies prior to assessment by flow cytometry (Figure 3.37).

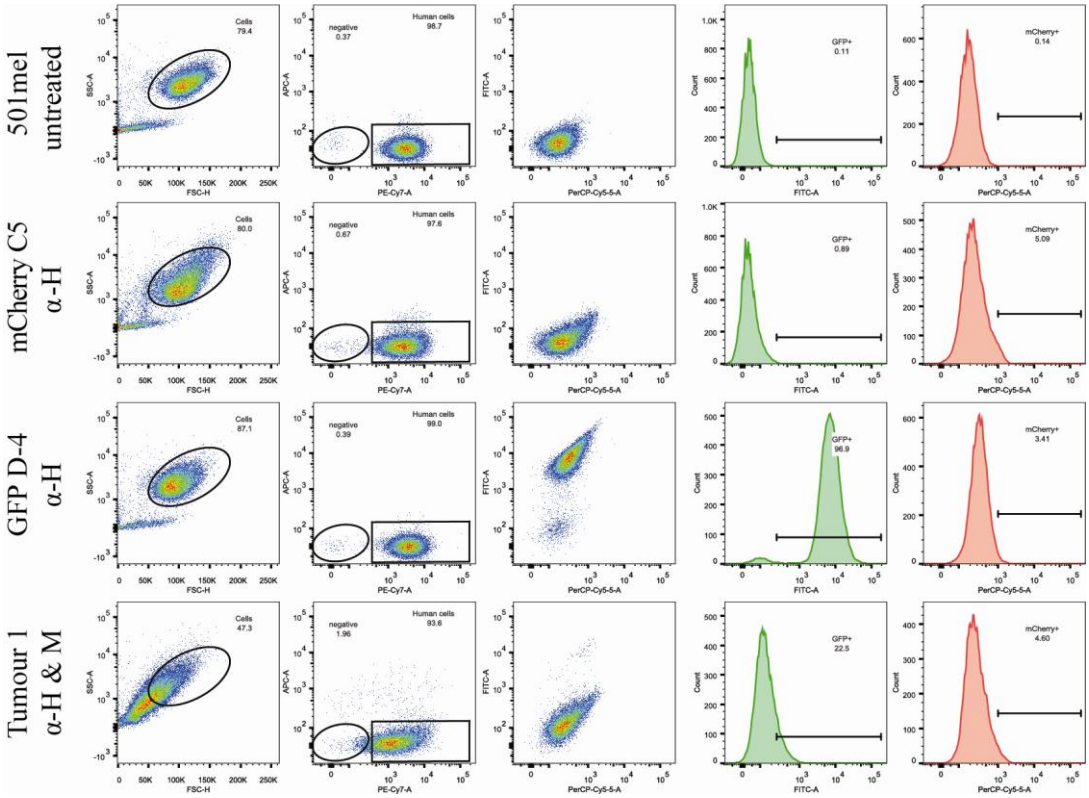


Figure 3.37: GFP clone D-4 expresses GFP after xenotransplanation into CD1 nude mice. GFP D-4 cells generated one tumour *in vivo*. After excision of the tumour, GFP D-4 cells were dissociated and fluorescence was assessed by flow cytometry. Untreated 501mel, mCherry C5 and GFP D-4 cells, grown *in vitro*, were used as controls. Cells were incubated with antibodies recognising human HLA-A,B,C (α-H) and/or mouse antibodies recognising TER-119, CD31, CD71 and CD45 (α-M).

Prior to the assessment of the clone, mCherry C5 and GFP D-4 cell lines only cultured *in vitro* were analysed for their fluorescent protein expression. The number of $mCherry^+$ cells in the mCherry C5 cell line was 5.09%, compared to 0.14% in the untreated control, which is lower than observed previously (Figure 3.36). The number of GFP^+ cells in this cell line was 0.89% compared to 0.11% in the control (Figure 3.37, second row). However, at this stage it was unclear if this was a true increase in GFP expression or an artefact. GFP expression in the GFP D-4 cell line was observed in 96.9%, while mCherry was expressed in 3.41% of cells (Figure 3.37, third row). In the GFP D-4 clone grown *in vivo* (tumour 1), 22.5% of the HLA-A,B,C-positive cells expressed GFP

and 4.6% expressed mCherry (Figure 3.37, fourth row). It was intriguing that 4.6% of cells started to express mCherry, however, similarly to the GFP D-4 cell line grown *in vitro* (Figure 3.37, third row) it was unclear if this was a true result or an artefact due to the presence of apoptotic cells. Additionally, it was surprising that only a small percentage of cells expressed GFP, compared to the GFP D-4 cell line grown *in vitro* (Figure 3.37, third row) suggesting that most cells stopped fluorescent protein expression. This was intriguing as a potential explanation could be silencing of promoters as reported previously (Frame et al., 2010). Alternatively, it is also possible that only those cells propagated that did not express GFP in the beginning, although this population was very small *in vitro* (3.1%, Figure 3.37, third row).

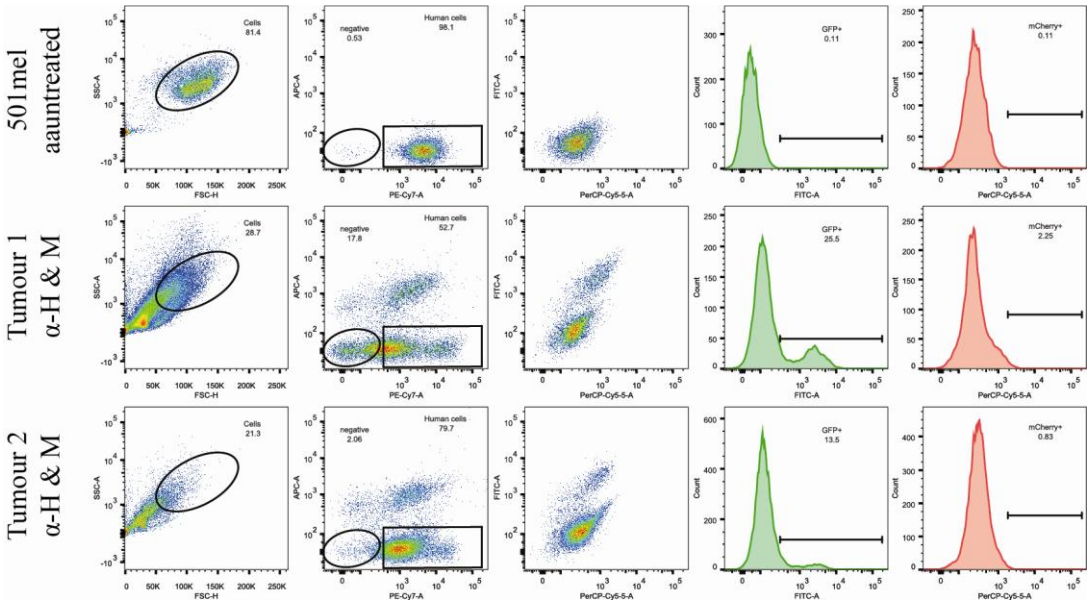


Figure 3.38: DUAL E5 tumour expressed GFP and mCherry after xenotransplanation. DUAL E5 cells generated two tumours *in vivo* (Tumour 1 and 2). After excision of the tumour, DUAL E5 cells were dissociated and fluorescence was assessed by flow cytometry. Untreated 501mel cells, grown *in vitro*, were used as control. Tumour cells were incubated with antibodies recognising human HLA-A,B,C (α-H) and mouse antibodies recognising TER-119, CD31, CD71 and CD45 (α-M).

Similar to the mouse that received mCherry C5 cells, the DUAL E5 clones also generated two tumours. While the GFP expression in tumour 1 was 25.5% (Figure 3.38, second row) compared to 0.11% in the untreated control, the percentage of GFP^+ cells in tumour 2 was 13.5% (Figure 3.38, third row). The percentage of mCherry-expressing

cells in both tumours, on the other hand, was 2.25% in tumour 1 and 0.83% in tumour 2, compared to 0.11% in the untreated control (Figure 3.38, second and third row).

To summarise, the mCherry C5 clone produced tumours that contained $mCherry^+$ and GFP^+ cells. Similarly, the tumours that originated from the clones GFP D-4 and DUAL E5 produced GFP^+ cells and a small percentage of $mCherry^+$ cells. Furthermore, the percentage of GFP^+ cells in the tumour was smaller than in the parental population grown *in vitro*. Consequently, the majority of the cells was negative for fluorescent protein expression.

3.5 Discussion

The first part of this chapter summarises the engineering of the dual lentiviral reporter plasmids. Subsequently, melanoma cells were transduced and cells containing the viral genome were selected with the antibiotic puromycin. mCherry and GFP expressions in transduced cells were analysed by microscopy and flow cytometry. Afterwards cells were sorted by flow cytometry to produce poly- and monoclonal cell populations of either mCherry- or GFP-expressing cells. To test whether changes in the microenvironment would affect *MITF* or *Brn2* promoter activity, monoclonal cell populations were transplanted into mice and a kinase inhibitor library screen was performed.

According to the cancer stem cell hypothesis only CSCs have the ability to self-renew and enable the long-term propagation of tumours, as demonstrated in several cancers (Al-Hajj et al., 2003; Bonnet and Dick, 1997; O'Brien et al., 2007). However, the phenotype-switching theory on the other hand, posits that through interconversion a CSC can acquire properties of proliferating or differentiating cells and vice versa. This would imply that there is no fixed cell state and that the cells are plastic. The cues for a

cell to change its phenotype will come from the microenvironment (Pinner et al., 2009; Thurber et al., 2011).

However, despite one of the assumptions of the phenotype-switching theory being that conversion can take place in both directions, we only observed a uni-directional change in phenotype *in vitro*, whereby the mCherry polyclonal cell population produced GFP^+ cells. *In vivo,* it seemed that some rate of interconversion might have taken place in the monoclonal cell lines because a cell line that was purely $mCherry^{positive}$ produced $mCherry^+$ and GFP^+ cells. Similarly, $GFP^{positive}$ cell lines produced GFP^+ and $mCherry^+$ cells, even though the percentage of $mCherry^+$ cells was low. While this could be an indication for phenotype-switching, it is also possible that cells started co-expressing fluorescent proteins without a change in phenotype.

Additionally, this *in vivo* data exemplified the concept of intertumour heterogeneity. In the case of mCherry C5, but more so in the DUAL E5 tumour samples, it was obvious that the two tumours that developed from both cell lines within the same animal expressed different numbers of $mCherry^+/GFP^+$ cells. This demonstrated that despite the fact that the parental population was the same, the tumours that developed from it were different. As the genetic composition of these tumours was the same at the time of inoculation, the changes in fluorescent protein expression within the tumours between the two samples, must have originated from differences in the microenvironment. This illustrates the crucial role the microenvironment plays on tumour development.

Previously, segregation of Brn2- and MITF-expressing cells has only been demonstrated to take place *in vivo* (Thurber et al., 2011). Therefore one explanation why this effect was not striking in our experiments, might have been due to the length of the *Brn2* and *MITF* promoters. These will be lacking crucial regulatory elements, potentially located upstream or downstream of the promoter sequence used. Despite the

promoters being able to respond to changes, such as activation by Sox10 or confluency *in vitro*, it is possible that more complex regulation is required *in vivo*. One example of this level of regulation is mediated by microRNAs (miRs), which can control the stability of mRNAs by inducing its silencing or degradation (Bartel, 2009). Some miRs are known regulators of MITF expression, such as miR-137 (Bemis et al., 2008), miR-182 (Segura et al., 2009), miR-340 (Goswami et al., 2010) or miR-218 (Guo et al., 2014). Interestingly, there are also miRs that regulate Brn2 expression, such as miR-211 (Boyle et al., 2011), inhibition of which increases Brn2 protein expression in melanocytes (Boyle et al., 2011). Overexpression in melanoma cells, on the other hand, leads to a decrease in invasion by decreasing Brn2 translation (Boyle et al., 2011). Furthermore, a comparison between melanocytes and melanoma cell lines demonstrated that miR-211 expression is decreased in the latter (Caramuta et al., 2010). On the basis of these results, physiologically-expressed miR-211 in melanocytes decreases Brn2 protein expression and might therefore provide the missing link between decreased MITF levels, which lead to a decrease in miR-211 expression and in turn to an increase in Brn2 protein levels as well as increased metastatic potential in melanoma cells.

These results demonstrate how crucial miRs are for the expression of certain proteins and therefore the determination of a phenotype. It is unlikely that miRs are the only mediators of phenotype-switching, but to date there is no clear mechanisms that might drive a change in phenotype. Therefore it is possible that the lack of miR binding sites in the reporters used here prevented an obvious change from GFP to mCherry expression and vice versa.

Other factors that can contribute to phenotype-switching might be post-translational modifications of Brn2 and MITF, such as phosphorylation and addition of small ubiquitin-like modifiers (SUMOylation). For Brn2, phosphorylation can lead to

differential promoter selectivity by changing its DNA binding capabilities (Nieto et al., 2007; Sunabori et al., 2008). Phosphorylation as a post-translational modification was also shown to affect the transcriptional activity of MITF, with increased phosphorylation being able recruit the p300/CREB-binding protein (CBP) co-activator more efficiently (Price et al., 1998).

Additionally, MITF was also shown to be a target of SUMOylation (Bertolotto et al., 2011; Murakami and Arnheiter, 2005). A missense substitution of glutamic acid to lysine at position 318 in MITF (E318K) impairs its SUMOylation, leading to an increase in colony formation, metastasis and invasion (Bertolotto et al., 2011). These examples demonstrate how crucial post-translational modifications are for the correct functioning of Brn2 and MITF. This is specifically the case for phenotype-switching, whereby Brn2 has to change from being an activator of MITF (*in vitro*) to a repressor of MITF (*in vivo*).

In our reporter system we would have been unable to detect any changes in post-translational modifications. This is due to the fact that we only measure promoter activity as opposed to post-translational modifications of Brn2 and MITF. Depending on the contribution of these modifications to phenotype-switching, it might have been difficult to observe this in our system, as we were measuring transcriptional activity of the *Brn2* and *MITF* promoters, instead.

To identify compounds that can affect *Brn2* or *MITF* promoter activity, the DUAL E5 cell line was used for the kinase inhibitor screen. From the screen, multiple compounds were identified that were able to induce GFP expression. As we were mainly interested in processes of migration and invasiveness, most kinases were not further assessed as they were involved in MITF protein regulation and investigated by other members of the group. We decided to focus on pathways that are implicated in melanomagenesis,

which led to the decision to assess Rho kinases and their inhibitors in more detail (Chapter 4). Rho kinases affect cell migration and are hypothesised to play a role in tumourigenesis. As the connection between Rho kinases and Brn2 function in melanoma was unknown, the Rho/ROCK pathway was an attractive target to explore for melanoma treatment.

Another mechanism that might be contributing to metastasis generation might be through Sox10-mediated activation of the *Brn2* promoter. The transcription factor Sox10 is expressed in neural crest cells (Kim et al., 2003) and involved in the development of glial cells (Britsch et al., 2001) and melanocytes (Southard-Smith et al., 1998). While Sox10 is expressed in melanoblasts, its expression is lost during melanocyte differentiation (Greenhill et al., 2011). Mutations in the *Sox10* gene have been identified to cause Waardenburg-Hirschsprung syndrome (Pingault et al., 1998) with patients suffering from this syndrome exhibiting hypopigmentation of the hair, skin, iris, as well as sensorineural deafness (Pingault et al., 1998).

Sox10 binds and activates the melanocyte-specific *MITF* promoter (Lee et al., 2000; Potterf et al., 2000; Verastegui et al., 2000) and has also been shown to activate the *DCT* gene (Jiao et al., 2004). Interestingly, it seems that Sox10 and MITF can regulate melanoblast-specific genes together (Jiao et al., 2004), potentially even Brn2. Although a direct interaction between Brn2 and Sox10 has not been reported before, both transcription factors are expressed in unpigmented melanocyte precursor cells and are down-regulated during differentiation (Cook et al., 2005). However, an argument that strengthens our results is the finding that Sox10 physically interacts with Brn2 (Smit et al., 2000).

Another finding that supports our observation is that Sox10 levels are increased in melanoma tissue and cell lines (Bakos et al., 2010; Flammiger et al., 2009; Shakhova et

al., 2012), and recently Sox10 has also been linked to invasion through its ability to regulate melanoma inhibitory activity (MIA) (Graf et al., 2014). Consequently silencing of Sox10 in human melanoma cells decreases colony formation *in vitro* and tumourigenesis *in vivo* (Shakhova et al., 2012). Furthermore, silencing of Sox10 in B16F10 cells reduced their migratory activity *in vitro* as well as *in vivo* using a lung metastasis animal model (Seong et al., 2012).

As Sox10 has been linked to invasiveness, we propose that one of the mechanisms to achieve this might be through an increase in Brn2 expression. However, we have not demonstrated whether an increase in *Brn2* promoter activity also leads to an increase in Brn2 protein expression. Nonetheless, knowing that Brn2 expression leads to an invasive phenotype (Pinner et al., 2009), alongside reports demonstrating increased Sox10 expression in melanoma and in invasion, opens up the possibility that Sox10 is mediating its invasive effects, at least in part, through Brn2.

To summarise the results from this chapter, while the dual reporter cell lines might have not fully represented endogenous promoter activity *in vivo*, they were still a useful tool for screening a kinase inhibitor library *in vitro*. We identified a ROCK inhibitor that increases GFP expression, activating the *Brn2* promoter, and therefore potentially inducing a phenotype that resembles that of de-differentiated cells. The next step is to confirm whether this compound affects endogenous *Brn2* promoter activity and to investigate in more detail the pathways that might be involved in metastasis and invasion.

4 The RhoA/ROCK pathway affect *Brn2* and *MITF* promoter activity in 501mel and SKmel28 cells

4.1 Introduction

4.1.1 Metastasis and invasion in melanoma

Melanoma is considered to be one of the most aggressive and dangerous tumours because of its metastasising properties (Miller and Mihm, 2006). For cells to metastasise, changes in cell adhesion have to occur in order to allow them to separate from the general tumour mass. Subsequently, cells will migrate from the primary tumour and intravasate to the lymphatic system from which they will eventually extravasate and colonise a secondary site (Hanahan and Weinberg, 2011). Once cells have colonised in the secondary site, they induce the generation of growth factors by their neighbouring cells to enable proliferation. In some cases, this process can take years as cells might assume a quiescent or dormant state first (Hoek and Goding, 2010).

During the process of metastasis and invasion of the surrounding tissue, cells are thought to undergo a process called epithelial-to-mesenchymal (EMT) transition, leading to changes in the gene expression profile of invasive cells (Hanahan and Weinberg, 2011). EMT was first described in embryonic epithelial cells during embryogenesis (Rubinfeld et al., 1997). However, as melanocytes originate from neural crest cells that also undergo an EMT-like transition to migrate to the epidermis during development, the process of EMT is also used in the context of de-differentiation and metastasis in melanoma. EMT is characterised by altered expression of genes, such as Twist, Snail, Slug and E-cadherin (Hanahan and Weinberg, 2011), which encodes for a transmembrane protein that is crucial for cell adhesion and for cell-to-cell interactions.

In melanoma, the T-box transcription factor TBX3 downregulates E-cadherin expression, thereby contributing to the progression from radial to vertical growth phase

(Rodriguez et al., 2008). Metastasising cancer cells also increase expression of N-cadherin, another transmembrane protein, allowing the metastasising cells to interact with stromal cells (Li et al., 2001). Additionally, in some cancer cells the cell adhesion molecule MCAM is overexpressed, facilitating the interaction of cancer cells with endothelial cells (Bogenrieder and Herlyn, 2002).

4.1.2 The Rho/ROCK pathway

While the general concept of metastasis formation has been investigated in many cancers, in melanoma this process is still not well understood. This has been delaying the progress of finding a long-lasting treatment for patients and therefore it is of primary interest to elucidate the molecular pathways involved in metastasis formation.

One of the key processes involved in migration is the RhoA/ROCK pathway (Sahai and Marshall, 2002). RhoA is a GTPase that belongs to the Rho-family proteins consisting of 18 members and four subgroups, one of which is the RhoA subgroup (Sahai and Marshall, 2002). The activation of RhoA is mediated by Rho guanine nucleotide exchange factors (Rho-GEFs), which allow guanosine triphosphate (GTP) to bind to RhoA (Sahai and Marshall, 2002). GTP is subsequently hydrolysed to guanosine diphosphate (GDP), which is catalysed by Rho-GTPase-activating proteins (Rho-GAPs) (Figure 4.1) (Sahai and Marshall, 2002).

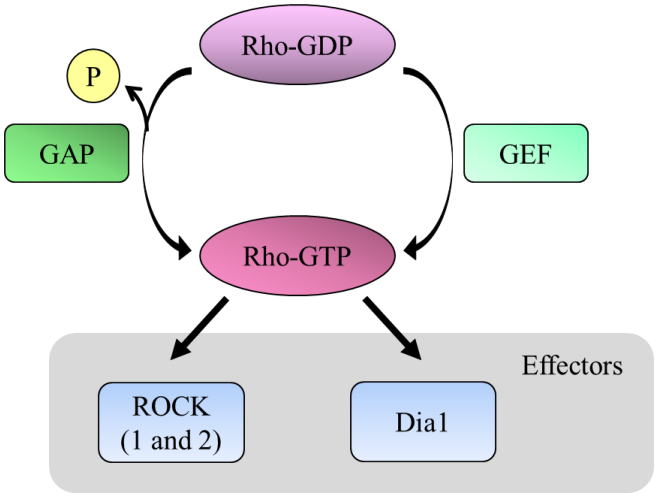


Figure 4.1: Schematic diagram of Rho protein regulation. Rho proteins can bind GDP and GTP. While inactive Rho proteins are bound to GDP, active Rho proteins bind GTP. The exchange from GDP to GTP is promoted by Rho guanine nucleotide exchange factors (GEFs). Once active, Rho proteins interact with effectors such as ROCK1 and 2, and diaphanous-related formin-1 (Dia1). The inactivation of Rho proteins happens either through their intrinsic activity to hydrolyse GTP to GDP and phosphate (P), or through Rho-GTPase-activating proteins (GAPs). Adapted from (Sahai and Marshall, 2002).

The activation of a Rho protein by the binding of GTP allows it to interact with effector molecules, which in turn can affect cell behaviour (Sahai and Marshall, 2002). Examples of effector molecules are the diaphanous-related formin-1 (Dia1) (Watanabe et al., 1999) and the serine/threonine ROCK kinases ROCK1 and ROCK2 (Watanabe et al., 1999). The latter two kinases are isoforms of each other with 64% homology between their kinase domains (Leung et al., 1996). While their expression is ubiquitous, ROCK1 is mainly expressed in liver, kidneys and lung (Morgan-Fisher et al., 2013) and ROCK2 is predominantly expressed in the brain and heart (Morgan-Fisher et al., 2013). Due to their high homology the kinases are activated similarly and share similar substrates. Nonetheless, they have also been reported to have distinct roles. For instance, while ROCK1 is involved in stress fibre formation and the process of focal adhesion, ROCK2 plays a role in myosin II-dependent phagocytosis (Yoneda et al., 2005).

One of the main roles of the Rho pathway is the control of the actin cytoskeleton (Hall, 2009). This is mediated through the ROCK1- and 2-induced phosphorylation of

proteins such as LIM kinases 1 and 2, the myosin regulatory light chain (MLC) and the myosin binding subunit of the MLC phosphatase (Amano et al., 2000).

ROCK kinases have been implicated in various processes such as the organisation of the cytoskeleton (Watanabe et al., 1999) and cell migration (Itoh et al., 1999; Somlyo et al., 2000) as well as in human diseases. Examples of diseases are cardiovascular disorders (Olson, 2008), neurodegenerative diseases (Zhou et al., 2003) and cancer (Lochhead et al., 2010).

To study the effect of ROCK proteins in these processes, mainly pharmacological inhibitors have been utilised, of which the two most common ones are Y27632 and fasudil, which has been approved in Japan for the treatment of cerebral vasospasm (Olson, 2008).

In a related research field, cells have been successfully generated by transforming mouse and human somatic cells to subsequently show properties and behaviour of tissue stem cells. These were consequently called iPS cells (Takahashi and Yamanaka, 2006). While the first attempts consisted of a cocktail of four to five transcription factors (Takahashi and Yamanaka, 2006), later other factors, such as ROCK inhibitors, were added to increase the efficiency of iPS cell generation (Park et al., 2008). This again points towards the important role of ROCK in the maintenance and induction of stem cells.

4.1.3 Rho/ROCK proteins in tumourigenesis

Metastatic cancer results from the transformation of benign cells to metastasising and invading cells. In order to metastasise, cells must be able to change their morphology, increase the motility, invade the neighbouring tissue and survive at distal sites from the primary tumour.

As the Rho/ROCK pathway is crucial for cell motility and morphology it is likely that it contributes to the process of invasion (Itoh et al., 1999; Somlyo et al., 2000). For this reason, it has been hypothesised that its inhibition might affect the formation of metastases (Itoh et al., 1999; Somlyo et al., 2000). In fact, inhibiting ROCK activity by Y27632 or fasudil *in vitro* blocks invasion in prostate cancer (Somlyo et al., 2000) and in glioma (Deng et al., 2010).

In melanoma, ROCK inhibition using the compound Y27632, alters cellular morphology and survival, and decreases invasion *in vitro* as well as leads to a reduction in melanoma tumour volume *in vivo* (Routhier et al., 2010). Using Wf-536, a different ROCK inhibitor, on mouse melanoma cell lines, leads to inhibition of invasion *in vitro* (Nakajima et al., 2003). Furthermore, the administration of this compound reduced the metastasis formation capability of cells in a spontaneous metastasis assay as well as in an experimental metastasis assay *in vivo*, without significantly altering the tumour volume in the mice (Nakajima et al., 2003).

4.1.4 Rho/ROCK proteins and Brn2

During development neural crest cells migrate from the neural crest to the epidermis and the hair follicle to develop into melanocytes. Therefore, it is possible that in melanoma, metastasising cells might have similar characteristics to neural crest cells. A crucial protein involved in the development of melanocytes from neural crest cells is the transcription factor Brn2 (Cook et al., 2003). During development Brn2 is downregulated to allow the melanoblasts to mature into melanocytes (Cook et al., 2003; Cook and Sturm, 2008). In explanted cultures from mouse embryos from E9 neural crest cells it was shown that Brn2 DNA binding activity was still present (Cook et al., 2003). In 2004, however, Goodall and colleagues showed that in murine E11.5

melanoblasts, Brn2 mRNA expression was not detectable (Goodall et al., 2004a). This can be explained by the fact that melanoblasts are more differentiated than neural crest cells and that Brn2 expression is mainly present in cells that are more stem-like (section 1.10.2). Additionally, it is possible that Brn2 is re-activated when melanoblasts or neural crest cells are placed in culture, possibly through activation of the MAPK pathway. Similarly, de-differentiation of human melanocytes using a mixture of different factors induces the expression of Brn2 and leads to the loss of pigmentation (Cook et al., 2003). This finding was confirmed and elaborated by retrovirally-mediated Brn2 overexpression in cultured mouse melanocytes (Goodall et al., 2004b). Moreover, Brn2 is also downregulated in response to the differentiating agents butyric acid and DMSO (Sturm et al., 1991).

Correspondingly, it is well documented that MITF is involved in the differentiation and development of melanocytes and therefore the induction of lineage specific genes (Cheli et al., 2010) and the generation of melanin (Bertolotto et al., 1996) (section 1.9.1). Interestingly, MITF is expressed in $Brn2^{low}$ cells and vice versa (Goodall et al., 2008), whereby the lack of MITF in these cells could account for the invasive properties of $Brn2^{+}$ cells (Pinner et al., 2009) and potentially mark melanoma stem cells.

This hypothesis is also supported by findings *in vivo*, whereby a subpopulation of low-pigmented melanoma cells, in which GFP expression was driven by *Brn2* promoter activity, was able to metastasise and regulate GFP expression after extravasation (Pinner et al., 2009). While this reinforces the hypothesis that Brn2 might be used as a marker for potential melanoma initiating cells, it also strengthens the argument of phenotype switching as well as the rheostat model: low pigmented cells, i.e. cells with

low MITF expression, containing high levels of Brn2, were able to metastasise into neighbouring tissues (Pinner et al., 2009).

Currently it is still unknown how Brn2 and ROCK interact to induce EMT and metastases, and in particular, if and how this interaction might be contributing to the metastatic properties of Brn2-positive melanoma stem cells.

MITF-depleted melanoma cells, which had undergone actin reorganization of the cytoskeleton, were more invasive and contained increased ROCK signalling (Carreira et al., 2006). Crucially, when these cells were treated with a ROCK inhibitor, the MITF depletion in these cells did not result in invasive cells. This suggested that ROCK activation was necessary for the invasion of melanoma cells.

4.1.5 Chapter objectives

Following on from the preliminary hit from the kinase inhibitor library screen (discussed in the previous chapter), there was an indication that the ROCK inhibition might affect *Brn2* promoter activity. It is clear that MITF levels affect ROCK activity but there is no direct indication of the mechanism of action of ROCK on Brn2.

The aims of this chapter are therefore:

- to investigate if activation of GTPase RhoA and the kinase ROCK1 lead to an increase in *Brn2* promoter activity
- to identify the effects of RhoA on Brn2 protein levels
- to explore the effect of ROCK inhibition on Brn2 protein levels
- to correlate these findings with effects on the *MITF* promoter and protein levels.

4.2 Results

4.2.1 RhoA activates the Brn2 promoter

As demonstrated in the first chapter (section 3.3.3), one of the preliminary hits from the kinase inhibitor screen included a Rho kinase (ROCK) inhibitor. The screen was set up to investigate pathways that might affect metastasis and invasion in melanoma. To this end, we primarily focussed on inhibitors that can activate the *Brn2* promoter.

As ROCK kinases are activated by the GTPase RhoA, we next investigated in more detail if the RhoA/ROCK pathway is involved in *Brn2* promoter activation. To this end, transfection experiments were performed with the wild-type (WT) p*Brn2*-luciferase (p*Brn2*-Luc) reporter plasmid. The WT *Brn2* promoter is made up of a 1.7 kilobases (kb) fragment upstream of a 168 basepair (bp) 5' untranslated region (UTR), followed by the luciferase gene (Figure 4.2).

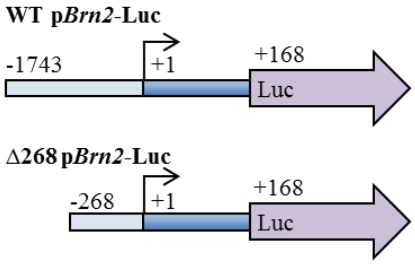


Figure 4.2: Diagram of the *Brn2* promoter-luciferase constructs. The WT p*Brn2*-Luc construct consists of a 1.7 kb fragment upstream of the 5' UTR, while Δ268 p*Brn2*-Luc construct contains a 268 bp fragment. Both promoter constructs comprise a 168 bp 5' UTR followed by the luciferase gene.

For transfection experiments, increasing amounts of a plasmid expressing WT and constitutively-active (CA) RhoA (RhoA WT and CA) were co-transfected into 501mel and SKmel28 cells together with the WT p*Brn2*-Luc plasmid (Figure 4.3).

The RhoA CA contains a Q63L mutation which leads to the expression of leucine instead of glutamine at position 63.

In 501mel cells (Figure 4.3A), 100 ng and 200 ng of the RhoA WT expression plasmid induced a small change in luciferase expression when transfected with WT p*Brn2*-Luc plasmid (10% decrease and 19% increase, respectively), whereas 100 ng and 200 ng of

the RhoA CA expression plasmid induced an increase of over 2-fold and 4.5-fold in luciferase expression, respectively, compared to the control.

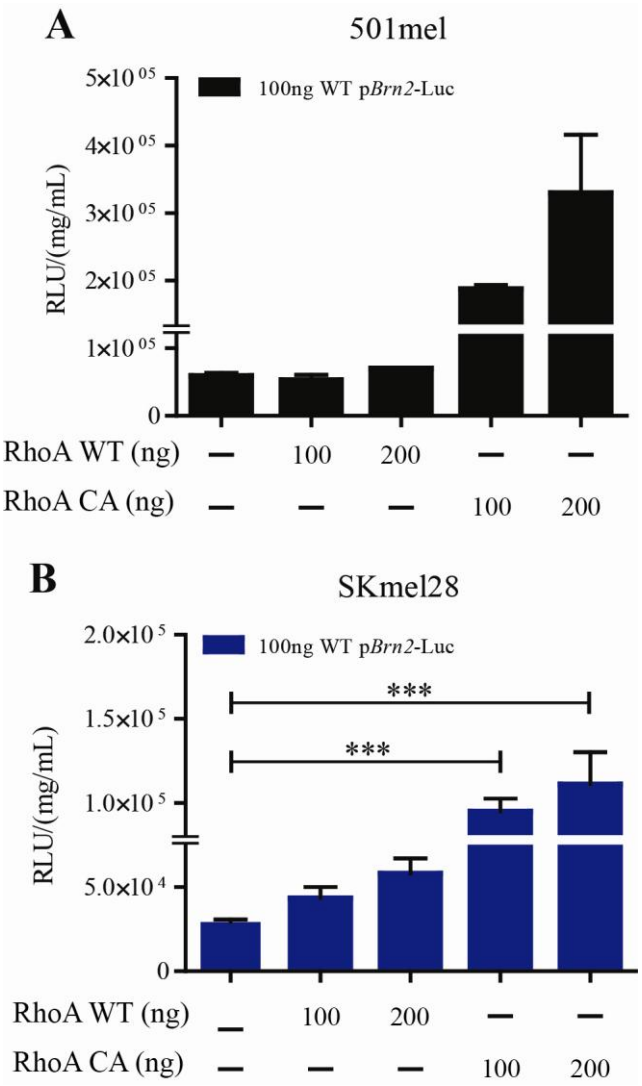


Figure 4.3: Constitutively-active RhoA activates the *Brn2* promoter. Indicated amounts of RhoA WT or CA were transfected into 501mel (**A**) or SKmel28 cells (**B**) together with 100 ng of the WT p*Brn2*-Luc construct. An empty vector was used to control for total amount of DNA. Luciferase expression was measured 24 h post-transfection. Results are expressed as the mean ± S.D., n=2 (501mel cells) n=3 (SKmel28 cells). Statistical analysis was performed using a one-way ANOVA followed by a post-hoc Tukey's test. *** = $p<0.001$

In SKmel28 cells, 100 ng and 200 ng of the plasmid expressing RhoA WT increased p*Brn2* activity (50% and 100%, respectively), while 100 ng and 200 ng of the RhoA CA expression plasmid induced a 3- and almost a 4-fold increase in *Brn2* promoter activity, compared to the control (Figure 4.3B).

4.2.2 RhoA-induced pBrn2 activation is not dependent on TCF/LEF1 binding site

The *Brn2* promoter contains binding sites for the transcription factors Pax3, TCF and LEF1 (Figure 3.3B). As these binding sites have been implicated in *Brn2* promoter activity (Bonvin et al., 2012), we next sought to investigate if RhoA-induced p*Brn2* activation was dependent on these transcription factors. To this end, we used a *Brn2* promoter deletion mutant, Δ268 p*Brn2*-Luc, containing a mutation in the TCF/LEF1 binding site (Δ268 TCF/LEF1 mut p*Brn2*-Luc) (Figure 4.2).

Compared to the WT p*Brn2*-Luc plasmid, the Δ268 p*Brn2*-Luc plasmids contains a 268 bp fragment upstream of the 5' UTR and both promoter constructs comprise a 168 bp fragment followed by the start codon for the luciferase gene (Figure 4.2).

To assess the activity of the deletion mutant Δ268 p*Brn2*-Luc, transfections were performed with increasing concentrations of the RhoA CA expression plasmid in 501mel and SKmel28 cells (Figure 4.4).

In 501mel cells, 50 ng and 100 ng of the plasmid expressing RhoA CA induced an over 20- and 40-fold increase in luciferase expression from the WT p*Brn2*-Luc construct (Figure 4.4A, black bars). The same amounts of RhoA CA expression plasmid induced only minor changes in the Δ268 *Brn2* promoter activity (Figure 4.4A, red bars).

The results demonstrate that in 501mel cells, the Δ268 p*Brn2*-Luc deletion mutant was still responsive and regulated by RhoA CA (Figure 4.4A). The luciferase expression from the Δ268 plasmid was higher than from the WT construct, while its induction by RhoA CA was less pronounced than for the WT. This suggests that the induction by RhoA CA requires key regulatory elements that were lacking in the Δ268 construct.

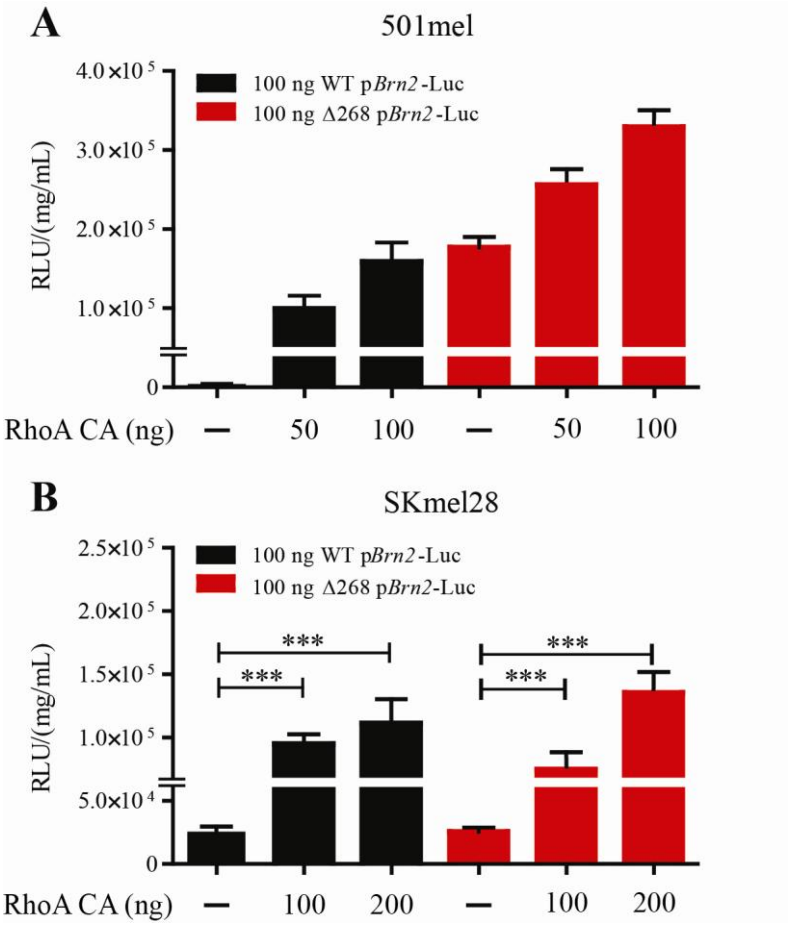


Figure 4.4: Constitutively-active RhoA induces *Brn2* promoter activation in WT and Δ268 p*Brn2*-luciferase constructs. Indicated amounts of RhoA CA were transfected into 501mel (**A**) and SKmel28 (**B**) cells together with 100 ng WT (black bars) or Δ268 (red bars) p*Brn2*-Luc plasmids and an empty vector to control for the total amount of DNA transfected. Luciferase expression was measured after 24 h post-transfection and results were normalised to the protein content per condition. Results are expressed as mean ± S.D. n=2 (501mel) or n=3 (SKmel28). Statistical analysis was performed using a one-way ANOVA followed by a post-hoc Tukey's test. *** = p<0.001

In SKmel28 cells, 100 ng and 200 ng of the RhoA CA expression plasmid induced a 3- and an almost 4-fold increase in WT *Brn2* promoter activity (black bars, p<0.001 in both conditions), respectively (Figure 4.4B). The same amounts co-transfected with the Δ268 p*Brn2*-Luc plasmid induced a 3-fold and over a 5-fold increase in p*Brn2* activity (red bars, p<0.001 in both conditions), respectively.

Despite having used different amounts of the RhoA CA expression plasmid in 501mel and SKmel28 transfections, the results suggest in both cell lines that the Δ268 p*Brn2*-Luc construct is functional and responsive to RhoA CA signalling.

To study the effects of TCF and LEF1 on the RhoA-induced *Brn2* promoter activation, a mutation in the TCF/LEF1 binding site was engineered previously in the Δ268 p*Brn2*-Luc (TCF/LEF1 mut p*Brn2*-Luc) (Goodall 2004) (Figure 4.5).

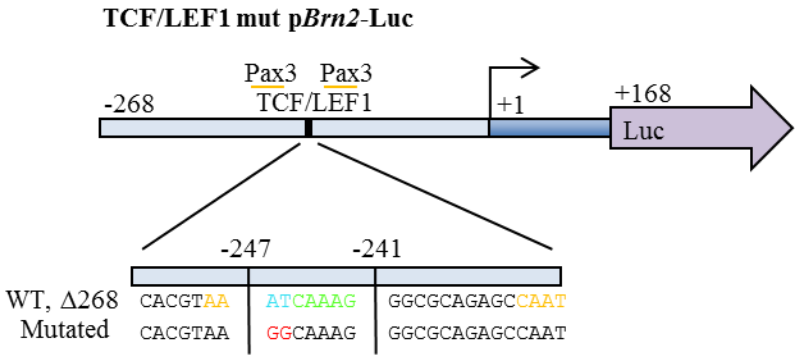


Figure 4.5: Schematic diagram of the TCF/LEF1 mutated p*Brn2*-Luc construct. The WT and the Δ268 *Brn2* promoter contain the TCF/LEF1 binding site (ATCAAAG (green)), as well as the binding sites for Pax3 (orange). In blue are the bases that are used by Pax3, TCF and LEF1. To generate the non-functional TCF/LEF1 binding site, two bases in the Δ268 p*Brn2*-Luc construct were mutated (red).

Co-transfections were performed with the Δ268 p*Brn2*-Luc plasmid with and without the mutated TCF/LEF1 binding site together with increasing amounts of RhoA CA expression plasmid in 501mel and SKmel28 cells (Figure 4.6).

In 501mel cells (Figure 4.6A), transfections with the Δ268 and the TCF/LEF1 mutated p*Brn2* construct demonstrated that the luciferase expression from the latter was much lower than from the Δ268 (80% decrease, $p<0.001$) (Figure 4.6A). 100 ng and 200 ng of the plasmid expressing RhoA CA induced a 40% and an 80% increase ($p<0.01$) in luciferase expression from the Δ268 p*Brn2*-Luc construct compared to the control (Figure 4.6A, red bars).

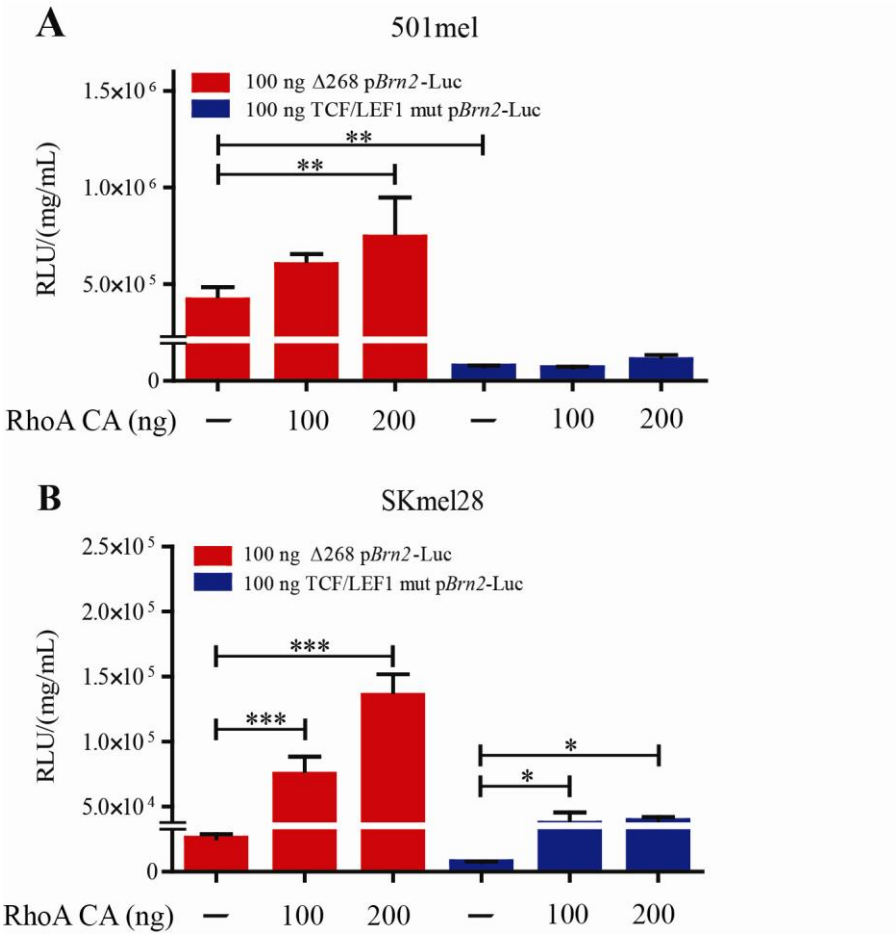


Figure 4.6: Constitutively-active RhoA activates the TCF/LEF1 mut p*Brn2*-Luc construct in SKmel28 cells. Indicated amounts of RhoA CA were transfected together with Δ268 (red bars) and TCF/LEF1 mut p*Brn2*-Luc constructs (blue bars) into 501mel (**A**) and SKmel28 cells (**B**). An empty vector was used to control for total amount of DNA. Luciferase expression was measured 24 h post-transfection and results were normalised to the protein content per well. The graphs represent mean ± S.D, n=3. Statistical analysis was performed using a one-way ANOVA followed by a post-hoc Tukey's test. * = $p<0.05$, ** = $p<0.01$, *** = $p<0.001$.

100 ng of the vector expressing RhoA CA did not affect the luciferase expression from the TCF/LEF1 mutated p*Brn2* strikingly and 200 ng only induced a small increase in luciferase expression (Figure 4.6A, blue bars).

However, in SKmel28 cells, increasing amounts of the RhoA CA expression plasmid induced luciferase expression from TCF/LEF1 mut p*Brn2* (5-fold, $p<0.05$) (Figure 4.6B, blue bars).

To summarise, in both cell lines the Δ268 plasmid was induced by RhoA CA to much higher absolute expression levels than the TCF/LEF1 mut p*Brn2*-Luc construct. However, in SKmel28 cells, the latter was still responsive to increasing concentrations of RhoA CA. Also note that the basal levels after transfection with the TCF/LEF1 mut

p*Brn2*-Luc plasmid were reduced when compared to the Δ268 p*Brn2*-Luc construct. Additionally, the basal level of Δ268 p*Brn2*-Luc activity was higher in 501mel than in SKmel28 cells (Figure 4.6A vs B, blue bars).

These transfection experiments demonstrate that the RhoA-induced *Brn2* promoter activation in SKmel28 cells might not solely depend on a functioning TCF/LEF1 binding site, as despite the TCF/LEF1 mutation, RhoA was still able to activate the promoter (Figure 4.6B, blue bars).

One explanation for this could be that the residual binding of the transcription factors TCF and LEF1 might be taking place, inducing luciferase expression. Additionally, there is a large difference between the quantity of luciferase from the TCF/LEF1 mut p*Brn2*-Luc construct compared with its backbone plasmid Δ268 p*Brn2*-Luc in both cell lines. The decrease of basal level of transcription could be due to the TCF/LEF1 mutation, which might affect the binding of other transcription factors, such as Pax3 (Figure 4.5).

One of the proteins that heavily utilises the TCF/LEF1 binding site is β-catenin. Therefore, to explain the differential RhoA-induced activation of the TCF/LEF1 mut p*Brn2*-Luc construct in 501mel and SKmel28 cells, it was important to investigate the expression of β-catenin in these cell lines next.

4.2.3 Cytoplasmic vs nuclear β-catenin expression in 501mel and SKmel28 cells

To assess the expression of β-catenin in 501mel and SKmel28 cells, cells were stained with an anti-β-catenin antibody and fluorescence was assessed by microscopy (Figure 4.7).

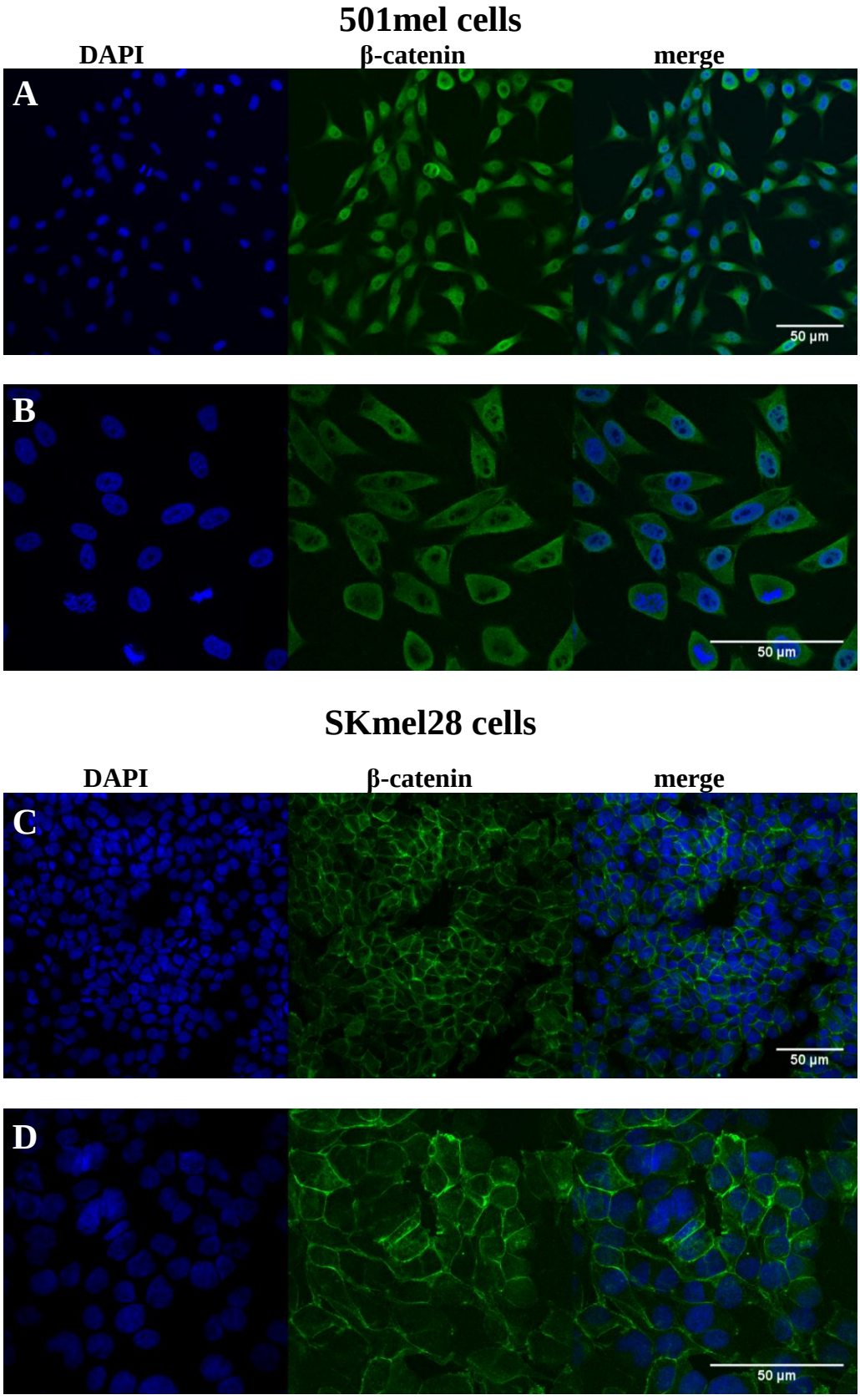


Figure 4.7: Differential β-catenin expression in 501mel and SKmel28 cells. 501mel cells (**A**, **B**) and SKmel28 (**C**, **D**) were stained with anti-β-catenin antibody, followed by an Alexa-Fluor 488 (green, second column) and counterstained with DAPI (blue, first column). Pictures were taken at 20x (**A**, **C**) and at 40x magnification (**B**, **D**). The scale bar represents 50 µm.

While 501mel cells express cytoplasmic and nuclear β-catenin (Figure 4.7A, B), SKmel28 cells exhibit primarily membrane-bound β-catenin with only a minor proportion present in the nucleus (Figure 4.7C, D).

This could explain the difference between the higher basal transcription levels of the TCF/LEF1 mutated *Brn2* promoter in 501mel compared to SKmel28 cells (Figure 4.6A vs B, blue bars).

4.2.4 Ectopic RhoA affects endogenous Brn2 protein expression

Following on from demonstrating that RhoA CA activates the exogenous *Brn2* promoter, we investigated whether RhoA CA also regulated endogenous Brn2 protein. To this end, 501mel cells were firstly transfected with a Myc epitope-tagged-RhoA CA expression plasmid and subsequently stained for Brn2 protein expression (Figure 4.8).

Due to the results that RhoA CA activated the *Brn2* promoter, our hypothesis was that RhoA CA would also increase endogenous Brn2 protein levels. However, when assessing the Brn2 protein expression in untransfected cells, 501mel cells exhibited a high level of heterogeneity (Figure 4.8B). In transfected cell populations (Figure 4.8A) there appears to be a lower level of Brn2 expression in cells expressing the RhoA CA-myc protein. One possible complicating factor is that Brn2 protein expression appears to fluctuate during the cell cycle. As the cells advance through G_1 to G_2 the size of the nucleus gradually increases, alongside Brn2 levels (unpublished data, Eda Suer). As the cells progress through mitosis, Brn2 levels decrease during metaphase and anaphase as the transcription factor is excluded from the chromatin and it only re-associates in late telophase. This effect may be exemplified in Figure 4.8A (asterisk), where smaller nuclei, presumably cells in G_1, express lower amounts of Brn2 protein. Therefore, due to the high level of heterogeneity and fluctuations of Brn2 in the cell cycle the effects of

RhoA CA on the endogenous Brn2 protein expression are hard to define precisely (Figure 4.8A, white arrows).

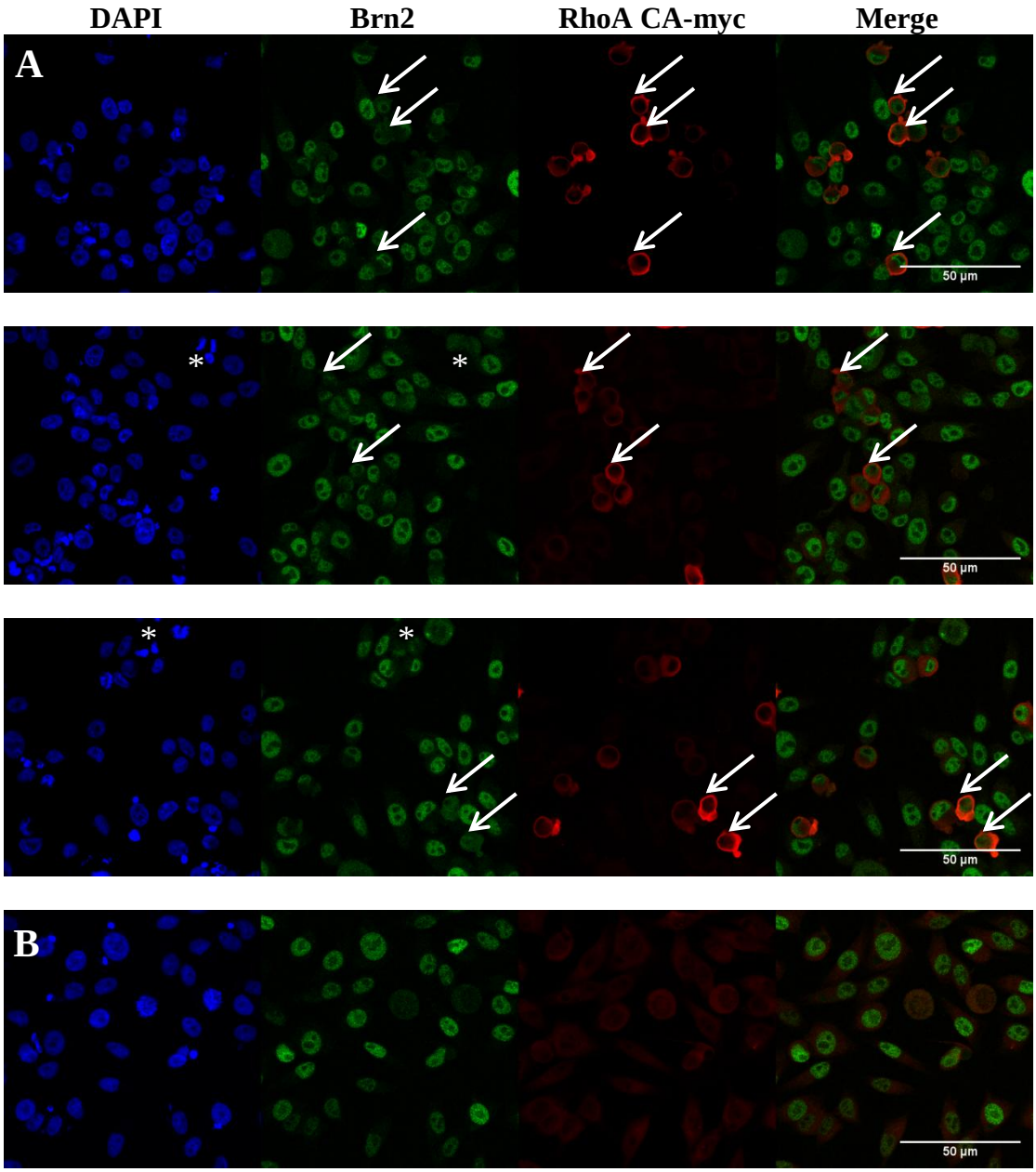


Figure 4.8: RhoA CA decreases Brn2 protein expression in 501mel cells. 501mel cells transfected with 400 ng of a RhoA CA-myc expression plasmid (**A**) and untransfected cells (**B**) were fixed 24 h post-treatment. Cells were stained with anti-Brn2 and anti-myc antibodies, followed by secondary Alexa-Fluor 488 (green) and 546 (red) antibodies, respectively. Cells were counterstained with DAPI (blue). Slides were analysed by fluorescence microscopy at 40x magnification. The scale bar represents 50 µm.

If ectopic RhoA CA indeed decreases Brn2 protein levels, it might suggest that activity of the *Brn2* promoter may not directly reflect protein levels. This effect is discussed more in later chapters (section 5.2.1).

4.2.5 RhoA decreases pMITF activity in 501mel and increases activity in SKmel28 cells

Having demonstrated that RhoA increased *Brn2* promoter activity in both 501mel and SKmel28 cells, we hypothesised that RhoA would induce a decrease in *MITF* promoter activity. To test this, luciferase assays with the vectors expressing RhoA WT and CA together with a p*MITF*-Luc plasmid were performed in 501mel and SKmel28 cells (Figure 4.9).

In 501mel cells, co-transfections with 100 ng and 200 ng of a RhoA WT expression plasmid decreased p*MITF* activity compared to the control (both by 40%), while the same amounts of RhoA CA induced a more striking decrease in promoter activity by 80% ($p<0.001$) (Figure 4.9A).

Interestingly, in SKmel28 cells, the same amounts of RhoA had the opposite effect. While RhoA WT did not change luciferase expression much, 100 ng and 200 ng of the RhoA CA expression plasmid increased p*MITF* activity 3- and 6-fold, respectively ($p<0.001$ in both cases) (Figure 4.9B).

Our hypothesis that RhoA might decrease *MITF* promoter activity was only confirmed in 501mel cells. The discrepancy between the effects of RhoA CA on the p*MITF*-Luc plasmid in 501mel and SKmel28 cells may be due to the differential modes of activity of RhoA and the potential involvement of other factors to induce *MITF* promoter activity.

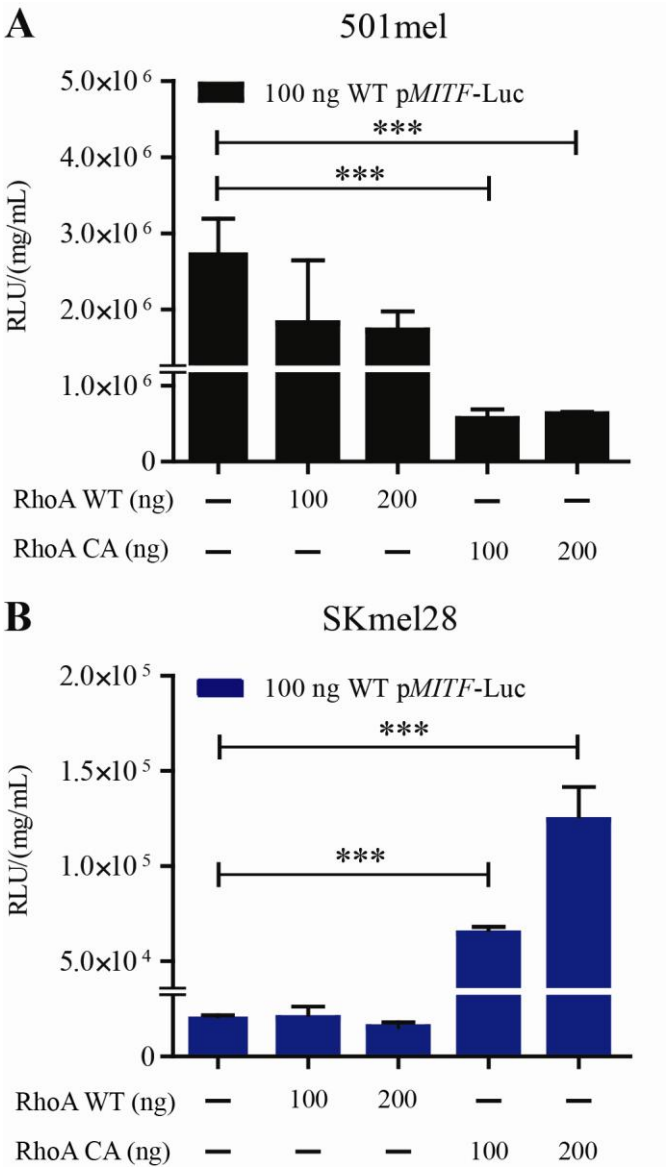


Figure 4.9: RhoA CA decreases and increases p*MITF* activity in 501mel and SKmel28 cells, respectively. Indicated amounts of RhoA WT and CA expression plasmids were transfected together with 100 ng p*MITF*-Luc into 501mel (**A**) and SKmel28 cells (**B**). To control for the total amount of DNA transfected in each condition, an empty vector was used as a control. Luciferase expression was measured 24 h post-transfection and normalised to the protein content per well. Results represent mean ± S.D, n=3. Statistical analysis was performed using a one-way ANOVA followed by a post-hoc Tukey's test. *** = $p<0.001$

4.2.6 ROCK1 decreases pBrn2 activity in 501mel and increases activity in SKmel28 cells

To investigate if the RhoA CA-induced effects on the *Brn2* promoter were also present downstream of RhoA signalling, luciferase assays were conducted with the effector kinase ROCK1.

As RhoA activates ROCK1 we investigated the effect of ROCK1 on the *Brn2* promoter regulation. We therefore co-transfected plasmids expressing the WT and CA forms of the kinase ROCK1 together with the WT *Brn2* promoter luciferase construct into 501mel and SKmel28 cells (Figure 4.10).

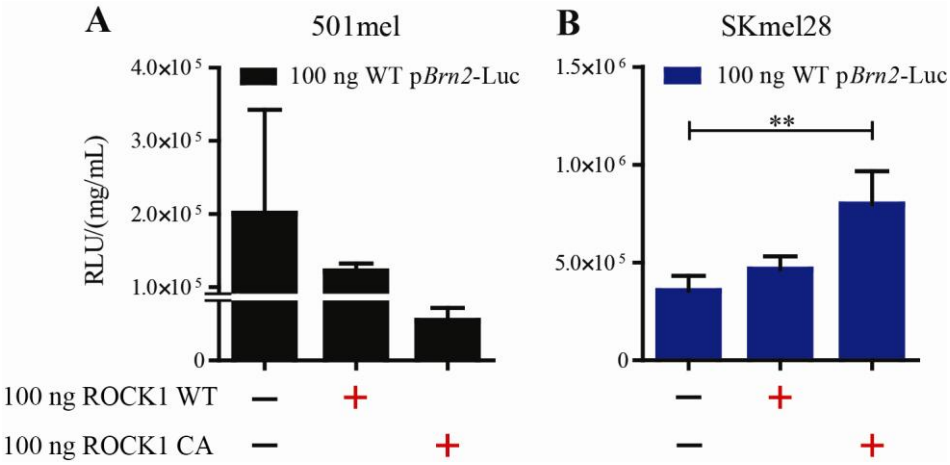


Figure 4.10: ROCK1 increases and decreases WT *Brn2* promoter activity in SKmel28 and 501mel cells, respectively. 100 ng of ROCK1 WT and CA expression plasmids were transfected into 501mel (**A**) and SKmel28 (**B**) cells together with 100 ng WT p*Brn2*-Luc plasmid. To control for the differences in the amount of DNA transfected in different conditions, an empty vector control was used. Luciferase expression was measured 24 h post-transfection. Results were normalised to the protein content and expressed as mean ± S.D, n=3. Statistical analysis was performed using a one-way ANOVA followed by a post-hoc Tukey's test. ** = $p<0.01$.

Interestingly, while RhoA induced luciferase activation of the WT p*Brn2*-Luc construct in 501mel cells (Figure 4.3A), ROCK1 had the opposite effect on the WT p*Brn2*-Luc construct (Figure 4.10A). In 501mel cells, ROCK1 WT and CA decreased luciferase expression by 40% and 70%, respectively, compared to the control (Figure 4.10A).

In SKmel28 cells, on the other hand, ROCK1 WT and CA led to an increase in luciferase expression by 30% and 130% ($p<0.05$), respectively, compared to the control (Figure 4.10B).

To summarise, in 501mel cells RhoA increases p*Brn2* activity while ROCK1 has the opposite effect. In SKmel28 cells, on the other hand, RhoA and ROCK1 both increase *Brn2* promoter activity. This is intriguing and might suggest that RhoA induces p*Brn2* activity via different pathways in these two cell lines.

4.2.7 ROCK1 decreases pMITF activity in 501mel and SKmel28 cells

To study the regulation of the *MITF* promoter by ROCK1, luciferase experiments were conducted with plasmids expressing WT and CA forms of ROCK1 and p*MITF*-Luc plasmids in 501mel and SKmel28 cells (Figure 4.11).

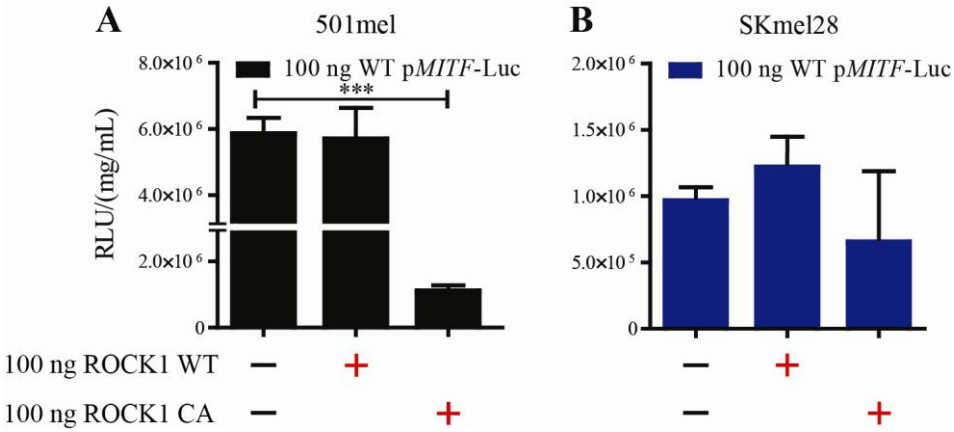


Figure 4.11: ROCK1 decreases *MITF* promoter activity in 501mel cells. Indicated amounts of plasmids expressing ROCK1 WT and CA were transfected into 501mel (**A**) and SKmel28 (**B**) cells together with 100 ng of the coding plasmid p*MITF*-Luc. To control for the amount of DNA transfected in each condition, an empty vector control was used. Luciferase expression was measured 24 h post-treatment and normalised to the protein content per well. Results are expressed as mean ± S.D, n=3. Statistical analysis was performed using a one-way ANOVA followed by a post-hoc Tukey's test. *** = $p<0.001$

In 501mel cells, ROCK1 WT did not affect luciferase expression strikingly, while ROCK1 CA decreased luciferase expression by 80% compared to the control ($p<0.001$) (Figure 4.11A).

In SKmel28 cells, no significant changes in luciferase expression upon co-transfections with ROCK1 WT or CA were detected (Figure 4.11B).

When comparing these results to the effect that RhoA induced on the *MITF* promoter, it is intriguing that in 501mel cells, RhoA and ROCK1 both decreased p*MITF* activity (Figure 4.9A and Figure 4.11A), while in SKmel28 cells, RhoA induced p*MITF* activity but ROCK1 did not elicit an effect (Figure 4.9B and Figure 4.11B).

Assuming that RhoA elicits its effect through its effector ROCK1, the results observed in 501mel cells are consistent. In SKmel28 cells on the other hand, there is a discrepancy between the RhoA-induced increase of the *MITF* promoter activity and the

lack of effect on the promoter activity following ROCK1 transfections. This suggests that in SKmel28 cells, RhoA might not be eliciting its activating effects on the *MITF* promoter through ROCK1 but rather utilising a different signalling network.

Interestingly, similar conclusions were made in regards to the RhoA- and ROCK1-induced effects on the *Brn2* promoter in these cell lines. However, to decipher the exact mechanism of action of RhoA and ROCK1, further experiments are necessary.

4.2.8 ROCK inhibitors increase Brn2 and decrease MITF protein expression

From the kinase inhibitor screen that was conducted earlier in 501mel cells, a ROCK inhibitor (ROCKi) activated the *Brn2* promoter (section 3.3.3). This was in line with the results above whereby ROCK1 decreased *Brn2* promoter activity from the WT p*Brn2*-Luc construct in 501mel cells (Figure 4.10). To confirm these results, we next investigated the effect of ROCK inhibition on Brn2 and MITF protein levels. To this end, 501mel cells were treated with two ROCK inhibitors from the library screen, #1 and #2 (Figure 4.12). As the compounds were dissolved in DMSO, it was used to control for any non-specific effects (Figure 4.12).

Brn2 protein was detected at 50-55 kDa and the β-actin loading control at 44 kDa (Figure 4.12). Both ROCKis increased Brn2 protein expression after 24 h compared to the DMSO control (Figure 4.12), confirming the outcome of the kinase inhibitor screen. These results correlate with the luciferase data that showed a decrease in *Brn2* promoter activity upon transfections with ROCK1 CA in 501mel cells (Figure 4.10A). 48 h post-treatment, Brn2 protein levels had returned to the DMSO-treated control levels.

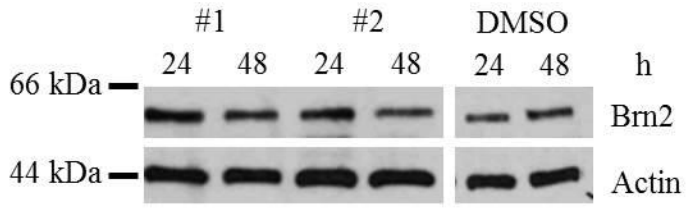


Figure 4.12: ROCK inhibitors affect Brn2 protein levels in 501mel cells. 501mel cells were treated with two ROCK inhibitors (#1 and #2) at 2.5 µM concentration. 24 h and 48 h post-treatment lysates were subjected to SDS-PAGE and Western blotted with the indicated antibodies.

To measure the MITF levels in the ROCKi-treated cells, the membranes were probed with anti-MITF antibodies (Figure 4.13).

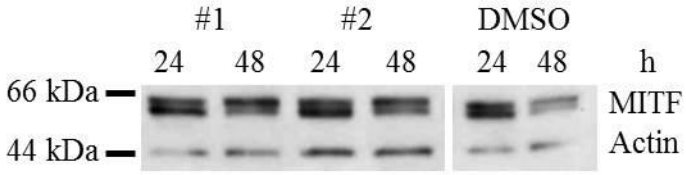


Figure 4.13: ROCK inhibitors affect MITF protein levels in 501mel cells. 501mel cells were treated with 2.5 µM of two ROCK inhibitors (#1 and #2). 24 h and 48 h post-treatment lysates were subjected to SDS-PAGE and Western blotted with the indicated antibodies.

The MITF antibody recognised the hyper-phosphorylated and hypo-phosphorylated forms of MITF (top bands, 60 kDa and 54 kDa, respectively, Figure 4.13) (Hemesath et al., 1998), while the anti-β-actin antibody was used to probe for actin as a loading control. At 24 h post-treatment, both inhibitors increase the ratio of the hypo-phosphorylated form over the hyper-phosphorylated form of MITF, while 48 h post-ROCKi treatment, the reverse was detected. This was intriguing as the hyper-phosphorylated form has been shown to be more transcriptionally active than the hypo-phosphorylated form (Price et al., 1998), and while at 24 h post-treatment Brn2 protein levels are increased (Figure 4.12), the less activate form of MITF is expressed (Figure 4.13). The reverse is true at 48 h post-treatment.

Interestingly, in luciferase experiments in 501mel cells, co-transfections with ROCK1 CA decreased *MITF* promoter activity (Figure 4.11A), which might be correlated with

the decrease in hyper-phosphorylated MITF protein, compared to the hypo-phosphorylated form, after ROCK1 inhibition (Figure 4.13).

4.2.9 ROCK inhibitor treatment leads to a short-term increase in Brn2, β-catenin and MITF protein levels in 501mel cells

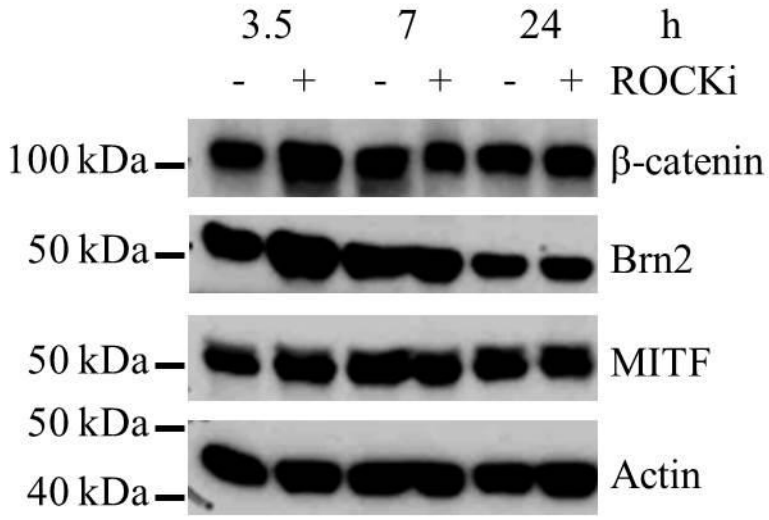


Figure 4.14: The ROCK inhibitor, Y27632 increases β-catenin, Brn2 and MITF levels. 501mel cells were treated with 5 µM of Y27632 for the indicated lengths of time. Lysates were subjected to SDS-PAGE and Western blotted with the indicated antibodies.

To evaluate the effect of ROCK inhibition on Brn2 and MITF protein levels at different time points, 501mel cells were treated with the ROCK inhibitor Y27632 for 3.5, 7, 24, 32 and 48 h. However, due to a decrease in protein expression in untreated control cells, time points after 24 h were discarded. The most striking changes were detectable at 3.5 h post-treatment (Figure 4.14). Brn2 and MITF protein levels were both increased at 3.5 h post-treatment compared to the untreated condition. At 7 h post-treatment, however, Brn2 and MITF protein levels had all dropped and there was no striking difference between the untreated and ROCKi-treated condition. Interestingly, at 24 h post-ROCKi treatment, Brn2 protein levels were decreased in both the untreated and the treated conditions compared to the previous time points (Figure 4.14). Also note that this blot only shows one band of MITF, which is likely due to different gel conditions.

From the luciferase results in Figure 4.6 it seemed the Wnt pathway might affect the RhoA/ROCK-induced effects on the *Brn2* promoter. We therefore also probed the membranes for β-catenin. Similarly to Brn2 and MITF protein at 3.5 h post-treatment, β-catenin levels were also elevated compared to untreated cells (Figure 4.14). Actin levels were detected to assess protein loading.

To summarise, the increase in Brn2 protein expression, detected using the two inhibitors from the kinase screen, was also observed with a different ROCK inhibitor, Y27632. However, while the two ROCKis from the screen increased Brn2 expression at 24 h post-treatment, Y27632 only increased Brn2 protein expression at 3.5 h post-treatment. This may be due to the fact that the ROCKis might not be isoform-specific and therefore might inhibit ROCK1 and 2 to varying degrees (Morgan-Fisher et al., 2013). As in this project we have only investigated the effect of the ROCK1 isoform on *Brn2* and *MITF* promoter activity, it is conceivable that ROCK2 might affect the expression of the transcription factors differently. This could account for the varying outcomes when using the ROCKis from the screen and Y27632.

4.3 Discussion

4.3.1 Key findings – Brn2 promoter

Luciferase assays demonstrated that RhoA activated the *Brn2* promoter in 501mel and SKmel28 cells. In 501mel cells, this activation was abrogated in TCF/LEF1 mutated *Brn2* promoter construct suggesting a role for the Wnt pathway. As β-catenin is the main mediator of the Wnt signalling pathway, 501mel and SKmel28 cells were stained for β-catenin, which demonstrated its differential expression in these two cell lines. While 501mel cells expressed mainly cytoplasmic and nuclear β-catenin, SKmel28 cells showed membrane-bound expression. This was intriguing as luciferase results with the

ROCK1 effector kinase showed differential effects on the *Brn2* promoter between the two cell lines. As ROCK1 is downstream of RhoA signalling, we hypothesised that it would have the same effect on the *Brn2* promoter as RhoA. While our hypothesis held true in SKmel28 cells where RhoA and ROCK1 both increased *Brn2* promoter activity, in 501mel cells RhoA increased and ROCK decreased p*Brn2* activity (Figure 4.15). In 501mel cells, this effect was confirmed using ROCK inhibitors, which increased Brn2 protein expression, demonstrated by western blotting.

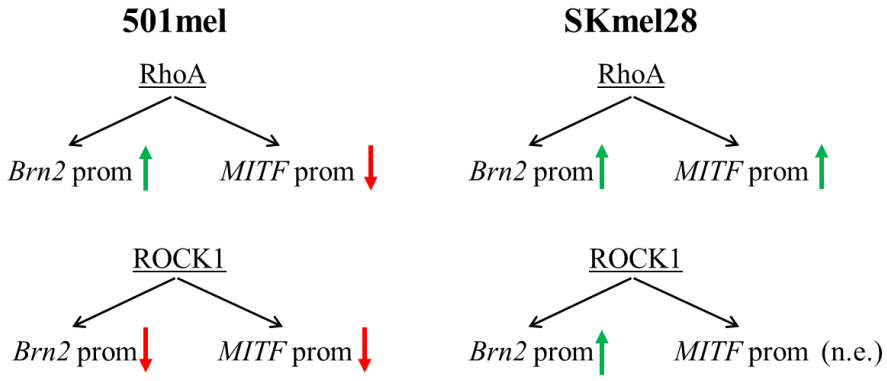


Figure 4.15: RhoA and ROCK1 induce differential effects of *Brn2* and *MITF* promoter activity in 501mel and SKmel28 cells. In 501mel cells co-transfections of RhoA and ROCK induce opposite effects on the *Brn2* promoter, while both decrease *MITF* promoter activity. In SKmel28 cells, RhoA and ROCK increase *Brn2* and *MITF* promoter activity. Green arrow = promoter activation, red arrow = promoter inhibition, n.e. = no effect.

This discrepancy between the effects of RhoA and ROCK on p*Brn2* in 501mel and SKmel28 cells could be explained by the differential mechanisms of action of RhoA. In 501mel cells RhoA-induced activation is dependent on a functioning TCF/LEF1 site and therefore most likely dependent on intact β-catenin signalling. In SKmel28 cells, however, activation of p*Brn2* by RhoA might be mediated through other factors than just the Wnt pathway as the TCF/LEF1 mutated *Brn2* promoter can still become activated. One way to explain this is by the differential sub-cellular localisation of β-catenin in 501mel (nuclear) and SKmel28 cells (membrane-associated). In 501mel cells, the RhoA-induced effects might be mediated by β-catenin and therefore a mutation in the TCF/LEF1 binding site will abrogate p*Brn2* activation. Consequently, as β-catenin is mainly membrane-bound in SKmel28 cells, the RhoA-induced p*Brn2*

activation might not solely depend on β-catenin, and therefore on TCF/LEF1. Consequently, mutation in this binding site will not fully inhibit RhoA-induced p*Brn2* activation.

Alternatively, because in 501mel cells, β-catenin is already located in the nucleus, as opposed to being associated with the cell membrane in SKmel28 cells, the basal level of TCF/LEF1 mutated p*Brn2* activity is higher in these 501mel cells compared to SKmel28 cells. However, in the event of RhoA-mediated signalling, in SKmel28 cells, β-catenin could be recruited to the nucleus to activate the *Brn2* promoter (as seen in Figure 4.6B). However, with higher basal levels in 501mel cells, even if β-catenin was recruited to the nucleus, the change in β-catenin levels might not be sufficient to increase p*Brn2* activity above basal levels.

4.3.2 Key findings – MITF promoter

Prior to the experiments involving the p*MITF* luciferase reporter, we hypothesised that in both cell lines RhoA would decrease *MITF* promoter activity as it had the opposite effect on the *Brn2* promoter. However, we observed a decrease in *MITF* promoter activity in 501mel cells and an increase in SKmel28 cells (Figure 4.15).

Subsequent transfections with ROCK1 expression plasmids in 501mel cells induced a decrease in *MITF* promoter activity while in SKmel28 cells ROCK1 expression did not affect *MITF* promoter activity. The effects produced by RhoA and by ROCK1 in 501mel cells are consistent under the premise that RhoA induces ROCK1 activation (Figure 4.1) and ROCK1 in turn affects the *MITF* promoter.

To explain the differential effects of RhoA and ROCK on the *MITF* promoter in the different cell lines, it is important to note that RhoA can also elicit effects through other proteins than ROCK1. Once RhoA is activated, it induces the transcription of the

DIAPH1 gene, which encodes the protein Dia1 that is responsible for the generation of stress fibres via actin polymerisation (Carreira et al., 2006; Watanabe et al., 1999). MITF is also able to activate Dia1 expression (Carreira et al., 2006). Additionally, using the *Brn2* promoter construct, we demonstrated that RhoA might be signalling through the Wnt pathway, which is intriguing when combined with the data that show differential expression of β-catenin in 501mel and SKmel28 cells.

To summarise, it is conceivable that depending on the cell line, *MITF* promoter activation might be mediated through: a) RhoA directly, b) Dia1 (which is also regulated by MITF), c) ROCK1 directly or d) through the Wnt pathway, which is activated by RhoA or ROCK1 (Figure 4.16).

As the importance of these factors may vary between different cell types, this might account for the differential effects of RhoA and ROCK on the *MITF* promoter in 501mel (decrease in p*MITF* activity, Figure 4.16A) and SKmel28 cells (increase in p*MITF* activity, Figure 4.16B). For instance, the second mechanism of p*MITF* regulation (through Dia1, b)) might contribute less in 501mel cells, as the overall effect of RhoA on p*MITF* is a decrease in activity.

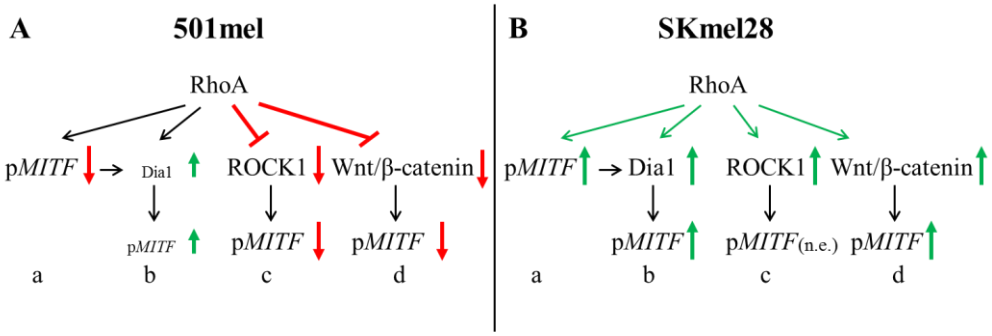


Figure 4.16: RhoA can affect *MITF* promoter activity via different pathways, depending on the cell line. There are different hypotheses how RhoA can affect *MITF* promoter function: **a)** RhoA can affect the *MITF* promoter directly leading to MITF expression, which in turn affects Dia1 expression; **b)** RhoA affects Dia1 expression, which in turn affects the *MITF* promoter; **c)** RhoA acts through the ROCK1 effector kinase, which subsequently affects the *MITF* promoter, possibly through another transcription factor or **d)** RhoA affects Wnt signalling/β-catenin directly, which in turn affects the *MITF* promoter, potentially through binding to the TCF/LEF1 binding site. In 501mel cells, the net effect of RhoA on *MITF* promoter is a decrease in its activity (**A**) while in SKmel28 cells, RhoA increases *MITF* promoter activity (**B**). Green arrow = promoter activation, red arrow = promoter inhibition, n.e. = no detectable effect.

However, to identify the precise mechanism of action of RhoA and ROCK on the *Brn2* and *MITF* promoters, more experiments will have to be conducted.

4.3.3 Rho family proteins and cancer

The activity of ROCK in tumour metastases formation is well established (section 4.1.3). Equally, it has long been known that Rho family GTPases regulate the actin cytoskeleton and matrix adhesion (Sahai and Marshall, 2002). However, it has also started to emerge that Rho family proteins play a role in cancer development (Clark et al., 2000; del Peso et al., 1997; Itoh et al., 1999; Qiu et al., 1995; van Golen et al., 2000; Yoshioka et al., 1998; Yoshioka et al., 1999), in particular RhoA and RhoC. *In vitro*, constitutively active RhoA induces transformation of NIH 3T3 mouse fibroblasts in the presence of constitutively-active Ras (Qiu et al., 1995). Furthermore, mouse fibroblast cells transformed with RhoA induce metastases by colony formation in lungs and secondary organs in mice, and retain this colony formation capacity in secondary xenotransplantation experiments (del Peso et al., 1997). RhoA expression in rat hepatoma cells also promotes invasion *in vitro* and *in vivo* (Yoshioka et al., 1998; Yoshioka et al., 1999). Interestingly, overexpression of RhoC in the poorly-metastatic human melanoma cell line A375P leads to enhanced metastasis formation, while blocking RhoC in the highly-metastatic human melanoma cell line A375M by a dominant-inhibitory Rho mutant abrogates metastases formation (Clark et al., 2000), confirming the importance of RhoC in metastases formation. Furthermore, overexpression of RhoC in human mammary epithelial cells leads to tumour formation with an invasive phenotype *in vivo*, demonstrating that RhoC can also function as a tumour oncogene (van Golen et al., 2000). Interestingly, the expression of RhoA and RhoC is increased in many cancer types, such as breast, colon and lung cancers (Fritz et

al., 1999). However, despite the high metastatic potential of melanoma cells, RhoA mutations have not been implicated in melanoma metastases formation to date.

Brn2, on the other hand, is thought to play a role in metastasis formation (Pinner et al., 2009) and together with our findings of RhoA-induced activation of the *Brn2* promoter as well as the modulation of the *MITF* promoter, it is conceivable that RhoA might contribute to metastasis formation by affecting Brn2 and MITF expression, potentially through Wnt signalling.

4.3.4 Rho family proteins and ROCK in the clinic

As Rho proteins have been implicated in various stages of tumour formation, different types of pharmacological agents were developed to interfere with these processes. Two of these agents are the farnesyltransferase inhibitors (Andreopoulou et al., 2013) and geranylgeranyltransferase I inhibitors (Zimonjic et al., 2013), which block the post-translational modification of Rho proteins that is needed for their GTPase activity. Other methods to interfere with Rho signalling involve the inhibition of guanine nucleotide exchange factors by introducing Rho mutants that only bind GDP (Feig, 1999). The disadvantage with these reagents is that they are not specific to one subtype of Rho proteins (Wang et al., 2003). Alternatively, it is also possible to inhibit the interaction between Rho proteins and their effectors (Vastrik et al., 1999). To specifically target Rho protein subtypes, Rho chimeras, consisting of negative regulators of Rho proteins (GAP), were developed (Wang et al., 2003). These are able to down-regulate individual Rho subtypes in human mammary epithelial breast cancer cells and in the metastatic A375M melanoma cell line decrease the invasive cell phenotypes (Wang et al., 2003).

Another method to interfere with Rho signalling cascade is by blocking the function of the Rho effector kinase ROCK. Similar to Rho proteins, ROCK kinases have also been implicated in tumour formation, demonstrating elevated levels in certain types of cancers such as testicular, bladder or renal cell carcinoma (Abe et al., 2008; Kamai et al., 2002; Kamai et al., 2003). Furthermore, ectopic expression of constitutively-active ROCK in normal rat kidney cells induced a transformed cellular phenotype (Pawlak and Helfman, 2002). Mutations in ROCK1 observed in human cancers were shown to have increased catalytic activity (Lochhead et al., 2010), resulting in their constitutive activation (Lochhead et al., 2010). In support of ROCK's involvement in metastasis formation, the comparison of invasive and non-invasive sarcoma cell lines showed elevated Rho/ROCK signalling in invasive cells (Rosel et al., 2008). Due to these findings, and the possibility of ROCK being involved in the formation of cancer metastases, ROCK inhibitors were investigated for cancer treatment by different groups (Nakajima et al., 2003; Routhier et al., 2010; Yoshioka et al., 1999) and demonstrated to decrease invasion *in vitro* and *in vivo*.

Contrary to these findings, our results have demonstrated that in one melanoma cell line, 501mel cells, ROCK1 decreases p*Brn2* activity while inhibition of ROCK1 increases Brn2 protein levels. Despite the fact that we have not performed functional studies to demonstrate the link between RhoA/ROCK pathway and *Brn2* promoter activity on invasion, it is clear that the decreased invasive potential of cancer cells demonstrated in the studies above might be cell line-/cancer type-specific, as well as dependent on the ROCK isoform the compounds are targeting.

4.3.5 Future work

The RhoA/ROCK pathway has been extensively studied in the context of tumour and metastasis formation. Brn2 has only recently emerged as a potential marker for de-differentiated cells, which also contain the ability to invade the surrounding tissues (Pinner et al., 2009). While cells expressing low levels of MITF, together with high levels of Brn2 expression have been strongly implicated in metastasis formation, a link between the RhoA/ROCK pathway and Brn2 expression was not previously established. Based on our preliminary results, we propose that the RhoA/ROCK pathway can activate the *Brn2*/*MITF* promoters (in SKmel28 cells) and that this pathway can therefore mediate metastasis formation and invasion in melanoma cells. To further investigate if our hypothesis is correct, the effect of RhoA or ROCK inhibitors on the Brn2 and MITF protein expression should be tested in SKmel28 cells. Additionally, it might be interesting to investigate in more detail why 501mel and SKmel28 cells show differences when transfected with RhoA or ROCK1 expression plasmids and whether the differential expression of β-catenin plays a role in this response. This would shed light on the mechanism of action of RhoA/ROCK and Brn2/MITF expression. Since this pathway seems to play a role in invasion, targeting it might open up avenues for the therapeutic intervention of metastasis generation in melanoma.

5 Differential regulation of the *MITF* and *Brn2* promoters by MAML1 and β-catenin

5.1 Introduction

In the previous chapter it was demonstrated that the *Brn2* and *MITF* promoters are regulated by RhoA and ROCK. These factors are known to contribute to invasion in melanoma. Two factors that are also linked to metastasis are the co-activator mastermind-like 1 (MAML1) and β-catenin, which play important roles in the Notch and Wnt pathways, respectively. In this part of the project we investigate the possible interplay between the Wnt and the Notch pathways and their effects on *Brn2* and *MITF* promoter activation.

5.1.1 Notch pathway

The role of the Notch pathway in melanomagenesis is controversial (section 1.6.2) as Notch can act as a tumour suppressor (Nicolas et al., 2003) but also as an oncogene (Balint et al., 2005). However, the Notch pathway also plays a role in the maintenance of stemness in murine melanocyte and melanoblasts (Moriyama et al., 2006). Notch activation is also linked with the induction of EMT in breast cancer cells (Leong et al., 2007). It therefore seems likely that Notch signalling could promote de-differentiation, invasion and metastasis formation in melanoma.

5.1.2 Interaction of Notch and the Wnt pathway in cancer

The Wnt pathway is one of the main activators of Brn2 (Goodall et al., 2004a) and its expression can promote melanoma invasion and is associated with migrating cells *in vivo* (Pinner et al., 2009). Given the potential role of Notch in melanoma de-differentiation, it would be interesting to investigate if components in the Notch and the

Wnt pathway interact to promote metastasis formation or stemness in certain cancer cells. However, there is little known about the interplay of these two pathways. Nevertheless, in mammalian cells GSK3-β, the kinase that is part of the 'destruction complex' that inhibits β-catenin from translocating to the nucleus, can phosphorylate the intracellular domain of the Notch2 receptor once it has been cleaved following binding of a ligand (Espinosa et al., 2003). This phosphorylation leads to a decrease in Notch-mediated transcription of target genes, such as Hes-1 (Espinosa et al., 2003). Interestingly, another report also demonstrated that GSK3-β phosphorylates the intracellular domain of Notch1 but instead of decreasing its ability to induce target gene expression, it protects Notch1 from being degraded (Foltz et al., 2002). In contrast to the first report, the latter demonstrates an activating role of GSK-3β in mammalian Notch signalling (Foltz et al., 2002). In addition, GSK-3β was also investigated with respect to its effect on other components of the Notch signalling pathway and was shown to decrease the transcriptional activity of MAML1 (on a transfected reporter plasmid) by directly interacting with the co-activator (Saint Just Ribeiro et al., 2009). However, the effects on Notch-targeted genes were not assessed.

Another component of the Notch pathway which may link to the Wnt pathway was investigated by Rodilla and colleagues (Rodilla et al., 2009). In this study a group of genes was identified, which are both regulated by the Notch pathway and lie downstream of the Wnt signalling. In colorectal cancer cells, which demonstrate a strong activity of Wnt signalling and therefore high levels of active β-catenin, Jagged1, a ligand for the Notch1 receptor, was upregulated (Rodilla et al., 2009). In colorectal cancer mouse models, containing a mutation in the APC gene, deletion of a *Jagged1* allele reduced tumour growth, further indicating that Wnt-mediated tumour formation might be influenced by a Notch pathway component (Rodilla et al., 2009). These results

were confirmed in the epidermis, where β-catenin activation induced the transcription of the *Jagged1* gene and regulated hair follicle maintenance (Rodilla et al., 2009). Interestingly, another study also highlighted the link between Jagged1 and β-catenin (Leong et al., 2007), showing that Notch pathway activation upon binding of Jagged1 to the Notch receptor decreased β-catenin activity (Leong et al., 2007). However, this response was not mediated by Wnt signalling (Leong et al., 2007). Other reports in colorectal cancer have demonstrated an interaction between the Notch and Wnt pathway components MAML1 and β-catenin, respectively (Alves-Guerra et al., 2007). While the Wnt pathway has been heavily implicated in the generation of colorectal carcinoma, mainly through nuclear β-catenin activity, the mechanism of its activation may vary from one tumour to another. However, this study showed that MAML1 is a co-activator of β-catenin *in vitro* and *in vivo* and that *in vivo* the latter recruits MAML1 to the *cyclin D1* and *c-Myc* promoters (Alves-Guerra et al., 2007). In this case, MAML1 acts independently of Notch signalling. This group also showed that siRNA-mediated knockdown of MAML1 and MAML2 led to cell death, potentially mediated by β-catenin-induced gene transcription of cyclin D1 and c-Myc (Alves-Guerra et al., 2007).

5.1.3 The Notch pathway, Brn2 and MITF

In melanoma, siRNA-mediated depletion of Brn2 in melanoma cell lines leads to decreased gene expression of components of the NOTCH pathway, such as the gene for the receptor *Notch1*, and the genes for two ligands for Notch2, *Jagged-2* (*JAG2)* and *Delta-like 1* (*DLL1)*, in one melanoma cell line (Thurber et al., 2011). However, this decrease was not as striking in a second melanoma cell line, indicating that this might be a cell line-specific effect. Conversely, silencing of MITF induced an upregulation of

the above-named genes as well as Brn2 (Thurber et al., 2011), in line with previous reports of Brn2 being a repressor of MITF (Goodall et al., 2008).

Based on these observations we hypothesised that the Notch pathway might be inducing the activation of Brn2, as this transcription factor is a marker for de-differentiated cells, which have the potential to invade and metastasise (Pinner et al., 2009).

5.1.4 Chapter objectives

- To investigate the role of Notch pathway components on the *Brn2* and *MITF* promoters.
- To investigate the potential interplay between Notch and Wnt pathway components.

Results

5.1.5 MAML1 activates the WT and Δ268 Brn2 promoter

As the Notch pathway plays a role in stem cell maintenance, it was next investigated if Notch pathway components would also increase *Brn2* promoter activity. To this end the WT p*Brn2*-Luc reporter plasmid was transfected into 501mel and SKmel28 cells together with plasmids encoding NICD, RBP-Jκ, MAML1 and Hes-1 (Figure 5.1).

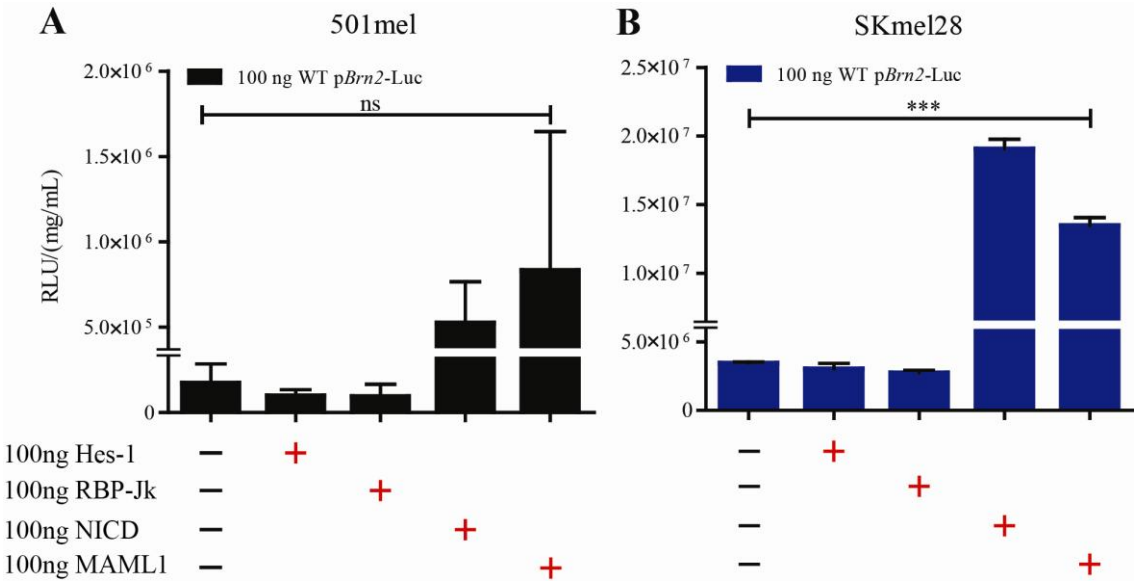


Figure 5.1: MAML1 and NICD activate the *Brn2* promoter in 501mel and SKmel28 cells. 100 ng of the indicated Notch pathway components were transfected into 501mel (A) and SKmel28 (B) cells together with 100 ng of the WT p*Brn2*-Luc plasmid. An empty vector was used to control for the DNA content per transfection. Luciferase expression was measured 24 h post-transfection and results were normalised to the protein content per well. Results are expressed as the mean ± standard deviation (S.D.), n=3. Statistical analysis was performed using a one-way ANOVA followed by a post-hoc Tukey's test. ns=not significant, *** = $p<0.001$

In 501mel cells, transfection of the Hes-1 and RBP-Jκ expression vectors decreased luciferase expression by 40% and 50%, respectively, while NICD and MAML1 induced the WT *Brn2* promoter activity by 2- and more than 3-fold, respectively, compared to the control (Figure 5.1A).

In SKmel28 cells, Hes-1 and RBP-Jκ had little effect on the WT *Brn2* promoter activity (10% and 20%, respectively), but NICD and MAML1 again increased WT *Brn2* promoter activity compared to the control (4.5- and 3-fold ($p<0.001$), respectively)

(Figure 5.1B). These results suggest that the *Brn2* promoter is responsive to Notch signalling.

To determine how Notch pathway components regulate the *Brn2* promoter, effects on the minimal Δ268 *Brn2* promoter deletion mutant (Chapter 4, Figure 4.2) were examined (Figure 5.2).

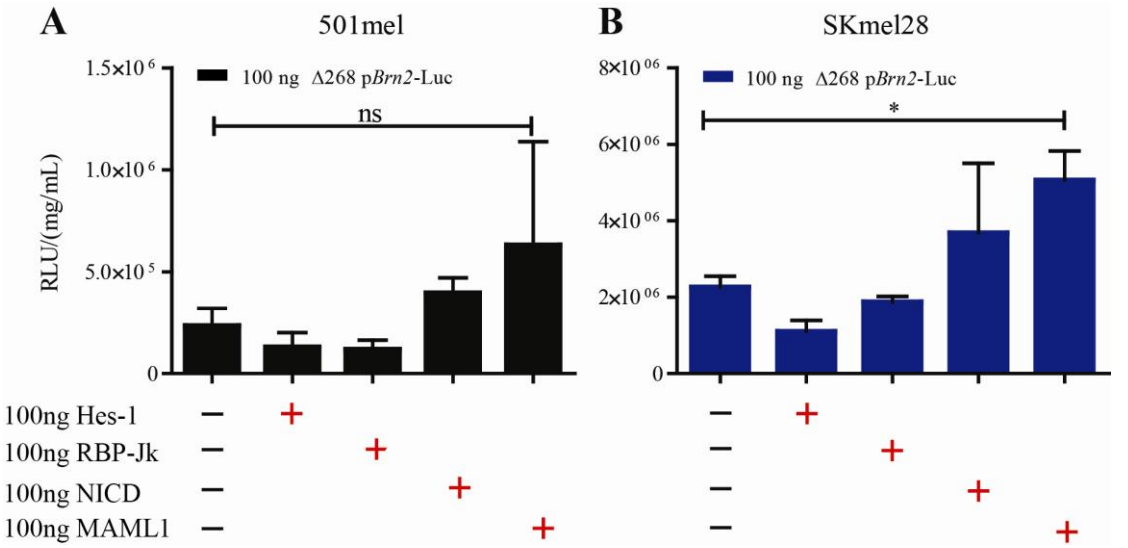


Figure 5.2: MAML1 activates the Δ268 p*Brn2* promoter in 501mel and SKmel28 cells. 100 ng of the indicated Notch pathway components were transfected into 501mel (**A**) and SKmel28 (**B**) cells together with 100 ng of the WT p*Brn2*-Luc plasmid. An empty vector was used to control for the amount of DNA used per transfection. Luciferase expression was measured 24 h post-transfection and results were normalised to the protein content per well. Results are expressed as the mean ± S.D., n=3. Statistical analysis was performed using a one-way ANOVA followed by a post-hoc Tukey's test. ns = not significant, * = $p<0.05$

In 501mel cells, again, Hes-1 and RBP-Jκ decreased the Δ268 *Brn2* promoter activity by 40% and 50%, respectively, compared to the control (Figure 5.2A). NICD and MAML1, on the other hand, increased Δ268 *Brn2* promoter activity by 70% and 170%, respectively, compared to the control.

In SKmel28 cells, Hes-1 and RBP-Jκ again decreased Δ268 *Brn2* promoter activity by 50% and 20%, respectively, compared to the control (Figure 5.2B), while NICD and MAML1 increased Δ268 *Brn2* promoter activity by 60% and 120% ($p<0.05$), respectively.

These results demonstrate that the regulation of the *Brn2* promoter in 501mel and SKmel28 cells is maintained in the minimal Δ268 *Brn2* promoter though to a lesser

degree than the full-length promoter. How the observed regulation of the *Brn2* promoter was achieved was not clear.

5.1.6 MAML1 does not cooperate with Pax3 to activate the Brn2 promoter

As MAML1 showed a consistent activation of the WT and the Δ268 *Brn2* promoters in 501mel and SKmel28 cells, further luciferase assays were conducted to investigate its mechanism of action.

Although it is possible that MAML1 binds the *Brn2* promoter directly, it has not been reported to possess sequence-specific DNA-binding activity and might therefore also activate the promoter by interacting with other transcription factors known to regulate the *Brn2* promoter such as Pax3 (Bonvin et al., 2012) or Sox10 (section 3.5).

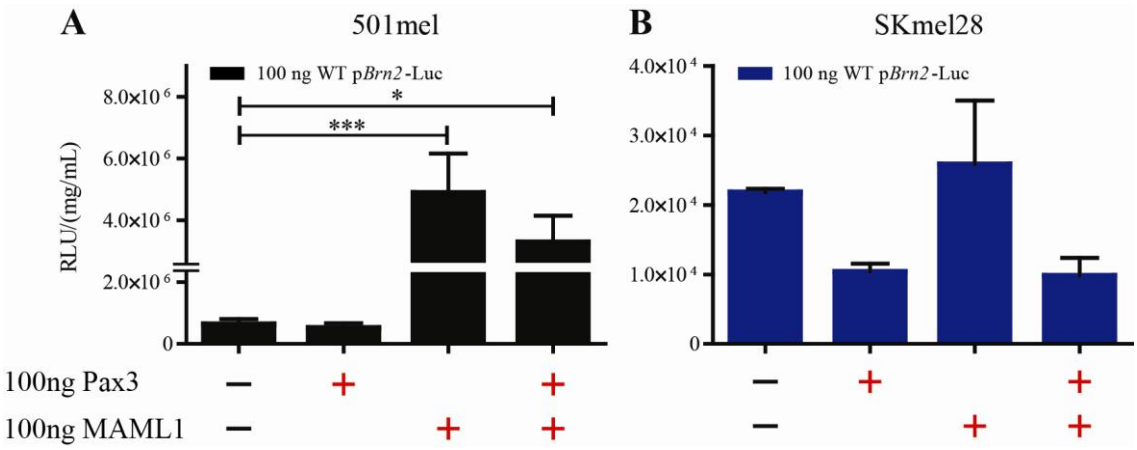


Figure 5.3: Pax3 and MAML1 do not have an additive effect on WT *Brn2* promoter activity. 100 ng of a Pax3 and 100 ng of a MAML1 expression plasmid, together with 100 ng WT p*Brn2*-Luc, were transfected into 501mel (**A**) and SKmel28 (**B**) cells. An empty plasmid was used to control for amount of DNA transfected. Luciferase expression was measured 24 h post-transfection and normalised to the protein content per well. Results are expressed as the mean ± S.D., n=3. Statistical analysis was performed using a one-way ANOVA followed by a post-hoc Tukey's test. * = $p<0.05$, *** = $p<0.001$.

In 501mel cells (Figure 5.3A), Pax3 by itself had little effect on the WT *Brn2* promoter activity (20% decrease), while MAML induced more than a 6.5-fold increase ($p<0.001$) compared to the control (Figure 5.1). Co-transfections of Pax3 and MAML1 expression plasmids led to a 4-fold ($p<0.05$) increase in the WT *Brn2* promoter activity, compared to the control. However, the luciferase expression was not higher than in the MAML1

only condition, suggesting no cooperative effect of Pax3 and MAML1 on the WT *Brn2* promoter activity in 501mel cells (Figure 5.3A).

In SKmel28 cells (Figure 5.3B), while MAML1 increased promoter activity by 20%, Pax3 decreased WT *Brn2* promoter activity by 50%, as did Pax3 and MAML1 together (70%), again suggesting that Pax3 and MAML1 do not induce an additive effect on the WT *Brn2* promoter activity in SKmel28 cells. Interestingly, in these transfection experiments, MAML1 did not induce as large an increase in WT *Brn2* promoter activation in SKmel28 cells as in the previous experiment (Figure 5.1). A potential explanation for this might be variation between luciferase experiments. As the luciferase expression in these experiments was lower than in the previous ones, it is conceivable that this was due to decreased transfection efficiency.

Another striking result was the lack of Pax3-induced activation of the WT *Brn2* promoter in SKmel28 cells (Figure 5.1B), compared to published results (Bonvin 2012). This however, might be explained by different experimental procedures whereby measurements were performed (36 h vs 24 h, published and performed by us, respectively).

5.1.7 Sox10 activates WT pBrn2 without cooperating with MAML1 to induce pBrn2 activation

Another transcription factor that induces WT *Brn2* promoter activation is Sox10 (section 3.5). To investigate whether MAML1-induced WT *Brn2* promoter activation is mediated through Sox10, luciferase assays were performed.

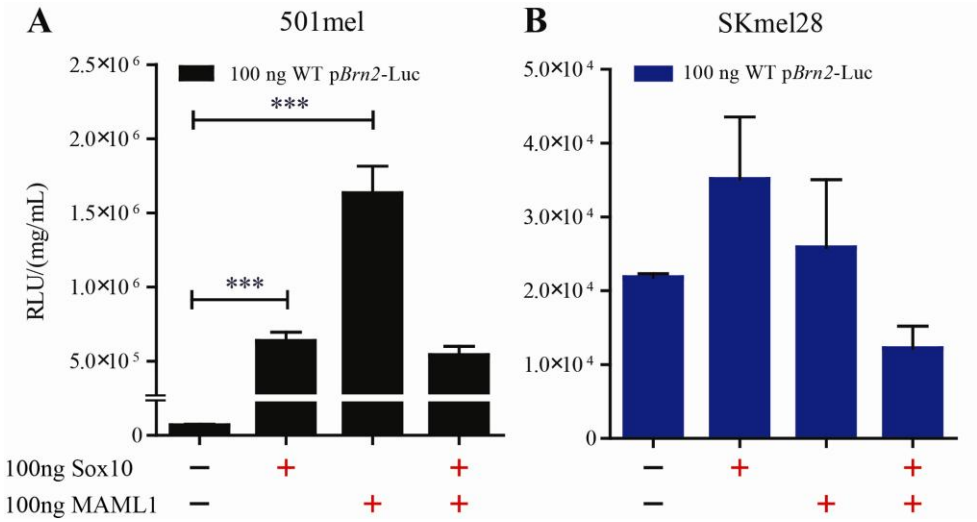


Figure 5.4: Sox10 does not cooperate with MAML1 to activate the WT *Brn2* promoter. 100 ng of Sox10 or MAML1 expression plasmids were transfected into 501mel (**A**) and SKmel28 (**B**) cells together with 100 ng WT p*Brn2*-Luc. An empty vector plasmid was used as a control for the variation in total DNA content per condition. Luciferase expression was measured 24 h post-transfection and normalised to protein content of the well. Results are expressed as the mean ± S.D., n=3. Statistical analysis was performed using a one-way ANOVA followed by a post-hoc Tukey's test. *** = $p<0.001$

In 501mel cells (Figure 5.4A), Sox10 and MAML1 separately induced an increase in WT *Brn2* promoter activity (more than 9.5- and 25-fold ($p<0.001$ for both), respectively). However, co-transfections with Sox10 and MAML1 expression plasmids, only led to an 8-fold increase in luciferase expression compared to the control, suggesting that Sox10 might be blocking the MAML1-induced activation of the *Brn2* promoter.

In SKmel28 cells (Figure 5.4B), Sox10 induced luciferase expression by 60%, while MAML1 increased luciferase expression by 20% and together with Sox10 induced a decrease by 40%, compared to the control.

To conclude, Sox10 and MAML1 do not cooperate to induce *Brn2* promoter activity and the MAML1 effect does not appear to be mediated by Sox10. In fact, while Sox10 and MAML1 on their own activate the WT *Brn2* promoter, in co-transfections, Sox10 seems to inhibit the MAML1-induced *Brn2* promoter activity in 501mel cells and activate the *Brn2* promoter to similar levels as Sox10 transfections only. This would suggest that MAML1-activated factors and Sox10 compete for the same binding site on

the *Brn2* promoter. Additionally, ectopically-overexpressed Sox10 might outcompete MAML1 in co-transfection experiments.

5.1.8 MAML1 and β-catenin show a synergistic activation of the WT pBrn2

Although Notch promotes de-differentiation in melanocytes, this pathway has not been known to directly regulate Brn2. Similarly, the ability of MAML1 to induce p*Brn2* activation has not been reported before. However, an indication about its mechanism of action comes from Alves-Guerra and colleagues who demonstrated that MAML1 can interact with β-catenin to induce transcription of target genes (Alves-Guerra et al., 2007). To test if MAML1-induced activation of p*Brn2* is mediated by β-catenin, co-transfection experiments with MAML1 and β-catenin expression plasmids together with the WT p*Brn2*-Luc construct were performed (Figure 5.5).

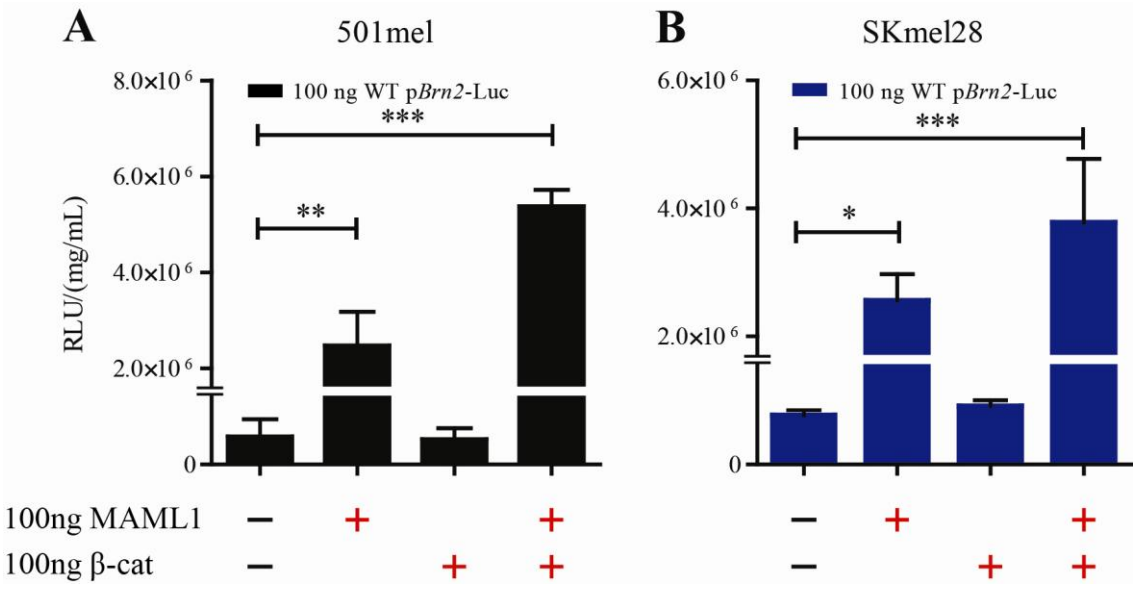


Figure 5.5: MAML1 and β-catenin cooperate to activate the WT *Brn2* promoter in 501mel and SKmel28 cells. 100 ng of MAML1 and β-catenin expression vectors were transfected into 501mel (**A**) and SKmel28 (**B**) cells together with 100 ng of the WT p*Brn2*-Luc construct. To control for the amount of DNA transfected in each condition, an empty vector was used. Luciferase was measured 24 h post-transfection and normalised to the protein content per well. Results are expressed as the mean ± S.D. n=3. Statistical analysis was performed using a one-way ANOVA followed by a post-hoc Tukey's test. * = $p<0.05$, ** = $p<0.01$, *** = $p<0.001$.

In 501mel cells, MAML1 induced a 3-fold activation of the WT *Brn2* promoter ($p<0.01$) while β-catenin had little effect on the WT *Brn2* promoter activation (10%

increase) (Figure 5.5A). However, co-transfections with β-catenin and MAML1 induced an 8-fold increase of the WT *Brn2* promoter activity ($p<0.001$) compared to the control (Figure 5.5A). These results confirmed that β-catenin enhances MAML1-induced activation of the WT *Brn2* promoter, despite β-catenin on its own not being able to achieve activation in this assays.

In SKmel28 cells, MAML1 alone induced 2-fold ($p<0.05$) WT *Brn2* promoter activity compared to control levels (Figure 5.5B). Again, β-catenin had a small effect on the WT *Brn2* promoter (20% increase) but co-transfection with the MAML1 expression plasmid induced a 4-fold increase in luciferase expression ($p<0.001$).

5.1.9 MAML1- and β-catenin-induced activation of the pBrn2 is dependent on the TCF/LEF1 binding site in SKmel28 cells

To investigate how β-catenin contributes to the MAML1-induced activation of the WT *Brn2* promoter, we conducted luciferase experiments using a TCF/LEF1 mutated p*Brn2*-Luc construct (Chapter 4 Figure 4.5). As the mutation was generated in the backbone of the Δ268 p*Brn2*-Luc plasmid, co-transfection experiments were firstly performed with the latter and MAML1 and β-catenin expression plasmids (Figure 5.6).

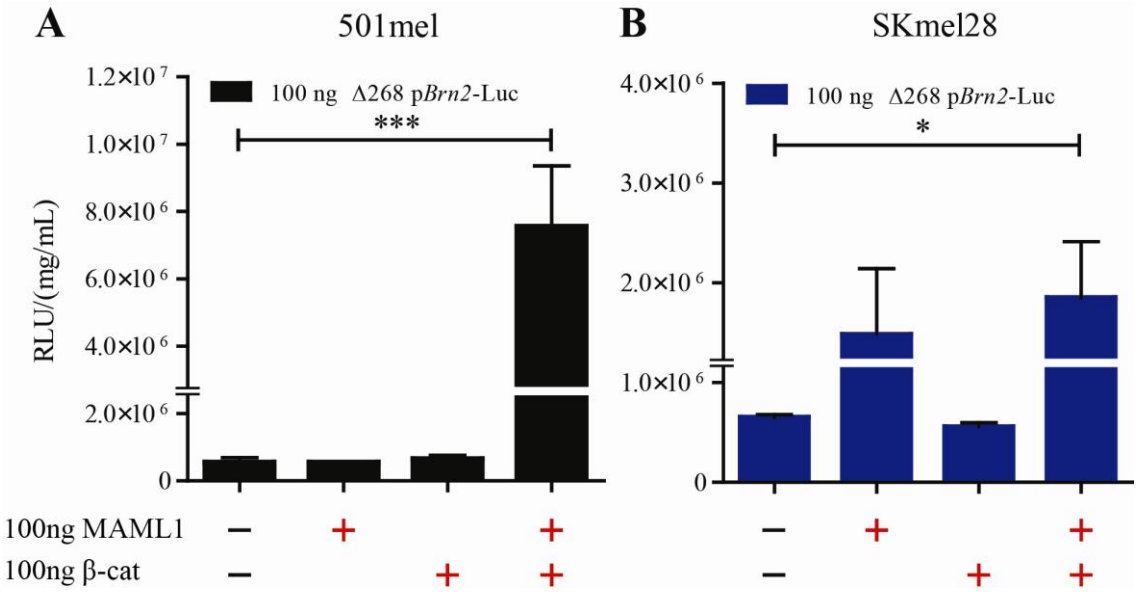


Figure 5.6: MAML1 and β-catenin cooperate to activate the Δ268 *Brn2* promoter in 501mel and SKmel28 cells. 100 ng of MAML1 and β-catenin expression vectors were transfected into 501mel (**A**) and SKmel28 (**B**) cells together with 100 ng of the Δ268 p*Brn2*-Luc construct. An empty vector was used to control for the amount of DNA transfected into each well. Luciferase was measured 24 h post-transfection and normalised to the protein content per well. Results are expressed as the mean ± S.D. n=3, performed in two independent experiments. Statistical analysis was performed using a one-way ANOVA followed by a post-hoc Tukey's test. * = $p<0.05$, *** = $p<0.001$

Contrary to the results above (Figure 5.2A), MAML1 did not induce a change in Δ268 *Brn2* promoter activity in 501mel cells in this experiment (Figure 5.6A), which was most likely due to the confluency of the cells. Similar to previous observations, β-catenin only slightly increased promoter activity (20% compared to control levels). Co-transfections with β-catenin and MAML1 expression plasmids induced almost a 14-fold increase in luciferase expression ($p<0.001$) (Figure 5.6A).

In SKmel28 cells, the activation of the Δ268 *Brn2* promoter followed a similar pattern to WT *Brn2* promoter activation: MAML1 induced a 2-fold increase in luciferase expression compared to the control. While β-catenin alone had almost no effect on the WT *Brn2* promoter activation (10% decrease), the combination of β-catenin and MAML1 induced an almost 3-fold increase ($p<0.05$).

In summary, luciferase activation of the WT p*Brn2*-Luc and Δ268 p*Brn2*-Luc constructs followed similar patterns upon transfections with MAML1 and β-catenin expression plasmids.

As there is clear involvement of β-catenin in MAML1-induced *Brn2* promoter activation and having previously demonstrated differential β-catenin protein expression in 501mel and SKmel28 cells (cytoplasmic and nuclear in 501mel and mainly membrane-associated in SKmel28 cells) (Chapter 4, Figure 4.7), we next sought to investigate how a TCF/LEF1 mutated binding site within the *Brn2* promoter would affect MAML1- and β-catenin-induced *Brn2* promoter activation. To this end, luciferase experiments were performed with TCF/LEF1 mut p*Brn2*-Luc. If MAML1 and β-catenin activate the *Brn2* promoter through the Wnt/β-catenin pathway, mutating the TCF/LEF1 binding site would attenuate or abrogate luciferase expression. Consequently, if the *Brn2* promoter containing the mutated TCF/LEF1 binding site is still activated by MAML1 and β-catenin, other factors must be involved in its activation.

In 501mel cells, despite the TCF/LEF1 mutation, MAML1 still induced a 4-fold increase in luciferase expression from the TCF/LEF1 mutated p*Brn2*-Luc construct (Figure 5.7A). β-catenin on its own also activated the TCF/LEF1 mut *Brn2* promoter by 70% but in combination with MAML1 the increase in activation was larger (11.5-fold, $p<0.001$) (Figure 5.7A).

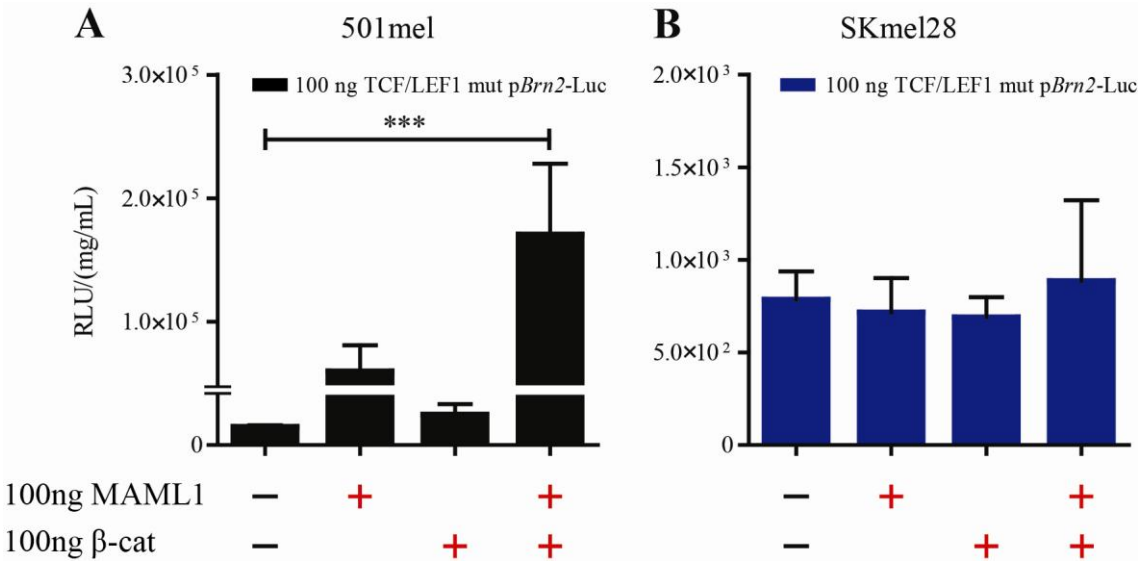


Figure 5.7: MAML1 and β-catenin cooperate to activate the TCF/LEF1 mutated *Brn2* promoter in 501mel. 100 ng of MAML1 and β-catenin expression plasmids alone or in combination were transfected into 501mel (**A**) and SKmel28 (**B**) cells together with 100 ng of the TCF/LEF1 mut p*Brn2*-Luc construct. An empty plasmid was used to control for the DNA amount per well. Luciferase was measured 24 h post-transfection and normalised to the protein content per well. Results are expressed as the mean ± S.D. n=3. Statistical analysis was performed using a one-way ANOVA followed by a post-hoc Tukey's test. *** = $p<0.001$

In SKmel28 cells, MAML1 and β-catenin had very little effect on the TCF/LEF1 mut *Brn2* promoter activation (10% in both conditions) (Figure 5.7B). Even the combination of β-catenin and MAML1 only induced a small increase in *Brn2* promoter activity compared to control levels (10%).

In conclusion, *Brn2* promoter activation by MAML1 and β-catenin in 501mel cells seems to be not solely dependent upon a functional TCF/LEF1 binding site as the promoter retains the capacity to be activated despite the mutation in the TCF/LEF1 site. Alternatively, it is possible that the promoter still retains some activity and that the nuclear β-catenin levels, present in 501mel cells are sufficient to induce activation.

In SKmel28 cells, however, the p*Brn2* activation upon treatment with MAML1 and β-catenin is abrogated, indicating that either this activation is mediated by or dependent upon a fully functioning TCF/LEF1 site or that the levels present in the nucleus are not sufficient to induce activation of the still partly functional promoter.

Note also that the basal luciferase levels upon transfections with the TCF/LEF1 mutated p*Brn2*-Luc construct are decreased compared to the Δ268 p*Brn2*-Luc construct (Figure 5.6) in 501mel and SKmel cells. This suggests that the TCF/LEF1 mutation inhibits general *Brn2* promoter activation by interfering or inhibiting the activation of the *Brn2* promoter by other factors. For instance, the binding sites for the transcription factor Pax3 overlaps with the TCF/LEF1 binding site. And thus, a mutation in the TCF/LEF1 binding site might influence/regulate the activity of Pax3 which might lead to a decrease in *Brn2* promoter activation.

5.1.10 MAML1 and ß-catenin-induced pBrn2 activation is mediated by the TCF/LEF1 site

A different approach to assess if a compound is acting through the Wnt pathway is by utilising the TOP/FOP-flash reporter system designed by the Clevers laboratory (Figure 5.8) (Barker and Clevers, 2006).

This system consists of the plasmids TOP-flash and FOP-flash that both contain a promoter-luciferase reporter combination. While the TOP-flash construct has multiple intact TCF/LEF1 binding sites, the promoter in the FOP-flash plasmid only consists of mutated TCF/LEF1 binding sites. To test if a factor-of-interest activates the Wnt pathway, transfections are performed with both plasmids and the ratio of TOP-flash over FOP-flash activation is calculated. If a factor-of-interest activates the Wnt pathway specifically, the ratio of luciferase expression of TOP- over FOP-flash will be high and vice versa.

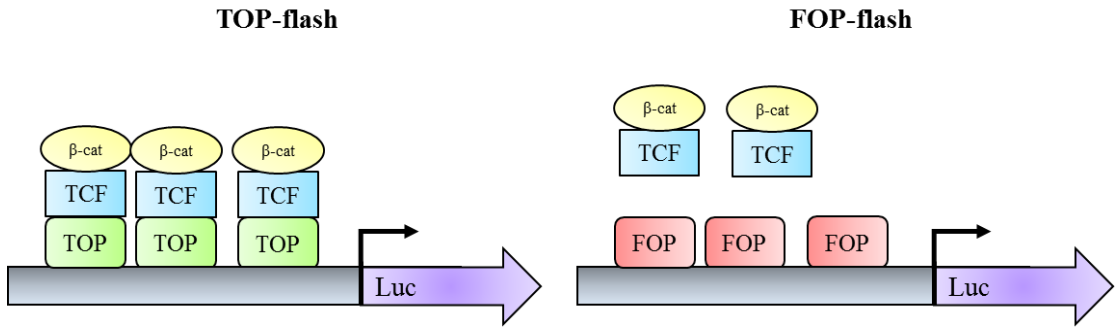


Figure 5.8: Schematic diagram of the TOP/FOP-flash plasmid system. The TOP/FOP-flash plasmid system allows testing if a compound is eliciting its effects through the Wnt pathway. Both plasmids both contain the luciferase gene that is transcribed upon promoter activation. While the TOP-flash plasmid contains a promoter consisting of intact TCF/LEF1 binding sites, the promoter in the FOP-flash plasmid is made up mutated TCF/LEF1 binding sites. If a compound is co-transfected with these plasmids and able to induce luciferase expression from the TOP-flash plasmid only, it indicates that it utilises the Wnt pathway for its mechanism of action. Adapted from (Barker and Clevers, 2006).

To confirm that the MAML1- and β-catenin-induced activation of the *Brn2* promoter in 501mel and SKmel28 cells is dependent, at least partly, upon functional TCF/LEF1 signalling, luciferase experiments using the TOP/FOP-flash reporter system were performed (Figure 5.9).

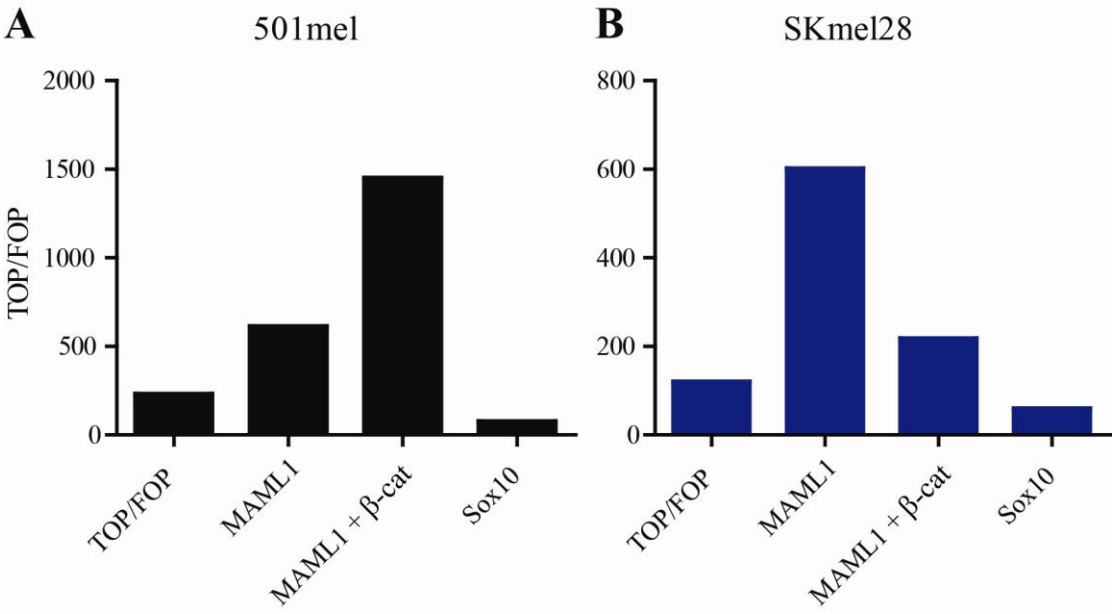


Figure 5.9: MAML1 and β-catenin induce luciferase expression from the TOP-flash plasmid in 501mel and SKmel28 cells. 100 ng of the indicated expression plasmids were transfected into 501mel (**A**) and SKmel28 (**B**) cells, together with 100 ng TOP- or FOP-flash plasmid constructs. To control for the total amount of DNA per condition, empty plasmids were used as a control. Luciferase was measured 24 h post-transfection and normalised to the protein content per well. Results are expressed as a ratio of TOP-flash/FOP-flash activation. n=2

In 501mel cells, MAML1 alone induced a 1.7-fold increase, while MAML1 and β-catenin together induced more than a 5-fold increased in the ratio of TOP-flash over FOP-flash activation compared to the control (Figure 5.9A).

Contrastingly, in SKmel28 cells, MAML1 alone induced a 4-fold increase, while MAML1 together with β-catenin induced an 80% increase of TOP- over FOP-flash luciferase expression compared to the control (Figure 5.9B).

In conclusion, these results demonstrate that in 501mel and SKmel28 cells, MAML1 alone and in combination with β-catenin require intact TCF/LEF1 binding sites to function to different degrees.

5.1.11 MAML1- and β-catenin-induced pBrn2 activation is mediated through TCF3

Having demonstrated that the TCF/LEF1 binding site plays a role in the MAML1- and β-catenin-induced activation of the *Brn2* promoter, the next step was to investigate the mechanism and the transcription factors that might be mediating this effect. To this end, plasmids expressing TCF3 and LEF1 were transfected separately and in combination with MAML1 and β-catenin expression plasmids, as well as with the WT *Brn2* promoter in luciferase assays (Figure 5.10).

In 501mel cells, transfections with β-catenin induced WT *Brn2* promoter activation by 40%, while TCF3, MAML1 and LEF1 induced almost a 6- ($p<0.001$), 5-fold ($p<0.001$) and 3.5-fold ($p<0.05$) activation of the WT *Brn2* promoter, respectively (Figure 5.10A). The combinations of β-catenin and TCF3 or LEF1 also induced a 9-fold ($p<0.001$) and a 6-fold ($p<0.001$) activation of the WT *Brn2* promoter, respectively. However, the largest increase was induced by MAML1 and TCF3 (21-fold activation, $p<0.001$), while transfections with MAML1 and LEF1 expression plasmids only induced a 4.5-fold ($p<0.01$) increase compared to the control (Figure 5.10A).

In SKmel28 cells, β-catenin did not increase luciferase expression while TCF3, MAML1 and LEF1 did (190% ($p<0.05$), 40% and 80% increase compared to the control, respectively) (Figure 5.10B). β-catenin and TCF3 induced the largest WT *Brn2* promoter activation leading to an almost 6-fold increase in luciferase expression ($p<0.001$), while β-catenin and LEF1 only induced luciferase expression by 150% ($p<0.05$). Co-transfections with MAML1 induced a 4.5-fold induction ($p<0.001$) of the p*Brn2*-Luc construct, while LEF1 increased the promoter activation by 40%, compared to the control (Figure 5.10B).

In summary, in 501mel and in SKmel28 cells, TCF3, MAML1 and LEF1 separately induced WT *Brn2* promoter activity to similar levels. However, combinations of MAML1 or β-catenin together with TCF3 expression plasmid induced the biggest increase in luciferase expression, which leads to the conclusion that TCF3, rather than LEF1, mediates the MAML1- and β-catenin-induced activation of WT p*Brn2*.

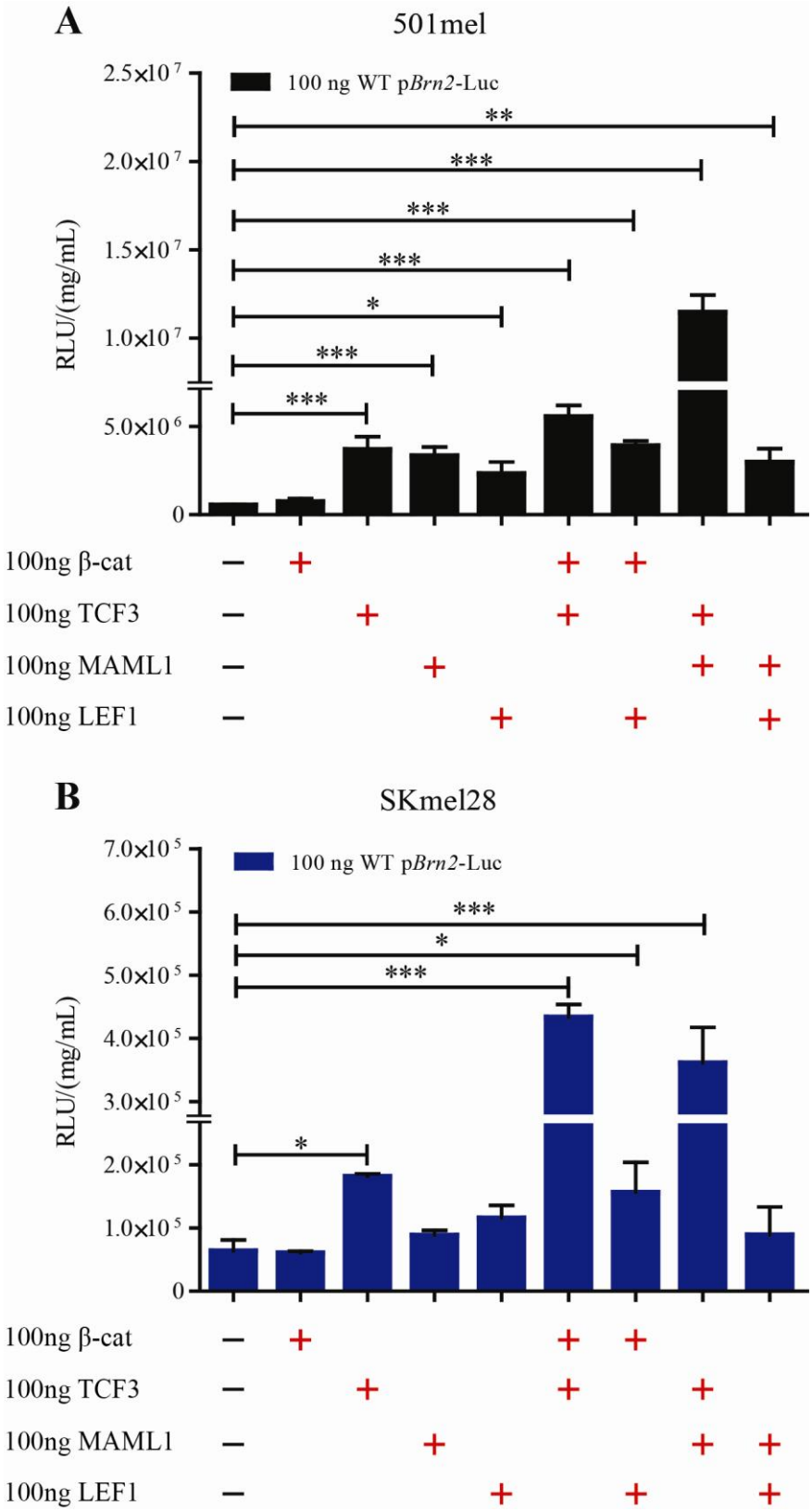


Figure 5.10: TCF3 on its own and in combination with β-catenin and MAML1 activates the WT *Brn2* promoter in 501mel and SKmel28 cells. 100 ng of the indicated expression plasmids were transfected into 501mel (**A**) and SKmel28 (**B**) cells together with 100 ng of the WT p*Brn2*-Luc plasmid. Luciferase was measured 24 h post-transfection and normalised to the protein content. Results are expressed as mean ± S.D, n=3. Statistical analysis was performed using a one-way ANOVA followed by a post-hoc Tukey's test. * = $p<0.05$, ** = $p<0.01$, *** = $p<0.001$

5.1.12 MAML1- and β-catenin-induced pMITF activation is mediated through LEF1

To investigate the effects of MAML1 and its potential mechanism of action on the *MITF* promoter, luciferase experiments were conducted with expression vectors of MAML1, β-catenin as well as TCF3 and LEF1 together with the WT *MITF* promoter-luciferase reporter (Figure 5.11A).

In 501mel cells (Figure 5.11A), β-catenin induced a small increase in luciferase expression (30%), while TCF3 decreased the activity of the *MITF* promoter by 80% compared to the control, suggesting that TCF3 may act to repress the *MITF* promoter. MAML1 and LEF1 on the other hand, both activated the promoter by 90%. Co-transfections with β-catenin and TCF3 or LEF1 expression plasmids had opposing effects. While the former induced a decrease (by 80%) the latter increased the *MITF* promoter activity (by 150%, $p<0.05$). A similar pattern was produced by co-transfections of the plasmid expressing MAML1 together with the TCF3 expression plasmid (inducing a decrease of 70%) or LEF1 (leading to the activation of the *MITF* promoter by 70%) (Figure 5.11A).

Transfections in SKmel28 cells had a similar effect on the *MITF* promoter, except for β-catenin expression plasmid alone, which induced a decrease in *MITF* promoter activity by 40%, as did TCF3 (50%) (Figure 5.11B). MAML1 increased promoter activity by 30% while LEF1 induced a 3-fold increase ($p<0.001$) of promoter activation. Again, co-transfections with the β-catenin expression plasmid together with the plasmid expressing TCF3 decreased the promoter activity by 80%, while β-catenin and LEF1 together induced a 2.5-fold activation ($p<0.01$), compared to the control.

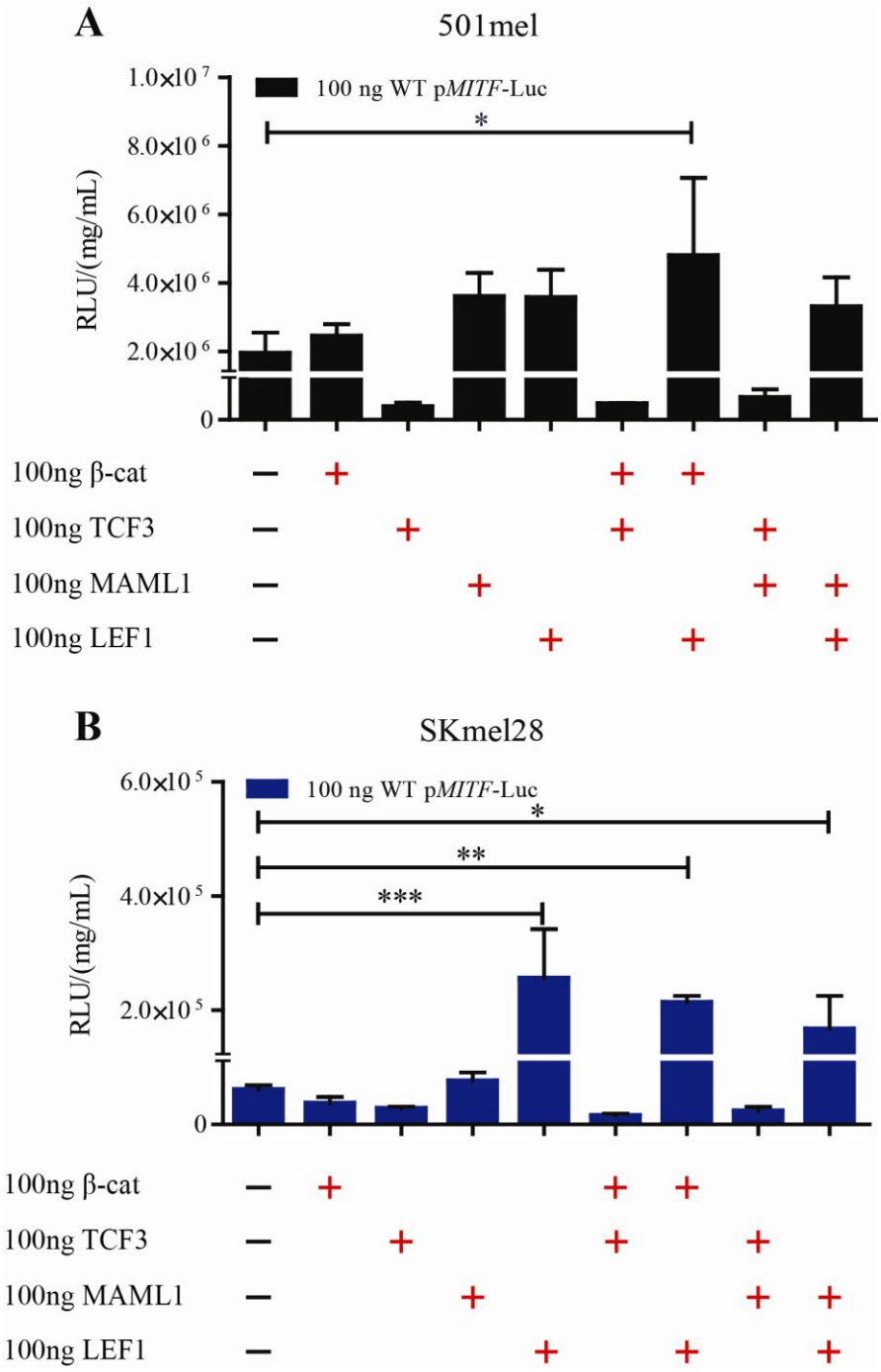


Figure 5.11: LEF1 on its own and in combination with β-catenin and MAML1 activates the *MITF* promoter in 501mel and SKmel28 cells. 100 ng of the indicated expression plasmids were transfected into 501mel (**A**) and SKmel28 (**B**) cells together with 100 ng of the p*MITF*-Luc plasmid. Luciferase was measured 24 h post-transfection and normalised to the protein content. Results are expressed as mean ± S.D, n=3. Statistical analysis was performed using a one-way ANOVA followed by a post-hoc Tukey's test. * = $p<0.05$, ** = $p<0.01$, *** = $p<0.001$

Co-transfections with MAML1 and TCF3 or LEF1 expression plasmids had a similar effect, inducing a decrease by 60% and an increase in *MITF* promoter activity by 180% ($p<0.05$), respectively.

To summarise, *MITF* promoter activity is up-regulated solely by the presence of the transcription factor LEF1 and combinations of LEF1 and MAML1 or β-catenin, while the transcription factor TCF3 exhibits the opposite effect by decreasing *MITF* promoter activity.

5.1.13 MAML1 effects on endogenous MITF protein expression in 501mel and SKmel28 cells

To investigate the effect of MAML1 on the endogenous *MITF* gene, 501mel and SKmel28 cells were transfected with a vector expressing FLAG-tagged MAML1 (Figure 5.12 and 5.13, respectively). Cells were subsequently stained for MITF, as well as MAML1-FLAG. To control for the background fluorescence produced by the secondary anti-FLAG antibody, untransfected cells were also stained with both antibodies.

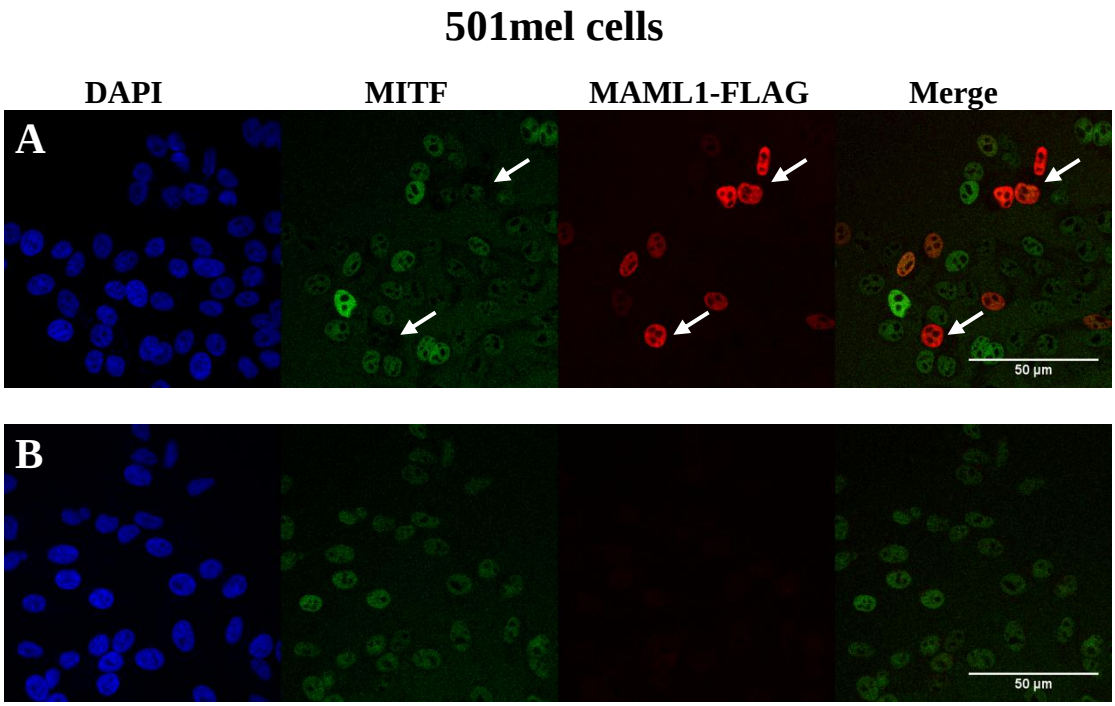


Figure 5.12: Ectopically-expressed MAML1 decreases endogenous MITF protein expression in 501mel cells. 400 ng of a plasmid expressing MAML1-FLAG were transfected into 501mel cells (**A**). 24 h post-transfection cells were fixed and stained with anti-MITF and anti-FLAG antibodies, followed by secondary antibodies Alexa-Fluor 488 (green, second column) and Alexa-Fluor 546 (red, third column), respectively. Cells were counterstained with DAPI (blue, first column). Pictures were taken at 40x magnification. The scale bar represents 50 µm. (**A**-transfected cells, **B**-untransfected control).

In cells ectopically expressing MAML1 the majority of cells showed a clear decrease in MITF protein expression (Figure 5.12A, white arrows) compared to untreated cells (Figure 5.12B). This might reflect a direct consequence of MAML1 expression, or might be related to cell cycle effects since it is well known that cycling cells are much more prone to transfection. Additionally, MITF is heterogeneously expressed in 501mel cells, most likely reflecting the degree of cell cycle regulation (Kao Chin Ngeow, personal communication).

The same procedure was applied to SKmel28 cells to assess endogenous *MITF* gene expression.

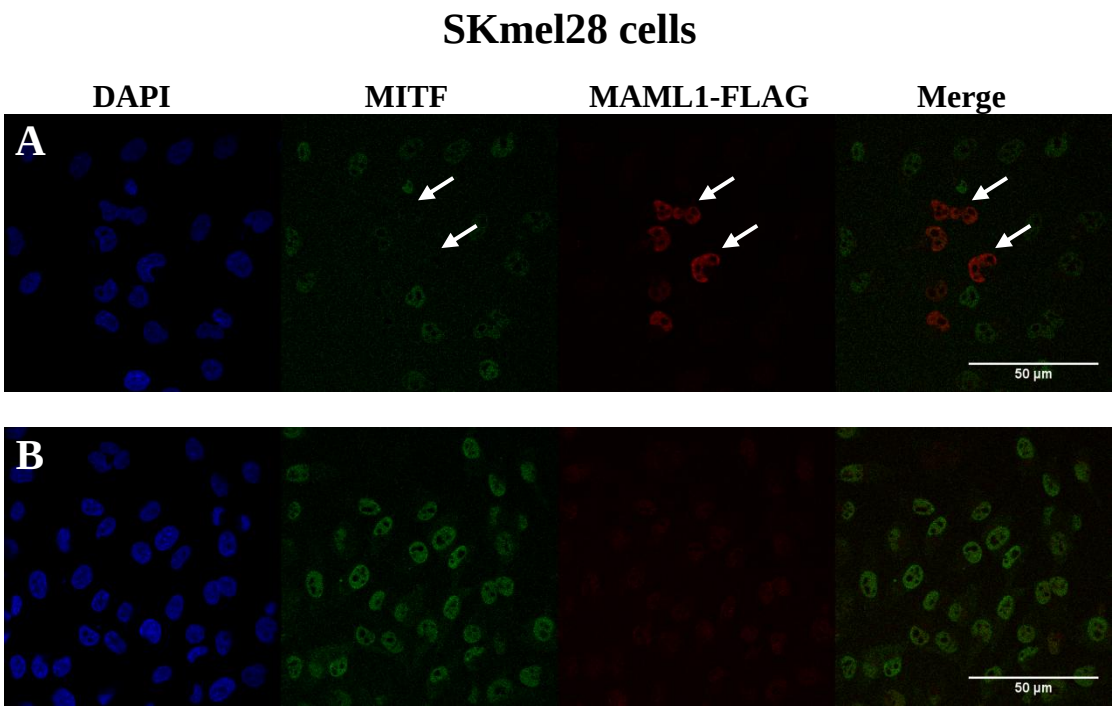


Figure 5.13: Ectopically-expressed MAML1 decreases endogenous MITF protein expression in SKmel28 cells. 400 ng of a plasmid expressing MAML1-FLAG were transfected into SKmel28 cells (**A**). 24 h post-transfection cells were fixed and stained with anti-MITF and anti-FLAG antibodies, followed by secondary antibodies Alexa-Fluor 488 (green, second column) and Alexa-Fluor 546 (red, third column), respectively. Cells were counterstained with DAPI (blue, first column). Pictures were taken at 40x magnification. The scale bar represents 50 µm. (**A**-transfected cells, **B**-untransfected control)

Similar to 501mel cells, SKmel28 cells also expressed varying levels of MITF protein while SKmel28 cells transfected with the MAML1 expression vector showed decreased levels of MITF (Figure 5.13A, white arrows) compared to untreated cells (Figure 5.13B).

5.1.14 MAML1 affects endogenous β-catenin protein expression in 501mel and SKmel28 cells

Having demonstrated that MAML1 and β-catenin interact to increase *Brn2* promoter activity in the luciferase assay, we investigated the effect of ectopic MAML1 expression on β-catenin protein levels. For this, the MAML1-FLAG-tagged expression vector was transfected into 501mel and SKmel28 cells and cells were stained with anti-β-catenin and anti-FLAG antibodies (Figure 5.14).

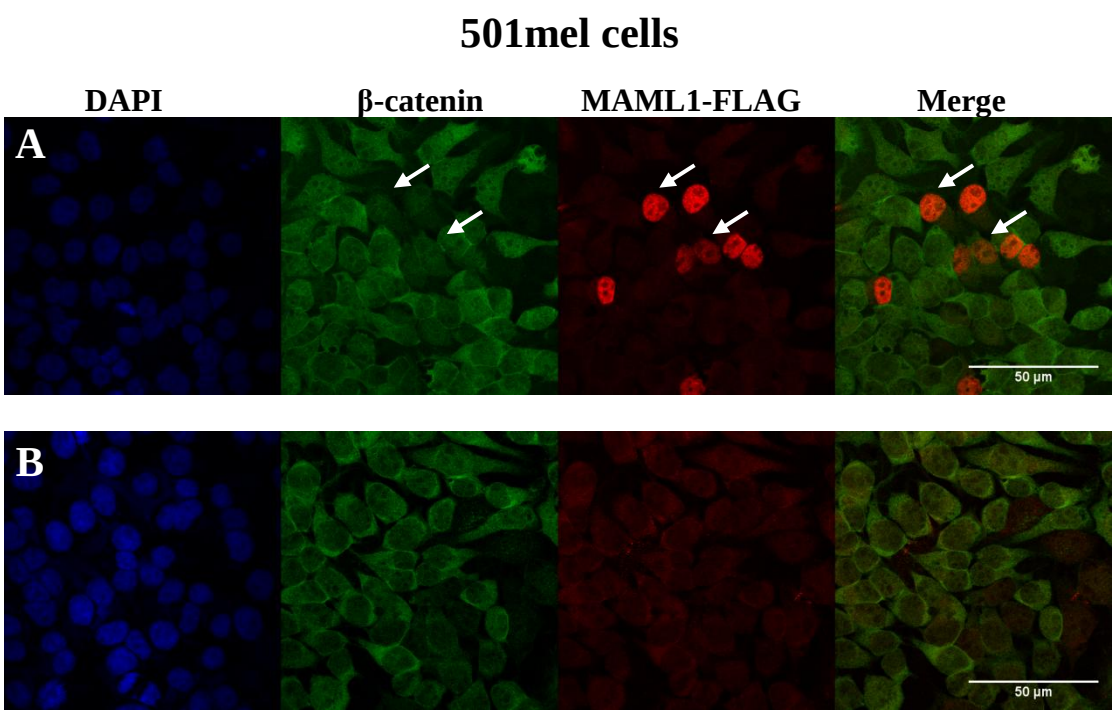


Figure 5.14: Ectopically-expressed MAML1 decreases endogenous β-catenin protein expression in 501mel cells. 400 ng of a plasmid expressing MAML1-FLAG were transfected into 501mel cells (**A**). 24 h post-transfection cells were fixed and stained with anti-β-catenin and anti-FLAG antibodies, followed by the secondary antibodies Alexa-Fluor 488 (green, second column) and Alexa-Fluor 546 (red, third column), respectively. Cells were counterstained with DAPI (blue, first column). Pictures were taken at 40x magnification. The scale bar represents 50 µm. (**A**-transfected cells, **B**-untransfected control)

501mel cells transfected with a MAML1 expression vector displayed lower β-catenin protein expression (Figure 5.14A, white arrows), although it is hard to determine whether this is a direct effect of MAML1 or an indirect consequence of the cell cycle in transfected cells. Again, as a control for the background fluorescence produced by the secondary antibody, untransfected cells were also stained with both antibodies (Figure 5.14B).

In SKmel28 cells, the effect of MAML1 on β-catenin expression was not as obvious as in 501mel cells. As β-catenin is expressed heterogeneously on the cell membrane (Figure 4.7C and D) it was difficult to detect changes in β-catenin expression upon ectopic MAML1 expression (Figure 5.15A).

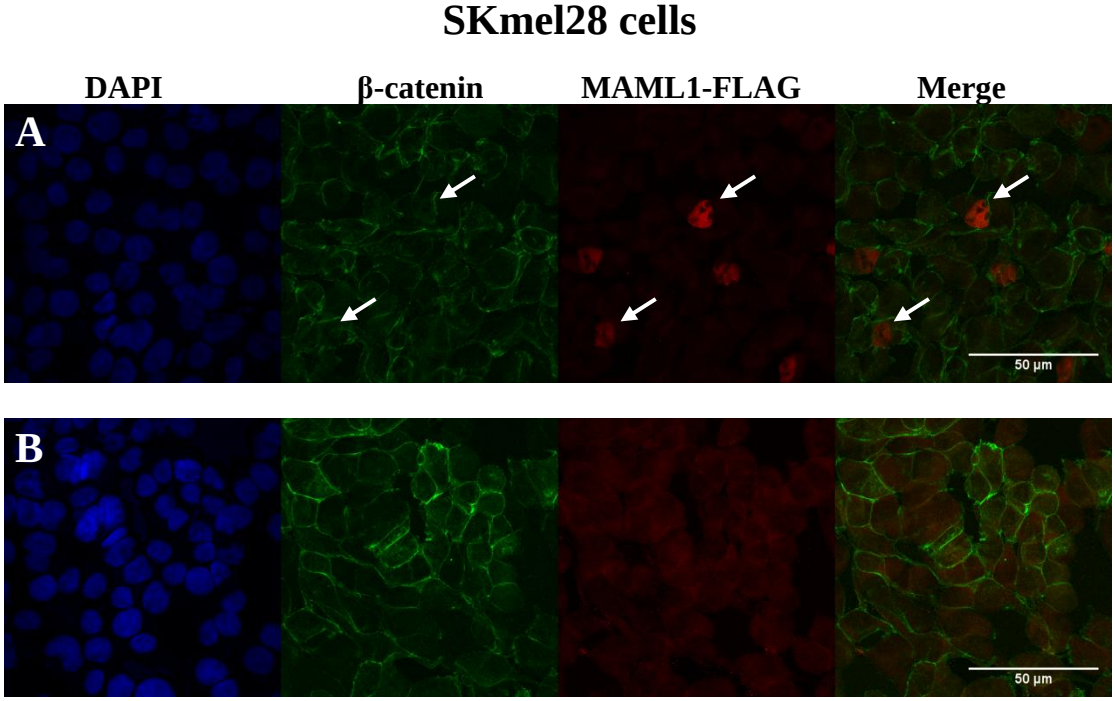


Figure 5.15: Ectopically-expressed MAML1 does not influence endogenous β-catenin protein expression in SKmel28 cells. 400 ng of a plasmid expressing MAML1-FLAG were transfected into SKmel28 cells (**A**). 24 h post-transfection cells were fixed and stained with anti-β-catenin and anti-FLAG antibodies, followed by the secondary antibodies Alexa-Fluor 488 (green, second column) and Alexa-Fluor 546 (red, third column), respectively. Cells were counterstained with DAPI (blue, first column). Pictures were taken at 40x magnification. The scale bar represents 50 µm. (**A**-transfected cells, **B**-untransfected control)

To summarise, while 501mel cells show decreased β-catenin protein levels upon transfections with MAML1, SKmel28 cells did not demonstrate any noticeable changes in membrane-bound β-catenin expression upon MAML1 transfection.

5.1.15 Silencing of MAML1 decreases MITF and β-catenin protein

To further investigate the effect of MAML1 on MITF, Brn2 and β-catenin protein levels in 501mel and SKmel28 cells, the MAML1 gene was silenced and western blotting was performed.

The functionality of the anti-MAML1 antibody was assessed in B16F10 and HEK293T cell lysates as these cell lines express MAML1 (Pournara et al., 2014) (Figure 5.16). The MAML1 antibody identified a protein at approximately 130 kDa (previously reported to be 140 kDa (Pournara et al., 2014).

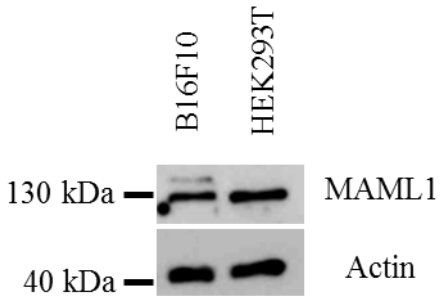


Figure 5.16: MAML1 is expressed in B16F10 and HEK293T cells. Lysates of B16F10 and HEK293T cells were subjected to SDS-PAGE and Western blotted with anti-MAML1 and anti-β-actin antibodies as indicated. Experiment was performed once.

To assess the effect of MAML1 depletion on β-catenin and MITF protein expression, 501mel cells were transfected with siRNAs against MAML1 and cell lysates were probed for antibodies detecting β-catenin and MITF (Figure 5.17). Preliminary observations have shown that up to 48 h post-transfection protein levels do not change. For this reason we decided to lyse the cells 48 h post-siRNA transfection. To control for the effects of siRNAs on protein expression, transfections with non-targeting siRNAs (CTL) were performed and lysates were also probed with indicated antibodies (Figure 5.17).

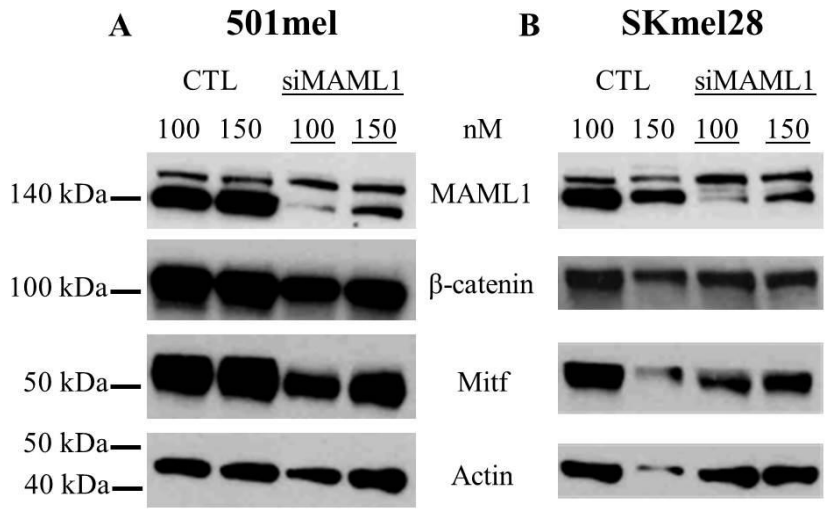


Figure 5.17: Silencing of MAML1 decreases β-catenin and MITF expression 501mel cells. 501mel (**A**) and SKmel28 (**B**) cells were transfected with 100 nM and 150 nM of siRNA against MAML1 (siMAML1) and control siRNA (siCtl). 48 h post-transfection cell lysates were subjected to SDS-PAGE and Western blotted with the indicated antibodies. Experiment was performed once.

The anti-MAML1 antibody identified the protein at 140 kDa and the anti-β-catenin antibody produced a band at 100 kDa, while the anti-MITF antibody produced two bands, indicating the hyper-phosphorylated and the hypo-phosphorylated protein forms at 60 and 54 kDa, respectively. Antibodies against β-actin were used as loading control and identified the protein at 42 kDa (Figure 5.17).

In 501mel cells, 100 nM and 150 nM siMAML1 treatment induced silencing of MAML1 (Figure 5.17A). Silencing was more pronounced in the 100 nM condition. Additionally, siMAML1 treatment decreased β-catenin expression (100 kDa) compared to 100 nM and 150 nM scrambled siRNA (CTL). The same was true for the MITF protein levels, while the β-actin levels were all comparable, suggesting that there were slight differences in loading of the proteins.

In SKmel28 cells (Figure 5.17B), the 150 nM condition was discounted because of low levels of actin. Instead, the 100 nM condition was compared. 100 nM siMAML1 induced silencing of MAML1 and decreased β-catenin and MITF protein levels (Figure 5.17B).

From the fluorescence microscopy pictures, where 501mel and SKmel28 cells transfected with MAML1 expression vectors showed a decrease in MITF and β-catenin protein expression (Figure 5.12 - 5.15), it was hypothesised that silencing of MAML1 would lead to an increase in MITF and β-catenin levels. However, the opposite was the case (Figure 5.17). The discrepancy could be due to the time point of protein level assessment, as the fluorescence microscopy pictures were taken 24 h post-transfection and the western blotting was performed 48 h post-transfection. However, the results of the siRNA silencing experiments are in agreement with the luciferase assays and indicate that MAML1 is likely to be a positive regulator of MITF expression.

5.1.16 Silencing of β-catenin decreases MAML1 levels in 501mel cells

To investigate how silencing of β-catenin influences MAML1 protein expression, 501mel and SKmel28 cells were transfected with siRNAs against β-catenin (siβ) (Figure 5.18).

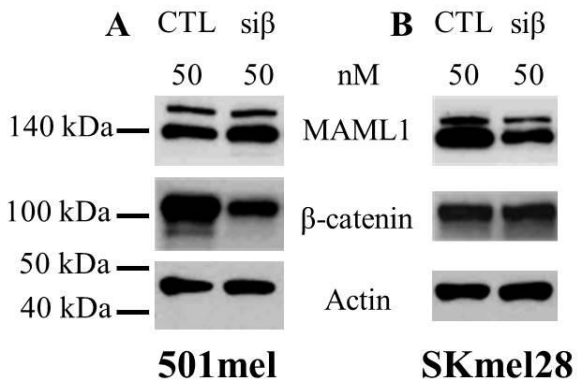


Figure 5.18: Silencing of β-catenin decreases MAML1 expression in SKmel28 cells. 501mel (**A**) and SKmel28 (**B**) were transfected with 50 nM siRNA against β-catenin (siβ) and control siRNA (CTL). 48 h post-transfection cell lysates were subjected to SDS-PAGE and stained with indicated antibodies. Experiment was performed once.

501mel cells, treated with 50 nM siβ, expressed lower levels of β-catenin compared to cells treated with 50 nM scrambled siRNA (CTL), which demonstrated that the silencing had worked (Figure 5.18A). MAML1 protein levels, however, were not affected. The anti-β-actin antibody was used as a loading control.

Silencing of β-catenin in SKmel28 cells was not as pronounced as in 501mel cells (Figure 5.18B) but 50 nM siβ still induced a decrease in MAML1 expression compared to the control condition. β-actin levels were consistent.

5.2 Discussion

5.2.1 Key findings

In this chapter we investigated the function of the Notch pathway component and transcriptional co-activator MAML1 and its potential effects on the *Brn2* and *MITF* promoters and protein levels in 501mel and SKmel28 cells. We demonstrated that MAML both on its own and in combination with β-catenin activates the WT and the truncated Δ268 *Brn2* promoter in 501mel and SKmel28 cells. While in 501mel cells mutation of the TCF/LEF1 binding site in the *Brn2* promoter did not fully abrogate MAML1- and β-catenin-induced promoter activation, in SKmel28 cells, MAML1 and β-catenin did not activate the TCF/LEF1 mutated p*Brn2*. This may suggest that in 501mel cells MAML1 and β-catenin utilise additional pathways to activate the *Brn2* promoter. However, it is also conceivable that this promoter retains a lower level of activity and therefore the nuclear β-catenin in 501mel cells can still induce activation of this promoter. In SKmel28 cells, on the other hand, nuclear β-catenin levels are low, as it is mainly membrane-associated, and therefore a mutation in the TCF/LEF1 site in the *Brn2* promoter, is likely to abrogate promoter activity.

In line with our hypothesis that the TCF/LEF1 binding site is involved in p*Brn2* activation, we next demonstrated that the transcription factor TCF3 was mediating the effect of β-catenin- and MAML1-induced p*Brn2* activation. Interestingly, MAML1 and β-catenin also activated the *MITF* promoter. However, this effect was mediated by

LEF1 in SKmel28 and 501mel cells, instead of TCF3 as shown to be the case for p*Brn2*.

Interestingly, immunofluorescence experiments demonstrated that overexpression of ectopic MAML1 decreases MITF protein expression in both cell lines, which contrasts with the luciferase experiments conducted before. The discrepancy between the luciferase experiments and the fluorescence microscopy pictures might be due to the techniques used. Luciferase assays measure the activity of the promoter and therefore transcription efficiency, while fluorescence microscopy assesses protein levels, which result from a combination of translation efficiency and protein stability, combined with mRNA stability and expression from the endogenous gene. The results acquired in luciferase assays might be due to MAML1 promoting promoter activation, but at the same time MAML1 might be increasing the turnover of the endogenous mRNA, which would result in lower MITF protein levels. Alternatively, MAML1 could also regulate translation directly or induce degradation of the MITF protein. Additionally, when assessing the activity of the *MITF* promoter in the luciferase plasmid, key regulatory elements present in the genomic DNA, such as binding sites for enhancers and repressors present within introns or located outside the short piece of promoter DNA used in these assays, are lacking in the luciferase construct. These might influence the expression of the endogenous *MITF* gene in a way not observed using the luciferase reporters.

Ectopic expression of MAML1 also decreased β-catenin protein levels in 501mel cells. However, in contrast to the immunofluorescence results, depletion of MAML1 by siRNAs decreased β-catenin and MITF protein levels, supporting results obtained using the luciferase system. siRNA-mediated depletion of β-catenin in 501mel cells had no

effect on MAML1 levels and only slightly decreased MITF protein levels, suggesting that there is no feedback from β-catenin to MAML1.

Alternatively, it is also possible that, similarly to MITF, MAML1 might also be acting as a rheostat. Low and high MAML1 levels decrease MITF and β-catenin protein expression, as demonstrated in siRNA experiments (Figure 5.17) and transfection experiments with subsequent staining of MITF and β-catenin (Figure 5.12-5.15). Medium levels, on the other hand, activate *Brn2* and *MITF* promoter activity (Figure 5.5). To verify this model, its robustness needs to be explained by staining for Brn2 expression and repeating these experiments in other cell lines.

Additionally, it is also important to consider that luciferase assays were conducted with *Brn2* and *MITF* promoters which will lack some regulatory elements that might be present in the genome. Therefore, staining of MITF and β-catenin after transfections with a MAML1 expression plasmid, followed by fluorescence microscopy, and siRNA depletion experiments might reflect the endogenous responses of the proteins more accurately.

5.2.2 MAML1 and cancer

Previously, the specific Notch pathway co-activator MAML1 was shown to interact with β-catenin in a Notch-independent way and induce cyclin D1 and c-Myc expression through binding to TCF/LEF1 binding sites in both promoters (Alves-Guerra et al., 2007). This is consistent with our findings in 501mel and SKmel28 cells, suggesting a role for MAML1- and β-catenin-induced *Brn2* promoter activation via TCF/LEF1 binding, implying a role for Wnt signalling. This is a novel finding concerning the regulation of *Brn2* promoter activity by a co-activator that has not yet been reported to affect its activity.

In melanoma cells, depletion of MAML1 decreases the Notch effectors Hes-1 and Hey-1 and induces cell senescence, differentiation, and melanin production (Kang et al., 2013). As our results demonstrated that MAML1 can activate p*Brn2* and p*MITF*, it is possible that these transcription factors contribute to the observations in the study above.

Interestingly, depletion of MITF in melanoma cell lines led to upregulation of Brn2, as well as the Notch pathway components Notch1, *JAG2* and *DLL1* (Thurber et al., 2011). As the effect on MAML1 was not documented, it is possible that depletion of MITF induced an increase in MAML1 expression which subsequently affected *Brn2* promoter activity and protein levels, thereby mediating MITF-induced effects on Brn2. Interestingly, chromatin immunoprecipitation sequencing data in the laboratory (unpublished) indicates that MITF binds 2 kb upstream from the MAML1 transcription start site raising the possibility that MAML1 is an MITF-regulated gene.

However, the role of MAML1 might not be straightforward, as indicated by the rheostat model. Varying protein levels might induce different effects on *MITF* and *Brn2* promoter activity as well as protein expression. Additionally, the function of MAML1 might vary depending on cellular context. In support of this, Shen and colleagues (Shen et al., 2006) and Zhao and colleagues (Zhao et al., 2007), have shown that MAML1 acts as a co-activator in different pathways. For instance, MAML1 is involved in muscle development by acting as a co-activator for Myocyte-specific enhancer factor 2C (MEF2C) (Shen et al., 2006). Most importantly, activation of Notch blocks muscle differentiation, suggesting that MAML1 functions independently of the Notch pathway (Shen et al., 2006). MAML1 is also a p53 co-activator and is recruited to p53-response elements on the promoter of p53 target genes (Zhao et al., 2007). Furthermore, upon activation, MAML1 increases the half-life of p53 and its phosphorylation/acetylation

(Zhao et al., 2007). These findings imply that depending on the interplay of signalling pathways on the cell type and the cell environment (Shen et al., 2006; Zhao et al., 2007), MAML1 could induce the activation of different promoters.

5.2.3 Differential regulation of the Brn2 and MITF promoters

Interestingly, while MAML1 activated the *Brn2* promoter, on its own and in combination with β-catenin, it also induced *MITF* promoter activity. When this was investigated in more detail, we observed that the activation of the two promoters was mediated by different co-factors (TCF3 and LEF1, respectively).

In the neural crest, when β-catenin signalling is active, and despite the fact that both promoters, *MITF* and *Brn2*, contain Wnt-responsive elements, only the MITF protein is expressed. It seemed puzzling that under these circumstances only MITF is expressed, even though both promoters could respond to Wnt signalling. One explanation for this would be through the presence of miRs, such as miR-211 (Boyle et al., 2011), as *Brn2* mRNA was not detected at E11.5 (Goodall et al., 2004a). However, our results demonstrate another possibility of differential regulation of both promoters containing the same Wnt-responsive elements. The two transcription factors TCF3 and LEF1 regulate the *Brn2* and *MITF* promoters, respectively, and therefore it is conceivable that the balance of these transcription factors might determine which promoter is activated. Similarly, the Hoek laboratory demonstrated that LEF1 is expressed in differentiated/proliferating cells, while TCF4 is expressed in de-differentiated/invasive cells (Eichhoff et al., 2011). Furthermore, LEF1 expression correlates with MITF protein expression, as does TCF4 protein with Wnt-5a expression, a Wnt pathway antagonist (Eichhoff et al., 2011). Additionally, LEF1 suppresses TCF4 and Wnt-5a expression, implying that cells assume either a differentiated/proliferative or a de-

differentiated/invasive phenotype (Eichhoff et al., 2011), confirming observations *in vivo* by the Sturm laboratory (Thurber et al., 2011).

5.2.4 Future work

In this part of the thesis we have demonstrated how MAML1, a co-activator implicated in the Notch pathway, can potentially act independently from that pathway, alone or in combination with β-catenin, to activate the *Brn2* and *MITF* promoters. However, to elucidate the precise mechanism of action of MAML1, it is imperative to firstly investigate whether MAML1 binds directly to the DNA and associates with other co-activators, such as LEF1 and TCF3. Secondly, it is important to investigate the functional implications of MAML1 expression on the invasive potential of cells. If MAML1 activates the *Brn2* promoter it might contribute to the de-differentiated and invasive phenotype, demonstrated by Pinner and colleagues (Pinner et al., 2009), in which case it might form a target for potential therapeutics to decrease the potential of melanoma cells to metastasise. This could be investigated *in vitro* using matrigel assays and *in vivo* using MAML1-depleted human melanoma cell lines, similar to MAML1 depletion experiments in B16F10 (Kang et al., 2013).

If demonstrated that MAML1 does have an effect on invasiveness and metastasis formation in human melanoma cells, it would be interesting to investigate if the MAML1-induced activation of p*Brn2* is mediated through **a)** the Notch pathway; **b)** a different pathway, as demonstrated by Shen and colleagues (Shen et al., 2006) and Zhao and colleagues (Zhao et al., 2007) or **c)** independently. If the former is the case, the effect of γ-secretase inhibitors could be evaluated on metastasis formation as these would interfere with Notch pathway activation. Previously, treatment with the γ-secretase inhibitor RO4929097 reduced proliferation of melanoma cell lines *in vitro* and

in vivo and decreased their tumour forming abilities in soft agar (Huynh et al., 2011). Additionally, once tumour formation was established, administration of RO4929097 led to tumour regression (Huynh et al., 2011). Subsequently, serial dilution experiments showed decreased tumour forming capability of tumour cells from mice that had been treated with RO4929097, compared to vehicle-treated tumour cells (Huynh et al., 2011). Furthermore, a Phase I study using RO4929097 in patients with advanced solid malignancies, including melanoma, showed preliminary evidence of anti-tumour activity, although this will need to be verified in further studies (Tolcher et al., 2012). However, it is also conceivable that the Notch pathway might not be mediating *Brn2* promoter activation by MAML1, in which case γ-secretase inhibitors might not be able to prevent *Brn2* promoter activation. Instead, specific MAML1 inhibitors could be used that would not interact with the Notch pathway. One such inhibitor is a fusion protein consisting of the Drosophila transcription factor Antennapedia and a dominant-negative form of MAML (Epenetos, 2009). This protein inhibits Notch activation by being internalised and transported to the nucleus (Epenetos, 2009).

In summary, while MAML1- and β-catenin-induced activation of the *Brn2* and *MITF* promoters are intriguing findings, it is necessary to demonstrate if this has implications for the behaviour of melanoma cells and if this pathway can be exploited for therapeutic targeting.

6 Discussion

6.1 Summary

In this project we aimed to gain insights into the mechanisms underlying phenotype-switching in melanoma cells, using lentivirally-generated reporter cell lines, by measuring the interconversion of GFP- to mCherry-expressing cells and vice versa. Additionally, we investigated pathways in melanoma that might be involved in metastasis formation and invasion of melanoma cells. *In vitro*, we screened a kinase inhibitor library and observed that the RhoA/ROCK pathway plays a role in *Brn2* promoter activity, a result validated in subsequent experiments. A second pathway involving the co-activator MAML1 and the protein β-catenin was also demonstrated to play a role in *Brn2* and *MITF* promoter activation.

6.2 Key findings

6.2.1 Chapter 3: Generation and testing of fluorescent lentiviral reporter constructs

- Dual reporter plasmids responded to changes in the microenvironment by expressing mCherry and GFP under the control of the *Brn2* and *MITF* promoters, respectively.
- Crude preparations of 501mel cells transduced with the p*Brn2*/p*MITF* dual reporter lentivirus showed that some cells were positive for mCherry (p*MITF)* only, some positive for GFP (p*Brn2*) only and some were dual positive.
- After FACS sorting, polyclonal $mCherry^{+}GFP^{-}$ cells produced GFP^{+} cells upon proliferation, whereas $GFP^{+}mCherry^{-}$ cells produced only GFP^{+} cells. Both cell populations also produced cells that were negative for both fluorescent signals. Monoclonal cell lines did not show clear signs of interconversion *in vitro*.

- Monoclonal cells transplanted *in vivo* maintained their fluorescence and some cells also expressed the "opposite" fluorescent protein to the one they expressed originally.
- Screening of a kinase inhibitor library identified several factors influencing the *Brn2* promoter, including the RhoA/ROCK pathway.

6.2.2 Chapter 4: RhoA/ROCK pathway affects pBrn2 and pMITF activities

- In 501mel cells, RhoA increased and ROCK decreased *Brn2* promoter activity, while in SKmel28 cells both compounds activated the promoter.
- In 501mel cells, RhoA and ROCK both decreased *MITF* promoter activity, while in SKmel28 cells ROCK had no effect and RhoA activated the *MITF* promoter.
- β-catenin is differentially expressed in 501mel and SKmel28 cells. In 501mel cells it is nuclear and cytoplasmic, while in SKmel28 cells it is located at the cell membrane.
- ROCK inhibition led to an increase in Brn2 protein expression in 501mel cells.

6.2.3 Chapter 5: Differential regulation of pBrn2 and pMITF by MAML1

- MAML1 activated the *Brn2* promoter in 501mel and SKmel28 cells and this effect was potentiated by β-catenin.
- MAML1- and β-catenin-induced *Brn2* promoter activation is mediated by the TCF/LEF1 binding site on the promoter.
- TCF3 mediates MAML1- and β-catenin-induced *Brn2* promoter activation, while LEF1 mediates MAML1- and β-catenin-induced *MITF* promoter activation.

- Overexpression of MAML1 decreased MITF and β-catenin protein levels.

6.3 Implications for melanoma biology

6.3.1 Implications of phenotype-switching for treatment of melanoma

The demonstration that phenotype-switching takes place in melanoma cells alters our perception of melanoma (heterogeneity) and its treatment. If treatment failure in melanoma, in addition to genetic resistance, is also due to cells having the capacity to change their phenotype, eradication of these cells would have to be accommodated into future treatment approaches.

Whether these drug-resistant cells are melanoma stem cells, tumour- or metastasis-initiating cells, is still a matter of debate. Nonetheless, it is crucial that these cells are also targeted alongside the bulk of the tumour. So far, the only possible intervention against melanoma stem cells trialled on patients is rituximab, a monoclonal antibody targeting CD20 (Pinc et al., 2012; Schlaak et al., 2012), a potential melanoma stem cell marker (Fang et al., 2005). The administration of rituximab directly into the lesion of a patient with chemotherapy-refractory metastatic melanoma produced lasting remission (Schlaak et al., 2012). The second pilot trial involving nine patients with stage IV metastatic melanoma, previously treated and rendered apparently disease-free, reported that at the time of publishing six patients were alive and five were recurrence-free (Pinc et al., 2012). Another application of monoclonal antibodies was the targeting of the ABCB5 efflux pump, which has been postulated to mark a pool of potential cancer stem cells (Frank et al., 2005; Schatton et al., 2008). Treatment with monoclonal antibodies induced cell-mediated cytotoxicity in ABCB5-expressing melanoma stem cells (Schatton et al., 2008) and increased cell sensitivity to the antibiotic doxorubicin (Frank et al., 2005). Similarly, targeting of the efflux drug ABCB8 in melanoma with short

hairpin RNAs also reduced doxorubicin resistance in these cells (Elliott and Al-Hajj, 2009).

Another route to target CSCs directly is differentiation therapy (Murphy et al., 2014). This approach has been demonstrated in glioblastoma, where upon administration of bone morphogenic protein 4, tumour growth was inhibited (Piccirillo and Vescovi, 2006). It is conceivable that if melanoma stem cells exist and exhibit characteristics of physiological stem cells, inducing them to be more resistant against therapy, differentiation of these cells might render them susceptible to conventional therapy. One way of achieving this might be by targeting the embryonic morphogen Nodal (Topczewska et al., 2006). Nodal is expressed in human metastatic tumours and its inhibition leads to a decrease in melanoma invasiveness and colony formation *in vitro* and a decrease in tumour growth and tumour size *in vivo* (Topczewska et al., 2006). More importantly, Nodal inhibition also induced a melanocytic phenotype of melanoma cells (Topczewska et al., 2006).

However, the limitation of the above-mentioned approaches is the possibility of a non-static population of melanoma/cancer stem cells. If these cells contain the ability to undergo phenotype-switching they might be able to evade anti-stem cell drug treatment. A solution to address the problem of phenotype-switching has been suggested by Saez-Ayala and colleagues, who have exploited the rheostat model for MITF to devise a treatment that drives expression of MITF to sensitise cells to treatment with a second drug (Saez-Ayala et al., 2013). After a screen for drugs that increase MITF levels in melanoma cells the differentiating agent methotrexate was identified (Saez-Ayala et al., 2013). Treatment with this drug elevates MITF-dependent tyrosinase gene expression. Subsequent administration of a prodrug, activated by tyrosinase, inhibits the enzyme dihydrofolate reductase thereby decreasing thymidine pools, as well as inducing DNA

double-strand breaks and apoptosis *in vitro* and *in vivo*. Increasing MITF levels therefore eradicates invasive and possibly MITF^{negative} stem cells (Saez-Ayala et al., 2013). The advantage of this two-step treatment is that it works regardless of *BRAF*, *MEK* or *p53* expression in the melanoma cells (Saez-Ayala et al., 2013).

To summarise, one of the main aims of melanoma therapy is to discover a treatment that can address the heterogeneous character of melanoma, both genetic and phenotypic. Due to this, the properties of the cells within the tumour can vary and one treatment alone might not be able to target all these populations. However, by combining treatments such as BRAF inhibition with differentiation therapy or with directed phenotype-switching, it might be possible to advance one step closer to fully eradicating the tumour.

6.3.2 Implications of the roles of MITF and Brn2 in invasion and metastasis

As RhoA and ROCK are known regulators of the cytoskeleton (Sahai and Marshall, 2002), it has been posited that the RhoA/ROCK signalling pathway affects metastasis and invasion in melanoma cells.

As Brn2 is increased and MITF is decreased in invasive cells (Pinner et al., 2009; Thurber et al., 2011), we hypothesised that there might be a link between RhoA/ROCK signalling and Brn2 expression, which could explain the invasive potential of Brn2^{+} cells. In this project we have shown that RhoA consistently increased *Brn2* promoter activity in 501mel and SKmel28 cells. Whether the effects are mediated by ROCK, will need to be further investigated, as in 501mel cells p*Brn2* activity decreased upon transfections with ROCK1 expression plasmids, while in SKmel28 cells it had the opposite effect. This demonstrated that the effects of the RhoA/ROCK pathway might be cell line-specific. Interestingly, in 501mel cells, alongside increasing p*Brn2* activity,

RhoA also decreased p*MITF* activity, which strengthens the link between RhoA and invasiveness, since decreased levels of MITF are a hallmark of invasive melanoma cells. However, the effects on p*MITF* activity were also cell-line specific as RhoA and ROCK differentially regulated this promoter in 501mel and SKmel28 cells. Nonetheless, these results demonstrate how the induction of RhoA-induced invasiveness could be mediated by increased *Brn2* promoter activity alongside decreased *MITF* promoter activity.

Another mechanism that could contribute to metastasis generation is the activation of the *Brn2* promoter by the co-activator MAML1, which has previously mainly been demonstrated to act within the Notch pathway (Wu et al., 2000). However, it can also act independently and interact with MEF2C, to contribute to muscle development (Shen et al., 2006) as well as interact with p53 (Zhao et al., 2007). In our experimental settings, MAML1-mediated p*Brn2* activation was potentiated by β-catenin. This was particularly interesting as the expression of β-catenin was strikingly different between 501mel and SKmel28 cells. Interestingly, while the interaction of MAML1 and β-catenin was demonstrated previously (Alves-Guerra et al., 2007), this link has not been made in the melanocyte lineage.

While our experiments might suggest that MAML1 acts independently of the Notch pathway to interact with β-catenin and activate the *Brn2* and *MITF* promoters, there is a possibility that the Notch pathway (through MAML1) and the Wnt pathway (through β-catenin) interact to induce promoter activation.

Furthermore, in our experimental settings MAML1 also activated the *MITF* promoter. At first it seems counterintuitive that MAML1 would induce the transcription of Brn2 and MITF, upon which Brn2 would repress MITF expression. However, this also seems

to be the case for Sox10-induced p*Brn2* and p*MITF* activation (Figure 6.1A). Although in physiological circumstances it is possible that simultaneous expression of MITF and Brn2 would lead to a transient increase in MITF, as Brn2 will repress MITF expression. Upon activation of another pathway that can inhibit Brn2 (X or Y), however, the inhibition on MITF is released and its expression is sustained (Figure 6.1).

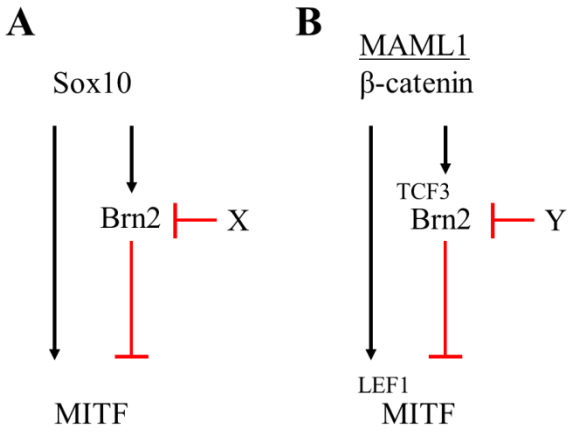


Figure 6.1: Diagram of a possible regulation of MITF and Brn2 protein expression by Sox10, MAML1 and β-catenin. Sox10 activates the expression of both Brn2 and MITF (**A**). Brn2 represses MITF expression, inducing a transient increase of MITF. Upon activation of a different pathway (X) that inhibits Brn2 activity, MITF expression is sustained. Similarly, β-catenin and potentially MAML1 can increase Brn2 and MITF expression (**B**), mediated by the transcription factors TCF3 and LEF1, respectively. This induces a transient increase in MITF protein. However, upon activation of a different pathway (Y), which inhibits Brn2, MITF expression can be sustained.

In line with this, MAML1 and β-catenin could be inducing the expression of Brn2 and MITF simultaneously, through TCF3 and LEF1, respectively, inducing a short-term, transient increase in MITF, until a second pathway (Y) could release the inhibition on MITF and allow sustained expression (Figure 6.1B).

The involvement of the RhoA/ROCK pathway and the MAML1- and β-catenin-mediated regulation of the *Brn2* and *MITF* promoters, opens up new avenues to pursue to elucidate the mechanisms involved in the generation of metastases and invasion.

6.4 Limitations of this project

The successful application of fluorescent reporter lentiviral systems has been demonstrated in prostate cancer where cell differentiation from a basal to a luminal

phenotype was observed (Frame et al., 2010). Nonetheless, it was also observed that silencing of certain promoters, such as the promoter for cytomegalovirus (CMV), takes place in these systems (Frame et al., 2010). Therefore, the advantages of using reporter lentiviral systems, such as the one used in this project, are very clear: They allow tracking of changes in gene expression over time, *in vitro* and *in vivo*, to investigate cell processes such as differentiation.

However, there are also some limitations with using lentiviral systems. The idea of using integration-competent viruses is useful in that it generates permanent expression of the genes of interest. However, due to the inability to influence the genomic locus the DNA will be inserted into, problems with promoter responsiveness or activity could arise.

Additionally, despite having used a full-length *Brn2* promoter, characterised and shown to be responsive *in vitro* (Goodall et al., 2004b), *in vivo* in its genomic locus the full responsiveness of the gene to microenvironmental changes is likely to require regulatory elements located further upstream or downstream of the promoter regions used here. This level of regulation would have not been present in reporters used to generate the cell lines and therefore the reporter cell lines are unlikely to respond to microenvironmental changes *in vivo* in the same way as endogenous promoters. Similar concerns arise from the use of the 2.3 kb *MITF* promoter.

Furthermore, in the dual lentivirus containing both the *Brn2* and *MITF* promoters, despite the built-in transcription block between the *Brn2* and the *MITF* promoters that was designed to prevent transcriptional read-through, it is still possible that the *MITF* promoter, located downstream of the *Brn2* promoter, would be co-activated together with the latter or that the presence of one promoter would influence the activity of the other.

To circumvent the problem of dual expression, it would have been possible to use two separate reporter viruses, either used separately or both transduced into the same cells, although this approach would also be accompanied with its own limitations. For instance, if cells are consecutively transduced with both viruses it would be difficult to ensure that the cells have the same amount of insertions of both promoter-fluorescent protein constructs, and therefore the interpretation of changes in fluorescence becomes more difficult.

The main limitations regarding the effect of the RhoA/ROCK and MAML1/β-catenin pathways on the *Brn2* and *MITF* promoter activities, stem from the nature of the luciferase assays. Due to time constraints, it was not possible to assess whether in the experiments in which two expression plasmids were co-transfected together with the p*Brn2*- or p*MITF*-Luc plasmids both proteins were expressed. It is conceivable that the expression of one protein might have affected the expression of the second. Further controls, including western blotting of the extracts used for the luciferase assays, will be used to verify that the potential regulators of the promoter-luciferase reporters are expressed as expected.

6.5 Future work

The problem of the size limitations that can be incorporated into the lentiviral backbone can be overcome by using a system that allows the delivery of larger genomic fragments of DNA, such as the PiggyBac transposon system (Zhao et al., 2014), consisting of a bacterial artificial chromosome. This would allow delivery of a larger fragment, encompassing more of the promoter region to ensure better physiological regulation. However, it might still be difficult to estimate the exact length of the DNA

needed to ensure full responsiveness, and the inclusion of intronic or 3' regulatory elements would still not be possible.

Another approach that has recently been used for gene editing is the clustered regularly interspaced short palindromic repeats (CRISPRs) system (Xue et al., 2014). Using this technique it is possible to integrate DNA fragments (delivered as RNA) into specific loci in the cell genome. This would allow insertion of the DNA encoding fluorescent proteins directly downstream of the endogenous promoter. This way, the endogenous promoter function should not be disrupted and fluorescent protein expression would monitor endogenous promoter activity more accurately.

To address the question of equal protein expression in luciferase experiments involving co-transfections, SDS-PAGE and western blotting would need to be conducted to ensure that both factors are expressed to equal amounts. Additionally, in order to uncover the mechanism of action of RhoA, ROCK and MAML1, it would be interesting to conduct biochemical analyses, such as co-immunoprecipitation experiments to study protein-protein interactions and to assess whether these factors act directly on the promoters or whether other cofactors are involved, as might be the case for MAML1 and β-catenin.

Finally, to advance the project and investigate if the RhoA/ROCK and MAML1/β-catenin pathway activation affects invasion and metastasis, functional assays will need to be conducted. These assays might involve matrigel invasion assays *in vitro* or *in vivo* transplantation of cells that were previously depleted of MAML1, RhoA or ROCK.

6.6 Conclusion

This project allowed the investigation of potentially new pathways that might (at least partly) explain the nature of invasive cells in melanoma or potentially melanoma stem cells. Further research will advance our understanding of these signalling pathways in melanoma and provide novel therapeutic targets.

7 References

Abe, H., T. Kamai, T. Tsujii, F. Nakamura, T. Mashidori, T. Mizuno, M. Tanaka, K. Tatsumiya, N. Furuya, A. Masuda, T. Yamanishi, and K. Yoshida. 2008. Possible role of the RhoC/ROCK pathway in progression of clear cell renal cell carcinoma. *Biomed Res*. 29:155-61.

Al-Hajj, M., M.S. Wicha, A. Benito-Hernandez, S.J. Morrison, and M.F. Clarke. 2003. Prospective identification of tumorigenic breast cancer cells. *Proc Natl Acad Sci U S A*. 100:3983-8.

Al Dhaybi, R., H. Sartelet, J. Powell, and V. Kokta. 2010. Expression of CD133+ cancer stem cells in childhood malignant melanoma and its correlation with metastasis. *Mod Pathol*. 23:376-80.

Alves-Guerra, M.C., C. Ronchini, and A.J. Capobianco. 2007. Mastermind-like 1 Is a specific coactivator of beta-catenin transcription activation and is essential for colon carcinoma cell survival. *Cancer Res*. 67:8690-8.

Amano, M., Y. Fukata, and K. Kaibuchi. 2000. Regulation and functions of Rho-associated kinase. *Exp Cell Res*. 261:44-51.

Andreopoulou, E., I.S. Vigoda, V. Valero, D.L. Hershman, G. Raptis, L.T. Vahdat, H.S. Han, J.J. Wright, C.M. Pellegrino, M. Cristofanilli, R.H. Alvarez, K. Fehn, S. Fineberg, and J.A. Sparano. 2013. Phase I-II study of the farnesyl transferase inhibitor tipifarnib plus sequential weekly paclitaxel and doxorubicin-cyclophosphamide in HER2/neu-negative inflammatory carcinoma and non-inflammatory estrogen receptor-positive breast carcinoma. *Breast Cancer Res Treat*. 141:429-35.

Arozarena, I., H. Bischof, D. Gilby, B. Belloni, R. Dummer, and C. Wellbrock. 2011. In melanoma, beta-catenin is a suppressor of invasion. *Oncogene*. 30:4531-43.

Bakos, R.M., T. Maier, R. Besch, D.S. Mestel, T. Ruzicka, R.A. Sturm, and C. Berking. 2010. Nestin and SOX9 and SOX10 transcription factors are coexpressed in melanoma. *Exp Dermatol*. 19:e89-94.

Balch, C.M., J.E. Gershenwald, S.J. Soong, J.F. Thompson, M.B. Atkins, D.R. Byrd, A.C. Buzaid, A.J. Cochran, D.G. Coit, S. Ding, A.M. Eggermont, K.T. Flaherty, P.A. Gimotty, J.M. Kirkwood, K.M. McMasters, M.C. Mihm, Jr., D.L. Morton, M.I. Ross, A.J. Sober, and V.K. Sondak. 2009. Final version of 2009 AJCC melanoma staging and classification. *J Clin Oncol*. 27:6199-206.

Balint, K., M. Xiao, C.C. Pinnix, A. Soma, I. Veres, I. Juhasz, E.J. Brown, A.J. Capobianco, M. Herlyn, and Z.J. Liu. 2005. Activation of Notch1 signaling is required for beta-catenin-mediated human primary melanoma progression. *J Clin Invest*. 115:3166-76.

Baltimore, D. 1974. The strategy of RNA viruses. *Harvey Lect*. 70 Series:57-74.

Barker, N., and H. Clevers. 2006. Mining the Wnt pathway for cancer therapeutics. *Nat Rev Drug Discov*. 5:997-1014.

Bartel, D.P. 2009. MicroRNAs: target recognition and regulatory functions. *Cell*. 136:215-33.

Bedogni, B., J.A. Warneke, B.J. Nickoloff, A.J. Giaccia, and M.B. Powell. 2008. Notch1 is an effector of Akt and hypoxia in melanoma development. *J Clin Invest*. 118:3660-70.

Bejar, J., Y. Hong, and M. Schartl. 2003. Mitf expression is sufficient to direct differentiation of medaka blastula derived stem cells to melanocytes. *Development*. 130:6545-53.

Bell, R.E., and C. Levy. 2011. The three M's: melanoma, microphthalmia-associated transcription factor and microRNA. *Pigment Cell Melanoma Res*. 24:1088-106.

Bemis, L.T., R. Chen, C.M. Amato, E.H. Classen, S.E. Robinson, D.G. Coffey, P.F. Erickson, Y.G. Shellman, and W.A. Robinson. 2008. MicroRNA-137 targets microphthalmia-associated transcription factor in melanoma cell lines. *Cancer Res*. 68:1362-8.

Bennett, D.C. 2008. Ultraviolet wavebands and melanoma initiation. *Pigment Cell Melanoma Res*. 21:520-4.

Bentley, N.J., T. Eisen, and C.R. Goding. 1994. Melanocyte-specific expression of the human tyrosinase promoter: activation by the microphthalmia gene product and role of the initiator. *Mol Cell Biol*. 14:7996-8006.

Bertolotto, C. 2013. Melanoma: from melanocyte to genetic alterations and clinical options. *Scientifica (Cairo)*. 2013:635203.

Bertolotto, C., P. Abbe, T.J. Hemesath, K. Bille, D.E. Fisher, J.P. Ortonne, and R. Ballotti. 1998. Microphthalmia gene product as a signal transducer in cAMP-induced differentiation of melanocytes. *J Cell Biol*. 142:827-35.

Bertolotto, C., K. Bille, J.P. Ortonne, and R. Ballotti. 1996. Regulation of tyrosinase gene expression by cAMP in B16 melanoma cells involves two CATGTG motifs surrounding the TATA box: implication of the microphthalmia gene product. *J Cell Biol*. 134:747-55.

Bertolotto, C., F. Lesueur, S. Giuliano, T. Strub, M. de Lichy, K. Bille, P. Dessen, B. d'Hayer, H. Mohamdi, A. Remenieras, E. Maubec, A. de la Fouchardiere, V. Molinie, P. Vabres, S. Dalle, N. Poulalhon, T. Martin-Denavit, L. Thomas, P. Andry-Benzaquen, N. Dupin, F. Boitier, A. Rossi, J.L. Perrot, B. Labeille, C. Robert, B. Escudier, O. Caron, L. Brugieres, S. Saule, B. Gardie, S. Gad, S. Richard, J. Couturier, B.T. Teh, P. Ghiorzo, L. Pastorino, S. Puig, C. Badenas, H. Olsson, C. Ingvar, E. Rouleau, R. Lidereau, P. Bahadoran, P. Vielh, E. Corda, H. Blanche, D. Zelenika, P. Galan, G. French Familial Melanoma Study, F. Aubin, B. Bachollet, C. Becuwe, P. Berthet, Y.J. Bignon, V. Bonadona, J.L. Bonafe, M.N. Bonnet-Dupeyron, F. Cambazard, J. Chevrant-Breton, I. Coupier, S. Dalac, L. Demange, M. d'Incan, C. Dugast, L. Faivre, L. Vincent-Fetita, M. Gauthier-Villars, B. Gilbert, F. Grange, J.J. Grob, P. Humbert, N. Janin, P. Joly, D. Kerob, C. Lasset, D. Leroux, J. Levang, J.M. Limacher, C. Livideanu, M. Longy, A. Lortholary, D. Stoppa-Lyonnet, S. Mansard, L. Mansuy, K. Marrou, C. Mateus, C. Maugard, N. Meyer, C. Nogues, P. Souteyrand, L. Venat-Bouvet, H. Zattara, V. Chaudru, G.M. Lenoir, M. Lathrop, I. Davidson, M.F. Avril, F. Demenais, R. Ballotti, and B. Bressac-de Paillerets. 2011. A SUMOylation-defective MITF germline mutation predisposes to melanoma and renal carcinoma. *Nature*. 480:94-8.

Bogenrieder, T., and M. Herlyn. 2002. Cell-surface proteolysis, growth factor activation and intercellular communication in the progression of melanoma. *Crit Rev Oncol Hematol*. 44:1-15.

Bohm, M., G. Moellmann, E. Cheng, M. Alvarez-Franco, S. Wagner, P. Sassone-Corsi, and R. Halaban. 1995. Identification of p90RSK as the probable CREB-Ser133 kinase in human melanocytes. *Cell Growth Differ*. 6:291-302.

Boiko, A.D., O.V. Razorenova, M. van de Rijn, S.M. Swetter, D.L. Johnson, D.P. Ly, P.D. Butler, G.P. Yang, B. Joshua, M.J. Kaplan, M.T. Longaker, and I.L. Weissman. 2010. Human melanoma-initiating cells express neural crest nerve growth factor receptor CD271. *Nature*. 466:133-7.

Bonnet, D., and J.E. Dick. 1997. Human acute myeloid leukemia is organized as a hierarchy that originates from a primitive hematopoietic cell. *Nat Med*. 3:730-7.

Bonvin, E., P. Falletta, H. Shaw, V. Delmas, and C.R. Goding. 2012. A phosphatidylinositol 3-kinase-Pax3 axis regulates Brn-2 expression in melanoma. *Mol Cell Biol*. 32:4674-83.

Boyle, G.M., S.L. Woods, V.F. Bonazzi, M.S. Stark, E. Hacker, L.G. Aoude, K. Dutton-Regester, A.L. Cook, R.A. Sturm, and N.K. Hayward. 2011. Melanoma cell invasiveness is regulated by miR-211 suppression of the BRN2 transcription factor. *Pigment Cell Melanoma Res*. 24:525-37.

Brambrink, T., R. Foreman, G.G. Welstead, C.J. Lengner, M. Wernig, H. Suh, and R. Jaenisch. 2008. Sequential expression of pluripotency markers during direct reprogramming of mouse somatic cells. *Cell Stem Cell*. 2:151-9.

Britsch, S., D.E. Goerich, D. Riethmacher, R.I. Peirano, M. Rossner, K.A. Nave, C. Birchmeier, and M. Wegner. 2001. The transcription factor Sox10 is a key regulator of peripheral glial development. *Genes Dev*. 15:66-78.

Brou, C., F. Logeat, N. Gupta, C. Bessia, O. LeBail, J.R. Doedens, A. Cumano, P. Roux, R.A. Black, and A. Israel. 2000. A novel proteolytic cleavage involved in Notch signaling: the role of the disintegrin-metalloprotease TACE. *Mol Cell*. 5:207-16.

Caramuta, S., S. Egyhazi, M. Rodolfo, D. Witten, J. Hansson, C. Larsson, and W.O. Lui. 2010. MicroRNA expression profiles associated with mutational status and survival in malignant melanoma. *J Invest Dermatol*. 130:2062-70.

Carreira, S., J. Goodall, I. Aksan, S.A. La Rocca, M.D. Galibert, L. Denat, L. Larue, and C.R. Goding. 2005. Mitf cooperates with Rb1 and activates p21Cip1 expression to regulate cell cycle progression. *Nature*. 433:764-9.

Carreira, S., J. Goodall, L. Denat, M. Rodriguez, P. Nuciforo, K.S. Hoek, A. Testori, L. Larue, and C.R. Goding. 2006. Mitf regulation of Dia1 controls melanoma proliferation and invasiveness. *Genes Dev*. 20:3426-39.

Carreira, S., B. Liu, and C.R. Goding. 2000. The gene encoding the T-box factor Tbx2 is a target for the microphthalmia-associated transcription factor in melanocytes. *J Biol Chem*. 275:21920-7.

Cheli, Y., S. Giuliano, T. Botton, S. Rocchi, V. Hofman, P. Hofman, P. Bahadoran, C. Bertolotto, and R. Ballotti. 2011. Mitf is the key molecular switch between mouse or human melanoma initiating cells and their differentiated progeny. *Oncogene*. 30:2307-18.

Cheli, Y., M. Ohanna, R. Ballotti, and C. Bertolotto. 2010. Fifteen-year quest for microphthalmia-associated transcription factor target genes. *Pigment Cell Melanoma Res*. 23:27-40.

Chien, A.J., E.C. Moore, A.S. Lonsdorf, R.M. Kulikauskas, B.G. Rothberg, A.J. Berger, M.B. Major, S.T. Hwang, D.L. Rimm, and R.T. Moon. 2009. Activated Wnt/beta-catenin signaling in melanoma is associated with decreased proliferation in patient tumors and a murine melanoma model. *Proc Natl Acad Sci U S A*. 106:1193-8.

Civenni, G., A. Walter, N. Kobert, D. Mihic-Probst, M. Zipser, B. Belloni, B. Seifert, H. Moch, R. Dummer, M. van den Broek, and L. Sommer. 2011. Human CD271-positive melanoma stem cells associated with metastasis establish tumor heterogeneity and long-term growth. *Cancer Res*. 71:3098-109.

Clark, E.A., T.R. Golub, E.S. Lander, and R.O. Hynes. 2000. Genomic analysis of metastasis reveals an essential role for RhoC. *Nature*. 406:532-5.

Clark, W.H. 1991. Tumour progression and the nature of cancer. *Br J Cancer*. 64:631-44.

Clark, W.H., Jr., D.E. Elder, D.t. Guerry, L.E. Braitman, B.J. Trock, D. Schultz, M. Synnestvedt, and A.C. Halpern. 1989. Model predicting survival in stage I melanoma based on tumor progression. *J Natl Cancer Inst*. 81:1893-904.

Clark, W.H., Jr., D.E. Elder, D.t. Guerry, M.N. Epstein, M.H. Greene, and M. Van Horn. 1984. A study of tumor progression: the precursor lesions of superficial spreading and nodular melanoma. *Hum Pathol*. 15:1147-65.

Collisson, E.A., A. De, H. Suzuki, S.S. Gambhir, and M.S. Kolodney. 2003. Treatment of metastatic melanoma with an orally available inhibitor of the Ras-Raf-MAPK cascade. *Cancer Res*. 63:5669-73.

Cook, A.L., P.D. Donatien, A.G. Smith, M. Murphy, M.K. Jones, M. Herlyn, D.C. Bennett, J.H. Leonard, and R.A. Sturm. 2003. Human melanoblasts in culture: expression of BRN2 and synergistic regulation by fibroblast growth factor-2, stem cell factor, and endothelin-3. *J Invest Dermatol*. 121:1150-9.

Cook, A.L., A.G. Smith, D.J. Smit, J.H. Leonard, and R.A. Sturm. 2005. Co-expression of SOX9 and SOX10 during melanocytic differentiation in vitro. *Exp Cell Res*. 308:222-35.

Cook, A.L., and R.A. Sturm. 2008. POU domain transcription factors: BRN2 as a regulator of melanocytic growth and tumourigenesis. *Pigment Cell Melanoma Res*. 21:611-26.

Cox, P.M., S.M. Temperley, H. Kumar, and C.R. Goding. 1988. A distinct octamer-binding protein present in malignant melanoma cells. *Nucleic Acids Res*. 16:11047-56.

Cully, M., H. You, A.J. Levine, and T.W. Mak. 2006. Beyond PTEN mutations: the PI3K pathway as an integrator of multiple inputs during tumorigenesis. *Nat Rev Cancer*. 6:184-92.

Damsky, W.E., D.P. Curley, M. Santhanakrishnan, L.E. Rosenbaum, J.T. Platt, B.E. Gould Rothberg, M.M. Taketo, D. Dankort, D.L. Rimm, M. McMahon, and M. Bosenberg. 2011. beta-catenin signaling controls metastasis in Braf-activated Pten-deficient melanomas. *Cancer Cell*. 20:741-54.

Davies, H., G.R. Bignell, C. Cox, P. Stephens, S. Edkins, S. Clegg, J. Teague, H. Woffendin, M.J. Garnett, W. Bottomley, N. Davis, E. Dicks, R. Ewing, Y. Floyd, K. Gray, S. Hall, R. Hawes, J. Hughes, V. Kosmidou, A. Menzies, C. Mould, A. Parker, C. Stevens, S. Watt, S. Hooper, R. Wilson, H. Jayatilake, B.A. Gusterson, C. Cooper, J. Shipley, D. Hargrave, K. Pritchard-Jones, N. Maitland, G. Chenevix-Trench, G.J. Riggins, D.D. Bigner, G. Palmieri, A. Cossu, A. Flanagan, A. Nicholson, J.W. Ho, S.Y. Leung, S.T. Yuen, B.L. Weber, H.F. Seigler, T.L. Darrow, H. Paterson, R. Marais, C.J. Marshall, R. Wooster, M.R. Stratton, and P.A. Futreal. 2002. Mutations of the BRAF gene in human cancer. *Nature*. 417:949-54.

Davis, H.E., M. Rosinski, J.R. Morgan, and M.L. Yarmush. 2004. Charged polymers modulate retrovirus transduction via membrane charge neutralization and virus aggregation. *Biophys J*. 86:1234-42.

De Strooper, B., W. Annaert, P. Cupers, P. Saftig, K. Craessaerts, J.S. Mumm, E.H. Schroeter, V. Schrijvers, M.S. Wolfe, W.J. Ray, A. Goate, and R. Kopan. 1999. A presenilin-1-dependent gamma-secretase-like protease mediates release of Notch intracellular domain. *Nature*. 398:518-22.

del Peso, L., R. Hernandez-Alcoceba, N. Embade, A. Carnero, P. Esteve, C. Paje, and J.C. Lacal. 1997. Rho proteins induce metastatic properties in vivo. *Oncogene*. 15:3047-57.

Delmas, V., F. Beermann, S. Martinozzi, S. Carreira, J. Ackermann, M. Kumasaka, L. Denat, J. Goodall, F. Luciani, A. Viros, N. Demirkan, B.C. Bastian, C.R. Goding, and L. Larue. 2007. Beta-catenin induces immortalization of melanocytes by suppressing p16INK4a expression and cooperates with N-Ras in melanoma development. *Genes Dev*. 21:2923-35.

Deng, L., G. Li, R. Li, Q. Liu, Q. He, and J. Zhang. 2010. Rho-kinase inhibitor, fasudil, suppresses glioblastoma cell line progression in vitro and in vivo. *Cancer Biol Ther*. 9:875-84.

Dorsky, R.I., R.T. Moon, and D.W. Raible. 1998. Control of neural crest cell fate by the Wnt signalling pathway. *Nature*. 396:370-3.

Downward, J. 2008. Targeting RAS and PI3K in lung cancer. *Nat Med*. 14:1315-6.

Dropulic, B. 2011. Lentiviral vectors: their molecular design, safety, and use in laboratory and preclinical research. *Hum Gene Ther*. 22:649-57.

Du, J., A.J. Miller, H.R. Widlund, M.A. Horstmann, S. Ramaswamy, and D.E. Fisher. 2003. MLANA/MART1 and SILV/PMEL17/GP100 are transcriptionally regulated by MITF in melanocytes and melanoma. *Am J Pathol*. 163:333-43.

Du, J., H.R. Widlund, M.A. Horstmann, S. Ramaswamy, K. Ross, W.E. Huber, E.K. Nishimura, T.R. Golub, and D.E. Fisher. 2004. Critical role of CDK2 for melanoma growth linked to its melanocyte-specific transcriptional regulation by MITF. *Cancer Cell*. 6:565-76.

Dunn, K.J., B.O. Williams, Y. Li, and W.J. Pavan. 2000. Neural crest-directed gene transfer demonstrates Wnt1 role in melanocyte expansion and differentiation during mouse development. *Proc Natl Acad Sci U S A*. 97:10050-5.

Duquenne, C., C. Psomas, S. Gimenez, A. Guigues, M.J. Carles, C. Barbuat, J.P. Lavigne, A. Sotto, J. Reynes, P. Guglielmi, C. Mettling, V. Francois, and P. Corbeau. 2014. The Two Human CXCR4 Isoforms Display Different HIV Receptor Activities: Consequences for the Emergence of X4 Strains. *J Immunol*.

Eichhoff, O.M., A. Weeraratna, M.C. Zipser, L. Denat, D.S. Widmer, M. Xu, L. Kriegl, T. Kirchner, L. Larue, R. Dummer, and K.S. Hoek. 2011. Differential LEF1 and TCF4 expression is involved in melanoma cell phenotype switching. *Pigment Cell Melanoma Res*. 24:631-42.

Eisen, T., D.J. Easty, D.C. Bennett, and C.R. Goding. 1995. The POU domain transcription factor Brn-2: elevated expression in malignant melanoma and regulation of melanocyte-specific gene expression. *Oncogene*. 11:2157-64.

Ellerhorst, J.A., V.R. Greene, S. Ekmekcioglu, C.L. Warneke, M.M. Johnson, C.P. Cooke, L.E. Wang, V.G. Prieto, J.E. Gershenwald, Q. Wei, and E.A. Grimm. 2011. Clinical correlates of NRAS and BRAF mutations in primary human melanoma. *Clin Cancer Res*. 17:229-35.

Elliott, A.M., and M.A. Al-Hajj. 2009. ABCB8 mediates doxorubicin resistance in melanoma cells by protecting the mitochondrial genome. *Mol Cancer Res*. 7:79-87.

Ellisen, L.W., J. Bird, D.C. West, A.L. Soreng, T.C. Reynolds, S.D. Smith, and J. Sklar. 1991. TAN-1, the human homolog of the Drosophila notch gene, is broken by chromosomal translocations in T lymphoblastic neoplasms. *Cell*. 66:649-61.

Emi, N., T. Friedmann, and J.K. Yee. 1991. Pseudotype formation of murine leukemia virus with the G protein of vesicular stomatitis virus. *J Virol*. 65:1202-7.

Epenetos, A., Kousparou, C. & Stylianou, S. . 2009. Inhibition of Notch signaling for the treatment of human carcinomas. *In* American Association for Cancer Research, A5502

Espinosa, L., J. Ingles-Esteve, C. Aguilera, and A. Bigas. 2003. Phosphorylation by glycogen synthase kinase-3 beta down-regulates Notch activity, a link for Notch and Wnt pathways. *J Biol Chem*. 278:32227-35.

Esposito, D., and R. Craigie. 1999. HIV integrase structure and function. *Adv Virus Res*. 52:319-33.

Fang, D., T.K. Nguyen, K. Leishear, R. Finko, A.N. Kulp, S. Hotz, P.A. Van Belle, X. Xu, D.E. Elder, and M. Herlyn. 2005. A tumorigenic subpopulation with stem cell properties in melanomas. *Cancer Res*. 65:9328-37.

Feig, L.A. 1999. Tools of the trade: use of dominant-inhibitory mutants of Ras-family GTPases. *Nat Cell Biol*. 1:E25-7.

Flammiger, A., R. Besch, A.L. Cook, T. Maier, R.A. Sturm, and C. Berking. 2009. SOX9 and SOX10 but not BRN2 are required for nestin expression in human melanoma cells. *J Invest Dermatol*. 129:945-53.

Foltz, D.R., M.C. Santiago, B.E. Berechid, and J.S. Nye. 2002. Glycogen synthase kinase-3beta modulates notch signaling and stability. *Curr Biol*. 12:1006-11.

Frame, F.M., S. Hager, D. Pellacani, M.J. Stower, H.F. Walker, J.E. Burns, A.T. Collins, and N.J. Maitland. 2010. Development and limitations of lentivirus vectors as tools for tracking differentiation in prostate epithelial cells. *Exp Cell Res*. 316:3161-71.

Francken, A.B., N.A. Accortt, H.M. Shaw, M. Wiener, S.J. Soong, H.J. Hoekstra, and J.F. Thompson. 2008. Prognosis and determinants of outcome following locoregional or distant recurrence in patients with cutaneous melanoma. *Ann Surg Oncol*. 15:1476-84.

Frank, N.Y., A. Margaryan, Y. Huang, T. Schatton, A.M. Waaga-Gasser, M. Gasser, M.H. Sayegh, W. Sadee, and M.H. Frank. 2005. ABCB5-mediated doxorubicin transport and chemoresistance in human malignant melanoma. *Cancer Res*. 65:4320-33.

Fritz, G., I. Just, and B. Kaina. 1999. Rho GTPases are over-expressed in human tumors. *Int J Cancer*. 81:682-7.

Fukunaga-Kalabis, M., A. Roesch, and M. Herlyn. 2011. From cancer stem cells to tumor maintenance in melanoma. *J Invest Dermatol*. 131:1600-4.

Garraway, L.A., and W.R. Sellers. 2006. Lineage dependency and lineage-survival oncogenes in human cancer. *Nat Rev Cancer*. 6:593-602.

Garraway, L.A., B.A. Weir, X. Zhao, H. Widlund, R. Beroukhim, A. Berger, D. Rimm, M.A. Rubin, D.E. Fisher, M.L. Meyerson, and W.R. Sellers. 2005a. "Lineage addiction" in human cancer: lessons from integrated genomics. *Cold Spring Harb Symp Quant Biol*. 70:25-34.

Garraway, L.A., H.R. Widlund, M.A. Rubin, G. Getz, A.J. Berger, S. Ramaswamy, R. Beroukhim, D.A. Milner, S.R. Granter, J. Du, C. Lee, S.N. Wagner, C. Li, T.R. Golub, D.L. Rimm, M.L. Meyerson, D.E. Fisher, and W.R. Sellers. 2005b. Integrative genomic analyses identify MITF as a lineage survival oncogene amplified in malignant melanoma. *Nature*. 436:117-22.

Giuliano, S., Y. Cheli, M. Ohanna, C. Bonet, L. Beuret, K. Bille, A. Loubat, V. Hofman, P. Hofman, G. Ponzio, P. Bahadoran, R. Ballotti, and C. Bertolotto. 2010. Microphthalmia-associated transcription factor controls the DNA damage response and a lineage-specific senescence program in melanomas. *Cancer Res*. 70:3813-22.

Goding, C.R. 2011. Commentary. A picture of Mitf in melanoma immortality. *Oncogene*. 30:2304-6.

Goodall, J., S. Carreira, L. Denat, D. Kobi, I. Davidson, P. Nuciforo, R.A. Sturm, L. Larue, and C.R. Goding. 2008. Brn-2 represses microphthalmia-associated transcription factor expression and marks a distinct subpopulation of microphthalmia-associated transcription factor-negative melanoma cells. *Cancer Res*. 68:7788-94.

Goodall, J., S. Martinozzi, T.J. Dexter, D. Champeval, S. Carreira, L. Larue, and C.R. Goding. 2004a. Brn-2 expression controls melanoma proliferation and is directly regulated by beta-catenin. *Mol Cell Biol*. 24:2915-22.

Goodall, J., C. Wellbrock, T.J. Dexter, K. Roberts, R. Marais, and C.R. Goding. 2004b. The Brn-2 transcription factor links activated BRAF to melanoma proliferation. *Mol Cell Biol*. 24:2923-31.

Gorden, A., I. Osman, W. Gai, D. He, W. Huang, A. Davidson, A.N. Houghton, K. Busam, and D. Polsky. 2003. Analysis of BRAF and N-RAS mutations in metastatic melanoma tissues. *Cancer Res*. 63:3955-7.

Goswami, S., R.S. Tarapore, J.J. Teslaa, Y. Grinblat, V. Setaluri, and V.S. Spiegelman. 2010. MicroRNA-340-mediated degradation of microphthalmia-associated transcription factor mRNA is inhibited by the coding region determinant-binding protein. *J Biol Chem*. 285:20532-40.

Graf, S.A., C. Busch, A.K. Bosserhoff, R. Besch, and C. Berking. 2014. SOX10 promotes melanoma cell invasion by regulating melanoma inhibitory activity. *J Invest Dermatol*. 134:2212-20.

Gray-Schopfer, V., C. Wellbrock, and R. Marais. 2007. Melanoma biology and new targeted therapy. *Nature*. 445:851-7.

Greenhill, E.R., A. Rocco, L. Vibert, M. Nikaido, and R.N. Kelsh. 2011. An iterative genetic and dynamical modelling approach identifies novel features of the gene regulatory network underlying melanocyte development. *PLoS Genet*. 7:e1002265.

Guldberg, P., P. thor Straten, A. Birck, V. Ahrenkiel, A.F. Kirkin, and J. Zeuthen. 1997. Disruption of the MMAC1/PTEN gene by deletion or mutation is a frequent event in malignant melanoma. *Cancer Res*. 57:3660-3.

Guo, J., J.F. Zhang, W.M. Wang, F.W. Cheung, Y.F. Lu, C.F. Ng, H.F. Kung, and W.K. Liu. 2014. MicroRNA-218 inhibits melanogenesis by directly suppressing microphthalmia-associated transcription factor expression. *RNA Biol*. 11:732-41.

Haass, N.K., K.S. Smalley, and M. Herlyn. 2004. The role of altered cell-cell communication in melanoma progression. *J Mol Histol*. 35:309-18.

Hacein-Bey-Abina, S., A. Garrigue, G.P. Wang, J. Soulier, A. Lim, E. Morillon, E. Clappier, L. Caccavelli, E. Delabesse, K. Beldjord, V. Asnafi, E. MacIntyre, L. Dal Cortivo, I. Radford, N. Brousse, F. Sigaux, D. Moshous, J. Hauer, A. Borkhardt, B.H. Belohradsky, U. Wintergerst, M.C. Velez, L. Leiva, R. Sorensen, N. Wulffraat, S. Blanche, F.D. Bushman, A. Fischer, and M. Cavazzana-Calvo. 2008. Insertional oncogenesis in 4 patients after retrovirus-mediated gene therapy of SCID-X1. *J Clin Invest*. 118:3132-42.

Hacein-Bey-Abina, S., C. Von Kalle, M. Schmidt, M.P. McCormack, N. Wulffraat, P. Leboulch, A. Lim, C.S. Osborne, R. Pawliuk, E. Morillon, R. Sorensen, A. Forster, P. Fraser, J.I. Cohen, G. de Saint Basile, I. Alexander, U. Wintergerst, T. Frebourg, A. Aurias, D. Stoppa-Lyonnet, S. Romana, I. Radford-Weiss, F. Gross, F. Valensi, E. Delabesse, E. Macintyre, F. Sigaux, J. Soulier, L.E. Leiva,

M. Wissler, C. Prinz, T.H. Rabbitts, F. Le Deist, A. Fischer, and M. Cavazzana-Calvo. 2003. LMO2-associated clonal T cell proliferation in two patients after gene therapy for SCID-X1. *Science*. 302:415-9.

Hall, A. 2009. The cytoskeleton and cancer. *Cancer Metastasis Rev*. 28:5-14.

Hanahan, D., and R.A. Weinberg. 2011. Hallmarks of cancer: the next generation. *Cell*. 144:646-74.

Hemesath, T.J., E.R. Price, C. Takemoto, T. Badalian, and D.E. Fisher. 1998. MAP kinase links the transcription factor Microphthalmia to c-Kit signalling in melanocytes. *Nature*. 391:298-301.

Hodgkinson, C.A., K.J. Moore, A. Nakayama, E. Steingrimsson, N.G. Copeland, N.A. Jenkins, and H. Arnheiter. 1993. Mutations at the mouse microphthalmia locus are associated with defects in a gene encoding a novel basic-helix-loop-helix-zipper protein. *Cell*. 74:395-404.

Hoek, K.S., and C.R. Goding. 2010. Cancer stem cells versus phenotype-switching in melanoma. *Pigment Cell Melanoma Res*. 23:746-59.

Hornyak, T.J., D.J. Hayes, L.Y. Chiu, and E.B. Ziff. 2001. Transcription factors in melanocyte development: distinct roles for Pax-3 and Mitf. *Mech Dev*. 101:47-59.

Hughes, A.E., V.E. Newton, X.Z. Liu, and A.P. Read. 1994. A gene for Waardenburg syndrome type 2 maps close to the human homologue of the microphthalmia gene at chromosome 3p12-p14.1. *Nat Genet*. 7:509-12.

Hussussian, C.J., J.P. Struewing, A.M. Goldstein, P.A. Higgins, D.S. Ally, M.D. Sheahan, W.H. Clark, Jr., M.A. Tucker, and N.C. Dracopoli. 1994. Germline p16 mutations in familial melanoma. *Nat Genet*. 8:15-21.

Huynh, C., L. Poliseno, M.F. Segura, R. Medicherla, A. Haimovic, S. Menendez, S. Shang, A. Pavlick, Y. Shao, F. Darvishian, J.F. Boylan, I. Osman, and E. Hernando. 2011. The novel gamma secretase inhibitor RO4929097 reduces the tumor initiating potential of melanoma. *PLoS One*. 6:e25264.

Iso, T., L. Kedes, and Y. Hamamori. 2003. HES and HERP families: multiple effectors of the Notch signaling pathway. *J Cell Physiol*. 194:237-55.

Itoh, K., K. Yoshioka, H. Akedo, M. Uehata, T. Ishizaki, and S. Narumiya. 1999. An essential part for Rho-associated kinase in the transcellular invasion of tumor cells. *Nat Med*. 5:221-5.

Jacobs, J.J., P. Keblusek, E. Robanus-Maandag, P. Kristel, M. Lingbeek, P.M. Nederlof, T. van Welsem, M.J. van de Vijver, E.Y. Koh, G.Q. Daley, and M. van Lohuizen. 2000. Senescence bypass screen identifies TBX2, which represses Cdkn2a (p19(ARF)) and is amplified in a subset of human breast cancers. *Nat Genet*. 26:291-9.

Jahner, D., and R. Jaenisch. 1985. Retrovirus-induced de novo methylation of flanking host sequences correlates with gene inactivity. *Nature*. 315:594-7.

Jiao, Z., R. Mollaaghababa, W.J. Pavan, A. Antonellis, E.D. Green, and T.J. Hornyak. 2004. Direct interaction of Sox10 with the promoter of murine Dopachrome Tautomerase (Dct) and synergistic activation of Dct expression with Mitf. *Pigment Cell Res*. 17:352-62.

Kageshita, T., C.V. Hamby, T. Ishihara, K. Matsumoto, T. Saida, and T. Ono. 2001. Loss of beta-catenin expression associated with disease progression in malignant melanoma. *Br J Dermatol*. 145:210-6.

Kamai, T., K. Arai, S. Sumi, T. Tsujii, M. Honda, T. Yamanishi, and K.I. Yoshida. 2002. The rho/rho-kinase pathway is involved in the progression of testicular germ cell tumour. *BJU Int*. 89:449-53.

Kamai, T., T. Tsujii, K. Arai, K. Takagi, H. Asami, Y. Ito, and H. Oshima. 2003. Significant association of Rho/ROCK pathway with invasion and metastasis of bladder cancer. *Clin Cancer Res*. 9:2632-41.

Kang, S., J. Xie, J. Miao, R. Li, W. Liao, and R. Luo. 2013. A knockdown of Maml1 that results in melanoma cell senescence promotes an innate and adaptive immune response. *Cancer Immunol Immunother*. 62:183-90.

Kao, H.Y., P. Ordentlich, N. Koyano-Nakagawa, Z. Tang, M. Downes, C.R. Kintner, R.M. Evans, and T. Kadesch. 1998. A histone deacetylase corepressor complex regulates the Notch signal transduction pathway. *Genes Dev*. 12:2269-77.

Kelly, P.N., A. Dakic, J.M. Adams, S.L. Nutt, and A. Strasser. 2007. Tumor growth need not be driven by rare cancer stem cells. *Science*. 317:337.

Kim, G., A.E. McKee, Y.M. Ning, M. Hazarika, M. Theoret, J.R. Johnson, Q.C. Xu, S. Tang, R. Sridhara, X. Jiang, K. He, D. Roscoe, W.D. McGuinn, W.S. Helms, A.M. Russell, S. Pope Miksinski, J. Fourie Zirkelbach, J. Earp, Q. Liu, A. Ibrahim, R. Justice, and R. Pazdur. 2014. FDA Approval Summary: Vemurafenib for Treatment of Unresectable or Metastatic Melanoma with the BRAF V600E Mutation. *Clin Cancer Res*.

Kim, J., L. Lo, E. Dormand, and D.J. Anderson. 2003. SOX10 maintains multipotency and inhibits neuronal differentiation of neural crest stem cells. *Neuron*. 38:17-31.

Kitano, S., T. Tsuji, C. Liu, D. Hirschborn-Cymerman, C. Kyi, Z. Mu, J.P. Allison, S. Gnjatic, J.D. Yuan, and J.D. Wolchok. 2013. Enhancement of tumor-reactive cytotoxic CD4+ T cell responses after ipilimumab treatment in four advanced melanoma patients. *Cancer Immunol Res*. 1:235-244.

Korman, J.B., and D.E. Fisher. 2013. Developing melanoma therapeutics: overview and update. *Wiley Interdiscip Rev Syst Biol Med*. 5:257-71.

Krop, I., T. Demuth, T. Guthrie, P.Y. Wen, W.P. Mason, P. Chinnaiyan, N. Butowski, M.D. Groves, S. Kesari, S.J. Freedman, S. Blackman, J. Watters, A. Loboda, A. Podtelezhnikov, J. Lunceford, C. Chen, M. Giannotti, J. Hing, R. Beckman, and P. Lorusso. 2012. Phase I pharmacologic and pharmacodynamic study of the gamma secretase (Notch) inhibitor MK-0752 in adult patients with advanced solid tumors. *J Clin Oncol*. 30:2307-13.

Lacy, K.E., S.N. Karagiannis, and F.O. Nestle. 2012. Advances in the treatment of melanoma. *Clin Med*. 12:168-71.

Lapidot, T., C. Sirard, J. Vormoor, B. Murdoch, T. Hoang, J. Caceres-Cortes, M. Minden, B. Paterson, M.A. Caligiuri, and J.E. Dick. 1994. A cell initiating human acute myeloid leukaemia after transplantation into SCID mice. *Nature*. 367:645-8.

Lee, M., J. Goodall, C. Verastegui, R. Ballotti, and C.R. Goding. 2000. Direct regulation of the Microphthalmia promoter by Sox10 links Waardenburg-Shah syndrome (WS4)-associated hypopigmentation and deafness to WS2. *J Biol Chem*. 275:37978-83.

Leong, K.G., K. Niessen, I. Kulic, A. Raouf, C. Eaves, I. Pollet, and A. Karsan. 2007. Jagged1-mediated Notch activation induces epithelial-to-mesenchymal transition through Slug-induced repression of E-cadherin. *J Exp Med*. 204:2935-48.

Leung, T., X.Q. Chen, E. Manser, and L. Lim. 1996. The p160 RhoA-binding kinase ROK alpha is a member of a kinase family and is involved in the reorganization of the cytoskeleton. *Mol Cell Biol*. 16:5313-27.

Li, G., K. Satyamoorthy, and M. Herlyn. 2001. N-cadherin-mediated intercellular interactions promote survival and migration of melanoma cells. *Cancer Res*. 61:3819-25.

Liew, D.N., H. Kano, D. Kondziolka, D. Mathieu, A. Niranjan, J.C. Flickinger, J.M. Kirkwood, A. Tarhini, S. Moschos, and L.D. Lunsford. 2011. Outcome predictors of Gamma Knife surgery for melanoma brain metastases. Clinical article. *J Neurosurg*. 114:769-79.

Lochhead, P.A., G. Wickman, M. Mezna, and M.F. Olson. 2010. Activating ROCK1 somatic mutations in human cancer. *Oncogene*. 29:2591-8.

Loercher, A.E., E.M. Tank, R.B. Delston, and J.W. Harbour. 2005. MITF links differentiation with cell cycle arrest in melanocytes by transcriptional activation of INK4A. *J Cell Biol*. 168:35-40.

Luo, Y., K. Dallaglio, Y. Chen, W.A. Robinson, S.E. Robinson, M.D. McCarter, J. Wang, R. Gonzalez, D.C. Thompson, D.A. Norris, D.R. Roop, V. Vasiliou, and M. Fujita. 2012. ALDH1A Isozymes are Markers of Human Melanoma Stem Cells and Potential Therapeutic Targets. *Stem Cells*.

Maelandsmo, G.M., R. Holm, J.M. Nesland, O. Fodstad, and V.A. Florenes. 2003. Reduced beta-catenin expression in the cytoplasm of advanced-stage superficial spreading malignant melanoma. *Clin Cancer Res*. 9:3383-8.

Maier, M.M., and M. Gessler. 2000. Comparative analysis of the human and mouse Hey1 promoter: Hey genes are new Notch target genes. *Biochem Biophys Res Commun*. 275:652-60.

Mamalis, A., M. Garcha, and J. Jagdeo. 2014. Targeting the PD-1 pathway: a promising future for the treatment of melanoma. *Arch Dermatol Res*. 306:511-9.

Matise, M.P., and A.L. Joyner. 1999. Gli genes in development and cancer. *Oncogene*. 18:7852-9.

McEvilly, R.J., M.O. de Diaz, M.D. Schonemann, F. Hooshmand, and M.G. Rosenfeld. 2002. Transcriptional regulation of cortical neuron migration by POU domain factors. *Science*. 295:1528-32.

McGill, G.G., M. Horstmann, H.R. Widlund, J. Du, G. Motyckova, E.K. Nishimura, Y.L. Lin, S. Ramaswamy, W. Avery, H.F. Ding, S.A. Jordan, I.J. Jackson, S.J. Korsmeyer, T.R. Golub, and D.E. Fisher. 2002. Bcl2 regulation by the melanocyte master regulator Mitf modulates lineage survival and melanoma cell viability. *Cell*. 109:707-18.

Michaloglou, C., L.C. Vredeveld, M.S. Soengas, C. Denoyelle, T. Kuilman, C.M. van der Horst, D.M. Majoor, J.W. Shay, W.J. Mooi, and D.S. Peeper. 2005. BRAFE600-associated senescence-like cell cycle arrest of human naevi. *Nature*. 436:720-4.

Miller, A.J., and M.C. Mihm, Jr. 2006. Melanoma. *N Engl J Med*. 355:51-65.

Montagut, C., S.V. Sharma, T. Shioda, U. McDermott, M. Ulman, L.E. Ulkus, D. Dias-Santagata, H. Stubbs, D.Y. Lee, A. Singh, L. Drew, D.A. Haber, and J. Settleman. 2008. Elevated CRAF as a potential mechanism of acquired resistance to BRAF inhibition in melanoma. *Cancer Res*. 68:4853-61.

Monzani, E., F. Facchetti, E. Galmozzi, E. Corsini, A. Benetti, C. Cavazzin, A. Gritti, A. Piccinini, D. Porro, M. Santinami, G. Invernici, E. Parati, G. Alessandri, and C.A. La Porta. 2007. Melanoma contains CD133 and ABCG2 positive cells with enhanced tumourigenic potential. *Eur J Cancer*. 43:935-46.

Morgan-Fisher, M., U.M. Wewer, and A. Yoneda. 2013. Regulation of ROCK activity in cancer. *J Histochem Cytochem*. 61:185-98.

Morgan, T.H. 1917. The Theory of the Gene. *The American Naturalist*. 51:513-544.

Morin, P.J., A.B. Sparks, V. Korinek, N. Barker, H. Clevers, B. Vogelstein, and K.W. Kinzler. 1997. Activation of beta-catenin-Tcf signaling in colon cancer by mutations in beta-catenin or APC. *Science*. 275:1787-90.

Moriyama, M., M. Osawa, S.S. Mak, T. Ohtsuka, N. Yamamoto, H. Han, V. Delmas, R. Kageyama, F. Beermann, L. Larue, and S. Nishikawa. 2006. Notch signaling via Hes1 transcription factor maintains survival of melanoblasts and melanocyte stem cells. *J Cell Biol*. 173:333-9.

Murakami, H., and H. Arnheiter. 2005. Sumoylation modulates transcriptional activity of MITF in a promoter-specific manner. *Pigment Cell Res*. 18:265-77.

Murakami, T., S. Toda, M. Fujimoto, M. Ohtsuki, H.R. Byers, T. Etoh, and H. Nakagawa. 2001. Constitutive activation of Wnt/beta-catenin signaling pathway in migration-active melanoma cells: role of LEF-1 in melanoma with increased metastatic potential. *Biochem Biophys Res Commun*. 288:8-15.

Murphy, G.F., B.J. Wilson, S.D. Girouard, N.Y. Frank, and M.H. Frank. 2014. Stem cells and targeted approaches to melanoma cure. *Mol Aspects Med*. 39C:33-49.

Nakajima, M., K. Hayashi, Y. Egi, K. Katayama, Y. Amano, M. Uehata, M. Ohtsuki, A. Fujii, K. Oshita, H. Kataoka, K. Chiba, N. Goto, and T. Kondo. 2003. Effect of Wf-536, a novel ROCK inhibitor, against metastasis of B16 melanoma. *Cancer Chemother Pharmacol*. 52:319-24.

Naldini, L. 1998. Lentiviruses as gene transfer agents for delivery to non-dividing cells. *Curr Opin Biotechnol*. 9:457-63.

Naldini, L., U. Blomer, P. Gallay, D. Ory, R. Mulligan, F.H. Gage, I.M. Verma, and D. Trono. 1996. In vivo gene delivery and stable transduction of nondividing cells by a lentiviral vector. *Science*. 272:263-7.

Nazarian, R., H. Shi, Q. Wang, X. Kong, R.C. Koya, H. Lee, Z. Chen, M.K. Lee, N. Attar, H. Sazegar, T. Chodon, S.F. Nelson, G. McArthur, J.A. Sosman, A. Ribas, and R.S. Lo. 2010. Melanomas acquire resistance to B-RAF(V600E) inhibition by RTK or N-RAS upregulation. *Nature*. 468:973-7.

Nelson, A.A., and H. Tsao. 2009. Melanoma and genetics. *Clin Dermatol*. 27:46-52.

New England BioLabs Inc. 2014. Double Digest Finder.

Nicolas, M., A. Wolfer, K. Raj, J.A. Kummer, P. Mill, M. van Noort, C.C. Hui, H. Clevers, G.P. Dotto, and F. Radtke. 2003. Notch1 functions as a tumor suppressor in mouse skin. *Nat Genet*. 33:416-21.

Nieto, L., G. Joseph, A. Stella, P. Henri, O. Burlet-Schiltz, B. Monsarrat, E. Clottes, and M. Erard. 2007. Differential effects of phosphorylation on DNA binding properties of N Oct-3 are dictated by protein/DNA complex structures. *J Mol Biol*. 370:687-700.

Nolan, G.P. 2014. Retroviral Systems - Phoenix helper-free retrovirus producer lines.

O'Brien, C.A., A. Pollett, S. Gallinger, and J.E. Dick. 2007. A human colon cancer cell capable of initiating tumour growth in immunodeficient mice. *Nature*. 445:106-10.

Ohno, H., S. Goto, S. Taki, T. Shirasawa, H. Nakano, S. Miyatake, T. Aoe, Y. Ishida, H. Maeda, T. Shirai, and et al. 1994. Targeted disruption of the CD3 eta locus causes high lethality in mice: modulation of Oct-1 transcription on the opposite strand. *EMBO J*. 13:1157-65.

Olson, M.F. 2008. Applications for ROCK kinase inhibition. *Curr Opin Cell Biol*. 20:242-8.

Omholt, K., S. Karsberg, A. Platz, L. Kanter, U. Ringborg, and J. Hansson. 2002. Screening of N-ras codon 61 mutations in paired primary and metastatic

cutaneous melanomas: mutations occur early and persist throughout tumor progression. *Clin Cancer Res*. 8:3468-74.

Omholt, K., D. Krockel, U. Ringborg, and J. Hansson. 2006. Mutations of PIK3CA are rare in cutaneous melanoma. *Melanoma Res*. 16:197-200.

Omholt, K., A. Platz, L. Kanter, U. Ringborg, and J. Hansson. 2003. NRAS and BRAF mutations arise early during melanoma pathogenesis and are preserved throughout tumor progression. *Clin Cancer Res*. 9:6483-8.

Omholt, K., A. Platz, U. Ringborg, and J. Hansson. 2001. Cytoplasmic and nuclear accumulation of beta-catenin is rarely caused by CTNNB1 exon 3 mutations in cutaneous malignant melanoma. *Int J Cancer*. 92:839-42.

Ossowski, L., and J.A. Aguirre-Ghiso. 2010. Dormancy of metastatic melanoma. *Pigment Cell Melanoma Res*. 23:41-56.

Paraiso, K.H., Y. Xiang, V.W. Rebecca, E.V. Abel, Y.A. Chen, A.C. Munko, E. Wood, I.V. Fedorenko, V.K. Sondak, A.R. Anderson, A. Ribas, M.D. Palma, K.L. Nathanson, J.M. Koomen, J.L. Messina, and K.S. Smalley. 2011. PTEN loss confers BRAF inhibitor resistance to melanoma cells through the suppression of BIM expression. *Cancer Res*. 71:2750-60.

Park, I.H., R. Zhao, J.A. West, A. Yabuuchi, H. Huo, T.A. Ince, P.H. Lerou, M.W. Lensch, and G.Q. Daley. 2008. Reprogramming of human somatic cells to pluripotency with defined factors. *Nature*. 451:141-6.

Pawlak, G., and D.M. Helfman. 2002. Post-transcriptional down-regulation of ROCKI/Rho-kinase through an MEK-dependent pathway leads to cytoskeleton disruption in Ras-transformed fibroblasts. *Mol Biol Cell*. 13:336-47.

Piccirillo, S.G., and A.L. Vescovi. 2006. Bone morphogenetic proteins regulate tumorigenicity in human glioblastoma stem cells. *Ernst Schering Found Symp Proc*:59-81.

Pinc, A., R. Somasundaram, C. Wagner, M. Hormann, G. Karanikas, A. Jalili, W. Bauer, P. Brunner, K. Grabmeier-Pfistershammer, M. Gschaider, C.Y. Lai, M.Y. Hsu, M. Herlyn, G. Stingl, and S.N. Wagner. 2012. Targeting CD20 in melanoma patients at high risk of disease recurrence. *Mol Ther*. 20:1056-62.

Pingault, V., N. Bondurand, K. Kuhlbrodt, D.E. Goerich, M.O. Prehu, A. Puliti, B. Herbarth, I. Hermans-Borgmeyer, E. Legius, G. Matthijs, J. Amiel, S. Lyonnet, I. Ceccherini, G. Romeo, J.C. Smith, A.P. Read, M. Wegner, and M. Goossens. 1998. SOX10 mutations in patients with Waardenburg-Hirschsprung disease. *Nat Genet*. 18:171-3.

Pinner, S., P. Jordan, K. Sharrock, L. Bazley, L. Collinson, R. Marais, E. Bonvin, C. Goding, and E. Sahai. 2009. Intravital imaging reveals transient changes in pigment production and Brn2 expression during metastatic melanoma dissemination. *Cancer Res*. 69:7969-77.

Potterf, S.B., M. Furumura, K.J. Dunn, H. Arnheiter, and W.J. Pavan. 2000. Transcription factor hierarchy in Waardenburg syndrome: regulation of MITF expression by SOX10 and PAX3. *Hum Genet*. 107:1-6.

Pournara, A., T. Holmlund, Y. Lu, R. Ceder, M. Putnik, R. Grafstrom, M. Vahter, and A.E. Wallberg. 2014. Arsenic-induced suppression of kidney cell proliferation and the transcriptional coregulator MAML1. *Metallomics*. 6:498-504.

Price, E.R., H.F. Ding, T. Badalian, S. Bhattacharya, C. Takemoto, T.P. Yao, T.J. Hemesath, and D.E. Fisher. 1998. Lineage-specific signaling in melanocytes. C-kit stimulation recruits p300/CBP to microphthalmia. *J Biol Chem*. 273:17983-6.

Prince, S., S. Carreira, K.W. Vance, A. Abrahams, and C.R. Goding. 2004. Tbx2 directly represses the expression of the p21(WAF1) cyclin-dependent kinase inhibitor. *Cancer Res*. 64:1669-74.

Qin, J.Z., L. Stennett, P. Bacon, B. Bodner, M.J. Hendrix, R.E. Seftor, E.A. Seftor, N.V. Margaryan, P.M. Pollock, A. Curtis, J.M. Trent, F. Bennett, L. Miele, and B.J. Nickoloff. 2004. p53-independent NOXA induction overcomes apoptotic resistance of malignant melanomas. *Mol Cancer Ther*. 3:895-902.

Qiu, R.G., J. Chen, F. McCormick, and M. Symons. 1995. A role for Rho in Ras transformation. *Proc Natl Acad Sci U S A*. 92:11781-5.

Quintana, E., M. Shackleton, H.R. Foster, D.R. Fullen, M.S. Sabel, T.M. Johnson, and S.J. Morrison. 2010. Phenotypic heterogeneity among tumorigenic melanoma cells from patients that is reversible and not hierarchically organized. *Cancer Cell*. 18:510-23.

Quintana, E., M. Shackleton, M.S. Sabel, D.R. Fullen, T.M. Johnson, and S.J. Morrison. 2008. Efficient tumour formation by single human melanoma cells. *Nature*. 456:593-8.

Raposo, G., and M.S. Marks. 2007. Melanosomes--dark organelles enlighten endosomal membrane transport. *Nat Rev Mol Cell Biol*. 8:786-97.

Reynolds, T.C., S.D. Smith, and J. Sklar. 1987. Analysis of DNA surrounding the breakpoints of chromosomal translocations involving the beta T cell receptor gene in human lymphoblastic neoplasms. *Cell*. 50:107-17.

Ricci-Vitiani, L., D.G. Lombardi, E. Pilozzi, M. Biffoni, M. Todaro, C. Peschle, and R. De Maria. 2007. Identification and expansion of human colon-cancer-initiating cells. *Nature*. 445:111-5.

Rimm, D.L., K. Caca, G. Hu, F.B. Harrison, and E.R. Fearon. 1999. Frequent nuclear/cytoplasmic localization of beta-catenin without exon 3 mutations in malignant melanoma. *Am J Pathol*. 154:325-9.

Rodilla, V., A. Villanueva, A. Obrador-Hevia, A. Robert-Moreno, V. Fernandez-Majada, A. Grilli, N. Lopez-Bigas, N. Bellora, M.M. Alba, F. Torres, M. Dunach, X. Sanjuan, S. Gonzalez, T. Gridley, G. Capella, A. Bigas, and L. Espinosa. 2009. Jagged1 is the pathological link between Wnt and Notch pathways in colorectal cancer. *Proc Natl Acad Sci U S A*. 106:6315-20.

Rodriguez, M., E. Aladowicz, L. Lanfrancone, and C.R. Goding. 2008. Tbx3 represses E-cadherin expression and enhances melanoma invasiveness. *Cancer Res*. 68:7872-81.

Roesch, A., M. Fukunaga-Kalabis, E.C. Schmidt, S.E. Zabierowski, P.A. Brafford, A. Vultur, D. Basu, P. Gimotty, T. Vogt, and M. Herlyn. 2010. A temporarily distinct subpopulation of slow-cycling melanoma cells is required for continuous tumor growth. *Cell*. 141:583-94.

Roesch, A., A. Vultur, I. Bogeski, H. Wang, K.M. Zimmermann, D. Speicher, C. Korbel, M.W. Laschke, P.A. Gimotty, S.E. Philipp, E. Krause, S. Patzold, J. Villanueva, C. Krepler, M. Fukunaga-Kalabis, M. Hoth, B.C. Bastian, T. Vogt, and M. Herlyn. 2013. Overcoming intrinsic multidrug resistance in melanoma by blocking the mitochondrial respiratory chain of slow-cycling JARID1B(high) cells. *Cancer Cell*. 23:811-25.

Rosel, D., J. Brabek, O. Tolde, C.T. Mierke, D.P. Zitterbart, C. Raupach, K. Bicanova, P. Kollmannsberger, D. Pankova, P. Vesely, P. Folk, and B. Fabry. 2008. Up-regulation of Rho/ROCK signaling in sarcoma cells drives invasion and increased generation of protrusive forces. *Mol Cancer Res*. 6:1410-20.

Routhier, A., M. Astuccio, D. Lahey, N. Monfredo, A. Johnson, W. Callahan, A. Partington, K. Fellows, L. Ouellette, S. Zhidro, C. Goodrow, A. Smith, K. Sullivan, P. Simone, L. Le, B. Vezuli, M. Zohni, E. West, D. Gleason, and B. Bryan. 2010. Pharmacological inhibition of Rho-kinase signaling with Y-27632 blocks melanoma tumor growth. *Oncol Rep*. 23:861-7.

Rubinfeld, B., P. Robbins, M. El-Gamil, I. Albert, E. Porfiri, and P. Polakis. 1997. Stabilization of beta-catenin by genetic defects in melanoma cell lines. *Science*. 275:1790-2.

Saez-Ayala, M., M.F. Montenegro, L. Sanchez-Del-Campo, M.P. Fernandez-Perez, S. Chazarra, R. Freter, M. Middleton, A. Pinero-Madrona, J. Cabezas-Herrera, C.R. Goding, and J.N. Rodriguez-Lopez. 2013. Directed phenotype switching as an effective antimelanoma strategy. *Cancer Cell*. 24:105-19.

Sahai, E., and C.J. Marshall. 2002. RHO-GTPases and cancer. *Nat Rev Cancer*. 2:133-42.

Saint Just Ribeiro, M., M.L. Hansson, M.J. Lindberg, A.E. Popko-Scibor, and A.E. Wallberg. 2009. GSK3beta is a negative regulator of the transcriptional coactivator MAML1. *Nucleic Acids Res*. 37:6691-700.

Sakuma, T., M.A. Barry, and Y. Ikeda. 2012. Lentiviral vectors: basic to translational. *Biochem J*. 443:603-18.

Salmon, P., and D. Trono. 2007. Production and titration of lentiviral vectors. *Curr Protoc Hum Genet*. Chapter 12:Unit 12 10.

Sanders, D.S., K. Blessing, G.A. Hassan, R. Bruton, J.R. Marsden, and J. Jankowski. 1999. Alterations in cadherin and catenin expression during the biological progression of melanocytic tumours. *Mol Pathol*. 52:151-7.

Schatton, T., and M.H. Frank. 2008. Cancer stem cells and human malignant melanoma. *Pigment Cell Melanoma Res*. 21:39-55.

Schatton, T., G.F. Murphy, N.Y. Frank, K. Yamaura, A.M. Waaga-Gasser, M. Gasser, Q. Zhan, S. Jordan, L.M. Duncan, C. Weishaupt, R.C. Fuhlbrigge, T.S. Kupper, M.H. Sayegh, and M.H. Frank. 2008. Identification of cells initiating human melanomas. *Nature*. 451:345-9.

Schatton, T., U. Schutte, N.Y. Frank, Q. Zhan, A. Hoerning, S.C. Robles, J. Zhou, F.S. Hodi, G.C. Spagnoli, G.F. Murphy, and M.H. Frank. 2010. Modulation of T-cell activation by malignant melanoma initiating cells. *Cancer Res*. 70:697-708.

Schlaak, M., P. Schmidt, C. Bangard, P. Kurschat, C. Mauch, and H. Abken. 2012. Regression of metastatic melanoma in a patient by antibody targeting of cancer stem cells. *Oncotarget*. 3:22-30.

Schroeter, E.H., J.A. Kisslinger, and R. Kopan. 1998. Notch-1 signalling requires ligand-induced proteolytic release of intracellular domain. *Nature*. 393:382-6.

Scott, G., S. Leopardi, S. Printup, and B.C. Madden. 2002. Filopodia are conduits for melanosome transfer to keratinocytes. *J Cell Sci*. 115:1441-51.

Segura, M.F., D. Hanniford, S. Menendez, L. Reavie, X. Zou, S. Alvarez-Diaz, J. Zakrzewski, E. Blochin, A. Rose, D. Bogunovic, D. Polsky, J. Wei, P. Lee, I. Belitskaya-Levy, N. Bhardwaj, I. Osman, and E. Hernando. 2009. Aberrant miR-182 expression promotes melanoma metastasis by repressing FOXO3 and microphthalmia-associated transcription factor. *Proc Natl Acad Sci U S A*. 106:1814-9.

Seong, I., H.J. Min, J.H. Lee, C.Y. Yeo, D.M. Kang, E.S. Oh, E.S. Hwang, and J. Kim. 2012. Sox10 controls migration of B16F10 melanoma cells through multiple regulatory target genes. *PLoS One*. 7:e31477.

Shakhova, O., D. Zingg, S.M. Schaefer, L. Hari, G. Civenni, J. Blunschi, S. Claudinot, M. Okoniewski, F. Beermann, D. Mihic-Probst, H. Moch, M. Wegner, R. Dummer, Y. Barrandon, P. Cinelli, and L. Sommer. 2012. Sox10 promotes the formation and maintenance of giant congenital naevi and melanoma. *Nat Cell Biol*. 14:882-90.

Shaner, N.C., P.A. Steinbach, and R.Y. Tsien. 2005. A guide to choosing fluorescent proteins. *Nat Methods*. 2:905-9.

Sharma, S.V., D.Y. Lee, B. Li, M.P. Quinlan, F. Takahashi, S. Maheswaran, U. McDermott, N. Azizian, L. Zou, M.A. Fischbach, K.K. Wong, K. Brandstetter, B. Wittner, S. Ramaswamy, M. Classon, and J. Settleman. 2010. A chromatin-mediated reversible drug-tolerant state in cancer cell subpopulations. *Cell*. 141:69-80.

Shen, H., A.S. McElhinny, Y. Cao, P. Gao, J. Liu, R. Bronson, J.D. Griffin, and L. Wu. 2006. The Notch coactivator, MAML1, functions as a novel coactivator for MEF2C-mediated transcription and is required for normal myogenesis. *Genes Dev*. 20:675-88.

Shi, H., G. Moriceau, X. Kong, M.K. Lee, H. Lee, R.C. Koya, C. Ng, T. Chodon, R.A. Scolyer, K.B. Dahlman, J.A. Sosman, R.F. Kefford, G.V. Long, S.F. Nelson, A. Ribas, and R.S. Lo. 2012. Melanoma whole-exome sequencing identifies (V600E)B-RAF amplification-mediated acquired B-RAF inhibitor resistance. *Nat Commun*. 3:724.

Singh, S.K., C. Hawkins, I.D. Clarke, J.A. Squire, J. Bayani, T. Hide, R.M. Henkelman, M.D. Cusimano, and P.B. Dirks. 2004. Identification of human brain tumour initiating cells. *Nature*. 432:396-401.

Skeen, J.E., P.T. Bhaskar, C.C. Chen, W.S. Chen, X.D. Peng, V. Nogueira, A. Hahn-Windgassen, H. Kiyokawa, and N. Hay. 2006. Akt deficiency impairs normal cell proliferation and suppresses oncogenesis in a p53-independent and mTORC1-dependent manner. *Cancer Cell*. 10:269-80.

Slominski, A., D.J. Tobin, S. Shibahara, and J. Wortsman. 2004. Melanin pigmentation in mammalian skin and its hormonal regulation. *Physiol Rev*. 84:1155-228.

Smit, D.J., A.G. Smith, P.G. Parsons, G.E. Muscat, and R.A. Sturm. 2000. Domains of Brn-2 that mediate homodimerization and interaction with general and melanocytic transcription factors. *Eur J Biochem*. 267:6413-22.

Somlyo, A.V., D. Bradshaw, S. Ramos, C. Murphy, C.E. Myers, and A.P. Somlyo. 2000. Rho-kinase inhibitor retards migration and in vivo dissemination of human prostate cancer cells. *Biochem Biophys Res Commun*. 269:652-9.

Sosman, J.A., K.B. Kim, L. Schuchter, R. Gonzalez, A.C. Pavlick, J.S. Weber, G.A. McArthur, T.E. Hutson, S.J. Moschos, K.T. Flaherty, P. Hersey, R. Kefford, D. Lawrence, I. Puzanov, K.D. Lewis, R.K. Amaravadi, B. Chmielowski, H.J. Lawrence, Y. Shyr, F. Ye, J. Li, K.B. Nolop, R.J. Lee, A.K. Joe, and A. Ribas. 2012. Survival in BRAF V600-mutant advanced melanoma treated with vemurafenib. *N Engl J Med*. 366:707-14.

Southard-Smith, E.M., L. Kos, and W.J. Pavan. 1998. Sox10 mutation disrupts neural crest development in Dom Hirschsprung mouse model. *Nat Genet*. 18:60-4.

Stahl, J.M., A. Sharma, M. Cheung, M. Zimmerman, J.Q. Cheng, M.W. Bosenberg, M. Kester, L. Sandirasegarane, and G.P. Robertson. 2004. Deregulated Akt3 activity promotes development of malignant melanoma. *Cancer Res*. 64:7002-10.

Steingrimsson, E., N.G. Copeland, and N.A. Jenkins. 2004. Melanocytes and the microphthalmia transcription factor network. *Annu Rev Genet*. 38:365-411.

Sturm, R.A., F. Bisshop, H. Takahashi, and P.G. Parsons. 1991. A melanoma octamer binding protein is responsive to differentiating agents. *Cell Growth Differ*. 2:519-24.

Sturm, R.A., and W. Herr. 1988. The POU domain is a bipartite DNA-binding structure. *Nature*. 336:601-4.

Sturm, R.A., B.J. O'Sullivan, J.A. Thomson, N. Jamshidi, J. Pedley, and P.G. Parsons. 1994. Expression studies of pigmentation and POU-domain genes in human melanoma cells. *Pigment Cell Res*. 7:235-40.

Sunabori, T., A. Tokunaga, T. Nagai, K. Sawamoto, M. Okabe, A. Miyawaki, Y. Matsuzaki, T. Miyata, and H. Okano. 2008. Cell-cycle-specific nestin expression coordinates with morphological changes in embryonic cortical neural progenitors. *J Cell Sci*. 121:1204-12.

Takahashi, K., K. Okita, M. Nakagawa, and S. Yamanaka. 2007. Induction of pluripotent stem cells from fibroblast cultures. *Nat Protoc*. 2:3081-9.

Takahashi, K., and S. Yamanaka. 2006. Induction of pluripotent stem cells from mouse embryonic and adult fibroblast cultures by defined factors. *Cell*. 126:663-76.

Takebe, N., P.J. Harris, R.Q. Warren, and S.P. Ivy. 2011. Targeting cancer stem cells by inhibiting Wnt, Notch, and Hedgehog pathways. *Nat Rev Clin Oncol*. 8:97-106.

Takeda, K., K. Yasumoto, R. Takada, S. Takada, K. Watanabe, T. Udono, H. Saito, K. Takahashi, and S. Shibahara. 2000. Induction of melanocyte-specific microphthalmia-associated transcription factor by Wnt-3a. *J Biol Chem*. 275:14013-6.

Thermo SCIENTIFIC. 2013. Multiple primer analyzer.

Thomas, A.J., and C.A. Erickson. 2008. The making of a melanocyte: the specification of melanoblasts from the neural crest. *Pigment Cell Melanoma Res*. 21:598-610.

Thomson, J.A., K. Murphy, E. Baker, G.R. Sutherland, P.G. Parsons, R.A. Sturm, and F. Thomson. 1995. The brn-2 gene regulates the melanocytic phenotype and tumorigenic potential of human melanoma cells. *Oncogene*. 11:691-700.

Thomson, J.A., P.G. Parsons, and R.A. Sturm. 1993. In vivo and in vitro expression of octamer binding proteins in human melanoma metastases, brain tissue, and fibroblasts. *Pigment Cell Res*. 6:13-22.

Thurber, A.E., G. Douglas, E.C. Sturm, S.E. Zabierowski, D.J. Smit, S.N. Ramakrishnan, E. Hacker, J.H. Leonard, M. Herlyn, and R.A. Sturm. 2011. Inverse expression states of the BRN2 and MITF transcription factors in melanoma spheres and tumour xenografts regulate the NOTCH pathway. *Oncogene*. 30:3036-48.

Tolcher, A.W., W.A. Messersmith, S.M. Mikulski, K.P. Papadopoulos, E.L. Kwak, D.G. Gibbon, A. Patnaik, G.S. Falchook, A. Dasari, G.I. Shapiro, J.F. Boylan, Z.X. Xu, K. Wang, A. Koehler, J. Song, S.A. Middleton, J. Deutsch, M. Demario, R. Kurzrock, and J.J. Wheler. 2012. Phase I study of RO4929097, a gamma secretase inhibitor of Notch signaling, in patients with refractory metastatic or locally advanced solid tumors. *J Clin Oncol*. 30:2348-53.

Topczewska, J.M., L.M. Postovit, N.V. Margaryan, A. Sam, A.R. Hess, W.W. Wheaton, B.J. Nickoloff, J. Topczewski, and M.J. Hendrix. 2006. Embryonic and tumorigenic pathways converge via Nodal signaling: role in melanoma aggressiveness. *Nat Med*. 12:925-32.

Tsao, H., V. Goel, H. Wu, G. Yang, and F.G. Haluska. 2004. Genetic interaction between NRAS and BRAF mutations and PTEN/MMAC1 inactivation in melanoma. *J Invest Dermatol*. 122:337-41.

Tsao, H., X. Zhang, E. Benoit, and F.G. Haluska. 1998. Identification of PTEN/MMAC1 alterations in uncultured melanomas and melanoma cell lines. *Oncogene*. 16:3397-402.

Untergasser, A., I. Cutcutache, T. Koressaar, J. Ye, B.C. Faircloth, M. Remm, and S.G. Rozen. 2012. Primer3--new capabilities and interfaces. *Nucleic Acids Res*. 40:e115.

Valyi-Nagy, I.T., G. Hirka, P.J. Jensen, I.M. Shih, I. Juhasz, and M. Herlyn. 1993. Undifferentiated keratinocytes control growth, morphology, and antigen expression of normal melanocytes through cell-cell contact. *Lab Invest*. 69:152-9.

van Golen, K.L., Z.F. Wu, X.T. Qiao, L.W. Bao, and S.D. Merajver. 2000. RhoC GTPase, a novel transforming oncogene for human mammary epithelial cells that partially recapitulates the inflammatory breast cancer phenotype. *Cancer Res*. 60:5832-8.

Vance, K.W., S. Carreira, G. Brosch, and C.R. Goding. 2005. Tbx2 is overexpressed and plays an important role in maintaining proliferation and suppression of senescence in melanomas. *Cancer Res*. 65:2260-8.

Vance, K.W., and C.R. Goding. 2004. The transcription network regulating melanocyte development and melanoma. *Pigment Cell Res*. 17:318-25.

Vastrik, I., B.J. Eickholt, F.S. Walsh, A. Ridley, and P. Doherty. 1999. Sema3A-induced growth-cone collapse is mediated by Rac1 amino acids 17-32. *Curr Biol*. 9:991-8.

Verastegui, C., K. Bille, J.P. Ortonne, and R. Ballotti. 2000. Regulation of the microphthalmia-associated transcription factor gene by the Waardenburg syndrome type 4 gene, SOX10. *J Biol Chem*. 275:30757-60.

Villanueva, J., A. Vultur, J.T. Lee, R. Somasundaram, M. Fukunaga-Kalabis, A.K. Cipolla, B. Wubbenhorst, X. Xu, P.A. Gimotty, D. Kee, A.E. Santiago-Walker, R. Letrero, K. D'Andrea, A. Pushparajan, J.E. Hayden, K.D. Brown, S. Laquerre, G.A. McArthur, J.A. Sosman, K.L. Nathanson, and M. Herlyn. 2010. Acquired resistance to BRAF inhibitors mediated by a RAF kinase switch in melanoma can be overcome by cotargeting MEK and IGF-1R/PI3K. *Cancer Cell*. 18:683-95.

Wagle, N., C. Emery, M.F. Berger, M.J. Davis, A. Sawyer, P. Pochanard, S.M. Kehoe, C.M. Johannessen, L.E. Macconaill, W.C. Hahn, M. Meyerson, and L.A. Garraway. 2011. Dissecting therapeutic resistance to RAF inhibition in melanoma by tumor genomic profiling. *J Clin Oncol*. 29:3085-96.

Walunas, T.L., D.J. Lenschow, C.Y. Bakker, P.S. Linsley, G.J. Freeman, J.M. Green, C.B. Thompson, and J.A. Bluestone. 1994. CTLA-4 can function as a negative regulator of T cell activation. *Immunity*. 1:405-13.

Wang, L., L. Yang, Y. Luo, and Y. Zheng. 2003. A novel strategy for specifically down-regulating individual Rho GTPase activity in tumor cells. *J Biol Chem*. 278:44617-25.

Watanabe, N., T. Kato, A. Fujita, T. Ishizaki, and S. Narumiya. 1999. Cooperation between mDia1 and ROCK in Rho-induced actin reorganization. *Nat Cell Biol*. 1:136-43.

Weber, J.S., R.R. Kudchadkar, B. Yu, D. Gallenstein, C.E. Horak, H.D. Inzunza, X. Zhao, A.J. Martinez, W. Wang, G. Gibney, J. Kroeger, C. Eysmans, A.A. Sarnaik, and Y.A. Chen. 2013. Safety, efficacy, and biomarkers of nivolumab with vaccine in ipilimumab-refractory or -naive melanoma. *J Clin Oncol*. 31:4311-8.

Wegner, M., D.W. Drolet, and M.G. Rosenfeld. 1993. POU-domain proteins: structure and function of developmental regulators. *Curr Opin Cell Biol*. 5:488-98.

Wellbrock, C., M. Karasarides, and R. Marais. 2004. The RAF proteins take centre stage. *Nat Rev Mol Cell Biol*. 5:875-85.

Wellbrock, C., and R. Marais. 2005. Elevated expression of MITF counteracts B-RAF-stimulated melanocyte and melanoma cell proliferation. *J Cell Biol*. 170:703-8.

Wellbrock, C., S. Rana, H. Paterson, H. Pickersgill, T. Brummelkamp, and R. Marais. 2008. Oncogenic BRAF regulates melanoma proliferation through the lineage specific factor MITF. *PLoS One*. 3:e2734.

Wernig, M., A. Meissner, R. Foreman, T. Brambrink, M. Ku, K. Hochedlinger, B.E. Bernstein, and R. Jaenisch. 2007. In vitro reprogramming of fibroblasts into a pluripotent ES-cell-like state. *Nature*. 448:318-24.

Widlund, H.R., M.A. Horstmann, E.R. Price, J. Cui, S.L. Lessnick, M. Wu, X. He, and D.E. Fisher. 2002. Beta-catenin-induced melanoma growth requires the downstream target Microphthalmia-associated transcription factor. *J Cell Biol*. 158:1079-87.

World Health Organization - International Agency for Research on Cancer. 2014. GLOBOCAN 2012: Estimated Cancer Incidence, Mortality and Prevalence Worldwide in 2012.

Wu, H., V. Goel, and F.G. Haluska. 2003. PTEN signaling pathways in melanoma. *Oncogene*. 22:3113-22.

Wu, L., J.C. Aster, S.C. Blacklow, R. Lake, S. Artavanis-Tsakonas, and J.D. Griffin. 2000. MAML1, a human homologue of Drosophila mastermind, is a transcriptional co-activator for NOTCH receptors. *Nat Genet*. 26:484-9.

Wullschleger, S., R. Loewith, and M.N. Hall. 2006. TOR signaling in growth and metabolism. *Cell*. 124:471-84.

Xue, W., S. Chen, H. Yin, T. Tammela, T. Papagiannakopoulos, N.S. Joshi, W. Cai, G. Yang, R. Bronson, D.G. Crowley, F. Zhang, D.G. Anderson, P.A. Sharp, and T. Jacks. 2014. CRISPR-mediated direct mutation of cancer genes in the mouse liver. *Nature*.

Yeh, I., A. von Deimling, and B.C. Bastian. 2013. Clonal BRAF mutations in melanocytic nevi and initiating role of BRAF in melanocytic neoplasia. *J Natl Cancer Inst*. 105:917-9.

Yoneda, A., H.A. Multhaupt, and J.R. Couchman. 2005. The Rho kinases I and II regulate different aspects of myosin II activity. *J Cell Biol*. 170:443-53.

Yoon, S., and R. Seger. 2006. The extracellular signal-regulated kinase: multiple substrates regulate diverse cellular functions. *Growth Factors*. 24:21-44.

Yoshioka, K., F. Matsumura, H. Akedo, and K. Itoh. 1998. Small GTP-binding protein Rho stimulates the actomyosin system, leading to invasion of tumor cells. *J Biol Chem*. 273:5146-54.

Yoshioka, K., S. Nakamori, and K. Itoh. 1999. Overexpression of small GTP-binding protein RhoA promotes invasion of tumor cells. *Cancer Res*. 59:2004-10.

Yu, S.F., T. von Ruden, P.W. Kantoff, C. Garber, M. Seiberg, U. Ruther, W.F. Anderson, E.F. Wagner, and E. Gilboa. 1986. Self-inactivating retroviral vectors designed for transfer of whole genes into mammalian cells. *Proc Natl Acad Sci U S A*. 83:3194-8.

Zhao, L., E.T. Ng, and P. Koopman. 2014. A piggyBac transposon- and gateway-enhanced system for efficient BAC transgenesis. *Dev Dyn*. 243:C1.

Zhao, Y., R.B. Katzman, L.M. Delmolino, I. Bhat, Y. Zhang, C.B. Gurumurthy, A. Germaniuk-Kurowska, H.V. Reddi, A. Solomon, M.S. Zeng, A. Kung, H. Ma,

Q. Gao, G. Dimri, A. Stanculescu, L. Miele, L. Wu, J.D. Griffin, D.E. Wazer, H. Band, and V. Band. 2007. The notch regulator MAML1 interacts with p53 and functions as a coactivator. *J Biol Chem*. 282:11969-81.

Zhou, Y., Y. Su, B. Li, F. Liu, J.W. Ryder, X. Wu, P.A. Gonzalez-DeWhitt, V. Gelfanova, J.E. Hale, P.C. May, S.M. Paul, and B. Ni. 2003. Nonsteroidal anti-inflammatory drugs can lower amyloidogenic Abeta42 by inhibiting Rho. *Science*. 302:1215-7.

Zimonjic, D.B., L.N. Chan, V. Tripathi, J. Lu, O. Kwon, N.C. Popescu, D.R. Lowy, and F. Tamanoi. 2013. In vitro and in vivo effects of geranylgeranyltransferase I inhibitor P61A6 on non-small cell lung cancer cells. *BMC Cancer*. 13:198.

Zuidervaart, W., S. Pavey, F.A. van Nieuwpoort, L. Packer, C. Out, W. Maat, M.J. Jager, N.A. Gruis, and N.K. Hayward. 2007. Expression of Wnt5a and its downstream effector beta-catenin in uveal melanoma. *Melanoma Res*. 17:380-6.

Zuo, L., J. Weger, Q. Yang, A.M. Goldstein, M.A. Tucker, G.J. Walker, N. Hayward, and N.C. Dracopoli. 1996. Germline mutations in the p16INK4a binding domain of CDK4 in familial melanoma. *Nat Genet*. 12:97-9.

8 Appendix

8.1 Funding secured as a result of this thesis

OSCI Seed Funding Grant, Directed phenotype switching as a differentiation therapy for melanoma

April 2012

8.2 Presentations relating to this thesis

Agkatsev, S., K.C. Ngeow, R. Freter, C. Goding, L.W. Seymour 2013.

Poster presentation. Development of dual fluorescent reporter viruses for melanoma subpopulations.

International Congress of the Society for Melanoma Research

Awarded poster prize